CELL ENVELOPE STRESS RESPONSE AND MECHANISMS OF ANTIBIOTIC RESISTANCE IN *BACILLUS SUBTILIS*

A Dissertation

Presented to the Faculty of the Graduate School

of Cornell University

In Partial Fulfillment of the Requirements for the Degree of

Doctor of Philosophy

by

Anna-Barbara Geertruida Hachmann

May 2010

CELL ENVELOPE STRESS RESPONSE AND MECHANISMS OF ANTIBIOTIC RESISTANCE IN *BACILLUS SUBTILIS*

Anna-Barbara Geertruida Hachmann, Ph. D.

Cornell University 2010

The bacterial cell envelope, consisting primarily of the cell membrane and the cell wall, is the most important physical and structural barrier. The cell wall provides the cell with structural strength and protects it from lysis due to the high turgor. The cytoplasmic membrane functions as a molecular sieve, controlling the transport of specific proteins, and nutrients. Because many aspects of the cell envelope are specific to bacteria, it is also a prime target for antibiotics. To date, at least 17 classes of antibiotics are available for treatment; however, to each class bacteria have developed resistance. This selective pressure within bacteria not only originates from the widespread use of antibiotics, it is also inherent in the natural environment of many soil dwelling prokaryotes which evolved to produce antibiotics as signaling molecules or for nutrient competition. Here, we have investigated the response of the Gram-positive model bacterium *Bacillus subtilis* to commonly used cell envelope active antibiotics. By combining global analytical techniques, including microarray analyses, proteomic studies, transposon mutagenesis, whole genome sequencing, and fluorescence and electron microscopy, we obtained a clearer picture of the response of *B. subtilis* to daptomycin, moenomycin, ramoplanin, fosfomycin, and duramycin. In addition, we discuss mechanisms of resistance to these antibiotics.

BIOGRAPHICAL SKETCH

Anna-Barbara Geertruida Hachmann, née Kleijn, was born on December 5th, 1978 in Bielefeld, Germany and grew up in the town of Tecklenburg.

After graduating from the Graf-Adolf-Gymnasium Tecklenburg in 1998, she worked for one year as laboratory assistant at Wiewelhove GmbH, a pharmaceutical company that specializes in contract manufacturing of solid forms in Ibbenbüren, Germany. She was responsible for analyzing raw materials and proprietary medicinal products according to the *Pharmacopoea Europaea* in the Department of Quality Control. It was during this time that she decided to persue a research career with a pharmaceutical background.

In October 1999 Anna began her studies of pharmacy at the Friedrich-Schiller University in Jena, Germany. From October 2003 until May 2004, she joined Dr. Hendrik van Veen in the Department of Pharmacology at the University of Cambridge, UK, where she explored structure activity relationships of the ATP-binding cassette multidrug transporter LmrA in *Lactococcus lactis*. She returned to Jena, to complete her pharmacy degree. In December 2004 she received her European pharmacist license.

Anna began her graduate studies at Cornell University in January 2005 where she joined Professor John D. Helmann's group in the Department of Microbiology. She was fascinated about studying mechanisms of antibiotic resistance at the level of transcriptional regulation in the Gram-positive model bacterium *Bacillus subtilis*. This dissertation summarizes her major findings.

Following the completion of her PhD, she will begin post-doctoral research with Professor Jon Clardy and Dr. David Rudner at Harvard Medical School, Boston.

ACKNOWLEDGMENTS

I am sincerely grateful to my advisor and mentor, Professor John D. Helmann, who has supported me throughout my graduate studies with his patience and knowledge while allowing me room to investigate different aspects of antibiotic resistance. This dissertation would not have been possible without his guidance.

It is a pleasure to thank my committee members, Associate Professor Ruth Collins, Professor Tadhg Begley, and Assistant Professor Hening Lin for their support and helpful advice. In addition, I would like to thank Professor Esther Angert, Professor Joseph Peters, Dr. Qiaojuan Shi, and Professor Anthony Hay for their assistance with various techniques.

During my graduate studies I was fortunate to work with a friendly and cheerful group of fellow students who encouraged me along the way and shared the excitement of “re”search. It was a privilege to work with Ahmed Gaballa, who is a wonderful mentor and friend, and has the ability to always put a smile on your face. I would like to thank the members of the Helmann lab and Winans lab, in particular Shawn MacLellan, Yun Luo, Veronica Guariglia-Oropeza, Tina Wecke, as well as Showey Yazdanian, Alex Fishman, Dominika Zgid, Paulina Gonzalez-Morelos, and my class mates for their friendship and many fond memories. I owe Cornell Outdoor Education and my climbing partners my love for climbing and the outdoors.

All this would not have been possible without the constant support from my husband and my family. With this I would also like to thank Nancy and Robert Nead (including the Zoo) for making us feel home away from home.

TABLE OF CONTENTS

LIST OF FIGURES

LIST OF TABLES

CHAPTER 1

INTRODUCTION

1.1 The cell envelope of Gram-positive bacteria

In Gram-positive bacteria, the cell is enclosed by the cytoplasmic membrane and the cell wall, which consists of peptidoglycan (PG) as well as wall- and lipo-teichoic acids (Fig. 1.1, Fig. 1.2). As a three-dimensional lattice of about 50 nm thickness, the cell wall functions as the most important physical barrier, providing the cell with structural strength and protecting it from lysis due to the high turgor (2, 65). These properties and its specificity to bacteria also render the cell wall a prime target for antibiotics (61) (Fig. 1.3).

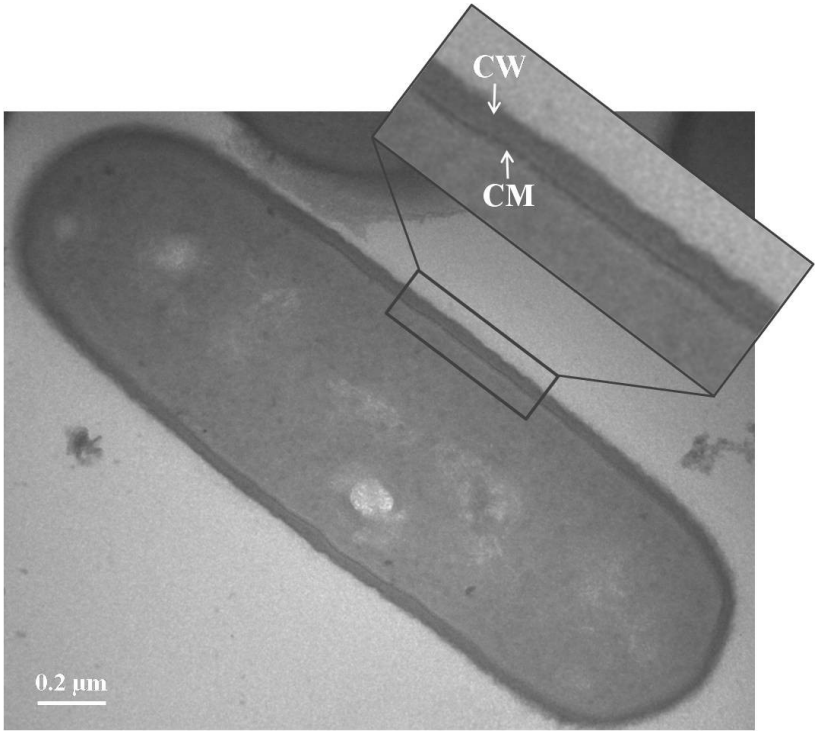

Figure 1.1. Electron micrograph of *Bacillus subtilis*.
The enlarged frame highlights the cytoplasmic membrane in dark gray (CM) and the cell wall in lighter gray (CW). Scale bar represents 0.2 µm.

The structural strength of the cell wall is a result of the high degree of polymerization of sugar chains with peptide bridges. In the Gram-positive model bacterium, *Bacillus subtilis*, this is mediated by high molecular weight penicillin binding proteins (HMW PBPs) (31, 40). These enzymes are bifunctional, acting as transglycosylases and transpeptidases, polymerizing the sugar and crosslinking the peptide moiety of lipid II to the growing PG (Fig. 1.2). The more peptide strands are crosslinked, the higher the mechanical strength and protection against osmotic lysis.

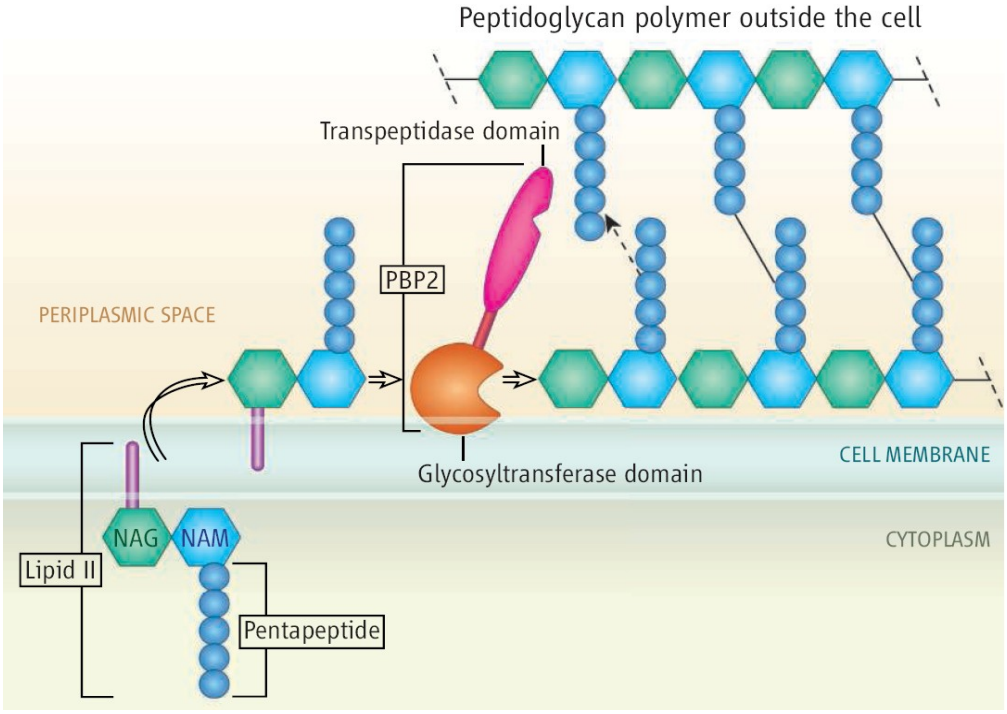

Figure 1.2. Peptidoglycan crosslinking by bi-functional penicillin binding proteins. Depicted are the final steps of peptidoglycan (PG) synthesis: lipid II is anchored in the membrane via undecaprenyl phosphate (63). After translocation to the outside of the membrane, it is built into the growing glycan chain by the glycosyltransferase activity, and crosslinked via the transpeptidase domain of penicillin binding proteins (PBP)s. NAG: N-acetyl glucosamine, NAM: N-acetyl muramic acid.

Summarized in Figure 1.3 are the different steps of PG synthesis in *B. subtilis*, with an emphasis on target sites of cell envelope active antibiotics. A central component during PG synthesis is lipid II. It consists of N-acetyl muramic acid (MurNAc) pentapeptide that is linked to N-acetyl glucosamine (GlcNAc) and anchored to the membrane by the released undecaprenylphosphate. During cell wall synthesis, lipid II is translocated to the outside of the membrane. After crosslinking by the action of transglycosylases and transpeptidases the undecaprenylphosphate moiety is recycled to the cytoplasmic side of the membrane (Fig. 1.3).

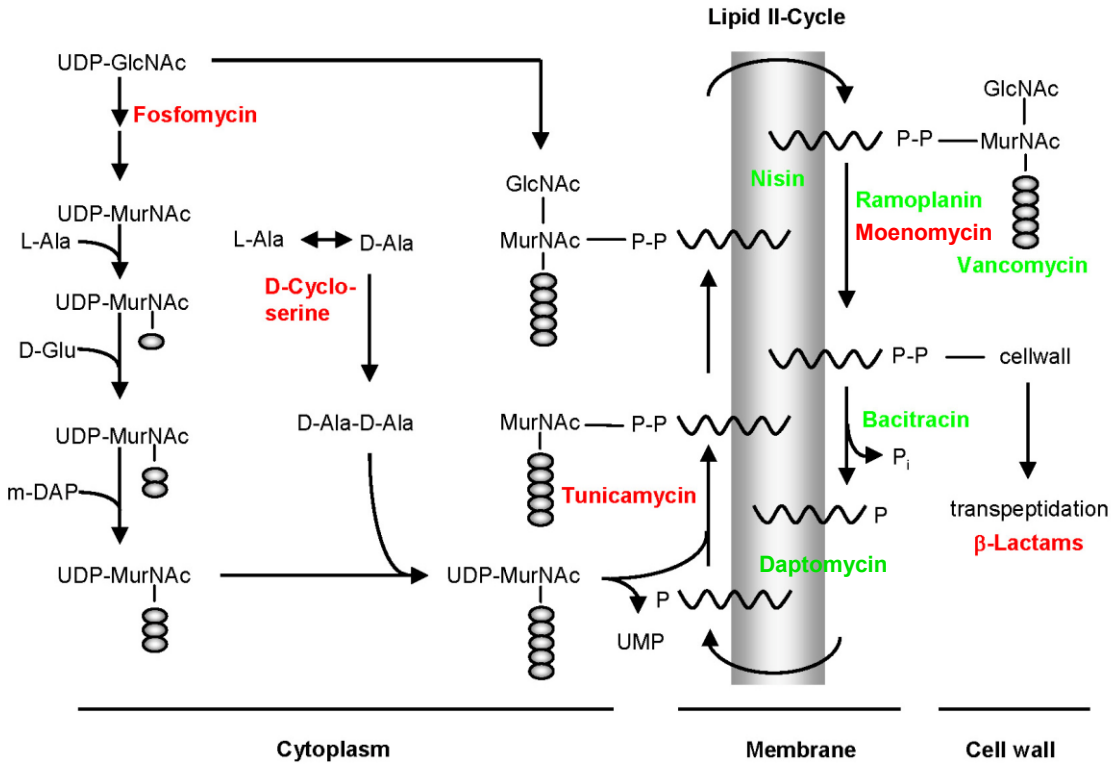

Figure 1.3. Peptidoglycan biosynthesis in *B. subtilis*.
Illustrated are key steps during cell wall synthesis together with antibiotics that target the membrane (daptomycin), peptidoglycan precursors (green), or cell wall synthesis enzymes (red). The curved line in the membrane depicts undecaprenyl phosphate, ovals: amino acids.
Adapted from (27)

In addition to PG, the Gram-positive cell wall contains teichoic acids (Fig. 1.4). As a polymer of polyol phosphates, they are responsible for the overall negative charge of the cell wall. This also allows them to chelate cations (in particular Mg^{2+}), and may create a pH gradient across the wall by sequestering protons that are expelled through the membrane (29). They serve as reservoirs of phosphates which can be mobilized under phosphate limiting conditions (19). Two types are present in Gram-positives; wall teichoic acids, which are linked to the cell wall, and lipoteichoic acids, which are anchored to the membrane and provide the main component of the hydrophobicity of the cell envelope (6). The charge of the cell wall can be regulated by the degree of D-alanylation, the coupling of D-alanine to the teichoic acids, which reduces the negative charge (7) (Fig. 1.4).

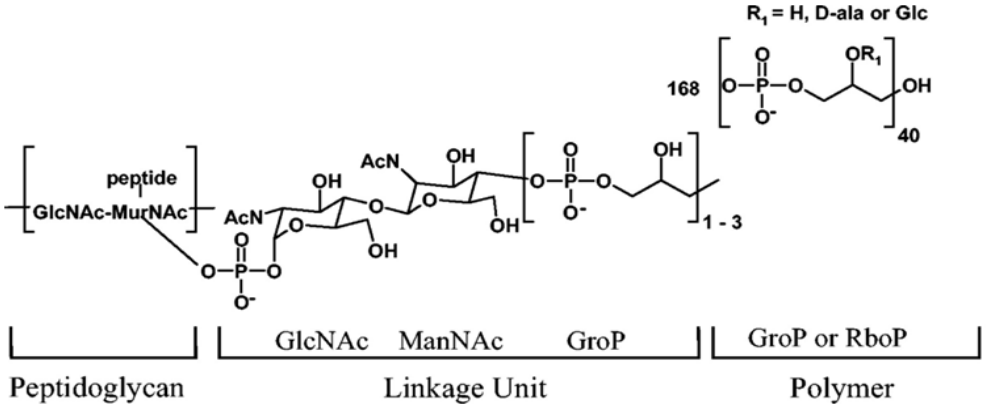

Figure 1.4. Structure of teichoic acids in *B. subtilis*.
Poly(glycerol phosphate) is covalently attached to peptidoglycan via disaccharide and one to three glycerol phosphate monomers. Hydroxyl groups on the main chain are often glucosylated or D-alanylated. GroP: glycerol phosphate; GlcNAc: *N*-acetylglucosamine; ManNAc: *N*-acetylmannosamine; Glc: glucose; MurNAc: *N*-acetylmuramic acid (5).

Wall teichoic acids are essential under certain condition. Attempts to delete genes that are involved in later teichoic acid synthesis steps have failed, indicating their essentiality. However, early synthesis genes are dispensable (Fig. 1.5) (16). It is believed that the toxicity of deleting late teichoic acid synthesis genes arises from accumulation of toxic intermediates or sequestration of essential metabolites (like undecaprenylphosphate), that are also used for PG synthesis (5, 11).

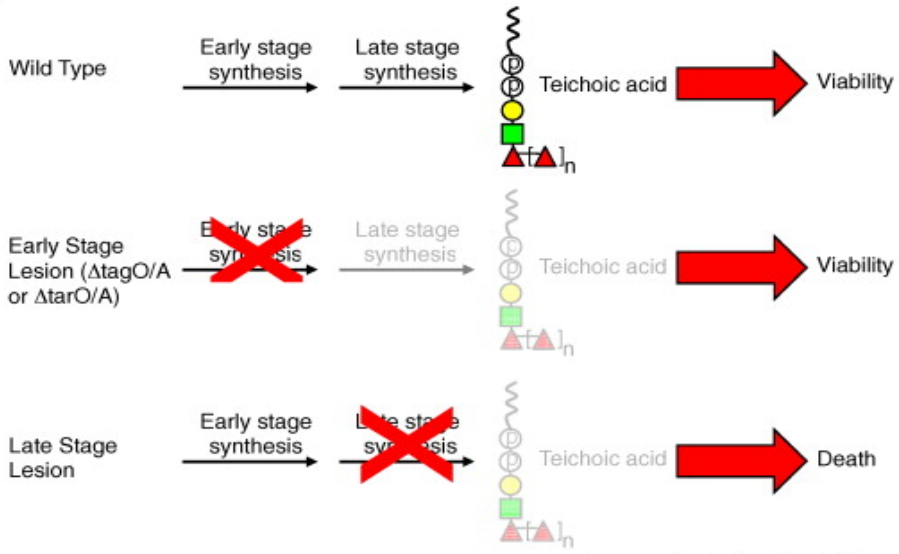

Figure 1.5. Essentiality of teichoic acids.
Teichoic acids are not required for viability in *B. subtilis* when early stages of the pathway are disrupted. Deletions in late stages of teichoic acid production are deleterious (16).

The *B. subtilis* membrane is composed of glycolipids and phospholipids (Fig. 1.6). Depending on the growth stage and culture medium used, the contents of the lipids vary. During logarithmic growth in rich media, the largest part is made up by the zwitterionic phosphatidylethanolamine (~50% PE), followed by glycolipids (~30% GL), and negatively charged phosphatidylglycerol (~16% PhG). Negatively charged cardiolipin (~0.8% CL) and positively charged lysyl-phosphatidylglycerol (~2.4%

LPG) are present to a smaller percentage (53).

Contrary to the fluid-mosaic model by Singer and Nicholson (50), lipids are now believed to aggregate in lipid domains (52). This was shown in the example of the negatively charged phosphatidylglycerol (PhG) in co-localization studies with the cell division inhibitor MinD (3). Strains that conditionally expressed *pgsA* (PhG synthase) were labeled with the membrane dye FM4-64, which preferentially stains negatively charged lipids. It was demonstrated that PhG localized in a spiral pattern along the long axis of the cell. Upon depletion of PgsA, the staining was delocalized, too. In addition, Barák *et al.* found MinD to co-localize with PhG using MinD-GFP (green fluorescent protein) in fluorescence resonance energy transfer studies (3). This further indicates a localization of the cell wall synthesis complex in regions of negatively charged lipids, supporting previous observations of a helical localization of PBPs (46).

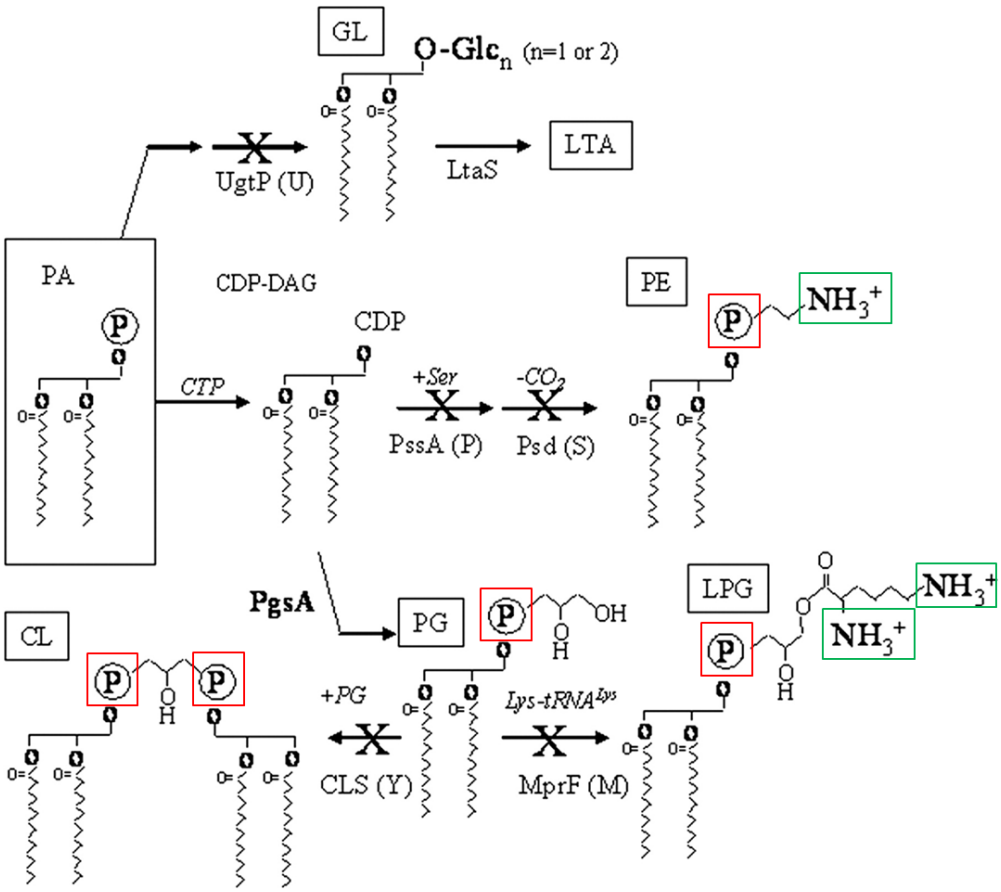

Figure 1.6. Membrane lipid biosynthesis in *B. subtilis*.
Phospholipids and glycolipids are derived from the precursor phosphatidic acid (PA). Positively or negatively charged moieties are shown in green or red, respectively. Phosphatidylethanolamine (PE), glycolipids (GL), phosphatidylglycerol (PG), cardiolipin (CL), lysyl-phosphatidylglycerol (LPG).
Adapted from (45)

1.2 Cell envelope stress response in *Bacillus subtilis*

Figure 1.7 illustrates the main cell envelope stress response (CESR) pathways in *B. subtilis*: two-component regulatory systems (TCS) and extracytoplasmic function (ECF) σ factors. TCS can sense perturbations to the cell envelope either through direct interaction with the histidine kinase (HK), or indirectly, for instance due to conformational changes. The HK is autophosphorylated and transfers the phosphate to its cognate response regulator (RR) (27). A well studied example is the LiaRS TCS (28). The LiaS HK is induced by a subset of antibiotics that target cell wall synthesis (e.g., vancomycin, bacitracin), and membrane active antibiotics (e.g., daptomycin) (Fig. 1.8). It then phosphorylates the RR, LiaR, which changes gene expression of a small regulon, including the phage shock protein A (PspA) family protein LiaH (20).

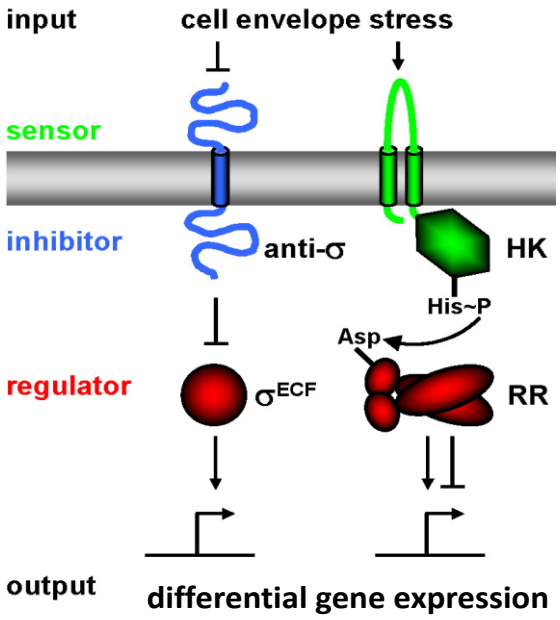

Figure 1.7. Cell envelope stress response systems in *B. subtilis*.
Extracytoplasmic Function σ factors (ECF) are shown left, two-component regulatory systems (TCS) right (HK = histidine kinase; RR = response regulator). Green: sensor protein, blue: inhibitory protein, red: transcriptional regulators; arrows signify activation, T-shaped lines: repression (27).

B. subtilis has seven known ECF σ factors, of which three are well studied; σ^M, σ^W, and σ^X (7, 8, 14, 23, 24). The analysis of σ^V, σ^Y, σ^Z, and YlaC, however, turned out to be rather complex, because precise inducing conditions, and therefore most regulon members, are not yet known (9, 33, 34, 44, 66). Generally, when inactive, ECF σ factors are sequestered by their respective anti-σ factor. Under certain stress conditions, the anti-σ releases the σ factor by degradation through proteolytical cleavage, or by conformational changes (Fig. 1.7) (64). Recruitment by the RNA polymerase core enzyme allow it to recognize a promoter region, where the domains 2 and 4 of the σ factor can bind to conserved -10 and -35 promoter sites and redirect gene expression of its regulon members (32).

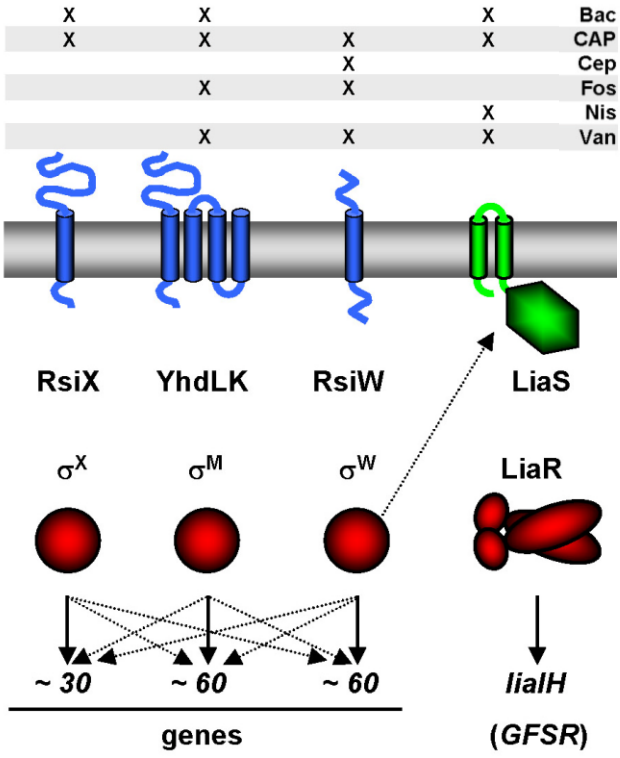

Figure 1.8. Induction of cell envelope stress response systems in *B. subtilis*.
Induction of ECF σ factors and the LiaRS TCS by Bac: bacitracin, CAP: cationic antimicrobial peptides, Cep: cephalosporin C, Fos: fosfomycin, Nis: nisin, Van: vancomycin. Color-coding: same as in Figure 1.7. Dotted arrows indicate cross-regulation/ regulatory overlap (27).

Figure 1.8 exemplifies antibiotics that can induce ECF σ factors in *B. subtilis*. Of note is a partial regulon overlap between different ECF σ factors, which is due to similarity between their promoter consensus sequences (33). Likewise, it can be seen that a particular stress or antibiotic can induce more than one σ factor (e.g., vancomycin, or bacitracin) (27).

1.3 Overview of cell envelope active antibiotics

Amongst the oldest classes of antibiotics are the β-lactams and glycopeptides. β-lactam antibiotics are comprised of penicillins, cephalosporins, and monobactams (Table 1.1). They owe their name to their central structural moiety, a β-lactam ring. The antimicrobial activity during cell wall synthesis is exerted by binding to transpeptidases as suicide inhibitors. Glycopeptides, like vancomycin, bind to the terminal, uncrosslinked D-Ala^4-D-Ala^5 residues of lipid II (Fig. 1.9).

Table 1.1. Cell envelope active antibiotics with their respective targets. Compounds are grouped by decade of introduction.

Decade	Compound (compound class)[1]	Bacterial target of action
1940s	Penicillins (beta-lactams)	Cell wall biosynthesis
	Nisin (peptide lantibiotic)	Cell wall/cell membrane
	Gramicidins (cationic cyclic peptides)	Cell membrane
	Polymyxins (cationic cyclic peptides)	Cell membrane
1950s	Vancomycin (glycopeptides)	Cell wall biosynthesis
1960s	Cephalosporin (beta-lactams)	Cell wall biosynthesis
	Moenomycin (glycolipid)	Cell wall biosynthesis
	Tunicamycin (nucleotide sugar analog)	Cell wall biosynthesis
1980s	Third generation cephalosporins	Cell wall biosynthesis
2000s	Carbapenemes (beta-lactams)	Cell wall biosynthesis
	Ramoplanin (lipoglycodepsipeptide)	Cell wall biosynthesis
	Daptomycin (cyclic lipopeptide)	Cell membrane
	Telavancin (lipoglycopeptide)	Cell wall/cell membrane

[1]See references for further detail (6, 36, 41, 47, 51, 59).

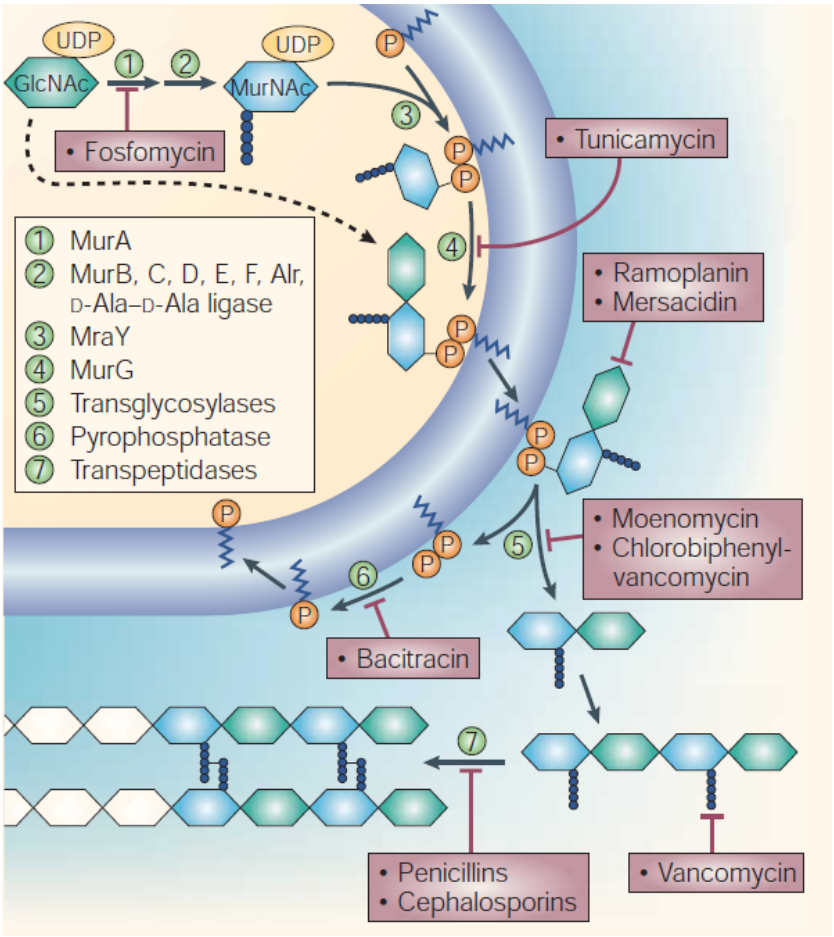

Figure 1.9. Targets of antibiotic action during cell wall synthesis.
Fosfomycin and tunicamycin target intracellular PG synthesis steps, which are catalyzed by MurA-MurG (steps 1-4). Ramoplanin and moenomycin inhibit the transglycosylation step. Bacitracin inhibits recycling of the lipid II carrier undecaprenyl phosphate. Vancomycin and β-lactams inhibit the transpeptidation reaction (61).

Here, a selection of antibiotics is discussed in more detail, with focus on cell envelope active antibiotics that are subject of the studies in subsequent chapters.

Daptomycin

Daptomycin is the first member of a new antibiotic class, the cyclic lipopeptides (Fig. 1.10). It was discovered in the early 1980's by Eli Lilly and Company as fermentation product of *Streptomyces roseosporus* (35). Initial clinical studies reported skeletal muscle toxicity as side-effect, and it was not until 2003, then marketed by Cubist Pharmaceuticals, that it was FDA approved to treat complicated skin and skin structure infections (22, 56). Additional applications include right-sided endocarditis and bacteraemia caused by Gram-positive pathogens (1).

A product of non-ribosomal peptide synthesis, daptomycin consists of 13 amino acids and a decanoyl side chain. Asp 3, Asp 7, Asp 9, MeGlu 12, and Orn 6 contribute to its overall charge of -3 (Fig. 1.10). Because of its negative net charge, the molecule needs to be administered with Ca^{2+}-ions to exert its full activity. It acts by disrupting the functional integrity of the membrane of Gram-positive bacteria. NMR and differential scanning calorimetry studies with liposomes have shown that daptomycin approaches the bacterial membrane in micelles. 14-16 molecules of daptomycin oligomerize in a 1:1 ratio with Ca^{2+} and orient their decanoyl side chains towards the center of the micelles (Fig. 1.11) (25, 48). The Ca^{2+}-ions function to buffer the negative charge of daptomycin, thereby allowing the complex to come closer to the cell envelope which is usually negatively charged because of teichoic acids in the cell wall and phospholipids in the membrane. Subsequently, daptomycin insert its decanoyl side chain into the membrane, which is followed by dissipation of the membrane potential and extrusion of K^{+}-ions. This, in turn, leads to arrest of DNA, RNA, and protein synthesis, and ultimately cell death, without cell lysis (Fig. 1.11) (49, 55).

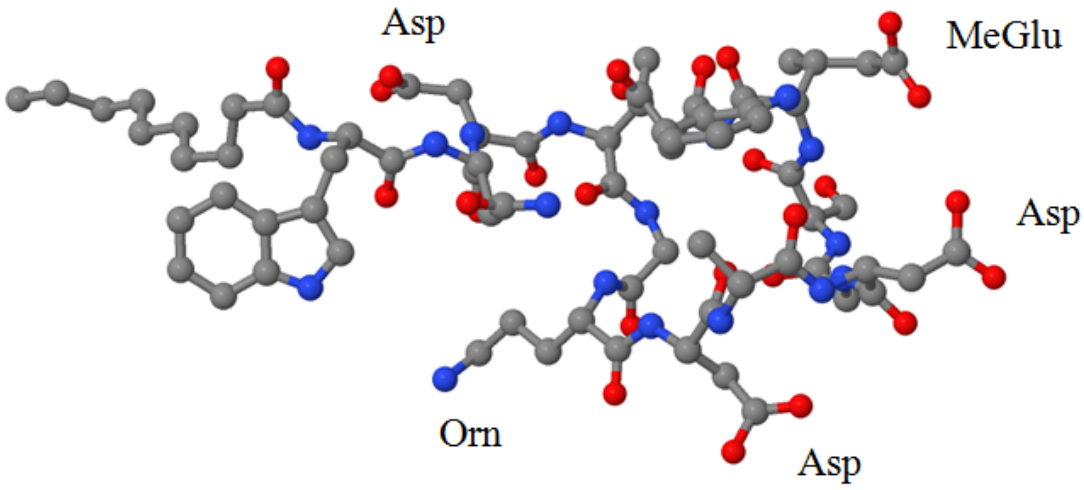

Figure 1.10. Structure of the cyclic lipopeptide daptomycin (PDB ID 1XT7).

Figure 1.11. Proposed mechanism of action of daptomycin.
14-16 molecules of daptomycin oligomerize into micelles with Ca^{2+} (yellow spheres) in a 1:1 molar ratio. In the proximity of the bacterial membrane daptomycin molecules dissociate and insert into the membrane, facilitated by Ca^{2+}. Modeled after (48).

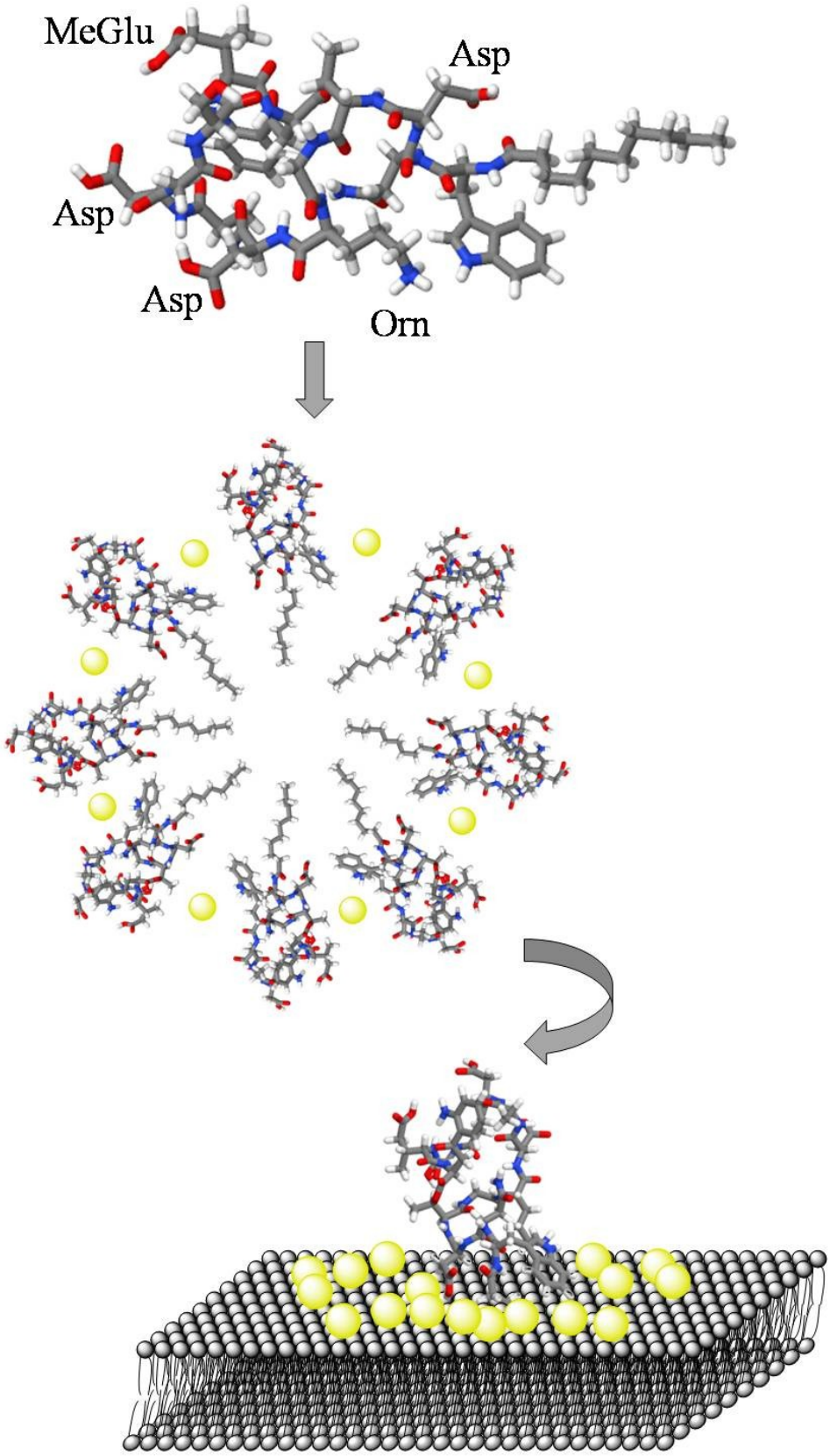
MeGlu
Asp
Asp
Asp
Orn

Moenomycin

Moenomycin is a phospho-glycolipid antibiotic produced by various strains of *Streptomyces*. It inhibits transglycosylases of Gram-positive bacteria by mimicking their substrate, lipid IV (lipid II with an additional disaccharide), during cell wall synthesis (Fig. 1.12). Also known as flavomycin or bambermycin, it is used as a growth promoter in animal feeding. It is not used in humans, however, because of poor absorption (39). In addition, it serves as a tool to study enzymes involved in cell wall synthesis (Fig. 1.13) (31). Structural analogs are currently being investigated by Walker *et al*. (38).

Besides its uses as a growth additive in animals, it was shown to decrease the frequency of transferable drug-resistance among Gram-negative pathogens and to reduce shedding of pathogenic bacteria, which is surprising, as it is mainly active against Gram-positive organisms. Furthermore, cross-resistance with other antibiotics and plasmid mediated resistance to moenomycin have not been described (39). The latter will be subject of our studies in Chapter 4.

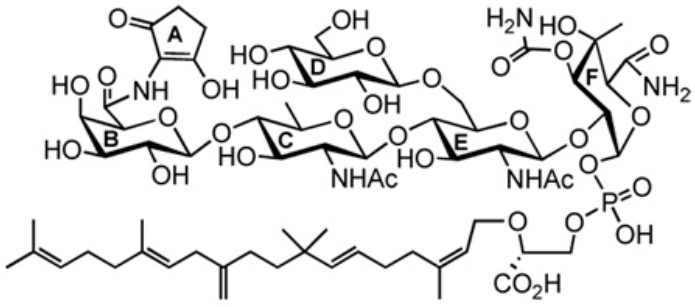

Moenomycin A (**1**)

Figure 1.12. Structure of the glycolipid moenomycin (57).

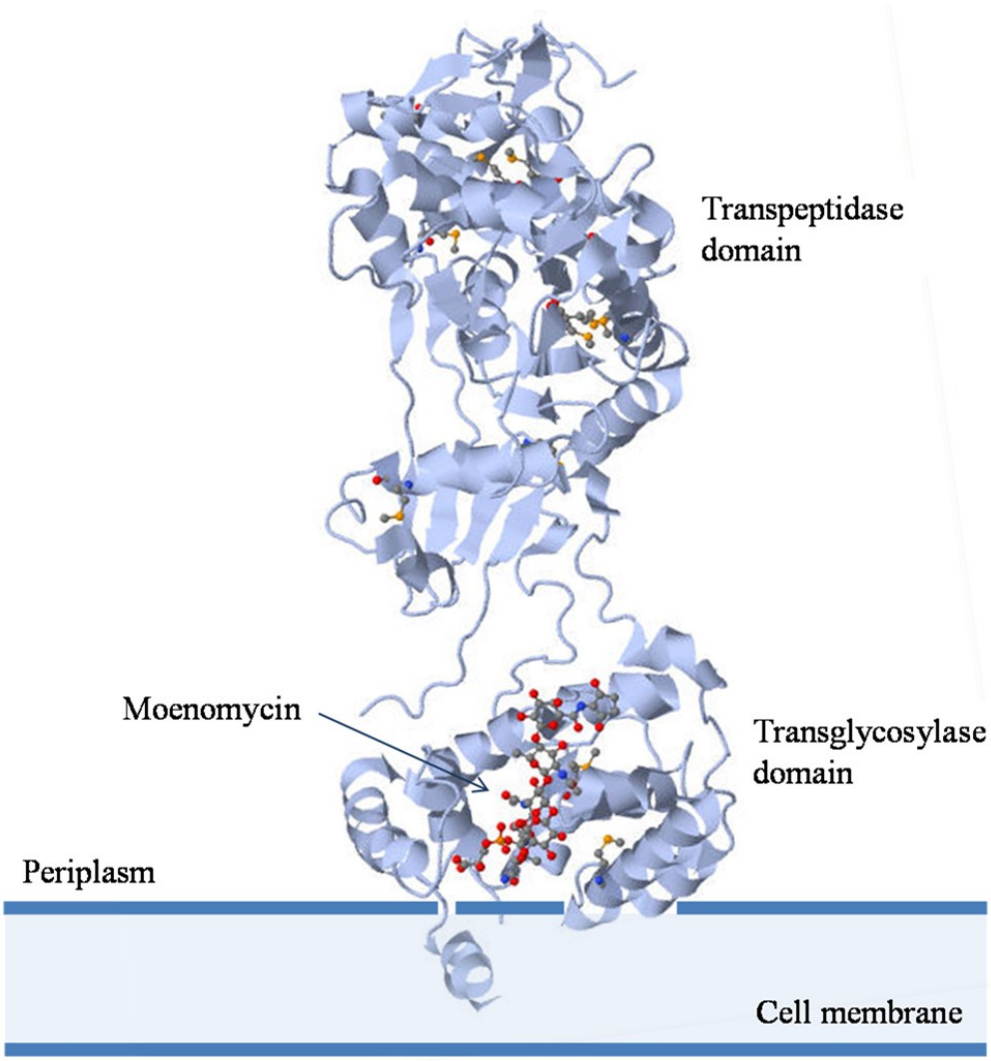

Figure 1.13. Moenomycin interaction with transglycosylase.
Crystal structure of moenomycin with the bi-functional PBP2 of *S. aureus* (PDB ID 2OLV, 2.80 Å, X-Ray diffraction).

Ramoplanin

The lipoglycodepsipeptide ramoplanin was discovered in the 1980s as part of an industrial drug discovery program targeted to find cell wall synthesis inhibitors. It is produced by non-ribosomal peptide synthesis in *Actinomycetes* spp., which indicates that it contains unusual amino acids. Here, seven out of 17 amino acids are in the D-form (see Chapter 5, Fig. 5.1) (6). The positively charged molecule is active against Gram-positive organisms, where it inhibits the transglycosylase reaction during PG synthesis by binding to lipid II, and probably also to the reducing ends of the growing glycan chain (17). Initial assumptions that it inhibits MurG by binding to lipid I were revised, because it is unlikely that ramoplanin, large and highly water soluble, can diffuse easily through membranes (42). It was shown that the ramoplanin aglycon binds lipid II preferentially over lipid I by a factor of five. Both form complexes that self-assemble into fibrils, which is a reason for its hydrolytic instability, making it not suitable for systemic administration (17). Regarding its clinical application, ramoplanin is in late stages of clinical trials for treatment of *Clostridium difficile* infections and prevention of enterococcal infections (Oscient Pharmaceuticals Corporation, Waltham, MA).

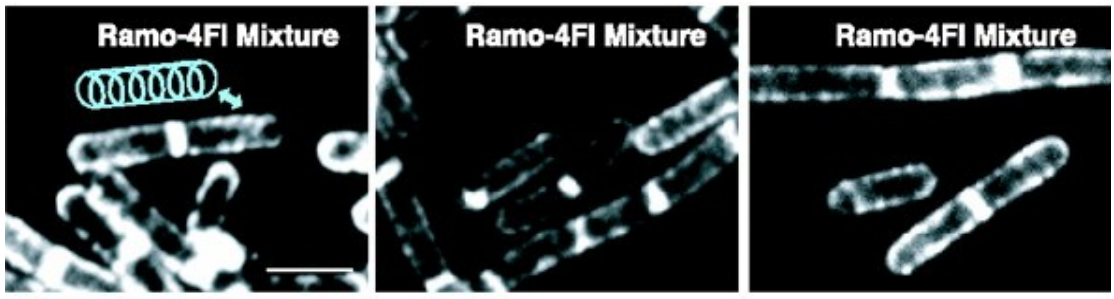

Figure 1.14. Imaging of peptidoglycan synthesis with fluorescent ramoplanin.
The micrographs depict a BodipyFl-labeled ramoplanin derivative. The fluorescent dye visualizes the helical pattern of active cell wall synthesis sites (58).

Hamburger *et al.* illustrate ramoplanin as a dimer in a 1.4 Å resolution crystal structure by use of detergents to mimic membrane properties (Fig. 1.15) (21). The two monomers are predicted to assemble as half-disks where residues 9–15 of each monomer interact in an antiparallel manner with six backbone-backbone hydrogen bonds. This structure also confirms previous assumptions that the hydrophobic polyprenyl chain inserts into the membrane, leaving the polar disaccharide in the aqueous region, and allowing the lipid II headgroup to interact with the hydrophilic face of the dimer (21).

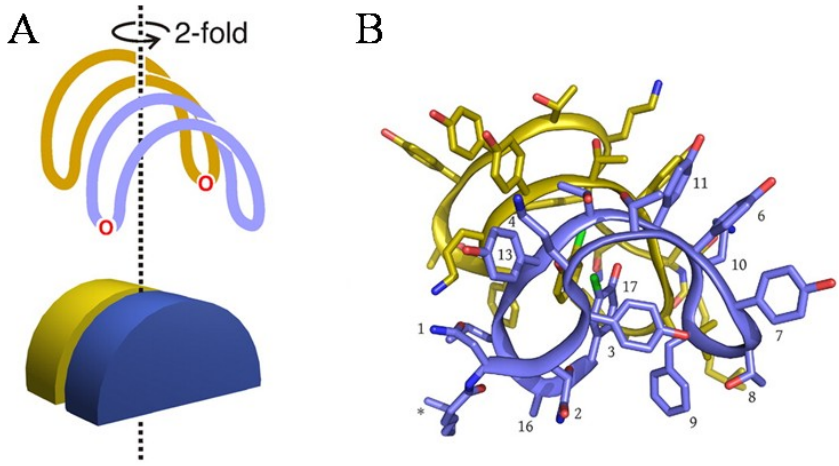

Figure 1.15. Structure of the ramoplanin dimer.
(A) shows a schematic view of the dimer, with one monomer blue and the other yellow. (B) depicts the structure of the dimer, with the peptide backbone and selected side chains of the blue monomer labeled. An asterisk marks the fatty acid moiety (21).

1.4 Mechanisms of antibiotic resistance

Because of its specificity to bacteria, the cell wall is a prime target for antibiotics. To date, at least 17 classes of antibiotics have been successfully produced or isolated (Table 1.1), but to each class, bacteria have developed resistance (47). This selective pressure within bacteria not only originates from the widespread use of antibiotics (in fact, 50% of current antibiotics are being used in agriculture and aquaculture (12)), it is also inherent in the natural environment of many prokaryotes (Fig. 1.16). Due to permanent competition for nutrients, many soil inhabiting bacteria have evolved to become prodigious antibiotic producers (26, 47).

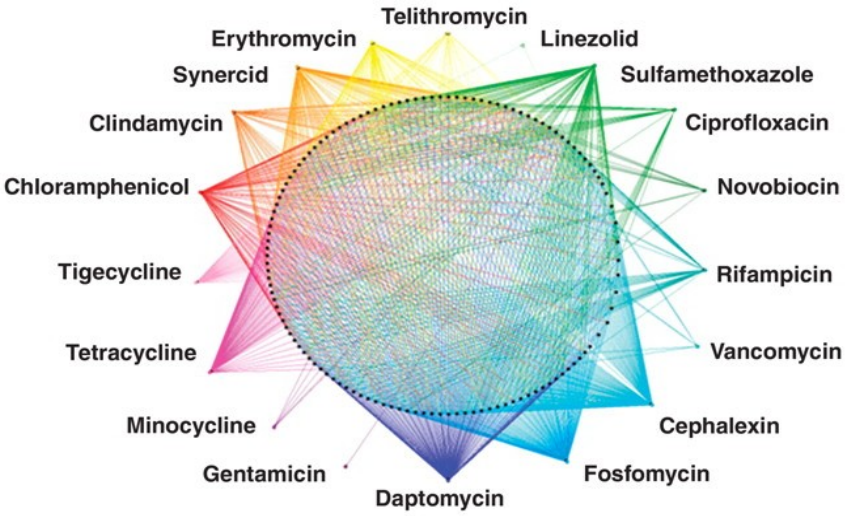

Figure 1.16. Antibiotic resistance profile of soil inhabiting bacteria.
The diagram demonstrates the density and diversity of resistance profiles of 480 bacterial isolates. Each of the 191 black dots corresponds to a different resistance profile, with each line symbolizing resistance to the antibiotic it points to (10).

Of note is the high prevalence of resistance to daptomycin in these isolates (Fig. 1.17). However, this is most likely due to the fact that many strains isolated from soil are *Streptomyces* spp., and daptomycin is produced by *S. roseosporus*. Producing strains have naturally evolved resistance mechanisms to their antibiotics.

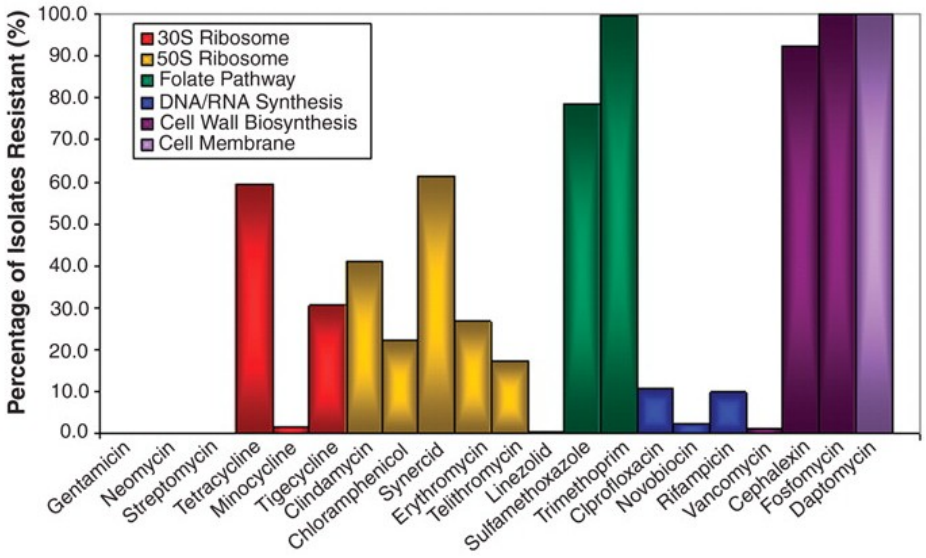

Figure 1.17. Resistance levels against tested antibiotics.
Soil isolates were each screened with 20 µg/ml antibiotic. Reproducible growth was defined as resistance (10).

Resistance also increased in clinical isolates. Fig. 1.18 shows increase of methicillin resistant *Staphylococcus aureus* (MRSA) in countries with extensive reporting (more than 250 *S. aureus* bacteraemias in at least three out of four years) (30). At the same time, the number of new antimicrobial drugs approved by the FDA between 1983 and 2007 decreased (18).

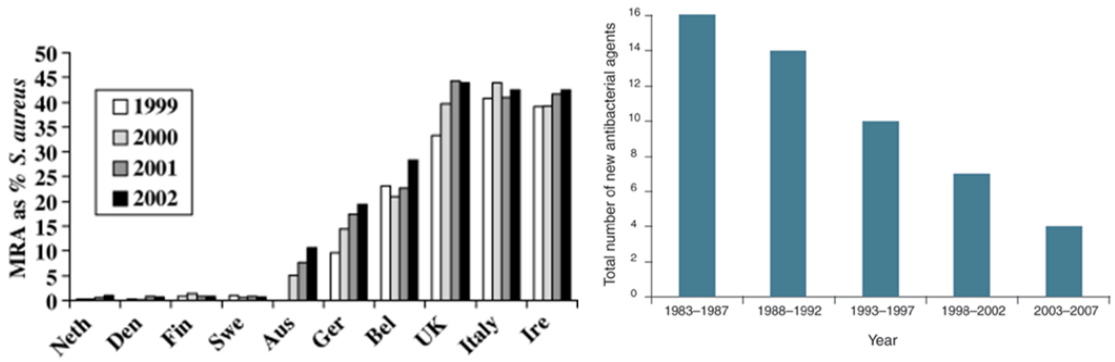

Figure 1.18. Increase of antibiotic resistance versus decrease of new antibiotics.
The percentage of *S. aureus* bacteraemias that are caused by MRSA increased despite the availability of anti-MRSA agents (30). The numbers of new, FDA approved antibiotics declined in the past 40 years(18).

Mechanisms of antibiotic resistance can generally be grouped into three categories. First, the antibiotic can be transported away from its site of action by pumps (e.g., ATP-binding cassette (ABC) transporters). Second, modification of the target can make it unreachable or unrecognizable for the antibiotic. Third, destruction or modification of the antibiotic can render the antibiotic ineffective (6, 60).

Figure 1.19 serves as example for the first group. Bacitracin is a peptide antibiotic that prevents dephosphorylation of undecaprenyl pyrophosphate (UPP). This inhibits essential UPP recycling, and therefore also cell wall synthesis (54).

When the BceRS two-component system (TCS) senses low concentrations of bacitracin, it increases expression of *bceAB*. BceAB is an ATP transporter that was shown to confer resistance to bacitracin (43). Whether it does so by exporting or importing the drug is still controversial (4, 13, 37). Importing would pump the antibiotic away from its site of action, if, in fact, bacitracin acts extracellularly.

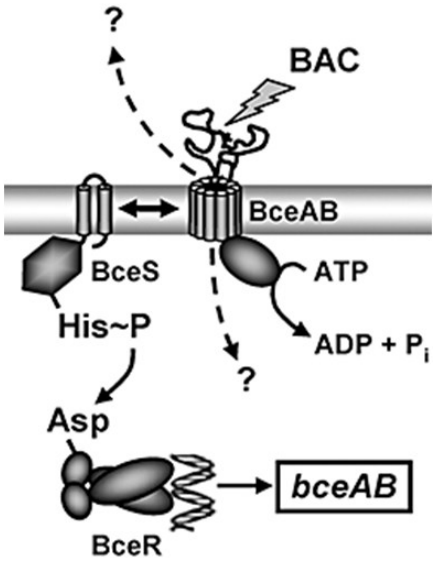

Figure 1.19. Part of the bacitracin stress response in *B. subtilis*.
The BceRS TCS regulates expression of the BceAB transporter which confers resistance to bacitracin (43). Solid lines: signal transduction, striped lines: bacitracin transport, box: genes encoding known bacitracin resistance determinants.

An example for target modification is displayed in Figure 1.20. Vancomycin resistance in enterococci can be achieved by target alteration, from the amide linkage in UDP-MurNAc(pep)3-D-Ala-D-Ala to the ester linkage in UDP-MurNAc(pep)3-D-Ala-D-Lac. This leads to a 1,000-fold drop in drug-binding affinity. The switch to D-Ala-D-Lac is regulated by the *vanA* operon. VanX, a D,D-dipeptidase, cleaves the terminal D-Ala. The dehydrogenase VanH converts pyruvate to lactate, which is ligated to D-Ala by VanA. Cell wall synthesis is not affected, as the terminal amino acid is cleaved during the transpeptidation step (60, 62).

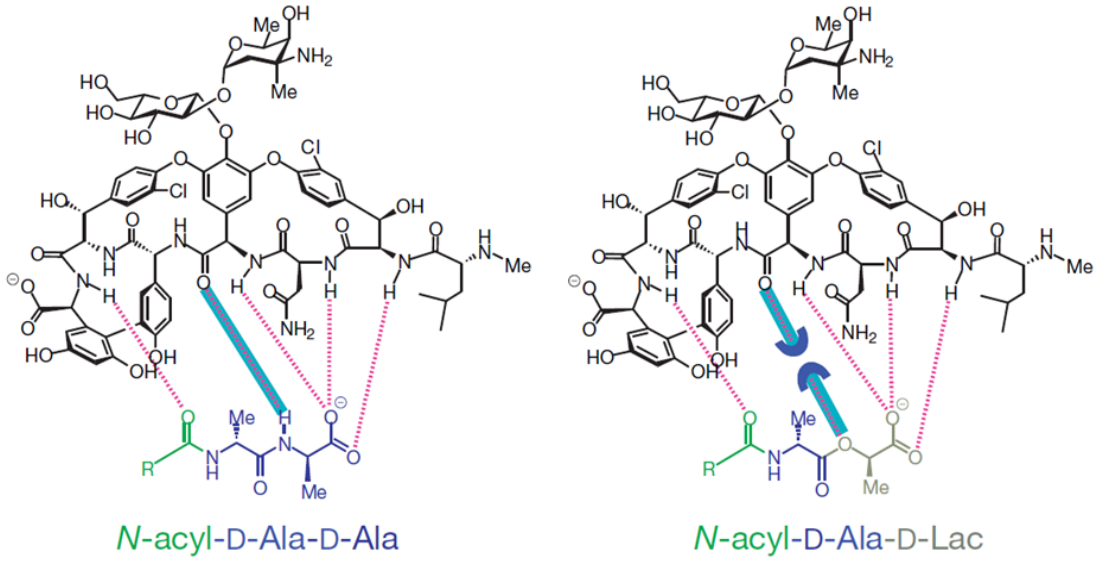

Figure 1.20. Mechanism of vancomycin resistance in enterococci.
Hydrogen bond formation between vancomycin and two D-alanine residues from lipid II (left) or D-alanine-D-lactate (right) (60).

The third group, destruction of an antibiotic, is exemplified by the action of β-lactamases (Fig. 1.21). Here, the β-lactam antibiotic penicillin is inactivated by the action of β-lactamases (also called penicillinases) in the periplasmic space of Gram-negative bacteria. Ring opening leads to penicilloic acid which can not bind to its target, the penicillin binding proteins (60).

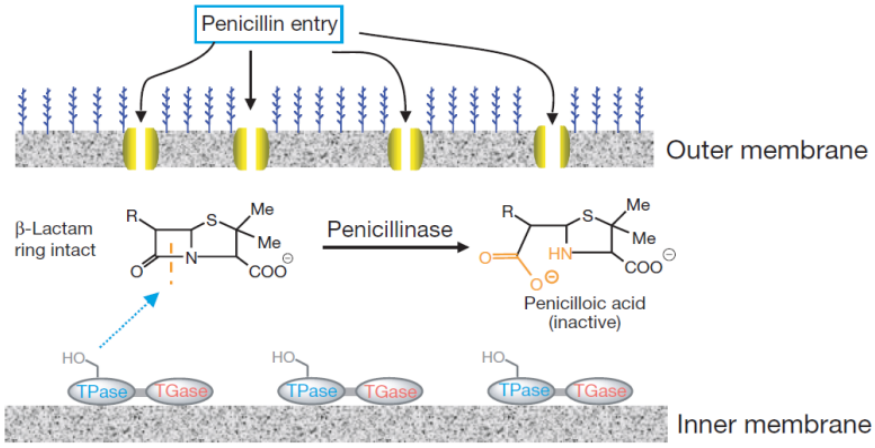

Figure 1.21. Inactivation of β-lactams by β-lactamase (penicillinase) (60).

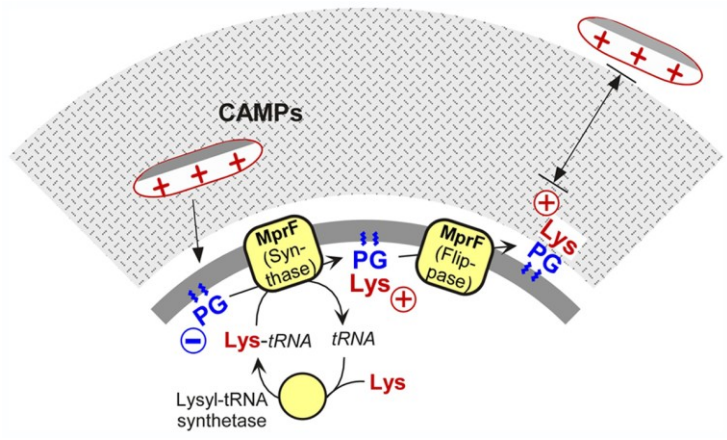

Figure 1.22. MprF mediated resistance to cationic antimicrobial peptides.
Transfer of lysine to phosphatidylglycerol decreases the negative charge of the membrane, and thereby leads to repulsion of positively charged peptides that target the cell membrane (15).

Last, but not least, resistance to antibiotics can also be obtained by indirect measures. Figure 1.22 shows how a change of the net charge of the bacterial membrane can affect the insertion ability of cationic antimicrobial peptides (CAMPs). The conversion of negatively charged phosphatidylglycerol to the positively charged lysyl-phosphatidylglycerol via Lys-tRNA, catalyzed by MprF, leads to a more neutralized membrane charge, which results in increased repulsion towards CAMPs (15).

REFERENCES

1. **Arbeit, R. D., D. Maki, F. P. Tally, E. Campanaro, and B. I. Eisenstein.** 2004. The safety and efficacy of daptomycin for the treatment of complicated skin and skin-structure infections. Clin Infect Dis **38:**1673-81.

2. **Archibald, A. R., I. C. Hancock, and C. R. Harwood.** 1993. Cell wall structure, synthesis, and turnover. ASM Press, Washington, DC.

3. **Barák, I., K. Muchova, A. J. Wilkinson, P. J. O'Toole, and N. Pavlendova.** 2008. Lipid spirals in Bacillus subtilis and their role in cell division. Mol Microbiol **68:**1315-27.

4. **Bernard, R., A. Guiseppi, M. Chippaux, M. Foglino, and F. Denizot.** 2007. Resistance to bacitracin in Bacillus subtilis: unexpected requirement of the BceAB ABC transporter in the control of expression of its own structural genes. J Bacteriol **189:**8636-42.

5. **Bhavsar, A. P., L. K. Erdman, J. W. Schertzer, and E. D. Brown.** 2004. Teichoic acid is an essential polymer in Bacillus subtilis that is functionally distinct from teichuronic acid. J Bacteriol **186:**7865-73.

6. **Breukink, E., and B. de Kruijff.** 2006. Lipid II as a target for antibiotics. Nat Rev Drug Discov **5:**321-32.

7. **Cao, M., and J. D. Helmann.** 2004. The Bacillus subtilis extracytoplasmic-function sigmaX factor regulates modification of the cell envelope and resistance to cationic antimicrobial peptides. J Bacteriol **186:**1136-46.

8. **Cao, M., P. A. Kobel, M. M. Morshedi, M. F. Wu, C. Paddon, and J. D. Helmann.** 2002. Defining the Bacillus subtilis sigma(W) regulon: a comparative analysis of promoter consensus search, run-off transcription/macroarray analysis (ROMA), and transcriptional profiling approaches. J Mol Biol **316:**443-57.

9. **Cao, M., L. Salzberg, C. S. Tsai, T. Mascher, C. Bonilla, T. Wang, R. W. Ye, L. Marquez-Magana, and J. D. Helmann.** 2003. Regulation of the Bacillus subtilis extracytoplasmic function protein sigma(Y) and its target promoters. J Bacteriol **185:**4883-90.

10. **D'Costa, V. M., K. M. McGrann, D. W. Hughes, and G. D. Wright.** 2006. Sampling the antibiotic resistome. Science **311:**374-7.

11. **D'Elia, M. A., K. E. Millar, T. J. Beveridge, and E. D. Brown.** 2006. Wall teichoic acid polymers are dispensable for cell viability in Bacillus subtilis. J

Bacteriol **188:**8313-6.

12. **Davies, J.** 2008. Resistance redux. Infectious diseases, antibiotic resistance and the future of mankind. EMBO Rep **9 Suppl 1:**S18-21.

13. **Dawson, R. J., K. Hollenstein, and K. P. Locher.** 2007. Uptake or extrusion: crystal structures of full ABC transporters suggest a common mechanism. Mol Microbiol **65:**250-7.

14. **Eiamphungporn, W., and J. D. Helmann.** 2008. The Bacillus subtilis sigma(M) regulon and its contribution to cell envelope stress responses. Mol Microbiol **67:**830-48.

15. **Ernst, C. M., P. Staubitz, N. N. Mishra, S. J. Yang, G. Hornig, H. Kalbacher, A. S. Bayer, D. Kraus, and A. Peschel.** 2009. The bacterial defensin resistance protein MprF consists of separable domains for lipid lysinylation and antimicrobial peptide repulsion. PLoS Pathog **5:**e1000660.

16. **Falconer, S. B., and E. D. Brown.** 2009. New screens and targets in antibacterial drug discovery. Curr Opin Microbiol **12:**497-504.

17. **Fang, X., K. Tiyanont, Y. Zhang, J. Wanner, D. Boger, and S. Walker.** 2006. The mechanism of action of ramoplanin and enduracidin. Mol Biosyst **2:**69-76.

18. **Fox, J. L.** 2006. The business of developing antibacterials. Nat Biotechnol **24:**1521-8.

19. **Grant, W. D.** 1979. Cell wall teichoic acid as a reserve phosphate source in Bacillus subtilis. J Bacteriol **137:**35-43.

20. **Hachmann, A. B., E. R. Angert, and J. D. Helmann.** 2009. Genetic analysis of factors affecting susceptibility of Bacillus subtilis to daptomycin. Antimicrob Agents Chemother **53:**1598-609.

21. **Hamburger, J. B., A. J. Hoertz, A. Lee, R. J. Senturia, D. G. McCafferty, and P. J. Loll.** 2009. A crystal structure of a dimer of the antibiotic ramoplanin illustrates membrane positioning and a potential Lipid II docking interface. Proc Natl Acad Sci U S A **106:**13759-64.

22. **Hawkey, P. M.** 2008. Pre-clinical experience with daptomycin. J Antimicrob Chemother **62 Suppl 3:**iii7-14.

23. **Helmann, J. D.** 2006. Deciphering a complex genetic regulatory network: the Bacillus subtilis sigmaW protein and intrinsic resistance to antimicrobial compounds. Sci Prog **89:**243-66.

24. **Helmann, J. D.** 2002. The extracytoplasmic function (ECF) sigma factors.

Adv Microb Physiol **46:**47-110.

25. **Ho, S. W., D. Jung, J. R. Calhoun, J. D. Lear, M. Okon, W. R. Scott, R. E. Hancock, and S. K. Straus.** 2007. Effect of divalent cations on the structure of the antibiotic daptomycin. Eur Biophys J **37:**421-433.

26. **Hopwood, D. A.** 2007. How do antibiotic-producing bacteria ensure their self-resistance before antibiotic biosynthesis incapacitates them? Mol Microbiol **63:**937-40.

27. **Jordan, S., M. I. Hutchings, and T. Mascher.** 2008. Cell envelope stress response in Gram-positive bacteria. FEMS Microbiol Rev **32:**107-46.

28. **Jordan, S., A. Junker, J. D. Helmann, and T. Mascher.** 2006. Regulation of LiaRS-dependent gene expression in bacillus subtilis: identification of inhibitor proteins, regulator binding sites, and target genes of a conserved cell envelope stress-sensing two-component system. J Bacteriol **188:**5153-66.

29. **Kemper, M. A., M. M. Urrutia, T. J. Beveridge, A. L. Koch, and R. J. Doyle.** 1993. Proton motive force may regulate cell wall-associated enzymes of Bacillus subtilis. J Bacteriol **175:**5690-6.

30. **Livermore, D. M.** 2004. The need for new antibiotics. Clin Microbiol Infect **10 Suppl 4:**1-9.

31. **Lovering, A. L., L. H. de Castro, D. Lim, and N. C. Strynadka.** 2007. Structural insight into the transglycosylation step of bacterial cell-wall biosynthesis. Science **315:**1402-5.

32. **Maetschke, S., M. Towsey, and J. Hogan.** 2006. Bacterial Promoter Modeling and Prediction for E. Coli and B. Subtilis with Beagle. *In* M. Bodén and T. L. Bailey (ed.), Workshop on Intelligent Systems for Bioinformatics (WISB 2006). CRPIT, 73, Hobart, Australia.

33. **Mascher, T., A. B. Hachmann, and J. D. Helmann.** 2007. Regulatory overlap and functional redundancy among Bacillus subtilis extracytoplasmic function sigma factors. J Bacteriol **189:**6919-27.

34. **Matsumoto, T., K. Nakanishi, K. Asai, and Y. Sadaie.** 2005. Transcriptional analysis of the ylaABCD operon of Bacillus subtilis encoding a sigma factor of extracytoplasmic function family. Genes Genet Syst **80:**385-93.

35. **McHenney, M. A., T. J. Hosted, B. S. Dehoff, P. R. Rosteck, Jr., and R. H. Baltz.** 1998. Molecular cloning and physical mapping of the daptomycin gene cluster from Streptomyces roseosporus. J Bacteriol **180:**143-51.

36. **Mogi, T., and K. Kita.** 2009. Gramicidin S and polymyxins: the revival of cationic cyclic peptide antibiotics. Cell Mol Life Sci **66:**3821-6.

37. **Ohki, R., Giyanto, K. Tateno, W. Masuyama, S. Moriya, K. Kobayashi, and N. Ogasawara.** 2003. The BceRS two-component regulatory system induces expression of the bacitracin transporter, BceAB, in Bacillus subtilis. Mol Microbiol **49:**1135-44.

38. **Ostash, B., E. H. Doud, C. Lin, I. Ostash, D. L. Perlstein, S. Fuse, M. Wolpert, D. Kahne, and S. Walker.** 2009. Complete characterization of the seventeen step moenomycin biosynthetic pathway. Biochemistry **48:**8830-41.

39. **Pfaller, M. A.** 2006. Flavophospholipol use in animals: positive implications for antimicrobial resistance based on its microbiologic properties. Diagn Microbiol Infect Dis **56:**115-21.

40. **Popham, D. L., and P. Setlow.** 1995. Cloning, nucleotide sequence, and mutagenesis of the Bacillus subtilis ponA operon, which codes for penicillin-binding protein (PBP) 1 and a PBP-related factor. J Bacteriol **177:**326-35.

41. **Price, N. P., and B. Tsvetanova.** 2007. Biosynthesis of the tunicamycins: a review. J Antibiot (Tokyo) **60:**485-91.

42. **Reynolds, P. E., and E. A. Somner.** 1990. Comparison of the target sites and mechanisms of action of glycopeptide and lipoglycodepsipeptide antibiotics. Drugs Exp Clin Res **16:**385-9.

43. **Rietkotter, E., D. Hoyer, and T. Mascher.** 2008. Bacitracin sensing in Bacillus subtilis. Mol Microbiol **68:**768-85.

44. **Ryu, H. B., I. Shin, H. S. Yim, and S. O. Kang.** 2006. YlaC is an extracytoplasmic function (ECF) sigma factor contributing to hydrogen peroxide resistance in Bacillus subtilis. J Microbiol **44:**206-16.

45. **Salzberg, L. I., and J. D. Helmann.** 2008. Phenotypic and transcriptomic characterization of Bacillus subtilis mutants with grossly altered membrane composition. J Bacteriol **190:**7797-807.

46. **Scheffers, D. J., L. J. Jones, and J. Errington.** 2004. Several distinct localization patterns for penicillin-binding proteins in Bacillus subtilis. Mol Microbiol **51:**749-64.

47. **Schmidt, F. R.** 2004. The challenge of multidrug resistance: actual strategies in the development of novel antibacterials. Appl Microbiol Biotechnol **63:**335-43.

48. **Scott, W. R., S. B. Baek, D. Jung, R. E. Hancock, and S. K. Straus.** 2007. NMR structural studies of the antibiotic lipopeptide daptomycin in DHPC micelles. Biochim Biophys Acta **1768:**3116-3126.

49. **Silverman, J. A., N. G. Perlmutter, and H. M. Shapiro.** 2003. Correlation of

daptomycin bactericidal activity and membrane depolarization in Staphylococcus aureus. Antimicrob Agents Chemother **47:**2538-44.

50. **Singer, S. J., and G. L. Nicolson.** 1972. The fluid mosaic model of the structure of cell membranes. Science **175:**720-31.

51. **Smith, W. J., and R. H. Drew.** 2009. Telavancin: a new lipoglycopeptide for gram-positive infections. Drugs Today (Barc) **45:**159-73.

52. **Somerharju, P., J. A. Virtanen, and K. H. Cheng.** 1999. Lateral organisation of membrane lipids. The superlattice view. Biochim Biophys Acta **1440:**32-48.

53. **Sonenshein, A. L., J. A. Hoch, and R. Losick (ed.).** 2002. Bacillus Subtilis and its closest relatives: from genes to cells. ASM Press, Washington, DC.

54. **Storm, D. R., and J. L. Strominger.** 1973. Complex formation between bacitracin peptides and isoprenyl pyrophosphates. The specificity of lipid-peptide interactions. J Biol Chem **248:**3940-5.

55. **Straus, S. K., and R. E. Hancock.** 2006. Mode of action of the new antibiotic for Gram-positive pathogens daptomycin: comparison with cationic antimicrobial peptides and lipopeptides. Biochim Biophys Acta **1758:**1215-23.

56. **Tally, F. P., M. Zeckel, M. M. Wasilewski, C. Carini, C. L. Berman, G. L. Drusano, and F. B. Oleson, Jr.** 1999. Daptomycin: a novel agent for Gram-positive infections. Expert Opin Investig Drugs **8:**1223-38.

57. **Taylor, J. G., X. Li, M. Oberthur, W. Zhu, and D. E. Kahne.** 2006. The total synthesis of moenomycin A. J Am Chem Soc **128:**15084-5.

58. **Tiyanont, K., T. Doan, M. B. Lazarus, X. Fang, D. Z. Rudner, and S. Walker.** 2006. Imaging peptidoglycan biosynthesis in Bacillus subtilis with fluorescent antibiotics. Proc Natl Acad Sci U S A **103:**11033-8.

59. **Wallhausser, K. H., G. Nesemann, P. Prave, and A. Steigler.** 1965. Moenomycin, a new antibiotic. I. Fermentation and isolation. Antimicrob Agents Chemother (Bethesda) **5:**734-6.

60. **Walsh, C.** 2000. Molecular mechanisms that confer antibacterial drug resistance. Nature **406:**775-81.

61. **Walsh, C.** 2003. Where will new antibiotics come from? Nat Rev Microbiol **1:**65-70.

62. **Walsh, F. M., and S. G. Amyes.** 2004. Microbiology and drug resistance mechanisms of fully resistant pathogens. Curr Opin Microbiol **7:**439-44.

63. **Wright, G. D.** 2007. Biochemistry. A new target for antibiotic development.

Science **315:**1373-4.

64. **Yoshimura, M., K. Asai, Y. Sadaie, and H. Yoshikawa.** 2004. Interaction of Bacillus subtilis extracytoplasmic function (ECF) sigma factors with the N-terminal regions of their potential anti-sigma factors. Microbiology **150:**591-9.

65. **Young, K. D.** 2003. Bacterial shape. Mol Microbiol **49:**571-80.

66. **Zellmeier, S., C. Hofmann, S. Thomas, T. Wiegert, and W. Schumann.** 2005. Identification of sigma(V)-dependent genes of Bacillus subtilis. FEMS Microbiol Lett **253:**221-9.

CHAPTER 2

GENETIC ANALYSIS OF FACTORS AFFECTING SUSCEPTIBILITY OF *BACILLUS SUBTILIS* TO DAPTOMYCIN

Daptomycin is the first of a new class of cyclic lipopeptide antibiotics used against multidrug-resistant Gram-positive pathogens. The proposed mechanism of action involves disruption of the functional integrity of the bacterial membrane in a Ca^{2+}-dependent manner. We have used transcriptional profiling to demonstrate that treatment of *Bacillus subtilis* with daptomycin strongly induces the *lia* operon including the autoregulatory LiaRS two-component system (homologous to *Staphylococcus aureus* VraSR). The *lia* operon protects against daptomycin and deletion of *liaH*, encoding a phage shock protein A (PspA)-like protein, leads to 3-fold increased susceptibility. Since daptomycin interacts with the membrane, we tested mutants with altered membrane composition for effects on susceptibility. Deletion mutations of *mprF* (lacking lysyl-phosphatidylglycerol) or *des* (lipid desaturase) increased daptomycin susceptibility, whereas overexpression of MprF decreased susceptibility. Conversely, depletion of the cell for the anionic lipid phosphatidylglycerol led to increased resistance. Fluorescently-labeled daptomycin localized to the septa and in a helical pattern around the cell envelope and was delocalized upon depletion of phosphatidylglycerol. Together, these results indicate that the daptomycin-Ca^{2+} complex interacts preferentially with regions enriched in anionic phospholipids and leads to membrane stresses that can be ameliorated by PspA family proteins.

The results of this study were published in A. B. Hachmann, E. R. Angert, and

J. D. Helmann. 2009. Antimicrob Agents Chemother 53:1598-609.

2.1 Introduction

Within the soil micro-environment bacteria compete for limiting nutrients by the production of antibiotics that serve to inhibit the growth of their competitors. Indeed, the majority of antibacterial compounds in clinical use are natural products of soil-dwelling organisms and, in many cases, are produced by *Streptomyces* spp. and related members of the actinomycetales (14). Many of these compounds target the synthesis of the peptidoglycan (PG) cell wall layer or disrupt membrane function. Those compounds in clinical use owe their selectivity to the fact that eukaryotic cells lack PG and have a different membrane lipid composition compared to most bacteria.

Antibiotics have also proven to be useful tools for microbial cell biology and have allowed the visualization of the subcellular location of cell envelope biosynthetic processes. For example, fluorescently-labeled vancomycin and ramoplanin, antibiotics that bind specifically to the uncrosslinked PG precursors and/or lipid II, have served to confirm the helical arrangement of the lateral cell wall biosynthetic complexes (15, 58) which was also shown in studies using green fluorescent protein (GFP)-tagged envelope proteins (53).

We have used *Bacillus subtilis* as a model system to investigate the genetic and physiological responses to both antibiotics and co-culture with antibiotic-producing strains. To date, our studies have focused on cell envelope antibiotics (including vancomycin, bacitracin, and fosfomycin) and bacteriocins such as nisin, duramycin, and sublancin (17, 43). Exposure to these compounds activates distinct cell envelope stress responses (CESRs) controlled by extracytoplasmic function (ECF) σ factors and

two-component regulatory systems (TCS) (34). In most cases, the activity of ECF σ factors and TCS is controlled by transmembrane sensors (anti-σ factors or membrane-bound histidine protein kinases, respectively) which thereby allow gene expression to be regulated in response to changes in the cell envelope. The identification of genes induced by a certain antibiotic stress provides insights into the nature of the antibiotic's target(s) and also aids in the identification of resistance functions, many of which are inducible by their cognate antibiotic (30).

Daptomycin, a cyclic lipopeptide antibiotic originally purified from *Streptomyces roseosporus* (46), is notable for its activity against methicillin-resistant *Staphylococcus aureus* (MRSA) and certain streptococci and enterococci. The mechanism of action of daptomycin has been controversial. Initial studies suggested that daptomycin inhibited lipoteichoic acid synthesis (6). However, these findings could not be verified (40). The current proposed mechanism of action involves the insertion of its decanoyl side chain into the cytoplasmic membrane in a Ca^{2+}-dependent manner. Subsequent oligomerization, followed by depolarization of the membrane potential and efflux of potassium ions, leads to arrest of protein, RNA, and DNA synthesis (56). It has been suggested that daptomycin approaches the bacterial membrane in the form of micelles composed of 14-16 daptomycin molecules and an equal number of Ca^{2+} ions which are proposed to help mask the negative charge of daptomycin. After insertion into the membrane, daptomycin dissipates the membrane potential and leads to cessation of macromolecule synthesis (24, 54, 56). Daptomycin treatment neither results in cell lysis nor does it enter the cytoplasm (6, 13).

Here, we have investigated the genetic and physiological responses of *B. subtilis* to daptomycin. Using transcriptional profiling, we demonstrate that

daptomycin strongly activated the LiaRS TCS which regulates the *liaIHGFSR* operon. Mutants defective for *liaH*, which encodes a phage shock protein A (PspA)-like membrane stress protein (35), were 3-fold more susceptible to daptomycin. This susceptibility was further exacerbated in cells additionally lacking the paralogous gene *pspA*. Fluorescence microscopy studies using Bodipy-FL labeled daptomycin together with strains having altered membrane lipid composition supports a model in which the daptomycin-Ca^{2+} complex interacts preferentially with regions enriched in anionic lipids (primarily phosphatidylglycerol (PhG) in *B. subtilis*) and is localized at new cell division septa and in a helical pattern along the long axis of the cell.

2.2 Materials and Methods

Bacterial strains and growth conditions. Strains and primers used in this study are listed in Tables 2.1 and 2.2. Deletion mutants were obtained by replacing genes with antibiotic resistance cassettes using long-flanking-homology PCR as described previously (43, 60) in the wild-type W168 (*trpC2*) or CU1065 (W168 *trpC2 att*SPβ). Unless otherwise noted, bacteria were cultured in Müller Hinton broth supplemented with 50 mg/L Ca^{2+} at 37°C with vigorous shaking. The following antibiotics were used for selection when necessary: spectinomycin 100 μg/mL, kanamycin 10 μg/mL, chloramphenicol 10 μg/mL, tetracycline 20 μg/mL, and erythromycin 1 μg/mL with lincomycin 25 μg/mL (mls: macrolide-lincomycin-streptogramin B resistance). Daptomycin and Bodipy-FL labeled daptomycin were provided by Cubist Pharmaceuticals (Lexington, MA). For microarray analyses (Table 2.3), cells were grown to mid-log phase from a 1:1000 dilution of overnight cultures. To determine the minimal inhibitory concentration (MIC), overnight cultures were

diluted 1:100, grown to mid-log, and re-diluted to 5 x 10^5 CFU/mL in Müller Hinton broth supplemented with 50 mg/L Ca^{2+}. At least 10 appropriate antibiotic concentrations close to the predicted MIC were added to the cultures at the beginning of the growth curve (including a control without antibiotics) in a total inoculum of 200 µL. Growth was measured spectrophotometrically (OD_{600}) using a Bioscreen incubator (Growth Curves USA, Piscataway, NJ) at 37°C with vigorous shaking by monitoring the absorbance every 20 minutes for 24 hours. Inhibition was defined as a final $OD_{600} < 0.05$ (at the 24 hour time point). The mode of the MIC of a minimum of triplicate experiments is shown in Table 2.4.

RNA preparation and microarray analyses. Cultures of W168 were grown to mid-log phase (OD_{600} of 0.4) and split into two flasks. One sample was treated with 1 µg/mL daptomycin (1X MIC) for 20 minutes; the other sample was used as non-treated control. Total RNA was isolated from three different biological replicas with the RNeasy Mini Kit (Qiagen Sciences, Maryland). After DNase treatment with TURBO DNA-free™ (Ambion), RNA concentrations were quantified using a NanoDrop spectrophotometer (NanoDrop Tech. Inc., Wilmington, DE). The corresponding cDNA was synthesized from 20 µg total RNA and differentially labeled according to manufacturer's instructions using the SuperScript™ Plus Indirect cDNA labeling System (Invitrogen). Before and after indirect labeling with Alexa Fluor 555 or Alexa Fluor 647 (at least 3 h at room temperature) cDNA was purified using the Qiagen PCR purification kit (Qiagen, Maryland) and quantified with NanoDrop. Both labeled cDNA populations were combined (approximately 100 pmoles coupled cDNA each), denatured, and hybridized to a microarray slide overnight at 42°C for 16-18 h. After washing, hybridized microarray slides were scanned with a GenePix™ 4000B

array scanner (Axon Instruments, Inc.). Our *B. subtilis* W168 microarrays, consisting of 4109 gene-specific antisense oligonucleotides (65-mers; Sigma-Genosys), were printed at the W.M. Keck Foundation Biotechnology Resource Laboratory, Yale University. Each slide contains 8,447 features corresponding to duplicates of each ORF-specific oligonucleotide, additional oligonucleotides of control genes, and 50% DMSO blank controls. Images were processed using the GenePix Pro 4.0 software package which produces (R,G) fluorescence intensity pairs for each gene. Each expression value is represented by at least six separate measurements (duplicate spots on each of three arrays). Mean values and standard deviations were calculated with MS Excel. The normalized microarray datasets were filtered to remove those genes that were not expressed at levels significantly above background in either condition (sum of mean fluorescence intensity <20). In addition, the mean and standard deviation of the fluorescence intensities were computed for each gene and those where the standard deviation was greater than the mean value were ignored. The fold induction values were calculated by using the signal intensities of daptomycin-treated samples divided by untreated samples. These data are available at NCBI's Gene Expression Omnibus (GEO) (http://www.ncbi.nlm.nih.gov/geo/) accessible via the Series accession number GSE13900. The graph in Fig.1 represents average results of triplicates.

Fluorescence microscopy. Cells were either treated with the lipophilic membrane dye FM® 4-64 (Invitrogen), with Bodipy-FL labeled vancomycin (vancomycin-BDP) (Invitrogen), or with Bodipy-FL labeled daptomycin (daptomycin-BDP) (Cubist Pharmaceuticals). Daptomycin-BDP is an N-BodipyFL-ornithine derivative of daptomycin. The activity of daptomycin-BDP was confirmed by

measuring the MIC of *B. subtilis* wild-type and a set of more susceptible mutants. In all cases, the MIC corresponded to about ten-fold higher MIC compared to daptomycin treatment. Furthermore, daptomycin-BDP was able to induce *cat-lacZ* reporter fusions to *liaI* independent of the solvent. 100 µl cells from exponential or stationary growth phases were incubated with 4 µl daptomycin-BDP 0.5 mg/mL in 50% DMSO for 10 min, with 2 µl vancomycin-BDP mixed 1:1 with vancomycin 0.1 mg/mL, or with 1µl FM® 4-64 0.5 µg/mL for 20 min. After washing in Müller Hinton broth the cells were mounted in the antifade reagent Citifluor (Ted Pella, inc.) on poly-L-lysine (Sigma-Aldrich) treated slides. Nomarski differential interference contrast (DIC) or fluorescent images were taken with an Olympus BX61 epifluorescent microscope with a 100× UPlanApo (N.A 1.35) objective. The microscope is equipped with fluorescence filter cubes for viewing DAPI, FITC, and Cy3. Images were acquired using a Cooke SensiCam with a Sony Interline chip. Image acquisition and post-processing were performed using SlideBook Software package (Intelligent Imaging).

Cluster analysis. Results of whole genome microarray analyses of *B. subtilis* with a set of antimicrobial compounds from our data and from a study by Hutter *et al.* (30) was compared by complete linkage clustering (arrangement based on treatment and genetic response similarity) using the Gene Cluster 3.0 software. The resulting cluster was visualized with Treeview 1.60 written by Michael Eisen (18).

Table 2.1. Strains used in this study.

strains	genotype, remarks, purpose	reference, construction[1]
W168	*trpC2*	BGSC no. 1A1
CU1065	W168 *trpC2 att*SPß	lab stock, (59)
HB5121	W168 *liaIHGFSR::spc*	LFH-PCR → W168
HB0934	CU1065 *liaGFSR::kan*	(43)
HB0920	CU1065 *liaH::kan*	(43)
HB0935	CU1065 *liaIH::tet*	(43)
HB0933	CU1065 *liaR::kan*	(43)
HB5337	CU1065 *mprF::kan*	(52)
HB5123	CU1065 *liaIH::tet mprF::kan*	HB5337 chr DNA → HB0935
HB0919	CU1065 *pspA::cat*	(4)
HB5124	CU1065 *liaH::kan pspA::cat*	HB0919 chr DNA → HB0920
HB5125	CU1065 *liaIH::tet pspA::cat*	HB0919 chr DNA → HB0935
HB5126	CU1065 *liaIH::tet mprF::kan pspA::cat*	HB0919 chr DNA → HB5123
HB0938	CU1065 *yhcYZ::cat*	T. Mascher, unpublished
HB5127	CU1065 *liaH::kan yhcYZ::cat*	HB0938 chr DNA → HB0920
HB0031	CU1065 *sigM::kan*	(12)
HB0020	CU1065 *sigW::mls*	(7)
HB7007	CU1065 *sigX::spc*	(27)
HB0097	CU1065 *sigX::spc sigM::kan*	(9)
HB0096	CU1065 *sigW::mls sigM::kan*	(11)
HB0030	CU1065 *sigX::spc sigW::mls*	M. Cao, unpublished
HB0982	CU1065 *sigM::kan sigW::mls sigX::spc*	(42)
HB5128	CU1065 *liaH::kan sigW::mls*	HB0020 chr DNA → HB0920
HB5129	CU1065 *liaH::kan pspA::cat sigW::mls*	HB0020 chr DNA → HB5124
HB5130	CU1065 *sigX::spc sigM::kan liaIH::tet*	HB0935 chr DNA → HB0097
HB5131	CU1065 *sigM::kan sigW::mls sigX::spc liaIH::tet*	HB0935 chr DNA → HB0982
HB5132	CU1065 *sigW::mls pspA::cat*	HB0919 chr DNA → HB0020
HB5133	CU1076 *sigM::kan sigW::mls sigX::spc pspA::cat*	HB0919 chr DNA → HB0982
HB5134	W168 *des::spc*	LFH-PCR → W168
HB5135	W168 *des::spc pspA::cat*	HB0919 chr DNA → HB5134
HB5346	CU1065 *ugtP::mls*	(52)
HB5361	CU1065 *pssA::spc*	(52)
HB5347	CU1065 *ywnE::tet*	(52)
HB5343	CU1065 *psd::mls*	(52)
HB5350	CU1065 *mprF::kan ugtP::mls*	(52)
HB5388	CU1065 *mprF::kan pssA::spc*	(52)
HB5344	CU1065 *psd::mls mprF::kan*	(52)
HB5136	CU1065 *mprF::kan pspA::cat*	HB0919 chr DNA → HB5337
HB5363	CU1065 P_{xylA}-*mprF* at *thrC* locus, spc^R	L. I. Salzberg, unpublished
BFA2809	W168 *trpC2 pgsA::pMutin4*	(2)
HB0950	CU1065 *att*SPß2Δ2*::*P_{lial}*-cat-lacZ*	(44)
HB0070	CU1065 *sigM::kan* SPß (P_M*-cat-lacZ*)	(9)
HB7022	CU1065 SPß7019 (P_X*-cat-lacZ*)	(27)
HB0050	CU1065 SPß*::*P_{sigW} *-cat-lacZ*	(28)
HB0021	CU1065 *sigW::mls* SPß*::*P_{sigW} *-cat-lacZ*	(12)

[1]Long-Flanking Homology (LFH-)PCR was applied as described previously to construct some of the deletions, using the primers listed in Table 2.2.

Table 2.2. Oligonucleotides used in this study.

no.	name	sequence[1]
2443	Lia-Do-Fwd(spc)	5-CGTTACGTTATTAGCGAGCCAGTCGCGGCTGCTATTTGTTTGCGCC-3
2444	Lia-Do-Rev	5-GGAGGGCTCTTCATCTGATCCG-3
2445	Lia-Up-Rev(spc)	5-CAATAAACCCTTGCCCTCGCTACGAAAAACGCCATGCACGAGGC-3
2446	Lia-Up-Fwd	5-GCTGTCACATTATGCGGCGC-3
3197	Des-Up-Fwd	5-CCCACTTCTCAACATTTGCAA-3
3198	Des-Up-Rev(spc)	5- CGTTACGTTATTAGCGAGCCAGTCCGACTTGCTTTGTCAGCTGT-3
3199	Des-Do-Fwd(spc)	5-CAATAAACCCTTGCCCTCGCTACGGTTTGTGTCATT TGGGCTAT-3
3200	Des-Do-Rev	5-CCCAAGCGTATCATGGAGAT-3

[1] Sequences complementary to antibiotic resistance cassettes for LFH-PCR are underlined.

2.3 Results and Discussion

Daptomycin strongly activates the LiaRS regulon in *B. subtilis.* Determination of antibiotic stimulons reveals the transcriptional responses to the imposed stress, and often provides clues to both the relevant mode of action and the induction of possible defense mechanisms (30). Here, we have used DNA-based microarrays to investigate the initial transcriptional responses to treatment of *B. subtilis* with daptomycin at the MIC of 1.0 μg/mL. As monitored after 20 minutes of exposure, daptomycin induced ~83 genes at least 2-fold and many of these are members of known antibiotic-responsive regulons (Fig. 1 and Table 2.3) (17, 44).

The strongest response to daptomycin treatment was the induction of the autoregulated *liaIHGFSR* operon which encodes the antibiotic-responsive LiaRS TCS (Table 2.3). Lia was named with reference to its strong induction by lipid-II-interacting antibiotics (35, 44), although it is now clear that there is an imperfect correlation between lipid II binding and induction (61). The *Staphylococcus aureus* VraSR system is orthologous to the LiaRS TCS (35). It has been implicated in mediating antibiotic resistance (22, 38), and was also strongly induced by daptomycin as deduced by microarray analyses (47).

In addition to the *liaI* operon itself, daptomycin induced several other genes in a LiaR-dependent manner. These included the *yhcYZ* operon, which was previously shown to be a direct target of LiaR activation (35) and the *yvrI* and *yvrL* genes. The *yvrI* gene has recently been shown to be a divergent member of the σ^{70} family of transcriptional regulators (41) and activates expression of oxalate decarboxylase (OxdC), a major cell wall protein (1). It is not yet clear if *yvrI* is a direct or indirect target of LiaR activation.

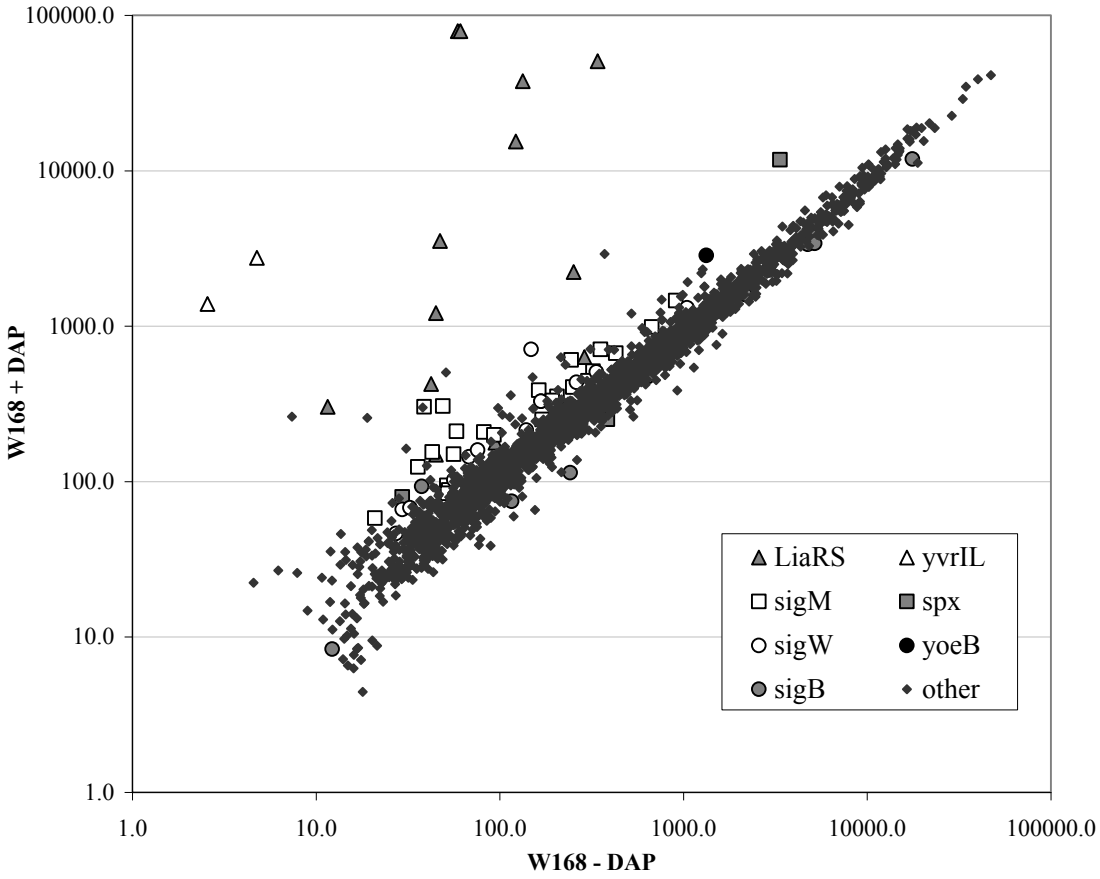

Figure 2.1. Daptomycin stimulon in *B. subtilis*.
The scatterplot represents the average expression levels of treated versus untreated cultures of *B. subtilis* W168 (daptomycin at MIC 1 µg/mL, 20 minutes) of triplicate microarray analyses. The legend lists highly expressed genes as grouped by their corresponding transcriptional regulators.

Table 2.3. Daptomycin stimulon.
Genes induced or repressed >2-fold are shown with their respective antibiotic-responsive regulator[1]

Gene	Signal Intensity[2] + DAP	Signal Intensity[2] - DAP	Fold Change	Gene Function[3]	Regulon
liaH	78930	59	1336	PspA homolog, cell membrane protection	LiaRS (35)
liaI	78935	61	1294	putative membrane protein	LiaRS (35)
liaG	37639	133	283	putative membrane-anchored protein	LiaRS (35)
liaF	50616	341	149	negative regulator of LiaR	LiaRS (35)
liaS	15435	122	126	TCS histidine kinase	LiaRS (35)
liaR	3535	47	75	TCS response regulator	LiaRS (35)
yhcY	149	45	3.3	TCS histidine kinase	LiaRS (35)
yhcZ	631	289	2.2	TCS response regulator	LiaRS (35)
yvrI	2754	4.8	574	σ factor yvrI	YvrI (41)
yvrL	1390	2.6	535	negative regulator of yvrI	YvrI (41)
yqjL	303	39	7.8	hydrolase; paraquat resistance	σ^{MW} (11)
ydaH	306	49	6.2	uncharacterized membrane protein	σ^{M} (10)
ypbG	211	58	3.6	marker for inhibition of cell wall biosynthesis	σ^{M} (10)
yebC	155	43	3.6	hypothetical conserved	σ^{M} (29)
ywaC	124	36	3.5	ppGpp synthase	σ^{M} (17, 48)
bcrC	358	115	3.1	similar to bacteriocin transport permease	σ^{M} (9)
rodA	150	56	2.7	cell-division membrane protein	σ^{M} (17)
yhdL	208	82	2.5	ECF anti-σ factor	σ^{M} (17)
maf	605	245	2.5	cell division and shape determination	σ^{M} (17)
murG	386	163	2.4	peptidoglycan biosynthesis	σ^{M} (17)
murB	710	353	2.0	UDP-N-acetylenolpyruvoyl glucosamine reductase	σ^{M} (17)
sigM	199	93	2.1	ECF σ factor	σ^{M} (26)
yuaF	707	148	4.8	hypothetical protein	σ^{W} (29)
yuaG	329	168	2.0	flotillin-like protein	σ^{W}(29)
yxjI	144	68	2.1	unknown	σ^{W}(29)
ywrE	159	76	2.1	unknown	σ^{W} (29)
ydjP	328	168	2.0	similar to chloroperoxydase	σ^{W} (29)
yoeB	2855	1332	2.1	protection against autolysins	YycFG (3, 51)
yfiC	11780	3349	3.5	similar to ABC transporter (ATP-binding protein)	
fabHA	1203	521	2.3	fatty acid biosynthesis	
fabHB	73	26	2.8	fatty acid biosynthesis	
yvcB	1214	45	27	unknown	
yvkN	302	12	26	unknown	
yvzA	424	42	10	unknown	
yvzC	261	10	26	hypothetical protein	
yvpB	257	19	14	hypothetical protein	
sdpI	2233	252	8.9	immunity protein for SdpC; signal transduction	SdpR (19)
ywdD	163	31	5.3	hypothetical protein	
ywdE	504	51	9.9	hypothetical protein	
ywfB	299	38	7.9	similar to Bacilysin biosynthesis protein	
yknU	2917	372	7.8	similar to ABC transporter (ATP-binding protein)	
hutM	126	40	3.2	histidine permease	
ypeB	469	151	3.1	sporulation protein	
yitI	630	215	2.9	probable acetyltransferase	

Table 2.3. (Continued)

Gene	Signal Intensity[2] + DAP	Signal Intensity[2] - DAP	Fold Change	Gene Function[3]	Regulon
rpmB	892	1631	0.5	ribosomal protein L28	
degR	115	216	0.5	activation of degradative enzymes (AprE, NprE, SacB)	
yisY	138	264	0.5	similar to chloride peroxidase	
ydgK	39	77	0.5	similar to bicyclomycin resistance protein	
yocH	759	1513	0.5	similar to cell wall-binding protein (autolysin)	YycFG (3, 51)
yxeQ	60	119	0.5	putative MmgE/Prp family protein	
lmrB	261	534	0.5	lincomycin-resistance	
rpsT	541	1140	0.5	ribosomal protein S20	
yxeM	66	156	0.4	similar to amino acid ABC transporter (binding protein)	
ywhE	386	926	0.4	*pbpG*, penicillin-binding protein (sporulation)	

[1] Induced genes controlled by regulator(s) known to be responsive to antibiotic-elicited stress are shown together with genes of predicted function or those with unknown function that are strongly induced (>5-fold). Induced and repressed genes were filtered to remove those with low overall expression levels (combined signal intensity <100). Altogether, daptomycin induced 83 genes at least 2-fold (234 genes ≥1.5-fold) and repressed 25 genes at least 2-fold (181 ≥1.5-fold) (NCBI GEO series accession GSE13900).

[2] "+DAP" and "-DAP" corresponds to average triplicates of the signal intensities of daptomycin-treated or untreated samples.

[3] Functions were assigned based on the SubtiList database or BSORF entry.

In *B. subtilis,* a number of genes involved in antibiotic resistance and cell wall metabolism are regulated by the extracytoplasmic function (ECF) σ-factors σ^W and σ^M. Daptomycin weakly induced 6 genes of the σ^W regulon (10, 12) and 19 genes of the σ^M regulon (17, 32) (Table 2.3). To monitor the transcriptional response of the *liaI*, *sigW*, and *sigM* genes to daptomycin treatment we used transcriptional (*cat-lacZ)* reporter fusions and found that all were induced by daptomycin (data not shown).

The phage-shock protein A homologs LiaH and PspA protect against daptomycin. Of the *liaIHGFSR* genes, *liaFSR* are well conserved within Gram-positive bacteria with a low G+C content. Only the bacilli also contain the phage-shock protein A homolog LiaH. *S. aureus* harbors the *liaFSR* orthologs SA1702 and *vraSR* (35). When tested for daptomycin susceptibility, Muthaiyan *et al.* observed an increased susceptibility of a *vraSR* mutant strain to daptomycin (0.78 μg/mL vs. 1.0 μg/mL for wild-type) (47). Here, we have used growth inhibition studies to examine whether the daptomycin induced *liaI* operon affects susceptibility to daptomycin. A deletion of the entire *liaI* operon significantly increased susceptibility from an MIC of 1.0 μg/mL for wild-type to an MIC of 0.3 μg/mL (Table 2.4). A null mutant of the negative regulator *liaF,* which overexpresses LiaIH (34, 35), did not appear to increase resistance.

To test for possible functional redundancy between *liaH* and its paralog *pspA* (which was not strongly induced by daptomycin treatment despite being part of the σ^W regulon) we tested single and double mutants of these loci. A *pspA* deletion showed almost no change of MIC compared to wild-type, but the double mutant *liaH pspA* further decreased the MIC by 2-fold relative to the *liaH* single mutant. These results indicate that the PspA (phage-shock-protein A) homologs, LiaH and PspA, both

contribute to decreased daptomycin susceptibility and that the induction of LiaH by daptomycin is adaptive.

The mechanisms by which PspA proteins protect cells against membrane-disruption are unclear, but are likely to involve direct interactions with the inner surface of the membrane (16). *Escherichia coli* PspA forms abundant, oligomeric ring-like structures that are speculated to coat the inner surface of the membrane, and thereby prevent proton leakage (39). In vitro, *E. coli* PspA binds preferentially to liposomes containing anionic lipids and suppresses proton leakage (39). LiaH has also been observed to be an abundant oligomeric protein with a similar ultrastructure (T. Mascher, personal communication). Together, these findings are consistent with the notion that daptomycin toxicity results from disruption of the membrane integrity and that the two *B. subtilis* PspA paralogs can counteract this disruptive effect.

ECF σ-factors also contribute to decreased daptomycin susceptibility. Since several σ^W and σ^M regulon members were upregulated upon daptomycin treatment, we tested null mutants of ECF σ-factor genes for daptomycin susceptibility. In the singly mutant strains, there was a slight decrease of MIC for *sigM* and *sigW* (0.8 μg/mL for both), whereas a *sigX* mutant was unaffected. Multiply mutant strains displayed even greater susceptibility with the lowest MIC noted for the *sigXM* double (0.6 μg/mL) and the *sigMWX* triple mutants (0.6 μg/ml) (Table 2.4). Increased daptomycin susceptibility in the multiply mutant strains is consistent with the recent demonstration that these three ECF σ factors have overlapping regulons and multiply mutant strains are often more susceptible to antibiotics than single mutants (42).

In *B. subtilis*, several ECF σ-factors have been implicated in conferring resistance to cell envelope-active antibiotics. For example, σ^X regulates the *dlt* operon

Table 2.4. Minimum inhibitory concentration of *B. subtilis* mutants and strains with altered membrane composition, or deletion of transcriptional regulators.

Strain/ Deletion Mutant	DAP MIC [μg/mL][2]	Strain/ Deletion Mutant	DAP MIC [μg/mL]
W168	1.0	*liaH pspA*	0.2
CU1065	1.0	*liaIH pspA*	0.2
LiaR-regulated		*liaIH mprF pspA*	0.2
liaIHGFSR[1]	0.3	*sigXM liaIH*	0.2
liaH	0.4	*sigMWX liaIH*	0.2
liaIH	0.4	*sigW pspA*	0.8
liaR	0.5	*sigMWX pspA*	0.5
liaF	1.0	**Membrane alterations**	
liaGFSR	0.5	W168 at 25°C	0.7
liaIH mprF	0.2	*des*[1] at 25°C	0.4
liaH yhcYZ	0.2	*des*[1]	0.9
yhcYZ	0.8	*des pspA*	0.9
ECF σ-regulated		*ugtP*	0.9
sigM	0.8	*pssA*	1.0
sigW	0.8	*ywnE*	1.0
sigX	1.0	*psd*	1.0
sigXM	0.6	*mprF*	0.5
sigWM	0.7	*mprF ugtP*	0.6
sigXW	0.9	*mprF pssA*	0.9
sigMWX	0.6	*psd mprF*	0.9
pspA	1.0	*mprF pspA*	0.5
LiaR/ECF σ-regulated		*mprF* overexpression	1.3
liaH sigW	0.3	*pgsA depletion*	8.0
liaH pspA sigW	0.2	IPTG induced *pgsA*	1.0

[1] Mutants derived from strain W168, other mutants derived from strain CU1065.
[2] MIC was determined by liquid growth inhibition experiments. Data represent the mode of the lowest daptomycin concentration that led to complete growth inhibition (minimum of triplicates).

and the *pssA ybfM psd* operon which reduce the net negative charge of the cell envelope by D-alanylation of teichoic acids and insertion of phosphatidylethanolamine into the membrane, respectively. As a result, mutants in *sigX* are more susceptible to cationic antimicrobial peptides (8). The σ^W regulon includes a large number of genes implicated in resistance against both small molecule inhibitors such as fosfomycin and peptide antibiotics such as sublancin and SdpC (4). Finally, the σ^M regulon has recently been shown to include many genes known to be important for cell envelope synthesis and *sigM* mutants are susceptible to some cell wall antibiotics such as moenomycin and bacitracin (17, 42). The identity of the ECF σ factor-dependent operons that confer daptomycin protection is not yet clear.

Mutants with altered membrane composition affect daptomycin susceptibility. Since the decanoyl side-chain of daptomycin is predicted to insert into the membrane, we tested whether susceptibility is influenced in strains altered in membrane lipid composition. Daptomycin susceptibility was measured for *B. subtilis* strains lacking phosphatidylethanolamine (*psd*, *pssA*), lysyl-phosphatidylglycerol *(mprF)*, glycolipids (*ugtP),* or cardiolipin (*ywnE*). Of the null mutants, only *mprF* showed a significant difference compared to wild-type (MIC 0.5 μg/mL vs. 1.0 μg/mL; Table 2.4). Moreover, overexpression of *mprF* led to slightly decreased susceptibility (MIC 1.3 μg/mL). MprF catalyzes the tRNA-dependent modification of phosphatidylglycerol (PhG) with lysine to form the positively charged lysyl-phosphatidylglycerol (LPhG) (57).

It has been shown earlier that a change in membrane charge due to *mprF* disruption affects the susceptibility to antimicrobial agents in *S. aureus* (49). Here, we speculate that the reduction of the net negative charge of the membrane upon

increased production of LPhG functions to reduce the affinity of a positively charged daptomycin-Ca^{2+} complex due to electrostatic repulsion. Indeed, previous studies of *S. aureus* strains that were selected for increased daptomycin resistance found that point mutations in *mprF* frequently occurred as an early event during selection (21). However, the effect of these mutations alone was quite modest and further selection led to additional mutations in the *yycFG* TCS and RNA polymerase subunit genes *rpoBC* (21). Since an *mprF* null mutant is more susceptible to daptomycin, we suggest that these *mprF* mutations may have been gain of function mutations. Independently, Jones *et al.* found that daptomycin resistance in *S. aureus* was correlated with increased translocation of LPhG from the inner to the outer leaflet of the membrane without changing the overall concentration of LPhG (33). An increase of *mprF* gene expression was not seen upon daptomycin treatment in *B. subtilis*, but an increase in positive charge through LPhG translocation to the outer leaflet, and an additional effect of reduction of the membrane net negative charge by σ^X, could together affect the ability of daptomycin to insert into the membrane.

The physical properties of the membrane are determined by both the membrane head-group composition and the length and desaturation of the fatty acyl side chains. In *B. subtilis*, the fluidity of the membrane is regulated, in large part, by the lipid desaturase Des which introduces *cis*-double bonds at Δ5 in response to reduction in temperature. The desaturase is under the control of the DesRK TCS (31). Deletion of *des* resulted in increased susceptibility to daptomycin and this effect was especially notable during growth at low temperatures (MIC at 25°C of 0.4 μg/mL vs. 0.7 μg/mL for wild-type). The underlying mechanisms of the effect of *des* deletion are not entirely clear. The increased rigidity of the membrane in a *des* mutant might facilitate

the membrane disruptive action of daptomycin, impair repair mechanisms by the cell, or the decrease in unsaturated fatty acyl moieties might affect interactions with the decanoyl side chain of daptomycin.

Depletion of phosphatidylglycerol greatly decreases daptomycin susceptibility. The effect of reducing the net negative charge of the cell membrane on daptomycin susceptibility was especially apparent when we studied a strain in which PhG could be depleted from cells using a conditionally expressed allele of *pgsA*. PgsA is required for the first step in PhG synthesis from phosphatidic acid (37). Depletion of this essential complex lipid, by transfer of cells to medium lacking the inducer IPTG, results in cells that lose the characteristic helical staining pattern associated with anionic-lipid favoring membrane dyes (e.g. FM 4-64). This strain continues to grow for several hours even in the absence of IPTG as they gradually become depleted of PhG (58). When PhG-depleted cells were sub-cultured in medium lacking IPTG, but containing daptomycin, they were able to grow in the presence of significantly higher daptomycin concentrations than wild-type. Conversely, when expression of *pgsA* was induced by IPTG addition, wild-type levels of daptomycin susceptibility were restored (Table 2.4). This increased resistance was specific for daptomycin: PhG-depleted cells were unaffected in susceptibility to vancomycin (which targets PG synthesis) and were increased in susceptibility to duramycin which interacts specifically with phosphatidylethanolamine (2). Presumably, in this case, depletion of PhG from the membrane led to an increase in the concentration of phosphatidylethanolamine.

The effects of membrane composition and charge on daptomycin insertion have also been studied by Jung *et al*. in artificial liposomes. By means of fluorescence spectroscopy, differential scanning calorimetry, and ^{31}P NMR, they found that

daptomycin (with Ca^{2+}) binds to acidic and neutral lipids in a different fashion and leads to a change of the structural organization of acidic membranes (induction of non-lamellar lipid phases and membrane fusion) (58). This again emphasizes the influence of membrane lipid composition on daptomycin susceptibility.

Daptomycin preferentially localizes to the cell septum and in a helical pattern along the cell wall. Fluorescent imaging with Bodipy-FL labeled daptomycin (daptomycin-BDP) was used to study the localization of daptomycin in the cell envelope in *B. subtilis*. Strikingly, daptomycin-BDP was not distributed evenly throughout the cell membrane, but rather in a complex, reproducible pattern. The highest concentration was found along the newly formed division septa, and in a helical pattern along the long axis of the cell, whereas no fluorescence was detected at the cell poles (Fig. 2A and 2B). This helical pattern and localization to the septa is reminiscent of localization studies of both the cell wall biosynthetic machinery (50) and anionic phospholipids (including PhG) in *B. subtilis* (56). Sites of active cell wall biosynthesis have been visualized using Bodipy-FL labeled vancomycin (vancomycin-BDP) (45).

We next compared the localization of daptomycin-BDP with vancomycin-BDP which binds to the D-Ala-D-Ala dipeptide of uncrosslinked PG (2). In separate labeling experiments, the daptomycin-BDP and vancomycin-BDP labeling showed very similar patterns (Fig. 2C). Since both antibiotics are bound to the same fluorophore, we were unable to carry out direct colocalization studies. However, pre-treatment with vancomycin did not affect labeling by daptomycin-BDP, nor did unlabeled daptomycin interfere with staining with vancomycin-BDP. This suggests that these two antibiotics may have distinct targets, as expected from prior work (2).

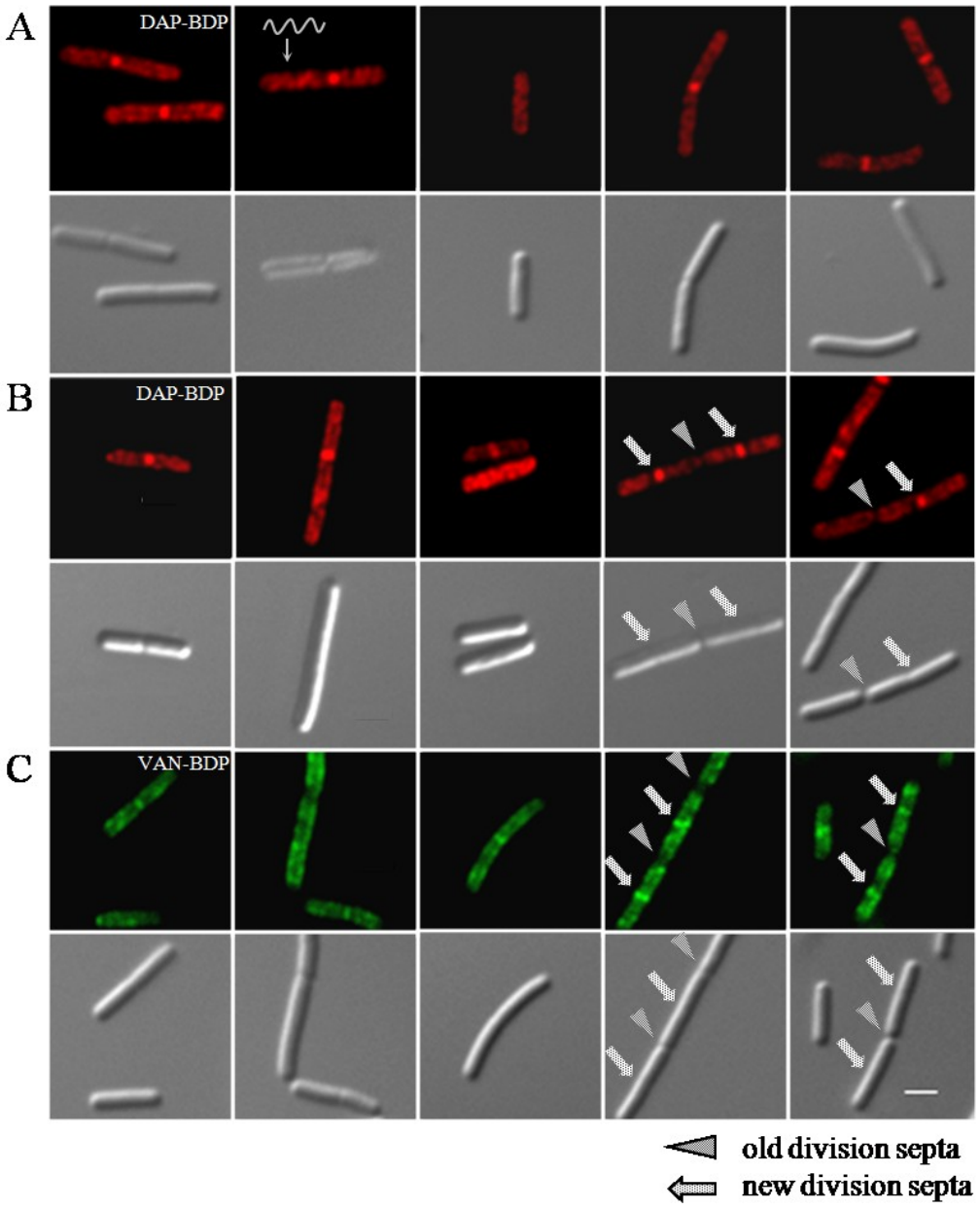

Figure 2.2. Daptomycin-BDP inserts preferentially at new division septa and in a spiral pattern.
Fluorescent and DIC micrographs of *B. subtilis* stained with daptomycin-BDP (DAP-BDP) and vancomycin-BDP (VAN-BDP). (A) *B. subtilis* W168 treated with daptomycin-BDP at two-fold MIC for 10 minutes (during exponential growth phase). (B). W168 treated with daptomycin-BDP at ten-fold MIC for 10 minutes. (C). W168 treated with equal amounts of vancomycin and vancomycin-BDP for 20 minutes. A and B show a spiral localization of daptomycin-BDP and the preferential insertion at newly formed division septa, similar to vancomycin-BDP (C). The arrowhead indicates old, the arrow new division septa. Scale bars represent 2 µm.

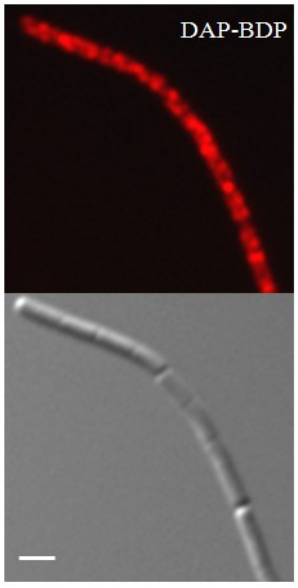

Figure 2.3. Daptomycin-BDP staining of stationary phase cells.
Fluorescent and DIC micrograph of stationary growth phase culture of *B. subtilis* W168 treated with daptomycin-BDP (DAP-BDP) at two-fold MIC for 10 minutes. The staining shows a similar insertion pattern compared to exponential growth phase cultures. Scale bars represent 2 μm.

Recently, Mascio *et al.* showed that daptomycin also exhibits bactericidal effects on *S. aureus* cells in stationary growth phases (albeit with higher MIC) (47) which prompted us to test daptomycin-BDP labeling in *B. subtilis* stationary cells. We observed a similar pattern as in exponentially growing cells (Fig. 3), albeit with less intense labeling at the division septa.

In light of the recently reported helical distribution of PhG in *B. subtilis* membranes (30) we next tested whether PhG depletion affects the observed staining pattern seen with daptomycin-BDP. Remarkably, cells depleted of PhG exhibited a significant loss of staining intensity and failed to exhibit the characteristic helical staining pattern seen in the non-depleted cells (Fig. 4C vs. 4A/B). Very similar effects were noted when the cells were stained instead with the membrane dye FM 4-64 (Fig. 4D vs. 4E) which is known to stain regions enriched in PhG (36, 39). Together, these results suggest that the characteristic staining pattern observed with daptomycin-BDP is due to a preferential interaction with the membrane in regions enriched in PhG, consistent with the effects of PhG depletion on daptomycin susceptibility as noted above.

Cluster analysis of the stimulons of daptomycin and other cell envelope active antibiotics. Analysis of the daptomycin stimulon and the effects of membrane mutations on susceptibility, combined with the preceding analysis of daptomycin-BDP localization, are all consistent with a primary mechanism of action involving insertion into the cell membrane in regions enriched in anionic lipids. However, recent studies of the transcriptional response of *S. aureus* to daptomycin led Muthaiyan *et al.* to suggest that daptomycin might interfere both with membrane integrity and PG biosynthesis (21).

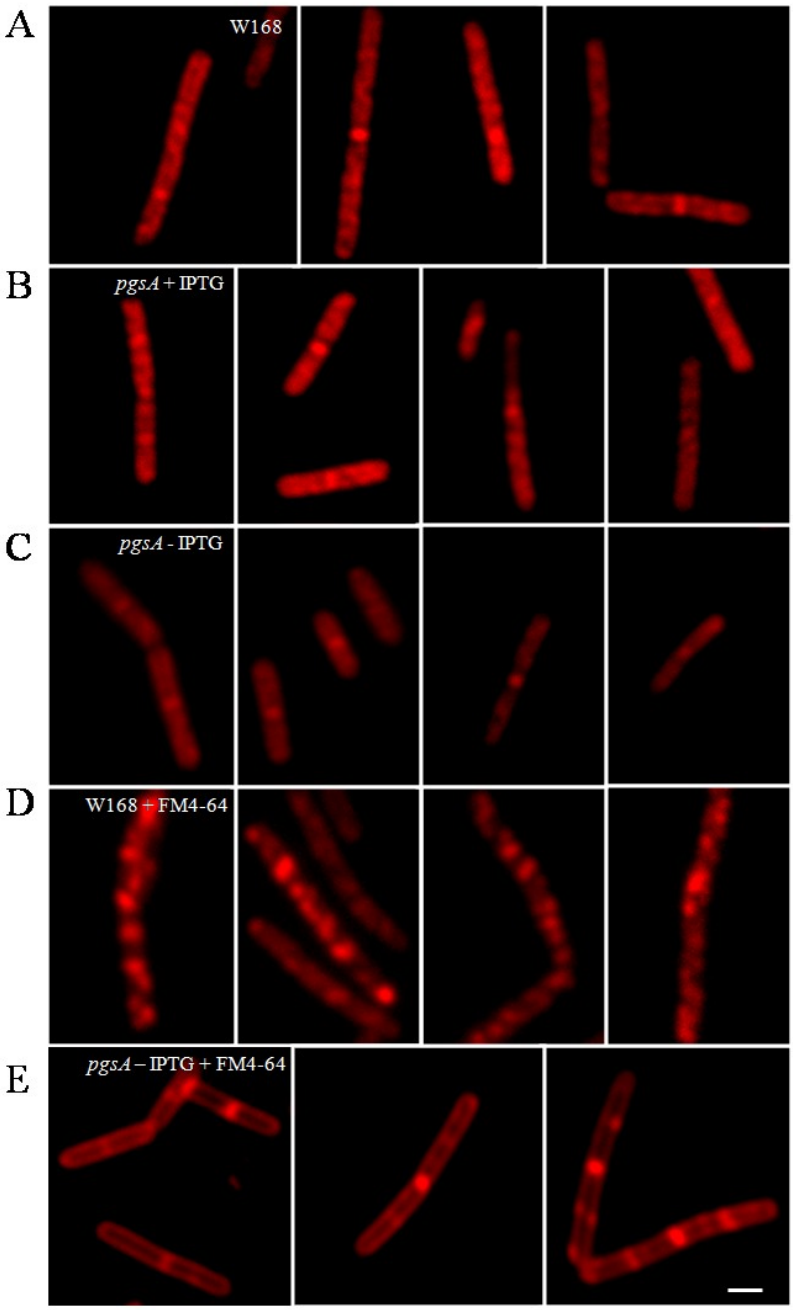

Figure 2.4. Correlation between daptomycin-BDP staining and anionic phospholipid content and distribution.
Fluorescent and DIC micrographs of **(A)** wild-type W168 and *pgsA*::pMutin grown in the **(B)** presence or **(C)** absence of 1 mM IPTG, stained with daptomycin-BDP at two-fold MIC for 10 minutes. Daptomycin-BDP delocalizes when *pgsA* is not expressed from the IPTG-inducible promoter suggesting preferential insertion of daptomycin in membrane lipid domains rich in anionic phosphatidylglycerol. **(D)** W168 and **(E)** *pgsA*::pMutin stained with the membrane lipid dye FM 4-64 in the absence of IPTG. Scale bars represent 2 μm.

In this organism, daptomycin induced genes characteristic of membrane-disrupting agents (e.g. m-chlorophenylhydrazone) as well as genes induced by cell wall synthesis inhibitors (e.g. vancomycin).

To determine whether the daptomycin stimulon of *B. subtilis* most closely resembled the stimulons for membrane-perturbing agents or cell wall synthesis inhibitors, we performed a hierarchical clustering analysis using datasets representing the transcriptional responses to daptomycin, vancomycin, moenomycin, and ramoplanin (our results), and 35 other antibiotics from a study by Hutter *et al.* (5). The daptomycin stimulon is most similar to a cluster of treatment conditions that includes compounds that inhibit PG synthesis (vancomycin, ristocetin, ramoplanin, and moenomycin) and that perturb membrane function (Triton X-114 and polymyxin B). All of these conditions induce the σ^M regulon and several compounds are strong inducers of the LiaRS TCS (Fig. 5). These results lead us to suggest that insertion of daptomycin into membrane regions enriched in anionic lipids may have multiple effects including both disruption of membrane function and perhaps interference with the assembly or function of cell wall biosynthetic complexes.

2.4 Conclusions

We here report a detailed genetic analysis of factors affecting daptomycin susceptibility in *B. subtilis*. Transcriptome analyses indicate that daptomycin induces sets of genes previously shown to be induced by exposure to membrane-active compounds and cell wall synthesis inhibitors. The LiaRS TCS is strongly induced by daptomycin, and genetic studies indicate that both LiaH and the paralog PspA contribute to decreased daptomycin susceptibility. By analogy with *E. coli* PspA (2),

these proteins are likely to help stabilize the membrane and prevent depolarization. These results are consistent with the expectation that daptomycin acts primarily on the membrane.

Analysis of strains with altered membrane composition suggests that daptomycin interacts preferentially with regions of the membrane enriched in anionic lipids including PhG, the dominant anionic lipid in *B. subtilis*. For example, a strain in which PhG is depleted becomes less susceptible to daptomycin although it retains normal (or even increased) susceptibility to other cell wall and membrane-active antibiotics. Conversely, strains lacking MprF, which synthesizes the cationic lipid LPhG, are more susceptible to daptomycin. Mutations in *mprF* have been previously associated with daptomycin resistance (23) although, in light of the results here, it seems likely that these are gain-of-function mutations that increase MprF levels or activity. Indeed, overexpression of *mprF* in *B. subtilis* decreases daptomycin susceptibility.

Cells depleted of PhG not only display decreased daptomycin susceptibility; they lose the characteristic helical staining pattern seen in wild-type cells treated with daptomycin-BDP. This may result directly from the reduction in levels of negatively charged membrane lipids which would thereby decrease the affinity of the positively charged daptomycin-Ca^{2+} complex for the membrane. Alternatively, or in addition, PhG depletion might result in altered composition or localization of membrane proteins, or cell envelope biosynthetic complexes. For instance, Campo *et al.* reported that reduced PhG led to delocalization of the translocation ATPase SecA in the *B. subtilis* membrane (20); and Barák *et al.* observed enrichment of the cell division protein MinD in anionic phospholipid spirals in the membrane (25, 55).

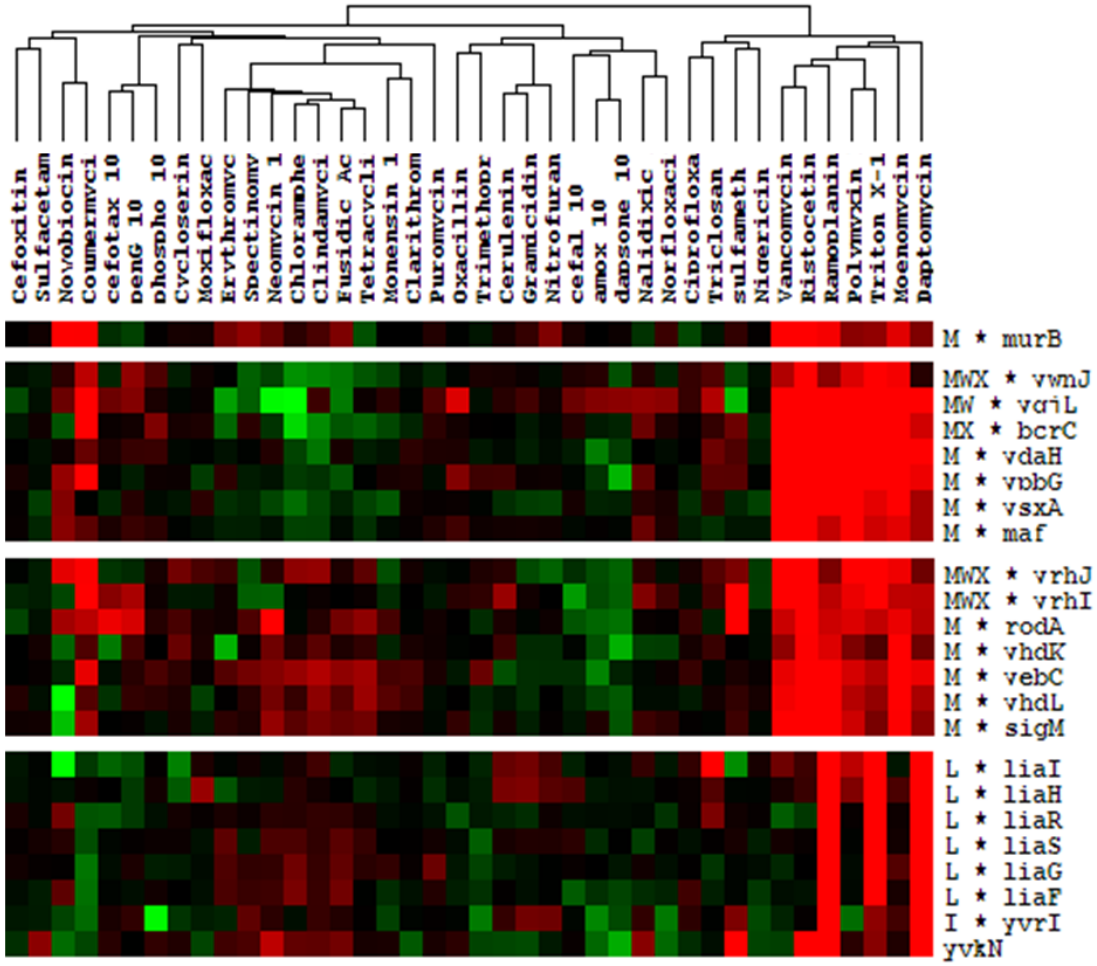

Figure 2.5. Cluster analysis of *B. subtilis* microarray studies with 40 different antimicrobial agents.
The gene expression patterns of daptomycin-treated *B. subtilis* are most closely related to those of cells treated with cell membrane and cell wall active antibiotics: moenomycin, triton X-114, polymyxin B, ramoplanin, ristocetin, and vancomycin. Cluster analysis was performed on whole genome datasets for each antibiotic (see Materials and Methods) and selected clusters enriched for daptomycin-induced genes are shown. Red indicates induction and green repression after treatment, whereas black corresponds to unchanged gene expression.

Daptomycin is used clinically as a reserve antibiotic against complicated skin and skin structure infections (21) as well as *S. aureus*-induced bacteremia and infective endocarditis (35). To date, reports about resistance to daptomycin in clinical settings have been relatively rare (41). To better understand the evolution of daptomycin resistance, *S. aureus* strains with increased daptomycin resistance (either selected in the laboratory or arising during clinical treatment) were chosen for DNA sequence analysis. These studies indicate that the evolution of resistance is a multigenic phenomenon. Often, mutations in *mprF* emerge early and other contributing mutations occur in the essential *yycFG* TCS and *rpoBC* genes (11). To date, there are no documented examples of high level daptomycin resistance emerging due to a single gene mutation. In light of these findings, it is interesting that cells depleted of PhG display such a dramatic decrease of susceptibility. However, null mutations that confer daptomycin resistance are unlikely to arise in *pgsA* since, at least in *B. subtilis*, it is an essential gene.

REFERENCES

1. **Antelmann, H., S. Towe, D. Albrecht, and M. Hecker.** 2007. The phosphorus source phytate changes the composition of the cell wall proteome in Bacillus subtilis. J Proteome Res **6:**897-903.

2. **Barák, I., K. Muchova, A. J. Wilkinson, P. J. O'Toole, and N. Pavlendova.** 2008. Lipid spirals in Bacillus subtilis and their role in cell division. Mol Microbiol **68:**1315-27.

3. **Bisicchia, P., D. Noone, E. Lioliou, A. Howell, S. Quigley, T. Jensen, H. Jarmer, and K. M. Devine.** 2007. The essential YycFG two-component system controls cell wall metabolism in Bacillus subtilis. Mol Microbiol **65:**180-200.

4. **Butcher, B. G., and J. D. Helmann.** 2006. Identification of Bacillus subtilis sigma-dependent genes that provide intrinsic resistance to antimicrobial compounds produced by Bacilli. Mol Microbiol **60:**765-82.

5. **Campo, N., H. Tjalsma, G. Buist, D. Stepniak, M. Meijer, M. Veenhuis, M. Westermann, J. P. Muller, S. Bron, J. Kok, O. P. Kuipers, and J. D. Jongbloed.** 2004. Subcellular sites for bacterial protein export. Mol Microbiol **53:**1583-99.

6. **Canepari, P., and M. Boaretti.** 1996. Lipoteichoic acid as a target for antimicrobial action. Microb Drug Resist **2:**85-9.

7. **Cao, M., B. A. Bernat, Z. Wang, R. N. Armstrong, and J. D. Helmann.** 2001. FosB, a cysteine-dependent fosfomycin resistance protein under the control of sigma(W), an extracytoplasmic-function sigma factor in Bacillus subtilis. J Bacteriol **183:**2380-3.

8. **Cao, M., and J. D. Helmann.** 2004. The Bacillus subtilis extracytoplasmic-function sigmaX factor regulates modification of the cell envelope and resistance to cationic antimicrobial peptides. J Bacteriol **186:**1136-46.

9. **Cao, M., and J. D. Helmann.** 2002. Regulation of the Bacillus subtilis bcrC bacitracin resistance gene by two extracytoplasmic function sigma factors. J Bacteriol **184:**6123-9.

10. **Cao, M., P. A. Kobel, M. M. Morshedi, M. F. Wu, C. Paddon, and J. D. Helmann.** 2002. Defining the Bacillus subtilis sigma(W) regulon: a comparative analysis of promoter consensus search, run-off transcription/macroarray analysis (ROMA), and transcriptional profiling approaches. J Mol Biol **316:**443-57.

11. **Cao, M., C. M. Moore, and J. D. Helmann.** 2005. Bacillus subtilis paraquat resistance is directed by sigmaM, an extracytoplasmic function sigma factor, and is conferred by YqjL and BcrC. J Bacteriol **187:**2948-56.

12. **Cao, M., T. Wang, R. Ye, and J. D. Helmann.** 2002. Antibiotics that inhibit cell wall biosynthesis induce expression of the Bacillus subtilis sigma(W) and sigma(M) regulons. Mol Microbiol **45:**1267-76.

13. **Cotroneo, N., R. Harris, N. Perlmutter, T. Beveridge, and J. A. Silverman.** 2008. Daptomycin exerts bactericidal activity without lysis of Staphylococcus aureus. Antimicrob Agents Chemother **52:**2223-5.

14. **D'Costa, V. M., K. M. McGrann, D. W. Hughes, and G. D. Wright.** 2006. Sampling the antibiotic resistome. Science **311:**374-7.

15. **Daniel, R. A., and J. Errington.** 2003. Control of cell morphogenesis in bacteria: two distinct ways to make a rod-shaped cell. Cell **113:**767-76.

16. **Darwin, A. J.** 2005. The phage-shock-protein response. Mol Microbiol **57:**621-8.

17. **Eiamphungporn, W., and J. D. Helmann.** 2008. The Bacillus subtilis sigma(M) regulon and its contribution to cell envelope stress responses. Mol Microbiol **67:**830-48.

18. **Eisen, M. B., P. T. Spellman, P. O. Brown, and D. Botstein.** 1998. Cluster analysis and display of genome-wide expression patterns. Proc Natl Acad Sci U S A **95:**14863-8.

19. **Ellermeier, C. D., E. C. Hobbs, J. E. Gonzalez-Pastor, and R. Losick.** 2006. A three-protein signaling pathway governing immunity to a bacterial cannibalism toxin. Cell **124:**549-59.

20. **Falagas, M. E., K. P. Giannopoulou, F. Ntziora, and K. Z. Vardakas.** 2007. Daptomycin for endocarditis and/or bacteraemia: a systematic review of the experimental and clinical evidence. J Antimicrob Chemother **60:**7-19.

21. **Friedman, L., J. D. Alder, and J. A. Silverman.** 2006. Genetic changes that correlate with reduced susceptibility to daptomycin in Staphylococcus aureus. Antimicrob Agents Chemother **50:**2137-45.

22. **Gardete, S., S. W. Wu, S. Gill, and A. Tomasz.** 2006. Role of VraSR in antibiotic resistance and antibiotic-induced stress response in Staphylococcus aureus. Antimicrob Agents Chemother **50:**3424-34.

23. **Hair, P. I., and S. J. Keam.** 2007. Daptomycin: a review of its use in the management of complicated skin and soft-tissue infections and Staphylococcus aureus bacteraemia. Drugs **67:**1483-512.

24. **Ho, S. W., D. Jung, J. R. Calhoun, J. D. Lear, M. Okon, W. R. Scott, R. E. Hancock, and S. K. Straus.** 2007. Effect of divalent cations on the structure of the antibiotic daptomycin. Eur Biophys J **37:**421-433.

25. **Holmes, R. L., and J. H. Jorgensen.** 2008. Inhibitory activities of 11 antimicrobial agents and bactericidal activities of vancomycin and daptomycin against invasive methicillin-resistant Staphylococcus aureus isolates obtained from 1999 through 2006. Antimicrob Agents Chemother **52:**757-60.

26. **Horsburgh, M. J., and A. Moir.** 1999. Sigma M, an ECF RNA polymerase sigma factor of Bacillus subtilis 168, is essential for growth and survival in high concentrations of salt. Mol Microbiol **32:**41-50.

27. **Huang, X., A. Decatur, A. Sorokin, and J. D. Helmann.** 1997. The Bacillus subtilis sigma(X) protein is an extracytoplasmic function sigma factor contributing to survival at high temperature. J Bacteriol **179:**2915-21.

28. **Huang, X., K. L. Fredrick, and J. D. Helmann.** 1998. Promoter recognition by Bacillus subtilis sigmaW: autoregulation and partial overlap with the sigmaX regulon. J Bacteriol **180:**3765-70.

29. **Huang, X., A. Gaballa, M. Cao, and J. D. Helmann.** 1999. Identification of target promoters for the Bacillus subtilis extracytoplasmic function sigma factor, sigma W. Mol Microbiol **31:**361-71.

30. **Hutter, B., C. Schaab, S. Albrecht, M. Borgmann, N. A. Brunner, C. Freiberg, K. Ziegelbauer, C. O. Rock, I. Ivanov, and H. Loferer.** 2004. Prediction of mechanisms of action of antibacterial compounds by gene expression profiling. Antimicrob Agents Chemother **48:**2838-44.

31. **Iwamoto, K., T. Hayakawa, M. Murate, A. Makino, K. Ito, T. Fujisawa, and T. Kobayashi.** 2007. Curvature-dependent recognition of ethanolamine phospholipids by duramycin and cinnamycin. Biophys J **93:**1608-19.

32. **Jervis, A. J., P. D. Thackray, C. W. Houston, M. J. Horsburgh, and A. Moir.** 2007. SigM-responsive genes of Bacillus subtilis and their promoters. J Bacteriol **189:**4534-8.

33. **Jones, T., M. R. Yeaman, G. Sakoulas, S.-J. Yang, R. A. Proctor, H.-G. Sahl, J. Schrenzel, Y. Q. Xiong, and A. S. Bayer.** 2008. Staphylococcus aureus Clinical Treatment Failures with Daptomycin are Associated with Alterations in Surface Charge, Membrane Phospholipid Asymmetry and Drug Binding. Antimicrob. Agents Chemother. **52:** 269-278.

34. **Jordan, S., M. I. Hutchings, and T. Mascher.** 2008. Cell envelope stress response in Gram-positive bacteria. FEMS Microbiol Rev **32:**107-46.

35. **Jordan, S., A. Junker, J. D. Helmann, and T. Mascher.** 2006. Regulation of

LiaRS-dependent gene expression in bacillus subtilis: identification of inhibitor proteins, regulator binding sites, and target genes of a conserved cell envelope stress-sensing two-component system. J Bacteriol **188:**5153-66.

36. **Jovanovic, G., L. J. Lloyd, M. P. Stumpf, A. J. Mayhew, and M. Buck.** 2006. Induction and function of the phage shock protein extracytoplasmic stress response in Escherichia coli. J Biol Chem **281:**21147-61.

37. **Jung, D., J. P. Powers, S. K. Straus, and R. E. Hancock.** 2008. Lipid-specific binding of the calcium-dependent antibiotic daptomycin leads to changes in lipid polymorphism of model membranes. Chem Phys Lipids **154:**120-128.

38. **Kato, Y., T. Suzuki, T. Ida, K. Maebashi, M. Sakurai, J. Shiotani, and I. Hayashi.** 2008. Microbiological and clinical study of methicillin-resistant Staphylococcus aureus (MRSA) carrying VraS mutation: changes in susceptibility to glycopeptides and clinical significance. Int J Antimicrob Agents **31:**64-70.

39. **Kobayashi, R., T. Suzuki, and M. Yoshida.** 2007. Escherichia coli phage-shock protein A (PspA) binds to membrane phospholipids and repairs proton leakage of the damaged membranes. Mol Microbiol **66:**100-9.

40. **Laganas, V., J. Alder, and J. A. Silverman.** 2003. In vitro bactericidal activities of daptomycin against Staphylococcus aureus and Enterococcus faecalis are not mediated by inhibition of lipoteichoic acid biosynthesis. Antimicrob Agents Chemother **47:**2682-4.

41. **MacLellan, S., T. Wecke, and J. Helmann.** 2008. A previously unidentified sigma factor and two accessory proteins regulate oxalate decarboxylase expression in Bacillus subtilis. Mol. Microbiol. **69:**954 - 967.

42. **Mascher, T., A. B. Hachmann, and J. D. Helmann.** 2007. Regulatory overlap and functional redundancy among Bacillus subtilis extracytoplasmic function sigma factors. J Bacteriol **189:**6919-27.

43. **Mascher, T., N. G. Margulis, T. Wang, R. W. Ye, and J. D. Helmann.** 2003. Cell wall stress responses in Bacillus subtilis: the regulatory network of the bacitracin stimulon. Mol Microbiol **50:**1591-604.

44. **Mascher, T., S. L. Zimmer, T. A. Smith, and J. D. Helmann.** 2004. Antibiotic-inducible promoter regulated by the cell envelope stress-sensing two-component system LiaRS of Bacillus subtilis. Antimicrob Agents Chemother **48:**2888-96.

45. **Mascio, C. T., J. D. Alder, and J. A. Silverman.** 2007. Bactericidal Action of Daptomycin against Stationary-Phase and Nondividing Staphylococcus aureus Cells. Antimicrob Agents Chemother **51:**4255-60.

46. **Miao, V., M. F. Coeffet-Legal, P. Brian, R. Brost, J. Penn, A. Whiting, S. Martin, R. Ford, I. Parr, M. Bouchard, C. J. Silva, S. K. Wrigley, and R. H. Baltz.** 2005. Daptomycin biosynthesis in Streptomyces roseosporus: cloning and analysis of the gene cluster and revision of peptide stereochemistry. Microbiology **151:**1507-23.

47. **Muthaiyan, A., J. A. Silverman, R. K. Jayaswal, and B. J. Wilkinson.** 2008. Transcriptional profiling reveals that daptomycin induces the Staphylococcus aureus cell wall stress stimulon and genes responsive to membrane depolarization. Antimicrob Agents Chemother **52:**980-90.

48. **Nanamiya, H., K. Kasai, A. Nozawa, C. S. Yun, T. Narisawa, K. Murakami, Y. Natori, F. Kawamura, and Y. Tozawa.** 2008. Identification and functional analysis of novel (p)ppGpp synthetase genes in Bacillus subtilis. Mol Microbiol **67:**291-304.

49. **Nishi, H., H. Komatsuzawa, T. Fujiwara, N. McCallum, and M. Sugai.** 2004. Reduced content of lysyl-phosphatidylglycerol in the cytoplasmic membrane affects susceptibility to moenomycin, as well as vancomycin, gentamicin, and antimicrobial peptides, in Staphylococcus aureus. Antimicrob Agents Chemother **48:**4800-7.

50. **Reynolds, P. E., and E. A. Somner.** 1990. Comparison of the target sites and mechanisms of action of glycopeptide and lipoglycodepsipeptide antibiotics. Drugs Exp Clin Res **16:**385-9.

51. **Salzberg, L. I., and J. D. Helmann.** 2007. An antibiotic-inducible cell wall-associated protein that protects Bacillus subtilis from autolysis. J Bacteriol **189:**4671-80.

52. **Salzberg, L. I., and J. D. Helmann.** 2008. Phenotypic and Transcriptomic Characterization of *Bacillus subtilis* Mutants with Grossly Altered Membrane Composition. J Bacteriol **190:**7797-7807.

53. **Scheffers, D. J., L. J. Jones, and J. Errington.** 2004. Several distinct localization patterns for penicillin-binding proteins in Bacillus subtilis. Mol Microbiol **51:**749-64.

54. **Scott, W. R., S. B. Baek, D. Jung, R. E. Hancock, and S. K. Straus.** 2007. NMR structural studies of the antibiotic lipopeptide daptomycin in DHPC micelles. Biochim Biophys Acta **1768:**3116-3126.

55. **Silverman, J. A., N. Oliver, T. Andrew, and T. Li.** 2001. Resistance studies with daptomycin. Antimicrob Agents Chemother **45:**1799-802.

56. **Silverman, J. A., N. G. Perlmutter, and H. M. Shapiro.** 2003. Correlation of daptomycin bactericidal activity and membrane depolarization in Staphylococcus aureus. Antimicrob Agents Chemother **47:**2538-44.

57. **Staubitz, P., H. Neumann, T. Schneider, I. Wiedemann, and A. Peschel.** 2004. MprF-mediated biosynthesis of lysylphosphatidylglycerol, an important determinant in staphylococcal defensin resistance. FEMS Microbiol Lett **231:**67-71.

58. **Tiyanont, K., T. Doan, M. B. Lazarus, X. Fang, D. Z. Rudner, and S. Walker.** 2006. Imaging peptidoglycan biosynthesis in Bacillus subtilis with fluorescent antibiotics. Proc Natl Acad Sci U S A **103:**11033-8.

59. **Vander Horn, P. B., and S. A. Zahler.** 1992. Cloning and nucleotide sequence of the leucyl-tRNA synthetase gene of Bacillus subtilis. J Bacteriol **174:**3928-35.

60. **Wach, A.** 1996. PCR-synthesis of marker cassettes with long flanking homology regions for gene disruptions in S. cerevisiae. Yeast **12:**259-65.

61. **Wecke, T., D. Zuhlke, U. Mader, S. Jordan, B. Voigt, S. Pelzer, H. Labischinski, G. Homuth, M. Hecker, and T. Mascher.** 2009. Daptomycin versus Friulimicin B: in-depth profiling of Bacillus subtilis cell envelope stress responses. Antimicrob Agents Chemother **53:**1619-23.

CHAPTER 3

PGSA DEPLETION LEADS TO HIGH DAPTOMYCIN RESISTANCE IN *BACILLUS SUBTILIS*

Resistance to antibiotics is of high concern in particular when considering the low number of new antibiotics discovered in the past 40 years. One of the newest antibiotics on the market, daptomycin, is a cyclic lipopeptide that disrupts the functional integrity of the cell membrane of Gram-positive pathogens in a Ca^{2+}-dependent manner. To date, few resistances against daptomycin have been reported with the highest stemming from laboratory isolates. Here, we present detailed genetic and phenotypic analyses of a daptomycin resistant isolate, Dap^R1, from the Gram-positive model bacterium *Bacillus subtilis*. This strain was obtained by serial passage with increasing daptomycin concentrations in the laboratory, and is 30-fold more resistant to daptomycin than the parent strain. In addition, Dap^R1 displays cross-resistance to cell wall active antibiotics, including vancomycin, moenomycin, and bacitracin. Dap^R1 is characterized by aberrant septum placement and by a thickened cell wall, especially at the cell poles. However, peptidoglycan analysis did not show significant changes compared to the parent strain. On a transcriptomic and proteomic level the strain deviates significantly from the parent strain. Solexa sequencing revealed 44 point mutations of which 31 changed protein sequence. An intermediate isolate of Dap^R1 that is 20-fold more resistant to daptomycin than wild-type, only has three point mutations; in the cell shape modulator gene *mreB*, the stringent response gene *relA*, and the phosphatidylglycerol synthase gene *pgsA*. We suggest that the high resistance of Dap^R1 can be attributed to the mutation in *pgsA*, resulting in a more

positively charged membrane, and a repulsive effect on the positively charged Ca^{2+}-daptomycin complex.

The majority of the studies in this chapter were performed by A. B. Hachmann, David Popham (Blacksburg, Virginia) contributed the quantification of muramic acids, and Haike Antelmann (Greifswald, Germany) carried out the proteomic analyses of Dap^R1 and W168.

3.1 Introduction

Daptomycin is a cyclic lipopeptide antibiotic used to treat complicated skin and skin structure infections caused by *Staphylococcus aureus* or enterococci. In addition, it has been approved to treat *S. aureus*-induced bacteremia and infective endocarditis (13). The mechanism of action involves the calcium ion dependent insertion of daptomycin into the bacterial membrane, followed by depolarization of the membrane potential and extrusion of potassium ions, leading to arrest of macromolecular synthesis and cell death (26, 27).

With over 500,000 patients treated since market approval, resistances to daptomycin developed rarely. According to the SENTRY Antimicrobial Surveillance Program from the United States for the years 2002-2008, 99.9% of methicillin resistant *S. aureus* treated with daptomycin had an MIC of 1.0 μg/ml or lower, with only a slight increase of MIC over time (http://www.gp-pathogens.com/data/default.cfm) (25). Previous studies targeting mechanisms of resistance to daptomycin were performed on clinical isolates and in vitro (14, 18). In-vitro isolation of resistant bacterial strains can give clues about the effectiveness of a certain antibiotic, and uncover information about mechanisms of resistance.

After serial passage with increasing daptomycin concentration, Friedman *et al.* characterized three *S. aureus* isolates that displayed increased daptomycin resistance (14). Mutations contributing to resistance were found in genes that encode for the membrane lipid modulator MprF, the two-component system YycFG, and RpoB/RpoC. MprF modifies membrane lipids by tRNA catalyzed lysinylation of phosphatidylglycerol, thereby increasing amounts of positively charged membrane lipids. This mutation is possibly a gain-of-function mutation as we found increased daptomycin susceptibility in an *mprF* deletion mutant and decreased susceptibility for MprF overexpression in *B. subtilis* (16). While the role of mutations in RpoB and RpoC was unknown, mutations in YycG could account for changes in cell wall metabolism, perhaps leading to decreased cell lysis (4).

To further investigate possible mechanisms of resistance to daptomycin, we isolated a mutant (Dap^R1) by serial passage in the Gram positive model bacterium *B. subtilis*. Here, we discuss the characterization of this daptomycin resistant strain, including possible mechanisms of resistance.

3.2 Materials and Methods

Bacterial strains and growth conditions. Unless otherwise noted, bacteria were cultured at 37°C with vigorous shaking using Müller Hinton broth supplemented with 50 mg/l Ca^{2+} as growth medium. The following antibiotics were used for selection when necessary: spectinomycin 100 µg/ml, kanamycin 10 µg/ml, chloramphenicol 10 µg/ml, tetracycline 20 µg/ml, and erythromycin 1 µg/ml with lincomycin 25 µg/ml (mls: macrolide-lincomycin-streptogramin B resistance). Table 3.1 lists the strains and primers used in this study. Deletion mutants were generated by

replacing genes with antibiotic resistance cassettes using long-flanking-homology PCR (21, 31) in the wild-type W168 (*trpC2*) or CU1065 (W168 *trpC2 att*SPβ). Daptomycin and Bodipy-FL labeled daptomycin were provided by Cubist Pharmaceuticals (Lexington, MA). The minimal inhibitory concentration (MIC) was determined by diluting overnight cultures 1:100, growing to OD_{600} of 0.4, and re-diluteding to 5 x 10^5 CFU/mL in Müller Hinton broth supplemented with 50 mg/l Ca^{2+}. At least 10 appropriate antibiotic concentrations close to the predicted MIC were added to the cultures at the beginning of the growth curve (including a control without antibiotics) in microtiter plates with a total inoculum of 200 µl. Growth was measured spectrophotometrically (OD_{600}) using a Bioscreen incubator (Growth Curves USA, Piscataway, NJ) at 37°C with vigorous shaking. The absorbance was recorded every 20 minutes for 24 hours. Inhibition was defined as a final $OD_{600} < 0.05$ (at the 24 hour time point). The mode of the MIC of a minimum of triplicate experiments is shown in Table 3.2 and Table 3.3.

RNA preparation and microarray analyses. Total RNA was isolated from three biological replicas of W168 and Dap^R1 grown to mid-log phase (OD_{600} of 0.4) using the RNeasy Mini Kit (Qiagen Sciences, Maryland). After DNase treatment with TURBO DNA-free™ (Ambion), RNA concentrations were quantified using a NanoDrop spectrophotometer (NanoDrop Tech. Inc., Wilmington, DE). cDNA was synthesized from 20 µg total RNA and differentially labeled according to manufacturer's instructions with the SuperScript™ Plus Indirect cDNA labeling System (Invitrogen). Before and after indirect labeling with Alexa Fluor 555 or Alexa Fluor 647 (at least 3 h at room temperature) cDNA was purified using the Qiagen MinElute PCR Purification Kit (Qiagen, Maryland) and quantified via NanoDrop.

Both labeled cDNA populations were combined (approximately 100 pmoles of labeled cDNA per sample), denatured, and hybridized to a microarray slide overnight at 42^{o}C for 16-18 h. After washing, hybridized microarray slides were scanned with a GenePix^{TM} 4000B array scanner (Axon Instruments, Inc.). Our *B. subtilis* W168 microarray slides were printed at the W.M. Keck Foundation Biotechnology Resource Laboratory (Yale University) with 4109 gene-specific antisense oligonucleotides (65-mers; Sigma-Genosys). In addition to duplicates of each ORF-specific oligonucleotide, the slides have additional oligonucleotides of control genes and 50% DMSO blank controls (8,447 features in total). The GenePix Pro 6.0 software package was used for image processing and analysis. Each expression value is represented by six separate measurements (duplicate spots on each of three arrays). Mean values and standard deviations of the normalized microarray datasets were calculated with MS Excel. Filtering was applied to remove genes that were not expressed at levels significantly above background (sum of mean fluorescence intensity <20). In addition, the mean and standard deviation of the fluorescence intensities were computed for each gene and those where the standard deviation was greater than the mean value were ignored. The fold change was calculated by using the signal intensities of Dap^{R}1 divided by W168.

Fluorescence microscopy. Cells were either treated with Bodipy-FL labeled vancomycin (vancomycin-BDP) (Invitrogen) or with Bodipy-FL labeled daptomycin (daptomycin-BDP) (Cubist Pharmaceuticals), an N-BodipyFL-ornithine derivative of daptomycin. 100 µl of W168 grown to exponential phase was incubated with 4 µl daptomycin-BDP 0.5 mg/mL in 50% DMSO for 10 min, or with 2 µl vancomycin-BDP mixed 1:1 with vancomycin 0.1 mg/ml for 20 min, Dap^{R}1 was incubated with 40

µl daptomycin-BDP, and 4µl vancomycin-BDP mix, respectively. After washing in Müller Hinton broth the cells were mounted in the antifade reagent Citifluor (Ted Pella, inc.) on poly-L-lysine (Sigma-Aldrich) treated slides. Nomarski differential interference contrast (DIC) or fluorescent images were taken with an Olympus BX61 epifluorescent microscope with a 100× UPlanApo (N.A 1.35) objective. The microscope is equipped with fluorescence filter cubes for viewing DAPI, FITC, and Cy3. Images were acquired using a Cooke SensiCam with a Sony Interline chip. Image acquisition and post-processing were performed using SlideBook Software package (Intelligent Imaging).

Transmission Electron Microscopy. Cells were prepared following a standard protocol of fixation in 2% glutaraldehyde followed by 2% OsO_4, both in 0.1% Na cacodylate buffer, followed by 2% aqueous uranyl acetate and dehydration in an ethanol/acetone series. Embedding was in Epon-araldite resin and thin sections taken on an LKB ultramicrotome. Grids were stained with Reynold's lead citrate and uranyl acetate and photographed in an FEI EM 201.

Peptidoglycan analysis. PG was purified from cells and digested with muramidase, and muropeptides were separated and quantified using HPLC as previously described (3, 22). For quantification of cell-associated muramic acid and dpm, culture samples were centrifuged, washed in cold 1 mM $MgCl_2$, and suspended in 6 N HCl. Following hydrolysis at 95°C for 4 h, muramic acid and dpm were determined by an amino acid/amino sugar analysis method (15, 23).

FAME analysis. W168 and Dap^R1 were grown to mid-exponential phase at 37 ^oC or 25 ^oC in LB. Cultures of two biological replicas were combined and frozen

cell pellets were submitted for fatty acid methyl ester (FAME) analysis at Microbial ID, Newark, DE (http://www.microbialid.com/).

Proteome and mass spectrometry analysis. *B. subtilis* strains were grown in LB-broth and harvested 1 hour after entry into the stationary phase at OD_{540} of 3.0. The TCA-precipitated extracellular, cell wall-associated and cytoplasmic proteins were prepared as described previously (1, 2) and resolved in a solution containing 2 M thiourea and 8 M urea. Protein content was determined using Bradford assay (5). For two-dimensional gel electrophoresis (2D-PAGE) 200 µg of the protein extracts were separated using non-linear immobilized pH gradients (IPG) in the pH range 4-7 for cytoplasmic proteins and 3-10 for extracellular and cell wall-associated proteins (Amersham Biosciences) and a Multiphor II apparatus (Amersham Pharmacia Biotech) as described previously (1). The resulting 2D gels were fixed in 40% (v/v) ethanol, 10% (v/v) acidic acid and stained with Colloidal Coomassie Brilliant Blue (Amersham Biosciences). Quantitative image analysis was performed from the Coomassie-stained 2D gels using the DECODON Delta 2D software (http://www.decodon.com). For standard identification of the proteins from 2D gels, spot cutting, tryptic digestion of proteins and spotting of resulting peptides onto the MALDI-targets (Voyager DE-STR, PerSeptive Biosystems) the Ettan Spot Handling Workstation was used (Amersham-Biosciences, Uppsala, Sweden) (12). The MALDI-TOF-TOF measurement of spotted peptide solutions was carried out on a Proteome-Analyzer 4800 (Applied Biosystems, Foster City, CA, USA) as described previously (12).

Table 3.1. Strains and oligonucleotides used in this study.

strains	genotype, remarks, purpose	reference, construction[1]
W168	*trpC2*	BGSC no. 1A1
CU1065	W168 *trpC2 att*SPß	lab stock (30)
Dap^{R}1	W168 daptomycin resistant isolate	this work
HB0106	CU1065 *bcrC::pMUTIN*	(8)
HB0148	CU1065 *ypbG::cat*	(9)
HB0152	CU1065 *yqjL::tet*	(9)
HB0154	CU1065 *yqjL::tet bcrC::pMUTIN*	(9)
HB0332	CU1065 *oppA*::mini-Tn*10* (spc^R)	(29)
HB5140	W168 *yokD*::Tn7SX (spc^R)	this work
HB5141	W168 *yrkPQ*::	LFH-PCR → W168
HB5142	W168 *yrkR*::	LFH-PCR → W168
HB5143	W168 *yrkO*::*kan*	LFH-PCR → W168
HB5144	W168 *yrkN*::*kan*	LFH-PCR → W168
HB5145	W168 *ykcC*::*spec*	LFH-PCR → W168
HB6050	CU1065 *sdpI::mls*	(6)
PS3301	*gerF::ermC*	(17)

no.	name	sequence[2]
4788	yrkO-Up-Fwd	5-ATGGATCCTCTCCTCTTTCCACACCTCA-3
4786	yrkO-Up-Rev(kan)	5-CCTATCACCTCAAATGGTTCGCTGGTCCAGAAAATGAACCCGTT-3
4787	yrkO-Do-Fwd(kan)	5-CGAGCGCCTACGAGGAATTTGTATCGAAGCTGACGTACGGCAAAGT
4789	yrkO-Do-Rev	5-AGAAGCTTCATCTTCGCAATCACCGAAC-3
4792	yrkN-Up-Fwd	5-TCTGTTCCTCAGGTACGGAT-3
4793	yrkN-Up-Rev(kan)	5-CCTATCACCTCAAATGGTTCGCTGGGCAGATCAGATTCCTTTGC-3
4794	yrkN-Do-Fwd(kan)	5-CGAGCGCCTACGAGGAATTTGTATCGCGCAATGGACGTGAAGATGA-3
4795	yrkN-Do-Rev	5-GATAAGCTCGCTGATCGTGA-3

[1]Long-Flanking Homology (LFH-)PCR was applied as described previously to construct some of the deletions, using the primers listed.

[2] Sequences complementary to antibiotic resistance cassettes for LFH-PCR are underlined.

Solexa Sequencing. Chromosomal DNA was isolated from W168 and Dap^{R}1, quantified by Nanodrop and submitted for sequencing. Sequencing was performed by the Cornell University Life Sciences Core Laboratories Center on an Illumina GA2 sequencer. The sequencing data was assembled using the W168 reference sequence with the Genebank accession number ABQK00000000 and aligned with MAQView. The sequencing coverage averaged 58-fold for W168 and 79-fold for Dap^{R}1.

3.3 Results and Discussion

Isolation and phenotypical characterization of the daptomycin resistant strain Dap^{R}1. In-vitro isolation of bacterial strains selected for antibiotic resistance allows studying mechanisms of resistance in a controlled environment. Here, we cultured a *B. subtilis* 168 wild-type strain continuously over 55 days with increasing daptomycin concentrations. Starting with sub-inhibitory concentrations of daptomycin (0.5 µg/ml, corresponding to half the MIC), the concentrations were increased every day by 0.5 µg/ml, up to 27.5 µg/ml. This ending concentration was chosen arbitrarily. Further passage of the strain in LB without addition of daptomycin for 10 days was carried out to ensure that the resistance phenotype was a stable feature and not due for example to adaptation. This strain, named Dap^{R}1, maintained its resistance to daptomycin at the selected concentration.

While having a similar growth rate like its parent strain, Dap^{R}1 lost two hallmarks of *B. subtilis* 168 - the ability to sporulate and natural competence. In addition, Dap^{R}1 displayed cross-resistance to other cell envelope antibiotics. The MIC of Dap^{R}1 increased two-fold compared to the parent strain when treated with the cell wall synthesis inhibitors vancomycin and bacitracin, or the pore former gramicidin.

Table 3.2. Minimum inhibitory concentrations of *B. subtilis* wild-type and Dap^{R}1 with different antibiotics.

Antibiotic	W168[1]	Dap^{R}1[1]
Daptomycin	1.0	27.5
Moenomycin[2]	10	>2000
Vancomycin	0.2	0.4
Bacitracin	500	1000
Gramicidin	300	>600
Fosfomycin	200	200
Tunicamycin	0.2	0.2
Ampicillin	20	20
Penicillin G	0.1	0.1
Nisin	90	100

[1] MIC in [µg/mL] was determined by liquid growth inhibition experiments. Data represent the mode of the lowest antibiotic concentration that led to complete growth inhibition (minimum of triplicates).
[2]endpoint determined after 10h, all others after 24h.

Table 3.3. Minimum inhibitory concentrations of *B. subtilis* mutants with daptomycin.

Strain	Daptomycin[1]
W168	1.0
CU1065	1.0
Dap^{R}1	27.5
bcrC	0.7
yqjL	1.1
bcrC yqjL	1.2
ypbG	0.9
yrkPQ	0.9
yrkR	1.0
yrkO	0.9
yrkN	0.9
sdpI	1.0
ykcC	1.0
yokD	0.8
oppA	0.7
gerF (*lgt*)	0.8

[1] MIC in [µg/mL] was determined by liquid growth inhibition experiments. Data represent the mode of the lowest antibiotic concentration that led to complete growth inhibition after 24h (minimum of triplicates).

Resistance to the transglycosylase inhibitor moenomycin was even more pronounced; the MIC increased more than 200-fold (Table 3.2, Table 3.3). Decreased susceptibility was not a universal feature with all cell envelope active compounds; the MIC of penicillin G, ampicillin, fosfomycin, and tunicamycin remained the same as wild-type. Taken together, Dap^{R}1 was found to have decreased susceptibility to cell wall and cell membrane antibiotics, possibly indicating common resistance mechanisms, for instance changes in the cell envelope.

Fluorescence Microscopy shows increased insertion of Bodipy FL-labeled daptomycin in septa and poles of Dap^{R}1. Light microscopic comparisons of Dap^{R}1 and its parent strain were inconclusive. In turn, fluorescence microscopic imaging depicts insertion of Bodipy Fl-labeled daptomycin in the septa and the poles of Dap^{R}1 (Fig. 3.1). The latter is surprising, because these results are in contrast to the parent strain, which had very low daptomycin insertion at old division septa or cell poles (16). Overall, the fluorescence intensity is lower in Dap^{R}1, even with 10-fold higher concentration of Bodipy FL-labeled daptomycin compared to the wild-type. This implies that daptomycin is still able to insert albeit with a changed pattern, likely due to changes in the cell envelope of Dap^{R}1.

Electron Microscopy of Dap^{R}1 reveals a thickened cell wall at the poles and irregular septum formation. In order to visualize alterations in the cell envelope of Dap^{R}1, we performed transmission electron microscopy (TEM). TEM of thin sectioned cells showed striking aberrances of the cell wall of Dap^{R}1 (Fig 3.2, Fig. 3.3). Whereas the wild-type cell has a characteristic rod-shape and regular septum formation, Dap^{R}1 stands out with a thickened cell wall at the poles. On average, the lateral cell walls were slightly thinner than in W168 (1.3-fold), but the polar walls were 3.2-fold thicker than that of the parent strain (Table 3.4). W168 cells were slightly longer and thicker than Dap^{R}1, 1.8 versus 1.7 μm long, respectively, and 0.6 versus 0.5 μm in diameter. Of further notice is the septum placement in Dap^{R}1. Invaginations and completed septa are formed aberrantly in Dap^{R}1, indicating that the regulation and placement of the cell division apparatus is affected.

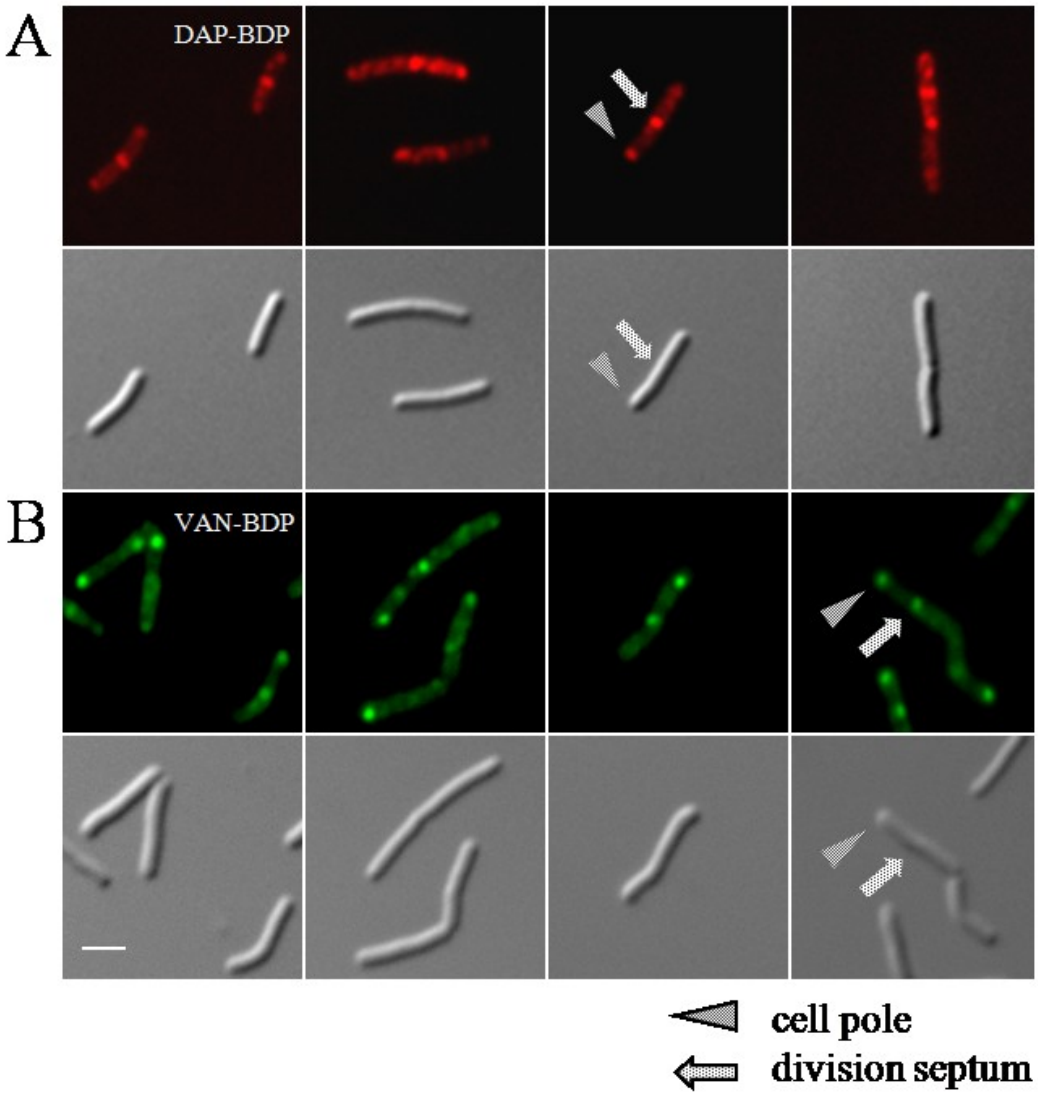

Figure 3.1. Daptomycin-BDP inserts in a spotted pattern and at cell poles and division septa in Dap^R1.
Fluorescent and DIC micrographs of Dap^R1 stained with daptomycin-BDP (DAP-BDP) and vancomycin-BDP (VAN-BDP). **(A)** Dap^R1 treated with daptomycin-BDP at two-fold MIC for 10 minutes (during exponential growth phase). **(B)**. Dap^R1 treated with equal amounts of vancomycin and vancomycin-BDP for 20 minutes. **(A)** shows a spotted localization of daptomycin-BDP and preferential insertion at division septa and cell poles, similar to vancomycin-BDP **(B)**. The arrowhead indicates cell poles, the arrow division septa. Scale bars represent 2 μm.

Together, these results are consistent with the notion of several mutations, but do not necessarily explain the resistance phenotype. A thicker cell wall was seen before in connection with vancomycin or daptomycin resistant *S. aureus* (7, 10). A partially thicker cell wall, only at the cell poles, has not been reported to our knowledge. Here, the increased thickness could pose a physical barrier for the tested antibiotics, leading to decreased susceptibility. In fact, this is supported by our observation of increased resistance to cell envelope active antibiotics of high molecular weight. Smaller antibiotics like penicillin G and ampicillin remained effective on Dap^{R}1.

The partially thicker cell wall and changes in septum formation let us wonder if the strain has alterations in its cytoskeleton, cell division, cell wall synthesis, or recycling apparatus. A defect in cell wall hydrolysis upon completion of cell division might result in the increased amount of peptidoglycan at the cell poles. A different explanation might be an elevated expression of cell wall synthesis proteins during cell division. It remains to be answered whether these alterations in the cell envelope architecture influence daptomycin insertion or mode of action.

Table 3.4. Comparison of cell wall thickness of W168 and Dap^{R}1.

Thickness in µm[1]	n	Mean	SD	Median	Sum	Minimum	Maximum
W168 wall[2]	16	0.038	0.006	0.038	0.614	0.030	0.053
Dap^{R}1 polar wall	18	0.121	0.034	0.126	2.181	0.074	0.221
Dap^{R}1 lateral wall	18	0.029	0.003	0.028	0.523	0.024	0.037

[1] measured from transmission electron micrographs
2 averages of lateral cell wall and polar cell wall

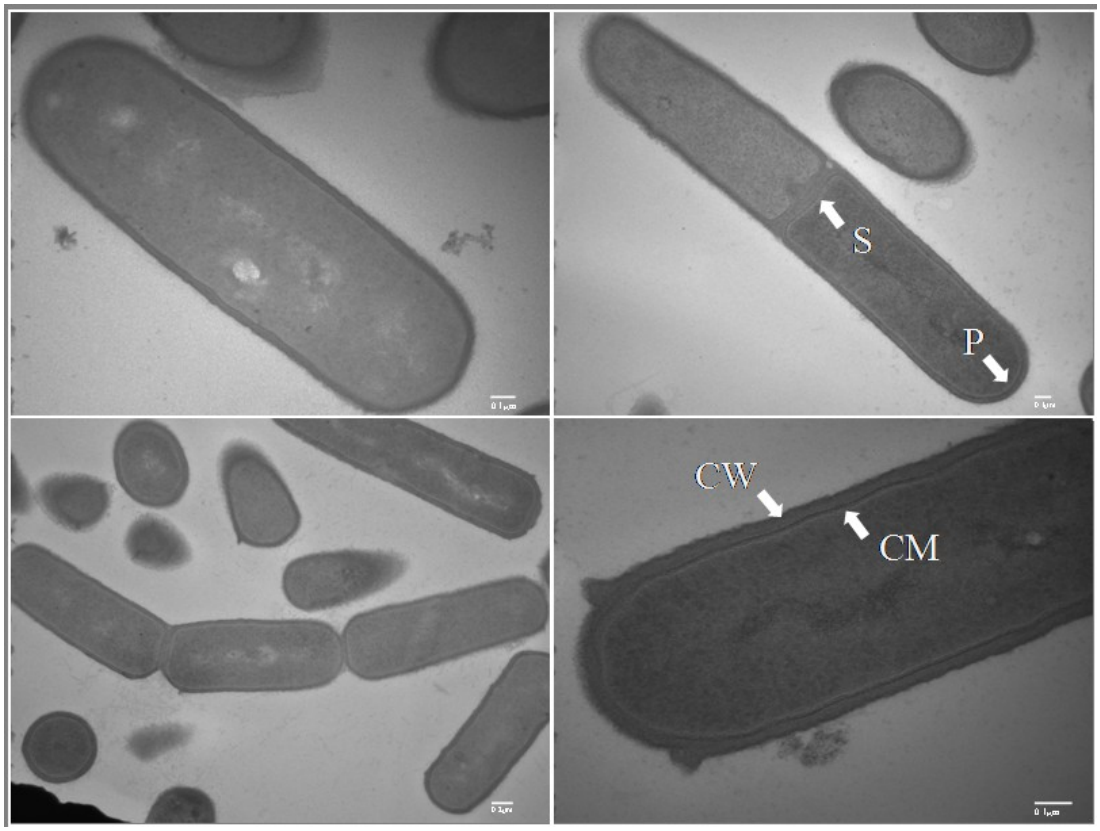

Figure 3.2. Transmission electron micrographs (TEM) of W168.
TEM of thin sliced W168 with regular septation and cell wall in the characteristic rod-shaped *B. subtilis* wild-type strain. The arrows indicate: CW=cell wall, CM=cell membrane, S=septum, P=pole. Scale bars represent 0.1 µm (except for bottom left, 0.2 µm).

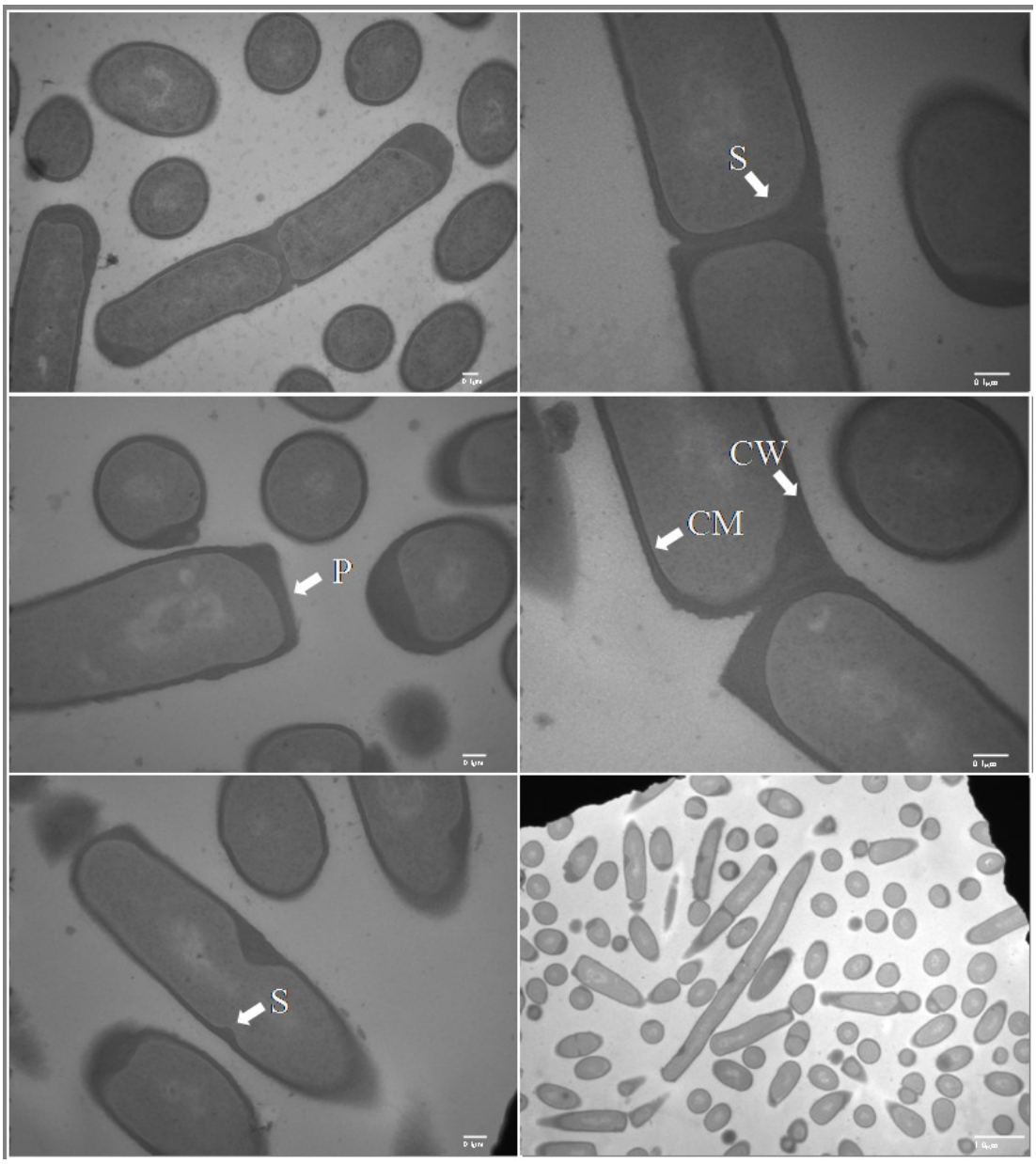

Figure 3.3. TEM of Dap^{R}1 reveal a thicker cell wall at the poles and irregular septum placement compared to W168 (Fig. 3.2).
Dap^{R}1 TEM with asymmetrical, aberrant septum placement and thicker cell wall at the cell poles and division septa. Overall, 68% of cells (n=142) displayed aberrant septa and thickened cell wall. The arrows indicate: CW=cell wall, CM=cell membrane, S=septum, P=pole. Scale bars represent 0.1 µm (except for bottom right, 1.0 µm).

Transcriptomic and proteomic comparison of W168 and Dap^{R}1 reveals differences in expression. To determine gene expression levels in Dap^{R}1 and obtain clues about possible changes on a genetic level that might lead to daptomycin resistance we conducted microarray based expression profiling of Dap^{R}1 and its parent strain. We isolated total RNA from Dap^{R}1 and W168 wild-type from exponentially growing cultures. The resulting microarrays revealed significant changes on gene expression levels between Dap^{R}1 and W168. Several genes with products involved in cell wall and teichoic acid synthesis were expressed more strongly in Dap^{R}1. In turn, genes encoding for metabolic proteins (e.g. maltose or ribose transporters) and surfactin synthases, competence and sporulation proteins were expressed at a higher level in the wild-type (Appendix, Table S3.1, Fig. 3.4). The latter is consistent with the loss of competence and sporulation deficiency in Dap^{R}1.

Most strongly expressed in Dap^{R}1 are the genes encoding the YrkPQ two-component system and its regulon members: *yrkR, yrkO, yrkN, ykcB, ykcC*. The regulation of the two-component system has been studied by Ogura *et al* (24). The YrkP response regulator autoregulates the *yrkPQR* operon, and induces expression of *yrkO, yrkP*, and *ykcBC*. YrkR is homolog to PsiE (phosphate starvation inducible protein E), YrkO is a conserved membrane protein with similarity to a transporter, YrkN has similarity to an acetyltransferase, YkcB and YkcC are conserved membrane proteins with similarities to glycosyl transferases. In addition, the LiaRS two-component system regulon members are expressed to a higher level in Dap^{R}1. Previously, they were shown to be induced upon daptomycin treatment. The PspA family protein LiaH protects against daptomycin, like its homolog in *Escherichia coli* which was shown to protect against membrane perturbing agents (11, 20).

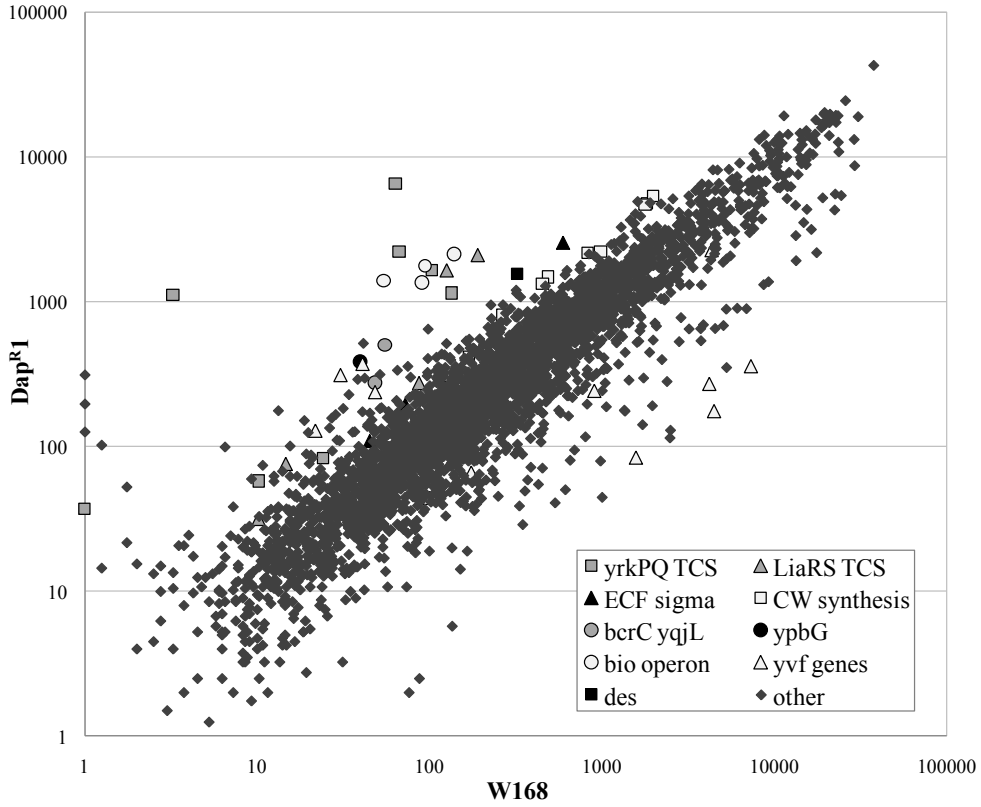

Figure 3.4. Comparison of Dap^{R}1 and W168 transcriptome.
The scatterplot represents expression levels of untreated mid-log cultures of *B. subtilis* Dap^{R}1 versus W168 of triplicate microarray analyses. The legend lists highly expressed genes, in part grouped by their corresponding transcriptional regulators.

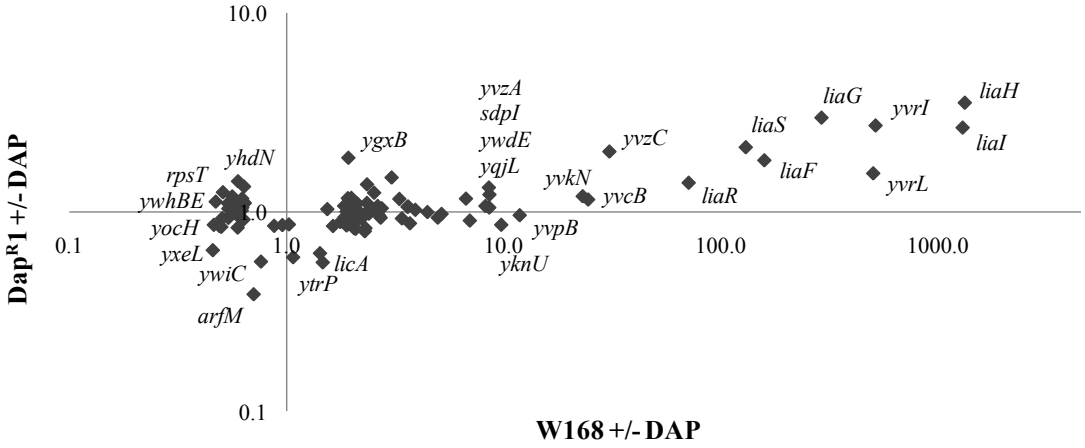

Figure 3.5. Dap^{R}1 and W168 gene expression ratios after daptomycin treatment.
The graph represents expression ratios of mid-log cultures of *B. subtilis* Dap^{R}1 versus W168 treated with daptomycin for 20 minutes at MIC levels (average of triplicate). Shown are only genes with a fold change >2 or <0.5.

Next, we were interested to see the changes on the transcriptomic level upon treatment with daptomycin (Appendix, Table S3.2, Fig. 3.5). Compared to the parent wild-type strain, Dap^{R}1 showed a weaker induction of the LiaRS two-component system including the regulon members. This can in part be explained by the fact that this regulatory system is already expressed to a high level in the mutant without treatment. A number of genes are induced in the wild-type, but are already expressed at a higher basal level in Dap^{R}1 without daptomycin treatment: *yqjL* (hydrolase; paraquat resistance), *bcrC* (bacteriocin transport permease), *ypbG* (marker for inhibition of cell wall biosynthesis), *maf* (cell division and shape determination), *murB* (UDP-N-acetylenolpyruvoyl glucosamine reductase), *murG* (peptidoglycan biosynthesis), and *sigM* (ECF σ factor). They are all involved in cell wall metabolism and could in part be responsible for the cell wall changes in Dap^{R}1. When tested for daptomycin susceptibility, deletion mutants of the above mentioned strains did not have a strong effect (Table 3.3). A *bcrC* deletion strain was slightly more sensitive to daptomycin with an MIC of 0.7 µg/mL, compared to W168 MIC of 1.0 µg/mL, but the other strains were close to wild-type within a 0.1 to 0.2 µg/mL range.

Proteomic analysis of Dap^{R}1. Differences on a transcriptomic level might not necessary reflect changes of the cellular proteome, especially as potential mutations can affect protein levels. Therefore, we set out to compare the cytosolic proteome, the extracellular proteome, and the cell wall proteome of Dap^{R}1 and W168 wild-type (Fig. 3.6-3.8). Proteins that also exhibited elevated gene expression in the corresponding microarray experiment are marked in Tables 3.5 and 3.6. Overall a lower number of proteins was changed; however, the proteins with the strongest changes in the proteomic analysis were also amongst the ones with the strongest expression changes

in the transcriptional studies. One strongly expressed protein was OppA, a binding protein of an oligopeptide ABC transporter. A deletion mutant of *oppA* was slightly more susceptible to daptomycin with an MIC of 0.7 µg/mL.

Interestingly, the exoproteome of Dap^{R}1 resembled that of an *lgt* deletion mutant (1). This mutant was shown earlier to cause shedding of at least 23 (lipo)proteins into the medium. The lipoproteine diacylglyceryl transferase (Lgt) modifies a cysteine residue in the lipobox of secretory lipoprotein precursors. Once exported, this lipid-modified cysteine residue serves to anchor the proteins to the membrane (28). Lgt, also called GerF, was not strongly altered in the microarray or proteomic analysis. However, this finding let us to test an *lgt* deletion strain for daptomycin susceptibility. With an MIC of 0.8 µg/mL it was slightly more susceptible than the wild-type. The strong resemblance of the two proteome gels led us wonder if Dap^{R}1 has a mutation in *lgt*, but this was not the case (see below).

Solexa sequencing of Dap^{R}1. Attempts to transfer the resistance phenotype of Dap^{R}1 to wild-type or to map the mutations in Dap^{R}1 by classical methods had failed. Therefore we mapped the mutations of this strain using Solexa/Illumina sequencing (http://www.illumina.com/) against the parent strain. We chose Solexa over other methods, because multiple *B. subtilis* 168 reference sequences are published, facilitating the assembly of sequencing reads. Even though the reads are shorter than with 454-based sequencing, the coverage is very high, and it is more accurate in detecting single nucleotide polymorphisms (SNP). Both sequences were assembled with MOSAIC using the published *B. subtilis* sequence with the Genebank accession number ABQK00000000 and aligned with MAQView. The sequencing coverage was relatively high, averaging 58-fold for W168 and 79-fold for Dap^{R}1.

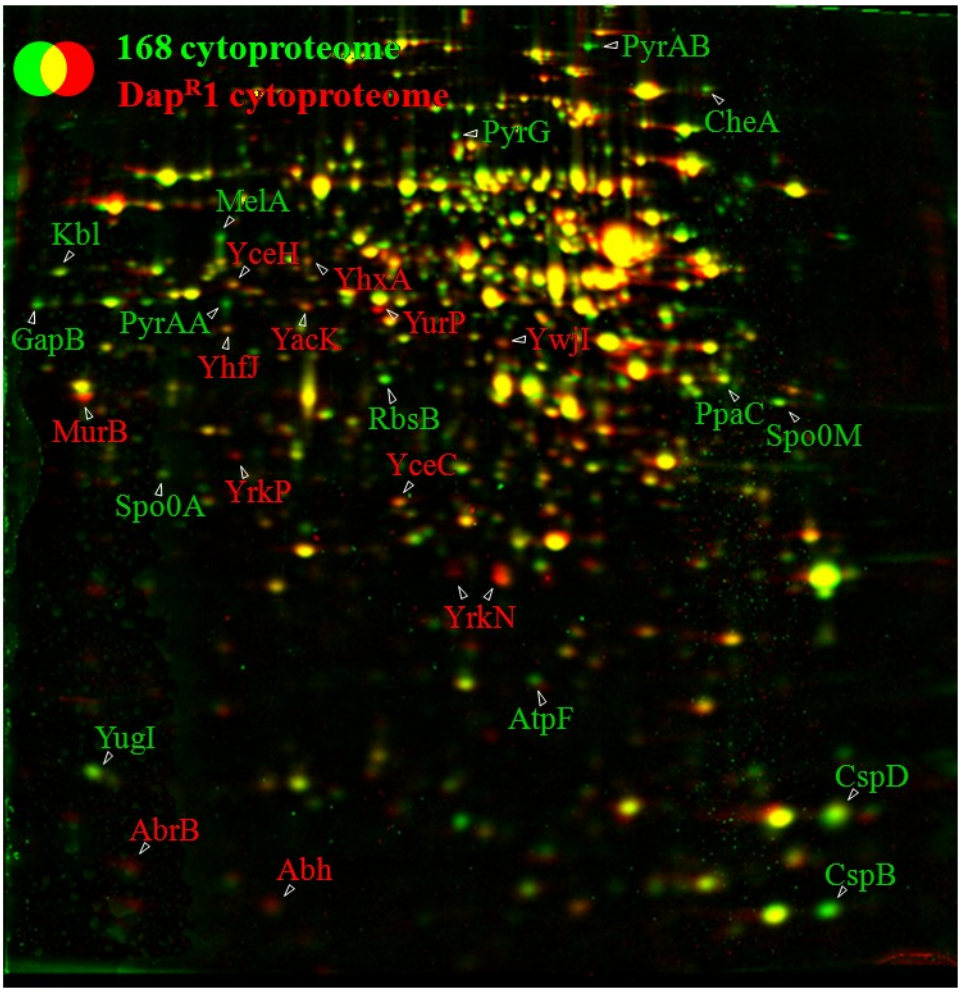

Figure 3.6. Cytoplasmic proteome.
Dual-channel image of the cytoplasmic proteome of Dap^{R}1 (red image) in comparison to W168 (green image). *B. subtilis* strains were grown in LB-broth and harvested 1 hour after entry into the stationary phase at OD_{540}=3.0. Cytoplasmic protein extracts were separated using 2D PAGE in the pH range 4-7 and the resulting 2D gels were stained with Coomassie Brilliant Blue. Quantification of the dual channel image was performed using the Decodon Delta 2D software (http://www.decodon.com). Proteins were identified using MALDI-TOF mass spectrometry as described previously (12). Proteins that display changed ratios in Dap^{R}1 compared to W168 are labeled in red (induced in Dap^{R}1) and green (repressed in Dap^{R}1). The respective protein induction and repression ratios of these proteins are listed in Table 3.7.

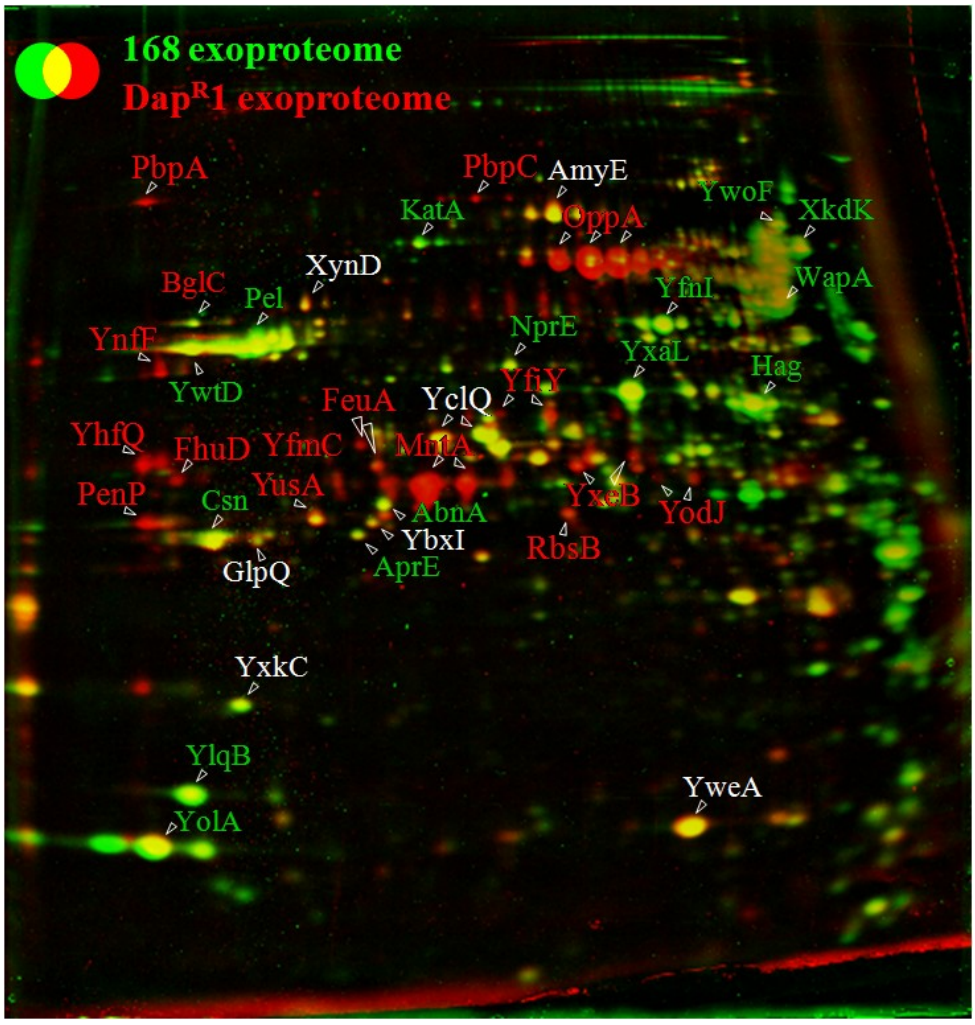

Figure 3.7. Extracellular proteome.
Dual-channel image of the extracellular proteome of Dap^{R}1 (red image) in comparison to W168 (green image). *B. subtilis* strains were grown in LB-broth and harvested 1 hour after entry into the stationary phase at OD_{540}=3.0. Extracellular proteins of the supernatant were precipitated with TCA and separated using 2D PAGE in the pH range 3-10 (1) and identified using MALDI-TOF mass spectrometry (12).Quantification of the dual channel image was performed using the Decodon Delta 2D software (http://www.decodon.com). Proteins with induced ratios in Dap^{R}1 compared to W168 are labeled in red. The expression ratios are listed in Table 3.8.

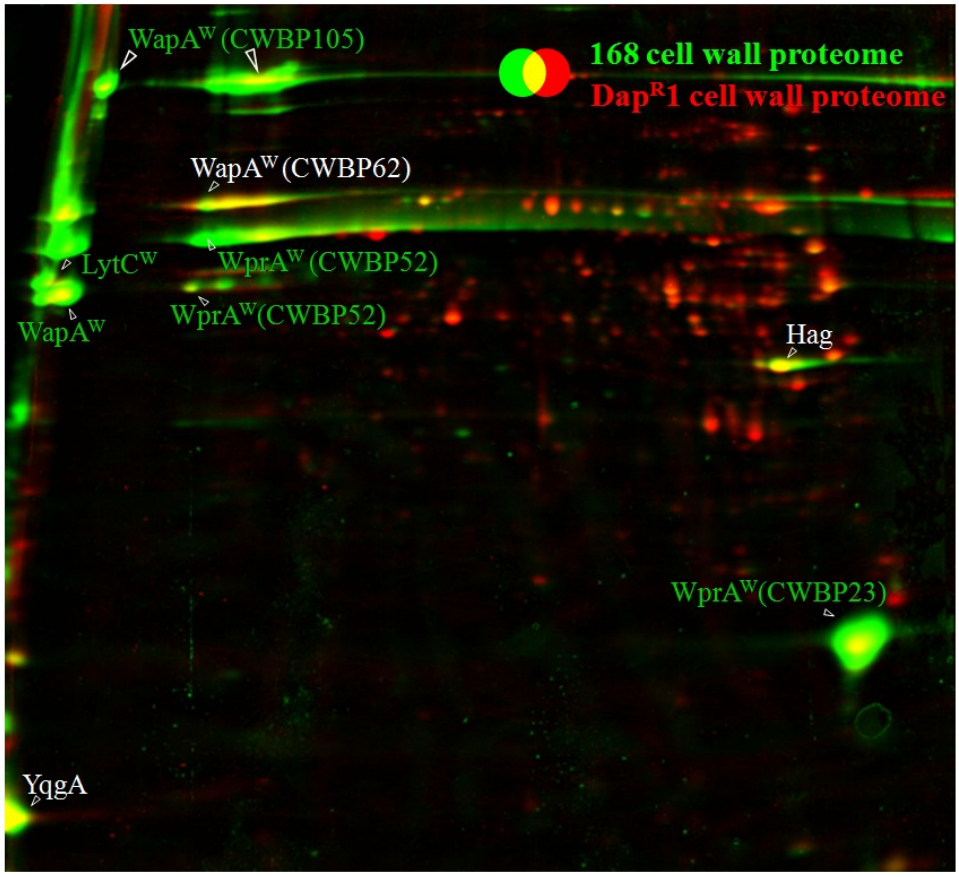

Figure 3.8. Cell wall proteome.
Dual-channel image of the cell wall proteome of Dap^{R}1 (red image) in comparison to W168 (green image). *B. subtilis* strains were grown in LB-broth and harvested 1 hour after entry into the stationary phase at OD_{540}=3.0. The cell wall-associated proteins were obtained after LiCl extraction from whole cells, precipitated with TCA and separated using 2D PAGE in the pH range 3-10 (1).The major cell wall-associated proteins (WapA, WprA) that are decreased in the cell wall fraction of Dap^{R}1are labeled in green. Note that cytoplasmic proteins accumulate in the acidic region (right) due to increased lysis in the cell wall proteome.

Table 3.5. Fold change of cytosolic protein expression of Dap^R1 and W168 without daptomycin treatment.

Protein	Ratio Dap^R1/W168	Protein Function
YrkN	5.97*	GCN5-related N-acetyltransferase
YrkP	2.43*	TCS, response regulator
MurB	4.56*	peptidoglycan synthesis
YurP	4.29	fructoselysine-6-P-deglycase
Abh	3.47*	transcriptional regulator of transition state genes (AbrB-like)
AbrB	2.17*	transcriptional pleiotropic regulator of transition state genes
YceC	2.62	tellurium resistance protein
YceH	2.16*	similar to toxic anion resistance protein
YacK	2.35	DNA integrity scanning protein DisA
YhfJ	1.83	similar to lipoate-protein ligase
AtpF	0.67	ATP synthase (subunit b)
CspC	0.32	cold-shock protein
CspD	0.63	cold-shock protein
YugI	0.60	putative RNA degradation protein
Spo0A	0.50	TCS response regulator central for the initiation of sporulation
Kbl	0.50	2-amino-3-ketobutyrate CoA ligase
PpaC	0.41	inorganic pyrophosphatase
MelA	0.36*	α -D-galactoside galactohydrolase
RbsB	0.34	ribose ABC transporter (ribose-binding protein)
GapB	0.23	glyceraldehyde-3-phosphate dehydrogenase
PyrG	0.49	CTP synthetase
PyrAB	0.28	carbamoyl-phosphate synthetase (catalytic subunit)
PyrAA	0.20	carbamoyl-phosphate synthetase (glutaminase subunit)

* genes also induced/repressed in Microarray

Table 3.6. Fold change of extracellular protein expression of Dap^{R}1 and W168 without daptomycin treatment.

Protein	Ratio Dap^{R}1/W168	Protein Function
YnfF	17.56	endo-xylanase
OppA	14.16	oligopeptide ABC transporter (binding protein)
YhfQ	13.52	iron(III) dicitrate-binding protein
FeuA	11.09	iron-uptake system (binding protein)
FhuD	8.46	ferrichrome ABC transporter (ferrichrome-binding protein)
PenP	7.84	beta-lactamase precursor
MntA	7.18	manganese ABC transporter (membrane protein)
YxeB	6.29	ABC transporter (binding protein)
PbpC	5.78	penicillin-binding protein 3
PbpA	5.70*	penicillin-binding protein 2A
BglC	3.88	endo-1,4-beta-glucanase
RbsB	3.68*	ribose ABC transporter (ribose-binding protein)
YfiY	3.25	iron(III) dicitrate transport permease
YodJ	3.17	D-alanyl-D-alanine carboxypeptidase
YusA	1.71	methionine-binding lipoprotein MetQ
XynD	1.55	endo-1,4-beta-xylanase (xylanase D)
AmyE	1.29	alpha-amylase
GlpQ	1.29	glycerophosphoryl diester phosphodiesterase
YweA	1.10	member of the processed secretome
Pel	0.97	pectate lyase
Csn	0.93	chitosanase
YwtD	0.82	murein hydrolase
WapA	0.78	cell wall-associated protein precursor
AprE	0.75	serine alkaline protease (subtilisin E)
AbnA	0.71*	arabinan-endo 1,5-alpha-L-arabinase
NprE	0.62	extracellular neutral metalloprotease
XynA	0.62	endo-1,4-beta-xylanase
YfnI	0.51*	glycerol phosphate lipoteichoic acid synthetase
YxaL	0.50	similar to serine/threonine protein kinase
Hag	0.49	flagellin protein
YolA	0.49	SPBc2 prophage-derived uncharacterized protein
XkdK	0.48*	phage-like element PBSX protein
YwoF	0.46	putative pectate lyase
YlqB	0.42*	hypothetical protein
KatA	0.32	vegetative catalase

* genes also induced/repressed in Microarray

Overall, Dap^{R}1 was found to carry 44 point mutations, of which 31 lead to a change of amino acid sequence (Table 3.8). As this is a high number of mutations, it is quite possible that many mutations occurred at random or to compensate for others, and are not responsible for resistance or the changed phenotype of Dap^{R}1. Three of the

31 SNPs in protein encoding genes are in essential genes, *nusA, mreB*, and *pgsA*, suggesting that they are mutations that alter protein activity. From the proteins that are affected by mutations, the SNPs in *pgsA, ywnE,* or *mreB*, are the most interesting ones that could have an effect on daptomycin resistance. We previously found a significant increase in daptomycin resistance upon depletion of the essential phosphatidyl glycerol synthase PgsA. This increased resistance could be due to a decrease in negatively charged lipids resulting in a stronger repulsion towards a calcium-daptomycin complex. We assume that this point mutation in Dap^R1 decreases protein activity without completely abolishing its function, because the strain is still viable with a similar growth rate like wild-type. Similarly, a mutation in *ywnE* which is involved in the production of the negatively charged membrane lipid, cardiolipin, could contribute to the repulsive effect. It is also worth noting that cardiolipin is a major component of the spore membrane (19).

Another mutation is in the essential protein MreB, which is involved in cell shape maintenance. The electron micrographs clearly show an altered cell shape for Dap^R1. Again, altered protein activity might be the case. Further interesting mutations are upstream of *murB*, and in the promoter region of *yrkO*, which could alter gene expression. Indeed, the microarrays show higher expression of both genes in Dap^R1.

Peptidoglycan analysis. The drastic changes of the cell wall of Dap^R1, as observed with electron microscopy, inspired us to perform peptidoglycan analysis of this strain to study its cell wall composition. Two independent methods, HPLC and incorporation and turnover of ^{14}C labeled N-acetylglucosamine were used to quantify muropeptides of the cell wall (Fig. 3.9). To our surprise, Dap^R1 did not stand out with a higher amount of muropeptides, when tested at different growth stages (early

exponential phase to stationary phase). This was confirmed by measuring muramic acids and di-amino-pimelic acids, which also were not significantly different from wild-type (data not shown). The thicker cell wall in Dap^R1 could thus be explained by several ideas. First, experimental lysis of the thicker cell wall of Dap^R1 could have been not as complete as that of wild-type, resulting in artificially lower values for measured peptidoglycan. This seems rather unlikely, as the samples were boiled in SDS for 30 minutes. Second, Dap^R1 perhaps does not contain much more muropeptides than the wild-type, as the increased thickness is localized only to the cell poles and does not surround the whole cell (the side walls were slightly thinner than in the wild-type). On average this might be evened out. Third, cell wall is not only composed of peptidoglycan; increased thickness might perhaps be due to teichoic acids, proteins, etc. To get a clearer image, further testing of cell wall components could be done.

Table 3.7. Single nucleotide polymorphisms in intergenic or protein coding regions.

#	Gene	Amino Acid change	Position within gene	Function of Gene Product
1	trnSL-Glu2	-	12 of 69	transfer RNA-Glu
2	intergenic	-	116bp us	116 bp upstream of start site of *ydjC* (unknown)
3	*guaA*	P477S	1429 of 1539	GMP synthetase
4	*yfhP*	R175H	524 of 981	unknown, may be a negative regulator for transcription of *yfhQ, fabL, sspE* and *yfhP*; σ^K-dependent promoter, similar to metal-dependent hydrolase
5	intergenic	-	225bp us	225 bp upstream of trnSL-Gly1 (transfer RNA-Gly)
6	intergenic	-	392bp us	392 bp upstream of *yhxA* (similar to adenosylmethionine-8-amino-7-oxononanoate aminotransferase)
7	*citR*	V50G	150 of 924	transcriptional repressor of the citrate synthase I (*citA*)
8	*med*	V151I	451 of 951	positive regulator of *comK*, upstream of *comZ*
9	*motB*	A222T	664 of 783	motility protein (flagellar motor rotation)
10	intergenic	-	372bp us	372 bp upstream of *rok* (repressor of *comK*)
11	intergenic	-	370bp us	370 bp upstream of *rok* (repressor of *comK*)
12	*ylbK*	A111V	332 of 780	similar to serine protease or patatin-like phospholipase
13	intergenic	-	26bp us	26 bp upstream of *murB* (UDP-N-acetylenolpyruvoyl-glucosamine reductase)
14	intergenic	-	137bp us	137 bp upstream of *fliK* (flagellar hook-length control)
15	*nusA**	Q112R	335 of 1113	transcription termination
16	*pgsA**	A64V	191 of 579	acidic phospholipid biosynthesis
17	*odhA*	S573T	1717 of 2823	2-oxoglutarate dehydrogenase (E1 subunit)
18	*kdgA*	P115S	343 of 588	2-keto-3-deoxygluconate-6-phosphate aldolase (σ^A-dependent)
19	*qcrC*	V210I	628 of 765	menaquinol:cytochrome c oxidoreductase
20	*qcrB*	H35Y	103 of 672	menaquinol:cytochrome c oxidoreductase
21	*serA*	R157G	469 of 1575	serine biosynthesis, phosphoglycerate dehydrogenase
22	intergenic	-	72bp us	72 bp upstream of *bmrU* (multidrug resistance protein)
23	*nusB*	N73D	217 of 393	transcription antitermination
24	*spoIIIAA*	R85G	253 of 921	stage III sporulation, mutants block sporulation after engulfment, mother-cell specific
25	*yqeG*	F5V	15 of 516	similar to HAD family phosphatase
26	*yqeB*	T95S	283 of 723	similar to ribosomal protein L29
27	intergenic	-	78bp us	78 bp upstream of *yrkO* (put. membrane protein), regulated by YrkPQ TCS
28	intergenic	-	101bp ds	101 bp downstream of *yrhP*, 10 bp downstream of *aapA* (amino acid permease)
29	intergenic	-	102bp ds	102 bp downstream of *yrhP* (homoserine/threonine efflux protein)
30	*yrhH*	A171T	511 of 540	similar to methyltransferase
31	*yrrC*	E795G	2384 of 2394	similar to exodeoxyribonuclease V alpha subunit
32	*yrrC*	M659K	1976 of 2394	similar to exodeoxyribonuclease V alpha subunit
33	*relA*	P305S	913 of 2202	GTP pyrophosphokinase, stringent response, mutant results in lowered induction of proteins involved in stress response and amino acid biosynthesis
34	*relA*	R177H	530 of 2202	GTP pyrophosphokinase, stringent response
35	*mreB**	A139V	416 of 1011	cell-shape determining protein
36	intergenic	-	68bp us	68 bp upstream of *araA* (L-arabinose isomerase converts D-galactose into D-tagatose)
37	*ytbE*	W127R	379 of 840	similar to 2,5-didehydrogluconate reductase
38	*ytbJ*	R354Q	1061 of 1074	similar to thiamin biosynthesis
39	*ytdP*	E479G	1436 of 2316	similar to transcriptional regulator (AraC/XylS family)

Table 3.7. (Continued)

#	Gene	AminoAcid change	Position within gene	Function of Gene Product
40	*cssS*	V342A	1025 of 1353	TCS HK, phosphorylates CssR, involved in cellular responses to protein secretion stress
41	*rnr*	T550M	1649 of 2337	ribonuclease R, nonspecific degradation of rRNA, 3'-5' exoribonuclease activity
42	*yvjB*	G344E	1031 of 1440	similar to carboxy-terminal processing protease
43	*ywnE*	I23T	68 of 1446	cardiolipin synthase
44	*tyrZ*	T9A	25 of 1239	tyrosyl-tRNA synthetase, minor; expressed when TyrS inactivated

* essential

Table 3.8. Fatty acid methyl esther analysis of *B. subtilis* wild-type and Dap^{R}1.

Fatty Acid	37°C		25°C	
[% content]	W168	Dap^{R}1	W168	Dap^{R}1
10:00	0.19	0.07	0.16	0.06
12:00	0.23	0.11	0.26	0.16
13:0 iso	0.13	0.15	0.13	0.11
13:0 anteiso	0.07	0.09	0.08	0.09
14:0 iso	1.28	0.57	0.88	0.35
14:1 ω5c	0	0	0.08	0
14:00	0.50	0.33	0.33	0.31
15:0 iso	15.70	17.32	15.64	14.15
15:0 anteiso	39.30	36.87	42.21	42.29
16:1 ω7c alcohol	0.12	0.17	0.93	0.55
16:0 iso	5.15	2.38	3.13	1.26
16:1 ω11c	0.27	0.54	1.91	2.17
16:1 ω5c	0	0	0.08	0
16:00	5.07	3.48	3.38	2.61
17:1 iso ω10c	0.34	1.02	2.78	3.78
17:0 iso	12.93	16.42	8.89	8.49
17:0 anteiso	16.51	18.01	15.08	17.89
17:00	0.19	0	0.11	0
17:0 2OH	0	0	0.14	0
18:1 ω9c	0.23	0.21	0.25	0.26
18:0 iso	0.15	0.10	0	0
18:00	0.75	0.78	0.60	0.62
19:0 iso	0.12	0.26	0	0.13
19:0 anteiso	0.15	0.26	0.11	0.20

Analysis of membrane fatty acids. The length and saturation status of phospholipids affects the physical properties of the bacterial cell membrane. The transcriptomic analysis has shown that the desaturase gene *des* is expressed to a higher level in Dap^{R}1, and we have found earlier an involvement of Des in daptomycin susceptibility (16). To test whether the saturation level or fatty acid composition is altered in Dap^{R}1, we submitted samples to Microbial ID for fatty acid methyl ester analysis (FAME) at 37 ^{o}C and 25 ^{o}C (Table 3.8). Overall, the composition and saturation of fatty acids in Dap^{R}1 or W168 was quite similar. At 37 ^{o}C, Dap^{R}1 showed a slight shift to longer fatty acids, with a decrease in C_{15} (15:0 anteiso) and increase in C_{17} (17:0 iso). At 25 ^{o}C, however, where an effect from the desaturase should be most pronounced, a slight shift to longer fatty acids can be seen again, but no increase in

saturation is visible when compared to W168. In contrast to the visible changes in the cell wall, the membrane phospholipid composition of Dap^{R}1 is very similar to that of its parent strain.

3.4 Conclusions.

One approach to study resistance to antimicrobial compounds is the characterization of clinical isolates of pathogenic strains, another makes use of evolving resistance *in vitro* through serial passage experiments. The latter serves as a controllable tool to monitor development of resistance over time. It is limited by the experimental set-up which does not reflect conditions present in patients or even conditions in nature (where antibiotics produced by micro-organisms might actually function as signaling molecules rather than killing factors).

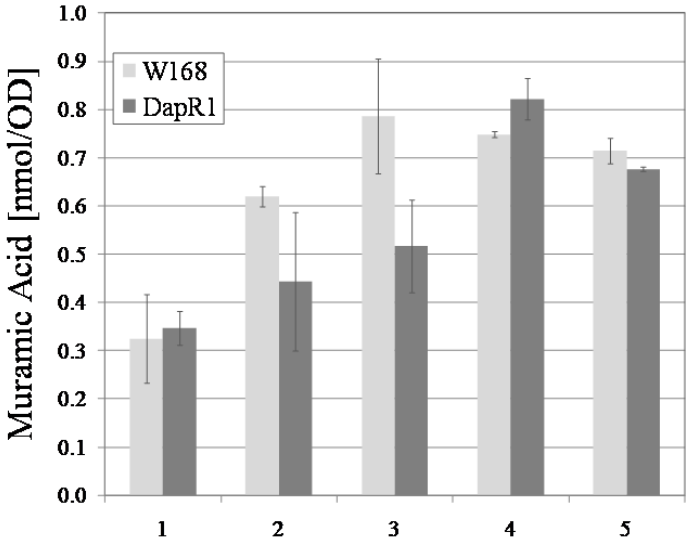

Figure 3.9. Muramic acid quantification in Dap^{R}1 and W168.
The x-axis corresponds to five sampling time points between OD_{600} of 0.3 and 3.0. The y-axis quantifies muramic acid normalized over optical density.

Also, the possibility of horizontal gene transfer is very limited under the present conditions. Nonetheless, we can learn a great deal from the frequency and amplitude of resistance. Here, we have used the Gram positive model bacterium *B. subtilis* to investigate daptomycin resistance.

The complex phenotype of the isolate Dap^R1 implied that more than one mutation is needed for daptomycin resistance. This idea was supported by our inability to transform the resistance phenotype from Dap^R1 to W168 wild-type. Similarly, attempts in our laboratory to select for resistance to daptomycin using transposon mutagenesis have been unsuccessful. Earlier, several mutations were found in *S. aureus* strains which were isolated with increasing daptomycin concentrations (14). Surprisingly, amongst the 44 point mutations in Dap^R1 was not a single one that was found previously in daptomycin resistant *S. aureus*, indicating the diversity between different bacterial species, and perhaps different mechanisms of daptomycin resistance.

The ease with which this resistant strain was obtained does not necessarily reflect a frequent occurrence of resistance in clinical settings, in particular as this study was done with the non-pathogenic *B. subtilis*, and as the incubation was performed continually over 55 days (much longer than average treatment in a patient). However, it should not be disregarded; instead, similar studies done with pathogenic strains, like (14), might uncover parallel resistance mechanisms that can be taken into account when considering treatment options or when developing new antibiotics.

REFERENCES

1. **Antelmann, H., H. Tjalsma, B. Voigt, S. Ohlmeier, S. Bron, J. M. van Dijl, and M. Hecker.** 2001. A proteomic view on genome-based signal peptide predictions. Genome Res **11:**1484-502.

2. **Antelmann, H., H. Yamamoto, J. Sekiguchi, and M. Hecker.** 2002. Stabilization of cell wall proteins in Bacillus subtilis: a proteomic approach. Proteomics **2:**591-602.

3. **Atrih, A., G. Bacher, G. Allmaier, M. P. Williamson, and S. J. Foster.** 1999. Analysis of peptidoglycan structure from vegetative cells of Bacillus subtilis 168 and role of PBP 5 in peptidoglycan maturation. J Bacteriol **181:**3956-66.

4. **Bisicchia, P., D. Noone, E. Lioliou, A. Howell, S. Quigley, T. Jensen, H. Jarmer, and K. M. Devine.** 2007. The essential YycFG two-component system controls cell wall metabolism in Bacillus subtilis. Mol Microbiol **65:**180-200.

5. **Bradford, M. M.** 1976. A rapid and sensitive method for the quantitation of microgram quantities of protein utilizing the principle of protein-dye binding. Anal Biochem **72:**248-54.

6. **Butcher, B. G., and J. D. Helmann.** 2006. Identification of Bacillus subtilis sigma-dependent genes that provide intrinsic resistance to antimicrobial compounds produced by Bacilli. Mol Microbiol **60:**765-82.

7. **Camargo, I. L., H. M. Neoh, L. Cui, and K. Hiramatsu.** 2008. Serial daptomycin selection generates daptomycin-nonsusceptible Staphylococcus aureus strains with a heterogeneous vancomycin-intermediate phenotype. Antimicrob Agents Chemother **52:**4289-99.

8. **Cao, M., and J. D. Helmann.** 2002. Regulation of the Bacillus subtilis bcrC bacitracin resistance gene by two extracytoplasmic function sigma factors. J Bacteriol **184:**6123-9.

9. **Cao, M., C. M. Moore, and J. D. Helmann.** 2005. Bacillus subtilis paraquat resistance is directed by sigmaM, an extracytoplasmic function sigma factor, and is conferred by YqjL and BcrC. J Bacteriol **187:**2948-56.

10. **Cui, L., X. Ma, K. Sato, K. Okuma, F. C. Tenover, E. M. Mamizuka, C. G. Gemmell, M. N. Kim, M. C. Ploy, N. El-Solh, V. Ferraz, and K. Hiramatsu.** 2003. Cell wall thickening is a common feature of vancomycin resistance in Staphylococcus aureus. J Clin Microbiol **41:**5-14.

11. **Darwin, A. J.** 2005. The phage-shock-protein response. Mol Microbiol **57:**621-8.

12. **Eymann, C., A. Dreisbach, D. Albrecht, J. Bernhardt, D. Becher, S. Gentner, T. Tam le, K. Buttner, G. Buurman, C. Scharf, S. Venz, U. Volker, and M. Hecker.** 2004. A comprehensive proteome map of growing Bacillus subtilis cells. Proteomics **4:**2849-76.

13. **Falagas, M. E., K. P. Giannopoulou, F. Ntziora, and K. Z. Vardakas.** 2007. Daptomycin for endocarditis and/or bacteraemia: a systematic review of the experimental and clinical evidence. J Antimicrob Chemother **60:**7-19.

14. **Friedman, L., J. D. Alder, and J. A. Silverman.** 2006. Genetic changes that correlate with reduced susceptibility to daptomycin in Staphylococcus aureus. Antimicrob Agents Chemother **50:**2137-45.

15. **González-Castro, M. J., J. López-Hernández, J. Simal-Lozano, and M. J. Oruña-Concha.** 1997. Determination of amino acids in green beans by derivitization with phenylisothiocyanate and high-performance liquid chromatography with ultraviolet detection. J. Chrom. Sci. **35:**181-185.

16. **Hachmann, A. B., E. R. Angert, and J. D. Helmann.** 2009. Genetic analysis of factors affecting susceptibility of Bacillus subtilis to daptomycin. Antimicrob Agents Chemother **53:**1598-609.

17. **Igarashi, T., B. Setlow, M. Paidhungat, and P. Setlow.** 2004. Effects of a gerF (lgt) mutation on the germination of spores of Bacillus subtilis. J Bacteriol **186:**2984-91.

18. **Jones, T., M. R. Yeaman, G. Sakoulas, S.-J. Yang, R. A. Proctor, H.-G. Sahl, J. Schrenzel, Y. Q. Xiong, and A. S. Bayer.** 2008. Staphylococcus aureus Clinical Treatment Failures with Daptomycin are Associated with Alterations in Surface Charge, Membrane Phospholipid Asymmetry and Drug Binding. Antimicrob. Agents Chemother. **52:** 269-278.

19. **Kawai, F., H. Hara, H. Takamatsu, K. Watabe, and K. Matsumoto.** 2006. Cardiolipin enrichment in spore membranes and its involvement in germination of Bacillus subtilis Marburg. Genes Genet Syst **81:**69-76.

20. **Kobayashi, R., T. Suzuki, and M. Yoshida.** 2007. Escherichia coli phage-shock protein A (PspA) binds to membrane phospholipids and repairs proton leakage of the damaged membranes. Mol Microbiol **66:**100-9.

21. **Mascher, T., N. G. Margulis, T. Wang, R. W. Ye, and J. D. Helmann.** 2003. Cell wall stress responses in Bacillus subtilis: the regulatory network of the bacitracin stimulon. Mol Microbiol **50:**1591-604.

22. **McPherson, D. C., and D. L. Popham.** 2003. Peptidoglycan synthesis in the

absence of class A penicillin-binding proteins in Bacillus subtilis. J Bacteriol **185:**1423-31.

23. **Meador-Parton, J., and D. L. Popham.** 2000. Structural analysis of *Bacillus subtilis* spore peptidoglycan during sporulation. J. Bacteriol. **182:**4491-4499.

24. **Ogura, M., T. Ohsawa, and T. Tanaka.** 2008. Identification of the sequences recognized by the Bacillus subtilis response regulator YrkP. Biosci Biotechnol Biochem **72:**186-96.

25. **Sader, H. S., A. A. Watters, T. R. Fritsche, and R. N. Jones.** 2007. Daptomycin antimicrobial activity tested against methicillin-resistant staphylococci and vancomycin-resistant enterococci isolated in European medical centers (2005). BMC Infect Dis **7:**29.

26. **Sauermann, R., M. Rothenburger, W. Graninger, and C. Joukhadar.** 2007. Daptomycin: A Review 4 Years after First Approval. Pharmacology **81:**79-91.

27. **Silverman, J. A., N. G. Perlmutter, and H. M. Shapiro.** 2003. Correlation of daptomycin bactericidal activity and membrane depolarization in Staphylococcus aureus. Antimicrob Agents Chemother **47:**2538-44.

28. **Tjalsma, H., A. Bolhuis, J. D. Jongbloed, S. Bron, and J. M. van Dijl.** 2000. Signal peptide-dependent protein transport in Bacillus subtilis: a genome-based survey of the secretome. Microbiol Mol Biol Rev **64:**515-47.

29. **Turner, M. S., and J. D. Helmann.** 2000. Mutations in multidrug efflux homologs, sugar isomerases, and antimicrobial biosynthesis genes differentially elevate activity of the sigma(X) and sigma(W) factors in Bacillus subtilis. J Bacteriol **182:**5202-10.

30. **Vander Horn, P. B., and S. A. Zahler.** 1992. Cloning and nucleotide sequence of the leucyl-tRNA synthetase gene of Bacillus subtilis. J Bacteriol **174:**3928-35.

31. **Wach, A.** 1996. PCR-synthesis of marker cassettes with long flanking homology regions for gene disruptions in S. cerevisiae. Yeast **12:**259-65.

CHAPTER 4

Tn7SX TRANSPOSON MUTAGENESIS: A TOOL TO STUDY ANTIBIOTIC RESISTANCE MECHANISMS IN *BACILLUS SUBTILIS*

Occurrence of antibiotic resistance is an increasing concern during chemotherapy. Understanding mechanisms causing the resistance can be valuable to target antimicrobial therapy more specificly, and for the design of new antibiotics to circumvent, or delay the development of resistance. In an effort to learn more about resistance to cell envelope active antibiotics, we have used Tn7SX transposon mutagenesis in the Gram-positive model bacterium *Bacillus subtilis*. Two main features of Tn7SX can result in decreased susceptibility: the transposon can insert into a gene and thereby, for instance, disrupt an antibiotic target, or it can lead to overexpression of downstream genes via its xylose inducible promoter, thereby initiating other ways of resistance. As a proof-of-principle we show that the transposon inserted multiple times independently into the *pssA-ybfM-psd* operon when selecting for duramycin resistance. The *pssA* operon synthesizes the membrane lipid target of duramycin, phosphatidyl ethanolamine. In addition, we obtained transposon insertions in 25 different genes that each conferred resistance to the transglycosylase inhibitor moenomycin. Moreover, coupling Tn7SX with replica plating allowed us to screen for increased susceptibility to the cell wall synthesis inhibitor fosfomycin. This type of screen could potentially identify new antibiotic targets demonstrating the versatility of the Tn7SX transposon mutagenesis system.

The majority of the studies in this chapter were performed by A. B. Hachmann, Christophe Bordi (Aix-Marseille Université, France) contributed to the identification

of duramycin-resistant transposants, and Michael Somuah (Kentucky State University) assisted with the fosfomycin susceptibility screening. Parts of the results of this study were published in C. Bordi, B. G. Butcher, Q. Shi, A. B. Hachmann, J. E. Peters, and J. D. Helmann. 2008. Appl Environ Microbiol 74:3419-25.

4.1 Introduction

Transposon mutagenesis serves as a valuable genetic tool for a variety of applications. The Tn7SX transposon mutagenesis system (Fig. 4.1) (6), adapted from the Tn7 transoposon and the EZ::TN transposase system by GeneHunter (50, 59), is characterized by high efficiency of transposition and random and stable insertions (6). Genes disrupted by the transposon can be identified for instance as antibiotic targets. Addition of xylose induces a P_{xylA} promoter in the transposon and can result in overexpression of downstream genes, thereby allowing for the identification of genes that can confer resistance to certain stresses.

We have used Tn7SX in *Bacillus subtilis* to discover resistance mechanisms to cell envelope active antibiotics. Here, we discuss Tn7SX insertions which we found to confer resistance to the cell envelope synthesis inhibitors moenomycin, penicillin G, cephalosporin C, and duramycin. In addition, we have used this system to screen for increased antibiotic susceptibility. We have found multiple ways in which cells can become more sensitive to the cell wall synthesis inhibitor fosfomycin, providing more details about mechanisms of detoxification.

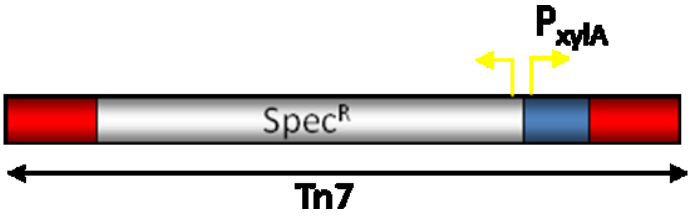

Figure 4.1. The Tn7SX transposon.
Insertions by Tn7SX can either disrupt gene function, or conditionally activate expression of downstream genes in the presence of xylose.

4.2 Materials and Methods

Bacterial strains and growth conditions. Bacteria were cultured at 37°C with vigorous shaking using Luria Bertani (LB) as growth medium.The following antibiotics were used for selection when necessary: spectinomycin 100 µg/mL, kanamycin 10 µg/mL, chloramphenicol 10 µg/mL, tetracycline 20 µg/mL, and erythromycin 1 µg/mL with lincomycin 25 µg/ml (mls: macrolide-lincomycin-streptogramin B resistance). The strains used in this study were derived from *Bacillus subtilis* wild-types W168 (*trpC2*) and CU1065 (W168 *trpC2 att*SPβ) and are listed in Table 4.1 and Table 4.4. Gene deletions were generated by replacing open reading frames with antibiotic resistance cassettes using long-flanking-homology PCR (42, 68). Moenomycin was kindly provided by Biovet JSC (Bulgaria).

Minimal inhibitory concentrations (MIC) were determined by diluting overnight cultures 1:100, growing to OD_{600} of 0.4, and re-diluteding to 5 x 10^5 CFU/mL in microtiter plates with a total inoculum of 200 µL. Growth was measured spectrophotometrically (OD_{600}) using a Bioscreen incubator (Growth Curves USA, Piscataway, NJ) at 37°C with vigorous shaking. The absorbance was recorded every 20 minutes for 24 hours. Inhibition was defined as a final $OD_{600} < 0.05$ (at the 24 hour time point). In most cases, *B. subtilis* wild-type or mutants treated with moenomycin did not result in a clear determinable MIC, but rather in a delayed lag phase. After 24h W168 was able to grow even with addition of 500µ/ml or 2000µ/ml moenomycin. Here, to compare different mutants, we used the ability to outgrow a certain moenomycin concentration after a particular time as a measure of susceptibility.

Table 4.1. Strains and oligonucleotides used in this study.
(additionol strains are listed in Table 4.4)

strains	genotype, remarks, purpose	reference, construction
W168	*trpC2*	BGSC no. 1A1
CU1065	W168 *trpC2 att*SPß	lab stock (67)
DPVB49	Δ*pbpD pbpG*::*kan pbpF*::Erm^r	(44)
HB0031	CU1065 *sigM::kan*	(12)

Tn7SX transposon mutagenesis. The pTn7SX transposon is characterized by a spectinomycin resistance marker and a xylose inducible promoter P_{xylA}, adapted from the EZ::TN transposase system by GeneHunter (Fig. 4.1) (59). For in-vitro transposon reactions proteins TnsA, TnsB, and TnsC* were used (Table 4.2). TnsC* carries an A225V gain-of-function mutation, resulting in loss of target specificity. For further details about this system see reference (6). We obtained a random and highly efficient transposition with approximately 55,000 clones per reaction, on average corresponding to one insertion per 75 base pairs.

Selection of duramycin-resistant mutants. The in-vitro transposition reaction was performed as described in (6). After gap-repair, the transformation of the transposition library into *B. subtilis* CU1065 cells was plated on solid LB containing spectinomycin and xylose to select for duramycin-resistant (Dur^r) mutants. After incubation for 5 h at 37°C, these plates were overlaid with 5 ml of soft LB agar (0.7%) containing spectinomycin, xylose, and 6 μg/ml duramycin and incubated at 37°C overnight. Clones were checked for insertion of Tn7SX into the *pssA* operon by PCR with primers 2369 and 1916. MICs for these resistant mutants and wild-type *B. subtilis* were determined by growth (optical density at 600 nm) after incubation overnight at 37°C in microtiter plates with LB containing 0, 1, 1.5, 2, 5, 20, 30, 40, 50, 75, 100, 150, and 200 μg/ml duramycin and either 2% xylose or glucose.

Selecting of moenomycin resistant mutants. This selection was carried out on LB agar plates with different concentrations of moenomycin using an amplified version of the Tn7SX library. Therefore, random Tn7SX in-vitro reaction was performed as described previously (6), with the following modifications. Two reactions were transformed into W168, grown over night in 20ml LB, combined, and chromosomal DNA was extracted. This was repeated with cultures grown with 2% xylose in order to induce the P_{xylA} promoter of the transposon. The libraries of chromosomal DNA were used to transform the transposon into different background strains (W168, CU1065, *sigM*, *pbpDFG*; Table 4.4). Most mutants were obtained by selecting at 0.4µg/ml moenomycin and 2% xylose, mutants M36 - M50 were selected at 10µg/ml , and M51-M56 at 1µg/ml. Mutants M89-M95 were obtained directly after in-vitro transposition and selected at 10µg/ml moenomycin. Mutants were confirmed by sequencing, linkage tests, and growth inhibition studies.

Screening of fosfomycin-sensitive mutants. Fosfomycin-sensitive (Fos^S) mutants were selected by plating *B. subtilis* W168 transformed with the amplified Tn7SX transposition library on solid LB plates containing spectinomycin, with or without 2% xylose. Supsequent transfer of the colonies into microtiter plates and replica plating on plates containing 30 µg/ml fosfomycin was used as a measure to identify fosfomycin sensitive mutants. MICs of these mutants were determined as described above (for duramycin), with the following concentrations of fosfomycin: 0, 10, 20, 30, 40, 50, 60, 70, 80, 100, 150, and 200 µg/ml. Insertions are summarized in Table 4.7.

Table 4.2. Tn7 proteins and their roles during transposition.

Protein	Function	Biochemical activities	Structural motifs or homologs
TnsA	transposase subunit	cutting at the 5' ends of Tn7	Type II restriction enzymes
TnsB	transposase subunit	cutting and joining at the 3' ends of Tn7	retroviral integrases and transposase DDE motif
TnsC	regulator/connector	ATP-dependent DNA binding and ATP hydrolysis	nucleotide-binding motif
TnsD	target selection – recognition of *attTn7*	sequence-specific DNA binding	none
TnsE	target selection – conjugal replication/lagging-strand DNA synthesis	structure-specific DNA binding: 3' recessed ends	none

Table adapted from Peters *et al*. (50)

4.3 Results and Discussion

Isolation of duramycin-resistant mutants. We used the Tn7SX transposon system to isolate mutants with increased resistance to the lantibiotic duramycin. Duramycin is a 10-amino-acid tetracyclic peptide produced by *Streptoverticillium cinnamoneum* that binds exclusively to ethanolamine phospholipids (29). Duramycin-resistant *B. subtilis* mutants have little or no phosphatidylethanolamine (PE) and cardiolipin, but the mutant loci were not determined (16).

Our first attempts to isolate Dur^r mutants by plating the *B. subtilis* transformants directly on duramycin-containing LB plates failed. Since duramycin resistance appears to be conferred by a change in membrane composition, we hypothesized that our method did not allow for sufficient growth in the absence of selection for the effects of Tn7SX insertions to manifest themselves as changes in the membrane lipid composition. Therefore, we plated the transformed cells on LB agar containing spectinomycin (for selection of the mutants) and xylose (to allow for upregulation from the P_{xylA} promoter) and incubated these plates for 5 h to allow time for potential alterations in membrane composition to become manifest. These plates

were then overlaid with 0.7% soft LB agar containing spectinomycin, xylose, and 6 μg/ml duramycin and incubated overnight. We obtained 60 clones resistant to duramycin upon restreaking on plates containing 10 μg/ml duramycin.

Since the *pssA-ybfM-psd* operon is required for the synthesis of PE and cardiolipin, we checked whether any of these mutations were at this locus and found that 53 of the 60 clones gave a PCR product consistent with insertion of Tn7SX within this region. We prepared chromosomal DNA from 10 of the 53 putative *pssA-ybfM-psd*::Tn7SX clones and used this to transform *B. subtilis* CU1065. Transformants were selected on spectinomycin, and in all cases subsequent testing revealed that these transformants were resistant to more than 200 μg/ml duramycin. This confirmed that the resistance phenotype was linked to disruption of the *pssA* operon by Tn7SX. Mapping of the Tn7SX junctions indicated that each insertion was unique, and they were found regularly spaced throughout all three genes of the operon. Analysis of chromosomal DNA from the other seven isolates indicated that the Dur^r phenotype was not linked to the mTn7SX insertion, suggesting that a second mutation (presumably within the *pssA-ybfM-psd* operon) was responsible for the resistance phenotype.

Phosphatidylserine (PS) synthase (encoded by *pssA*) catalyzes the formation of PS, the first step in PE synthesis (Fig. 4.2). PS is rapidly converted to PE by PS decarboxylase (encoded by *psd*). Therefore, the disruption of these genes results in a lack of PE in the membrane and insensitivity to duramycin (60). The function of YbfM is unknown; however, we have shown that nonpolar mutations within its gene do not result in duramycin resistance (60). Therefore, the insertions that we isolated within this gene are predicted to be polar on the downstream *psd* gene. Since we

obtained multiple unique insertions across the *pssA-ybfM-psd* operon, we suspect that we have saturated the screen, indicating that there are no other genes within the *B. subtilis* genome that, when disrupted or overexpressed, result in duramycin resistance.

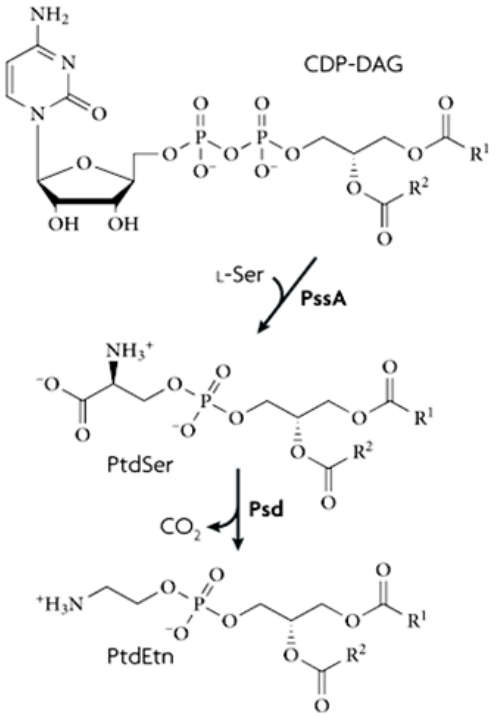

Figure 4.2. Synthesis of phosphatidylethanolamine.
PssA catalyses synthesis of phosphatidylserine (PtdSer) from CDP-diacylglycerol (CDP-DAG). PtdSer is decarboxylated by Psd to phosphatidylethanolamine (PtdEtn) (71).

Moenomycin – an antibiotic with one cellular target, but many mechanisms of resistance. In *Bacillus subtilis*, peptidoglycan is synthesized by high molecular weight (HMW) penicillin binding proteins (PBP) that are bifunctional, performing both transglycosylation and transpeptidation reactions (Table 4.3). The glycolipid moenomycin binds to and inhibits HMW PBPs by mimicking the membrane bound disaccharide substrate of the growing glycan chain (Fig. 4.3).

Moenomycin is a strong inducer of the extracytoplasmic σ factor (ECF) σ^M in

B. subtilis (see Chapter 5, Table 5.3). This is consistent with the fact that σ^M is induced by other cell wall active agents, and that it regulates genes involved in cell envelope synthesis and regulation, shape determination and cell division. In turn, a *sigM* deletion strain is much more sensitive to moenomycin than wild-type W168 (Fig. 4.4).

Table 4.3. High molecular weight penicillin binding proteins in *B. subtilis*.

Gene	Protein	Function	Localization
ponA	PBP1	cell division-specific transglycosylase/ transpeptidase, vegetative	septal (shown by immuno-fluorescence, GFP-fusion) (49, 53, 62)
pbpD	PBP4	not known, vegetative	distributed along membrane with distinct spots at periphery (GFP) (53, 62)
pbpF	PBP2c	synthesis of spore peptidoglycan, vegetative, late stages of sporulation	distributed along membrane, redistributed to prespore during sporulation (GFP) (43, 61, 62)
pbpG	PBP2d	synthesis of spore peptidoglycan, sporulation	distributed along membrane (GFP), redistributed to prespore during sporulation (43, 61, 62)

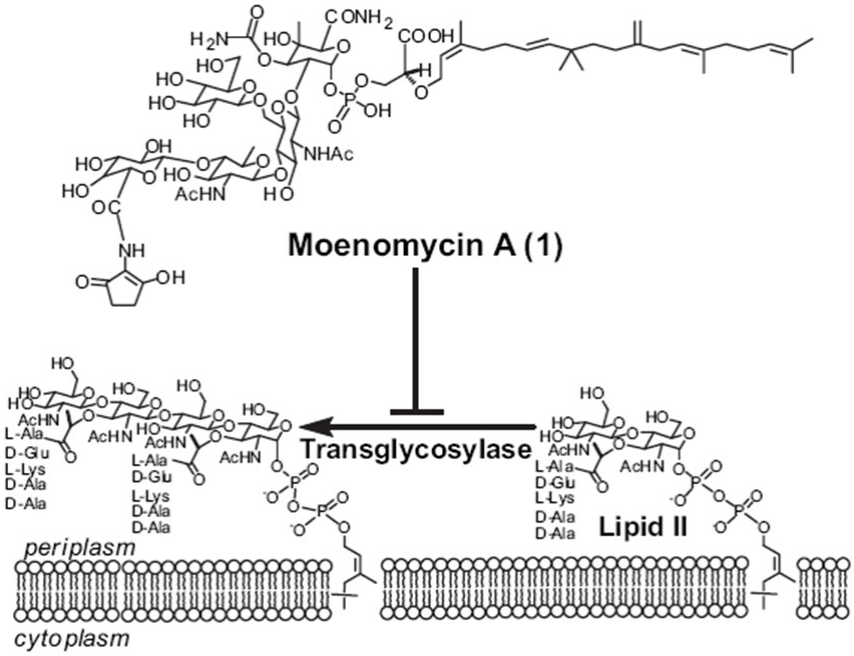

Figure 4.3. Structure and target of moenomycin.
The growing peptidoglycan chain is crosslinked by extracytoplasmic domains of transglycosylases. Moenomycin is a glycolipid antibiotic that mimics the sugar component of lipid II and therefore binds to transglycosylases (13).

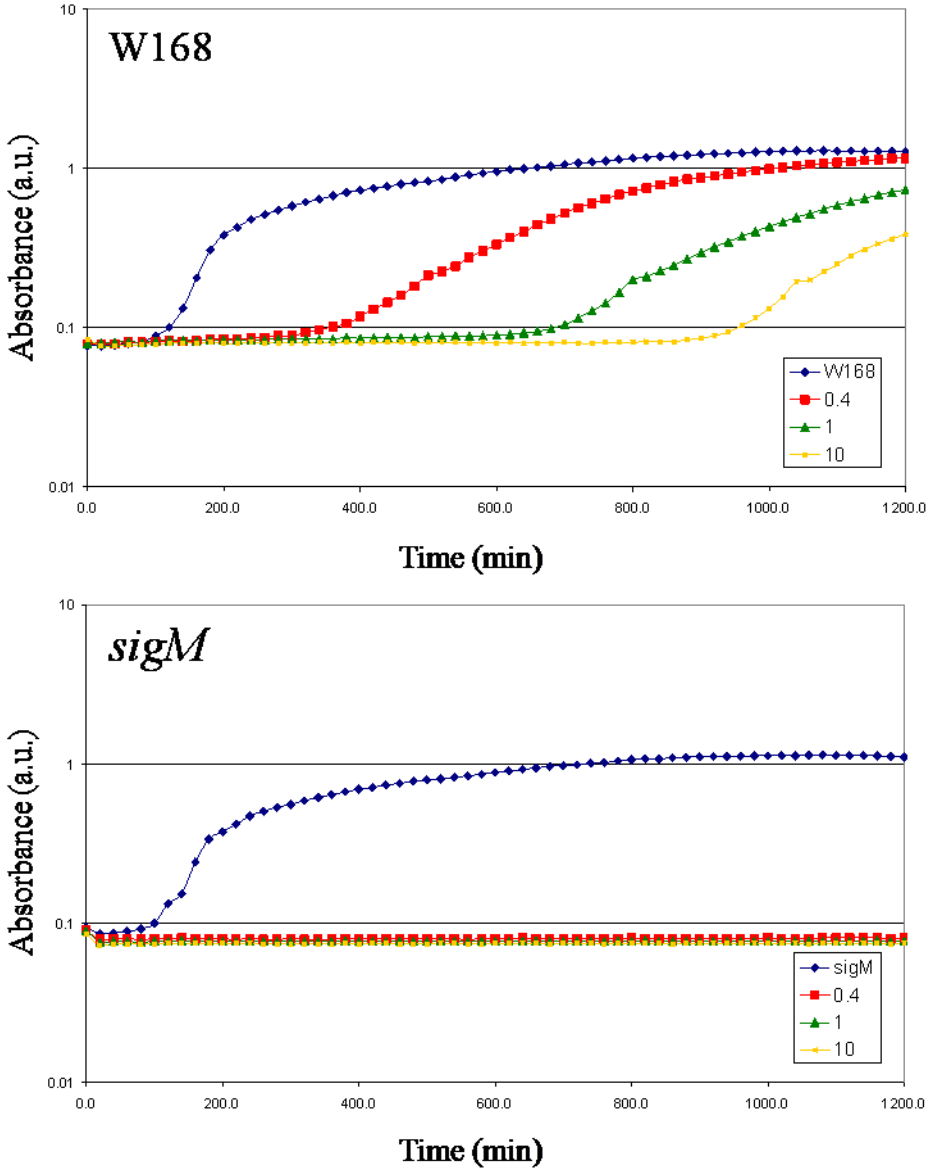

Figure 4.4. Growth inhibition of W168 and a sigM deletion by moenomycin.
The graph measures absorbance over time. The colors of the growth curves represent different moenomycin concentrations: blue 0µg/ml, red 0.4 µg/ml, green 1.0µg/ml, and yellow 10 µg/ml. Both strains grow equally fine without moenomycin (blue). Whereas wild-type W168 outgrows moenomycin after a prolonged lag-phase, *sigM* is much more susceptible at the shown concentrations.

Produced by *Streptomyces* species, the transglycosylase inhibitor moenomycin is highly active against a broad range of Gram-positive organisms (25). Poor absorption limited its effectiveness in humans; however, it is widely used as a growth promoter in animal feeding. Although having been used for more than 30 years in the animal industry (25), reports about resistance to moenomycin have been rare (10).

A plausible mechanism of resistance would include upregulation of an alternative transglycosylase. Popham *et al.* have shown that a *B. subtilis* mutant lacking all four HMW PBPs (which are known transglycosylases) was still viable (44). As could be expected, this strain was resistant to moenomycin. This indicates that another enzyme could perform the transglycosylase function (since the strain was viable), but is structurally not too similar to the known transglycosylases, or else it would be a target for moenomycin. In fact, no homologs have been found to date. One option could involve a partial synthesis of peptidoglycan subunits to oligomers at the cytoplasmic side of the cell membrane before being flipped to the periplasm. This phenomenon prompted us to take a closer look at mutations that could affect resistance to moenomycin. In particular we wondered if the xylose inducible promoter of the Tn7SX transposon would be useful to direct our search towards the alternative transglycosylase; if overexpressed through addition of xylose, this could confer resistance to moenomycin.

To increase the likelihood of finding a transposon insertion upstream of a transglycosylase, we used a triple mutant missing three out of the four HMW PBPs, *pbpDFG*. We were unable to use the quadruple deletion mutant, which misses all four HMW PBPs, because it is no longer competent, grows at a slower rate, and lyses earlier than wild-type (data not shown). In addition, we also used a *sigM* deletion as a

background strain, because it is much more susceptible to moenomycin (Fig. 4.4); and σ^M regulates *ponA*, one of the four HMW PBPs that are targeted by moenomycin. In an independent study we found *ponA* expressed at a lower level in a *sigM* deletion strain (Chapter 5, Table 5.3); this perhaps increases the chance for upregulation of an alternative transglycosylase.

To our great surprise, we readily obtained moenomycin resistant mutants using Tn7SX transposon mutagenesis (detailed in Table 4.4, summarized in Table 4.5). We found 95 insertions in 25 different genes and two in intergenic regions that decreased susceptibility to moenomycin (Fig. 4.5). Most phenotypes are independent of xylose, meaning, they are caused by gene disruption with the transposon. However, in two mutants the resistance is clearly dependent on addition of xylose. One has a Tn7SX insertion in the YdfH histidine kinase gene of a two-component regulatory system (TCS), with the xylose inducible promoter facing towards the response regulator. We hypothesize that the addition of xylose drives expression of the response regulator and thereby upregulates expression of genes that can confer resistance. In the next paragraphs, we will focus on a subset of insertions in more detail.

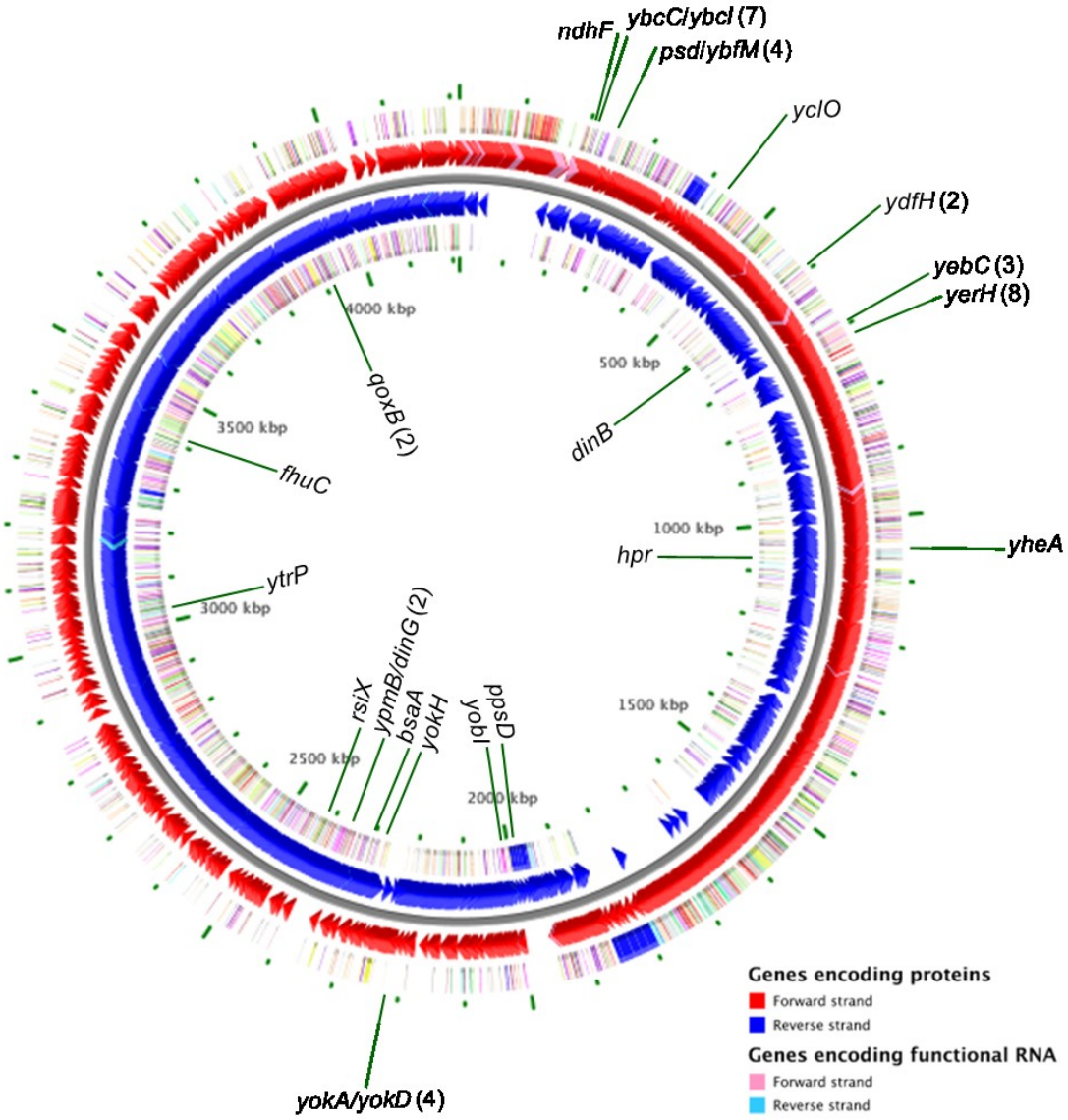

Figure 4.5. Distribution of moenomycin resistant Tn7SX insertions across the *B. subtilis* chromosome.
Ilustrated are genes on the forward (red) or reverse (blue) strand that were disrupted by the Tn7SX transposon. The number of different insertions obtained in separate transposition events in a gene is given in parenthesis (no number indicates one insertion in the respective gene). The chromosome map was created using BacMap (64).

Table 4.4. Moenomycin resistant Tn7SX insertions in W168, CU1065, *sigM*, and *pbpDFG*.

Strain	Gene	Tn7SX insertion site[1]	Gene Function	Down-stream gene	moenomycin out-growth after X min.[3] without/ with xylose		Strain back-ground[4]
M01	*qoxB*	970 (-)	cytochrome aa3 quinol oxidase (subunit I)	*ywzA* (transglycosylase associat. protein)	300	320	W168
M02	*ybcD*	959 (+)	conserved unknown	*ybcF* (carbonic anhydrase)	360	300	W168
M03	*yerH*	143 (-)	putative lipoprotein	*yerI (kinase)*			W168
M04	*ydfH*	383 (+)	TCS histidine kinase	*ydfI* (TCS RR)	660	400	W168
M05	*yerH*	143 (-)	putative lipoprotein	*yerI*			
M06	*yerH*	420 (-)	putative lipoprotein	*yerI*	260	260	CU1065
M07	*yerH*	493 (-)	putative lipoprotein	*yerI*	300	260	CU1065
M08	*yerH*	465 (-)	putative lipoprotein	*yerI*	300	280	CU1065
M09	*ypmB*	30 (-)	similar to propeptide PepSY	*aspB* (aspartate aminotransferase)	340	160	CU1065
M10	*ypmB*	30 (-)	similar to propeptide PepSY	*aspB*	n.t.	n.t.	CU1065
M11	*yerH*	493 (-)	putative lipoprotein	*yerI*	n.t.	n.t.	CU1065
M12	-		sequencing gave no hits		240	240	CU1065
M13	*dinG*	2102 (-)	ATP dependent DNA helicase	*ypmAB*	240	240	CU1065
M14	*ypmB*	30 (-)	similar to propeptide PepSY	*aspB*	n.t.	n.t.	CU1065
M15	*yclO*	89 (+)	ferrichrome ABC transporter	yclP (permease)	260	260	CU1065
M16	*ypmB*	30 (-)	similar to propeptide	*aspB*	n.t.	n.t.	CU1065
M17	*dinG*	2258 (-)	ATP dependent DNA helicase	*ypmAB*	n.t.	n.t.	CU1065
M18	*ypmB*	30 (-)	similar to propeptide PepSY	*aspB*	n.t.	n.t.	CU1065
M19	*ypmB*	30 (-)	similar to propeptide PepSY	*aspB*	n.t.	n.t.	CU1065
M20	*yerH*	420 (-)	putative lipoprotein	*yerI*	n.t.	n.t.	CU1065
M21	*yerH*	475 (-)	putative lipoprotein	*yerI*	260	220	W168
M22	*ydfH*	938 (+)	histidine kinase	*ydfI*	720	380	W168
M23	-		no hits		240	240	W168
M24	*ypmB*	30 (-)	similar to propeptide PepSY	*aspB*	220	180	W168
M25	*yerH*	1183 (-)	putative lipoprotein	*yerI*	240	240	W168
M26	*ybcD*	144 (-)	conserved unknown	*ybcF*	240[2]	220[2]	W168
M27	-		no hits		680	660	W168
M28	-		no hits		240	240	W168
M29	*ypmB*	30 (-)	similar to propeptide PepSY	*aspB*	n.t.	n.t.	W168
M30	*ybcI*	51 (-)	conserved unknown	*ybcL*(transporter)	520	500	W168
M31	*ydfH*	938 (+)	histidine kinase	*ydfI*	240	240	W168
M32	*ypmB*	30 (-)	similar to propeptide PepSY	*aspB*	n.t.	n.t.	W168
M33	*fhuC*	744 (+)	ferrichrome ABC transporter	*yvrP* (exporter)	240	240	W168
M34	*yebC*	284 (-)	putative membrane protein	*yebD* (unknown)	260	300	W168
M35	*ybcD*	1690 (+)	conserved unknown	*ybcF*	180	160	W168
M36	*ytrP*	1656 (+)	diguanylate cyclase-related enzyme	*yttP* (transcriptional regulator)	520	280	*sigM*
M37	*ybcD*	680 (-)	conserved unknown	*ybcF*	800	520	*sigM*
M38	*ybcD*	680 (-)	conserved unknown	*ybcF*	520	280	*sigM*
M39	*ybcD*	680 (-)	conserved unknown	*ybcF*	n.t.	n.t.	*sigM*
M40	*ybcD*	680 (-)	conserved unknown	*ybcF*	n.t.	n.t.	*sigM*
M41	*ybcD*	680 (-)	conserved unknown	*ybcF*	n.t.	n.t.	*sigM*
M42	*ybcD*	680 (-)	conserved unknown	*ybcF*	n.t.	n.t.	*sigM*
M43	*ybcD*	680 (-)	conserved unknown	*ybcF*	n.t.	n.t.	*sigM*
M44	*ybcD*	680 (-)	conserved unknown	*ybcF*	n.t.	n.t.	*sigM*
M45	*ybcD*	680 (-)	conserved unknown	*ybcF*	n.t.	n.t.	*sigM*
M46	*ybcD*	680 (-)	conserved unknown	*ybcF*	n.t.	n.t.	*sigM*
M47	*ybcD*	680 (-)	conserved unknown	*ybcF*	n.t.	n.t.	*sigM*
M48	*ybcD*	680 (-)	conserved unknown	*ybcF*	n.t.	n.t.	*sigM*
M49	*ybcD*	680 (-)	conserved unknown	*ybcF*	n.t.	n.t.	*sigM*
M50	*ybcD*	680 (-)	conserved unknown	*ybcF*	n.t.	n.t.	*sigM*
M51	*dinB*	43 (+)	nuclease inhibitor	*ydgF*(amino acid permease)	720	480	*sigM*

Table 4.4. (Continued)

Strain	Gene	Tn7SX insertion site[1]	Gene Function	Down-stream gene	moenomycin out-growth after X min.[3] without/ with xylose		Strain back-ground
M52	*dinB*	43 (+)	nuclease inhibitor	*ydgF*	420	320	*sigM*
M53	*dinB*	43 (+)	nuclease inhibitor	*ydgF*	540	300	*sigM*
M54	*dinB*	43 (+)	nuclease inhibitor	*ydgF*	n.t.	n.t.	*sigM*
M55	*yerH*	144 (-)	putative lipoprotein	*yerI*	200	200	*sigM*
M56	*ppsD*	184 (-)	plipastatin synthetase	*ppsE*	240	260	*sigM*
M57	-		no hits		860	760	*pbpDFG*
M58	*yebC*	206 (-)	putative membrane protein	*yebD*	880	980	*pbpDFG*
M59	-		no hits		560	720	*pbpDFG*
M60	*psd*	37 (-)	phosphatidylserine decarboxylase (DC)	*ybfN* (unknown)	220	260	*pbpDFG*
M61	*psd*	278 (+)	phosphatidylserine DC		140[2]	n.t.	*pbpDFG*
M62	*psd*	44 (-)	phosphatidylserine DC	*ybfN* (unknown)	n.t.	n.t.	*pbpDFG*
M63	*psd*	54 (-)	phosphatidylserine DC	*ybfN* (unknown)	n.t.	n.t.	*pbpDFG*
M64	*ybfM*	20 (-)	in *pssA-ybfM-psd* operon		140[2]	n.t.	*pbpDFG*
M65	*ypmB*	30 (-)	similar to propeptide PepSY		120[2]	n.t.	*pbpDFG*
M66	*yebC*	297 (-)	putative membrane protein		500[2]	n.t.	*pbpDFG*
M67	*ybcD*	199 (-)	conserved unknown		180[2]	180[2]	*pbpDFG*
M68	*yerH*	103 (-)	putative lipoprotein	*yerI*	240[2]	n.t.	CU1065
M69	*ypmB*	27 (-)	similar to propeptide PepSY		n.t.	n.t.	CU1065
M70	*ybcC*	211 (+)	conserved unknown	*ybcD*	340[2]	n.t.	CU1065
M71	*yokA*	486 (-)	DNA recombinase	*yokB* (lipoprotein)	380[2]	300[2]	CU1065
M72	*yokD*	599 (+)	similar to aminoglycoside N3-acetyltransferase		200[2]	n.t.	CU1065
M73	*yokD*	10 (+)	similar to acetyltransferase		380[2]	380[2]	CU1065
M74	*yokH*	481 (-)	unknown	*yokF* (nuclease?)	220[2]	n.t.	CU1065
	or		(both have similar sequence)				
	yobM	412 (-)	unknown	*yobN* (oxidase)	220[2]	n.t.	CU1065
M75	*rsiX*	880 (-)	σ^X anti σfactor		340[2]	n.t.	CU1065
M76	*interg.*	(+)	177bp upstream of *bsaA* (peroxidase)	*ypbQ*	380[2]	380[2]	CU1065
M77	*yerH*	499 (-)	putative lipoprotein	*yerI*	n.t.	n.t.	CU1065
M78	*yerH*	420 (-)	putative lipoprotein	*yerI*	n.t.	n.t.	CU1065
M79	*yokA*	305 (-)	DNA recombinase	*yokB*	n.t.	n.t.	CU1065
M80	*yerH*	103 (-)	putative lipoprotein	*yerI*	n.t.	n.t.	W168
M81	*ydfH*	938 (+)	histidine kinase	*ydfI*	660[2]	140[2]	W168
M82	*ybcD*	136 (-)	conserved unknown	*ybcF*	n.t.	n.t.	W168
M83	*ybcD*	1688 (+)	conserved unknown	*ybcF*	n.t.	n.t.	W168
M84	*ybcI*	51 (-)	conserved hypothetical	*ybcL*	300[2]	n.t.	W168
M85	*ypmB*	27 (-)	similar to propeptide PepSY		n.t.	n.t.	W168
M86	*yobI*	1303 (-)	conserved hypothetical		180[2]	n.t.	W168
M87	*yerH*	1183 (-)	putative lipoprotein	*yerI*	n.t.	n.t.	W168
M88	*yerH*	1019 (-)	putative lipoprotein	*yerI*	n.t.	n.t.	W168
M89	*hpr*	3 (-)	ScoC transcriptional regulator	-	300	280	W168
M90	*interg.*	(-)	20bp downstream of *yheA*	*yheC*	180	180	W168
M91	*yerH*	436 (-)	putative lipoprotein	*yerI*	320	n.t.	W168
M92	*ybcD*	680 (-)	conserved unknown	*ybcF*	280	300	W168
M93	-		no hits		300	300	W168
M94	*ndhF*	388 (-)	NADH dehydrogenase (subunit 5), upstream of *ybcD*	*ybcD*	300	300	W168
M95	*qoxB*	738 (-)	cytochrome aa3 quinol oxidase (subunit I)	*ywzA*	320	340	W168

Table 4.4. (Continued)

Strain	Gene	Tn7SX insertion site[1]	Gene Function	Down-stream gene	moenomycin out-growth after X min.[3] without/ with xylose		Strain back-ground
	W168		wild-type		670	650	W168
	CU1065		wild-type		850	860	CU1065
	pbpDFG		LFH deletion		950	800	W168
	sigM		LFH deletion		no growth	no growth	CU1065
	pssA		LFH deletion		300[2]	n.t.	CU1065
	psd		LFH deletion		200[2]	n.t.	CU1065

[1] orientation of xylose inducible promoter in relation to gene (same orientation = (+), opposite orientation = (-))
[2] tested at 1µg/ml, all others at 10µg/ml moenomycin.
[3] moenomycin treatment did not result in a clear determinable MIC, but rather in a delayed lag phase. To compare different mutants, we used the ability to outgrow a certain moenomycin concentration[2] after a particular time as a measure of susceptibility.
[4] Tn7SX insertions are sorted by strain background.

Table 4.5. Moenomycin resistant Tn7SX insertions summary.

Insertion in…	Orientation[2]/ Background	Gene Function[3]	Inducible promoter upstream of…	Xylose dependency
ybcD (21/5X)[1]	+/- W168, *sigM*, *pbpDFG*	conserved unknown (*ybcC*)	*ybcF* (carbonic anhydrase)	slight
ybcC (1X)	+ CU1065	conserved unknown	*ybcF* (carbonic anhydrase)	no
ybcI (2/1X)	- W168	conserved hypothetical	-	no
yerH (17/8X)	- W168, *sigM*, CU1065	putative lipoprotein	*yerD* (ferredoxin-dep. glutamate synthase)	slight
ypmB (12/1X)	- W168, CU1065 *pbpDFG*	similar to propeptide PepSY	-	slight
dinG (2/2X)	- CU1065	ATP dependent DNA helicase	-	no
yebC (3/3X)	- W168, *pbpDFG*	putative membrane protein	-	no
psd (4/3X)	+/- *pbpDFG*	phosphatidylserine decarboxylase	-	no
ybfM (1X)	- *pbpDFG*	in *pssA-ybfM-psd* operon	*psd* (PS decarboxylase)	no
dinB(4/1X)	+ *sigM*	nuclease inhibitor	*ydgF* (amino acid permease)	slight
ydfH (4/2X)	+ W168	TCS histidine kinase	*ydfI* (response regulator)	yes
yokA (2/2X)	- CU1065	DNA recombinase	*yokB* (lipoprotein)	slight
yokD (2/2X)	+ CU1065	similar to aminoglycoside N3-acetyltransferase	*yokA* (DNA recombinase)	no
hpr (1X)	- W168	ScoC, transcriptional regulator	-	no
qoxB (2/2X)	- W168	cytochrome aa3 quinol oxidase (subunit I)	*ywzA* (transglycosylase associated protein)	no
ytrP (1X)	+ *sigM*	diguanylate cyclase-rel. enzyme	*yttP* (transcr. regulator)	yes
ppsD (1X)	- *sigM*	plipastatin synthetase	-	no
intergenic (1X)	- W168	ds of *yheA* and *yheC*	*yheC* (reg. by SpoIIID)	no
intergenic (1X)	+ CU1065	us of *bsaA* (peroxidase)	*ypgQ* (metal phosphohydrolase)	no
ndhF (1X)	- W168	NADH dehydrogenase	-	no
rsiX (1X)	- CU1065	σ^X anti σ factor	-	no
yobI (1X)	- W168	conserved hypothetical	-	no
yokH (1X)	- CU1065	unknown	-	no
yclO (1X)	+ CU1065	ferrichrome ABC transporter	*yclP* (permease)	no
fhuC (1X)	+ W168	ferrichrome ABC transporter	*yvrP* (efflux transporter)	no

[1] Parentheses: (number of total insertions / number of independent insertions X) in respective gene.
[2] "+ or –" corresponds to the orientation of the xylose inducible promoter of Tn7SX relative to the gene.
[3] Function/Similarity based on Subtilist entries.

The YdfHI two-component system regulon confers resistance to moenomycin. Four Tn7SX insertions were found in the histidine kinase gene of the YdfHI TCS. According to the sequencing results they are in two different insertion sites in W168 (Table 4.4). All four are oriented in the same way, with the xylose inducible promoter facing the downstream response regulator gene *ydfI*. Susceptibility assays with moenomycin in liquid cultures showed that this strain was more resistant than W168 upon addition of 2% xylose, which drives expression of the P_{xylA} promoter of Tn7SX. Without addition of xylose, the strain was as susceptible as W168 for most of the time; a subset showed decreased susceptibility without xylose. This could either be due to a slight leakiness of the xylose driven promoter, or in case that the histidine kinase acts as a phosphatase, the disruption by the transposon could also lead to increased amounts of phosphorylated response regulator.

The YdfHI TCS has not been studied very well. Kobayashi *et al.* examined 24 out of 30 TCS pairs in *B. subtilis* by cloning them into an isopropyl-β-d-galactopyranoside (IPTG)-inducible expression vector (pDG148), inducing for two hours, followed by microarray analysis (34). Even though induction for two hours starting from early logarithmic phase is a very long time frame which can lead to secondary effects being present in the transcriptional analysis, we took the published regulon members as a starting point (Table 4.6; (34)). A total of 29 genes were altered in their expression at least four fold, 21 genes were induced, and eight genes were repressed. A gene that caught our interest was *ykuD* (34).

Table 4.6. Regulon members of the YdfHI two-component regulatory system. Genes that were at least 4-fold induced or repressed are shown (adapted from Kobayashi *et al*. (34))

Gene	Gene Function
Induced:	
ydfE	putative flavoprotein
ydfH	TCS, histidine kinase
ydfI	TCS, response regulator
ydfJ	putative proton metabolite efflux transporter
ydfT	*cotP*, spore coat protein
ydgJ	putative transcriptional regulator (MarR family)
ydjM	conserved hypothetical protein
ykuD	*ldt*, L,D-transpeptidase
pyrR	transcriptional attenuation of the pyrimidine operon / uracil phosphoribosyltransferase activity
proJ	glutamate 5-kinase (proline biosynthesis)
proH	pyrroline-5-carboxylate reductase (proline biosynthesis)
yqjD	Propanoyl-CoA carbon dioxide ligase
ysbA	murein hydrolase regulator LrgA
rbsR	transcriptional repressor of the ribose operon
rbsK	ribokinase
rbsD	ribose ABC transporter (membrane protein)
rbsA	ribose ABC transporter (ATP-binding protein)
rbsC	ribose ABC transporter (permease)
rbsB	ribose ABC transporter (ribose-binding protein)
licC	PTS lichenan-specific enzyme IIC component
yydH	putative peptide zinc metalloprotease protein
Repressed:	
lctE	L-lactate dehydrogenase
lctP	L-lactate permease
yqxL	magnesium transport protein corA
ywcJ	formate/nitrite transporter
ywbH	holin-like protein cidA
cydC	ABC transporter required for expression of cytochrome bd (ATP-binding protein)
cydB	cytochrome bd ubiquinol oxidase (subunit II)
cydA	cytochrome bd ubiquinol oxidase (subunit I)

YkuD was found to be a sporulation protein, under the regulation of σ^K, with a LysM domain, typical for peptidoglycan binding proteins (35). More recently, it was renamed Ldt, for L,D-transpeptidase (14, 40). Cremniter *et al*. report Ldt to have activity in *Enterococcus faecium*, catalyzing the transpeptidation between the third amino acid of lipid II during peptidoglycan (PG) synthesis (Fig. 4.6). In vitro, the ortholog in *B. subtilis* catalyzes the condensation between two *meso*-diaminopimelic acid[3] residues (40), instead of the third and the fourth amino acid that are used during regular peptidoglycan synthesis. This alternative pathway leads to resistance to glycopeptide and β-lactam antibiotics in *E. faecium*, as the specific target is missing in both cases. Here, a potential induction of *ldt* through the YdfHI TCS is intriguing, because this could lead to upregulation of an alternative cell wall synthesis pathway, circumventing the need for the four known HMW PBPs. However, preliminary results are discouraging. Deletions of both *ldt* and its paralog *yciB* were not more susceptible to moenomycin or other cell wall active antibiotics (our unpublished results, and (7)); though this has not been tested in a mutant missing all four HMW PBPs. An involvement of Ldt or YciB in resistance could also be tested by ectopic overexpression. Focusing on the YdfHI TCS, a comprehensive analysis of the regulon members (for instance by microarray, but with shorter induction periods), chip, or transcriptional fusions, could shed light on the involvement in moenomycin resistance.

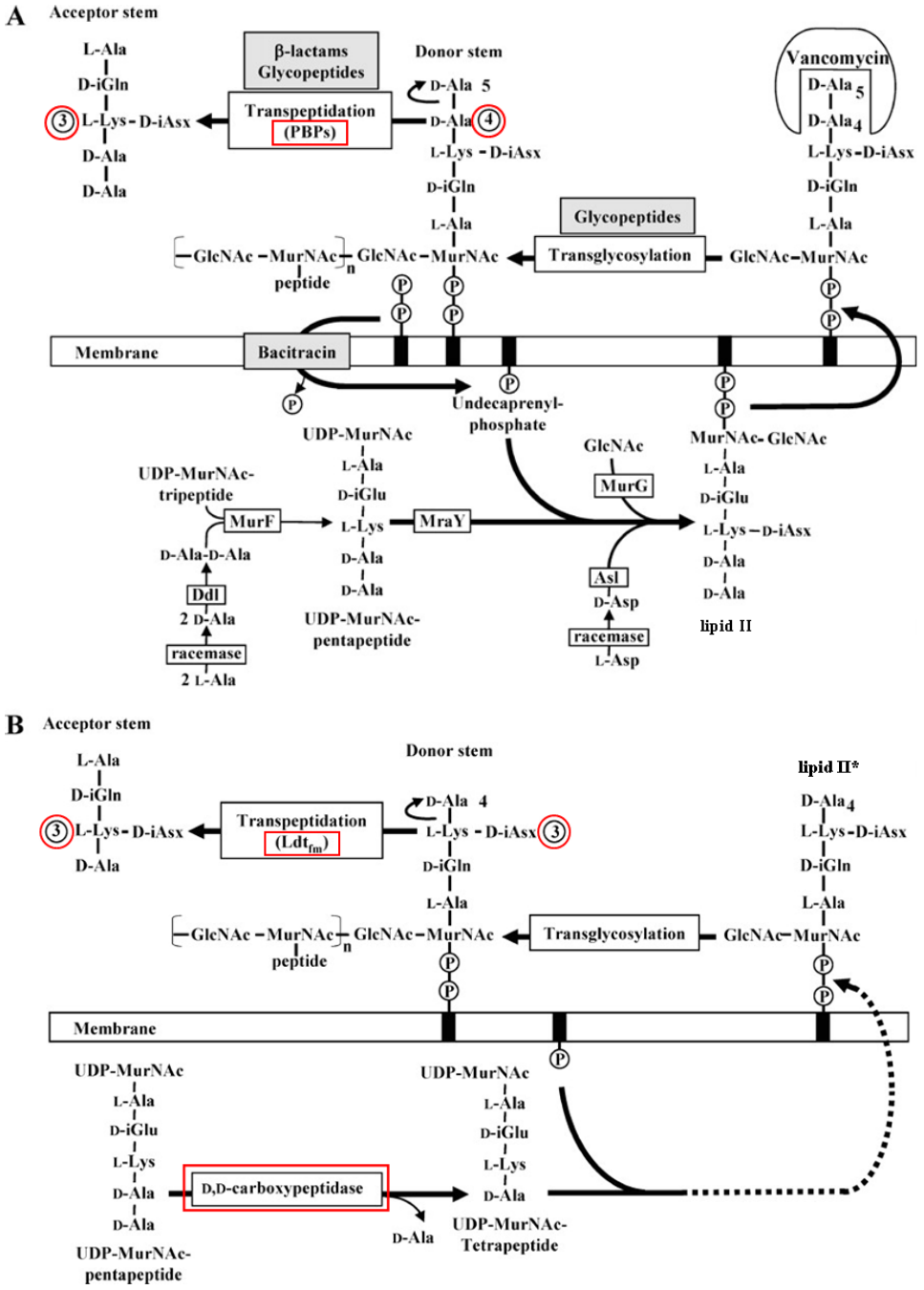

Figure 4.6. Regular and alternative cell wall synthesis pathways in *E. faecium*.
(A) Regular peptidoglycan synthesis. The extracellular polymerization and cross-linking of peptidoglycan is mediated by penicillin-binding proteins (D,D-transpeptidases). (B) An alternative peptidoglycan synthesis uses L,D-transpeptidases (Ldt) which circumvent the need for regular penicillin-binding proteins. Ldt requires the pentapeptide precursor of lipid I to be cleaved to a tetrapeptide by a D,D-carboxypeptidase (14).

YbcC and YbcI, two conserved hypotheticals. The Tn7SX transposon is inserted 24 times in the genes *ybcC* (22X) and *ybcI* (2X), with six different insertion sites in *ybcC* (previously annotated as *ybcC* and *ybcD*). The xylose inducible promoter is not uniformly oriented in the same directions in these insertions. When searched with NCBI blast, both proteins are listed as conserved hypothetical proteins, and similar proteins are also not annotated. *ybcI* is located about 1kb further downstream of *ybcC*, separated by *ybcF* (similar to carbonic anhydrase), and *ybcH* (hypothetical protein) (17, 28).

When compared to closely related *Bacillus* species, it is notable that *ybcC* is not present in *B. pumilis*. In *S. aureus* the *ybcC* and *ybcI* genes are direct neighbors (http://string.embl.de). Using the String software with a maximum of ten interactions and one additional node, all three genes, *ybcC, ybcD* (still shown as separate genes), and *ybcI*, are interconnected due to being in the same neighborhood, and due to co-occurrence across genomes (Fig. 4.7). Connnected with the three genes is *ndhF*, encoding a NADH-quinone oxidoreductase subunit, which is directly upstream of *ybcC*. The only other interaction that stands out is with *rasP*, coding for a zinc-metalloprotease that cleaves RsiW, the anti-σ^W ECF σ factor, though *rasP* is only connected to *ybcI*. Due to the fact that both genes are not yet annotated and do not have a particular motif (only regions of low complexity, when analysed with EMBL-SMART), the reason for moenomycin resistance is not yet clear. However, the frequent occurrence of transposon insertions in these two genes leading to moenomycin resistance remains worthy of investigation.

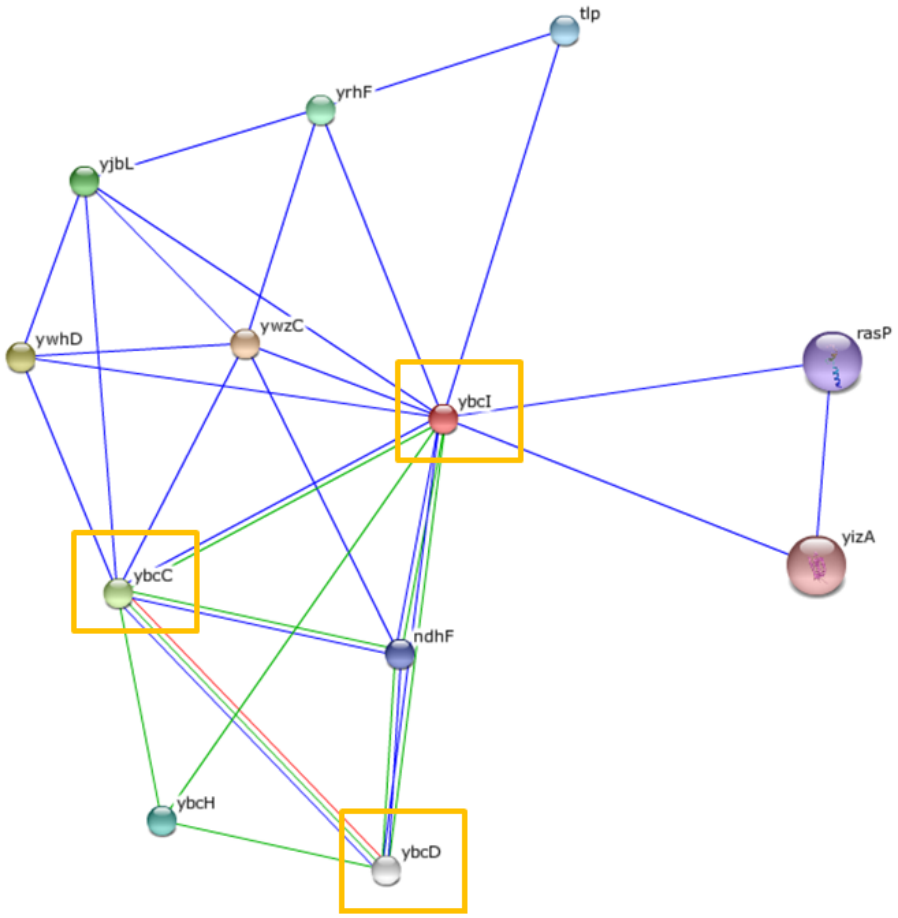

Figure 4.7. Putative interaction network of *ybcI*.
STRING analysis of protein associations based on: co-ocurrence across genomes (blue), genetic neighborhood (green), gene fusions (red). Displayed connections have a confidence score of 0.6 or higher. Adapted from http://string.embl.de/ (30)

The sex-pheromone homolog YerH. 17 Tn7SX insertions were found in *yerH*, of which eight are independent (at different insertion sites). The insertions occurred in three different backgrounds, W168, CU1065, and the *sigM* deletion. The P_{xylA} promoter faced opposite the gene orientation, towards *yerD* (encoding a protein with similarity to a ferredoxin-dependent glutamate synthase (52, 58)), though the resistance was independent of xylose. According to UniProtKB, YerH is anchored to

the membrane, has a signal peptide (1-18), and is likely to be lipidated at cysteine-19 via N-palmitoyl or S-diacylglycerol.

YerH is homolog to CamS (44% identity) of *Staphylococcus aureus*, which processes the sex pheromone staph-cAM373. The latter is a heptapeptide and potential intergeneric inducer of transfer-proficient genetic elements (20). Similar to CamS are Eep in *E. faecalis* and Lsp in *Escherichia coli*. Eep stands for enhanced expression of pheromone, a metallopeptidase that cleaves signal peptides of lipoproteins to yield octapeptides (3). These peptides act as aggregation pheromones, inducing conjugation between different *E. faecalis* strains. Eep is 44% identical to YluC in *B. subtilis*, which is a RIP peptidase that degrades the anti σ factor RsiW through intramembrane proteolysis (15). At this point, the correlation between the disruption of the lipoprotein YerH and decreased moenomycin susceptibility are not known.

YpmB – an extracellular protease? 12 Tn7SX insertions were obtained in *ypmB* in three different background strains, W168, CU1065, and the triple deletion of the HMW PBPs *pbpDFG*. Upon addition of xylose, the strains were slightly more resistant to moenomycin, although no gene is directly downstream in the same orientation as the P_{xylA} promoter. YpmB has a PepSY domain, which is found in the propeptide of members of the MEROPS peptidase family M4, containing for instance the thermostable thermolysins (EC 3.4.24.27), and related thermolabile neutral proteases (bacillolysins) (EC 3.4.24.28). Extracellular proteases are often produced as propeptides with dual function: an intramolecular chaperone necessary for the folding of the polypeptide (FTP domain) and an inhibitor preventing premature activation of the enzyme (PepSY domain, IPR011096) (8, 65).

ypmB is part of the *dinG ypmA ypmB aspB* operon. The transposon insertion could perhaps have a polar effect on *aspB*, encoding an aspartate aminotransferase (Fig. 4.8, Fig. 4.9). Effects from *ypmB* disruption on moenomycin resistance or potential polar effects remain to be tested.

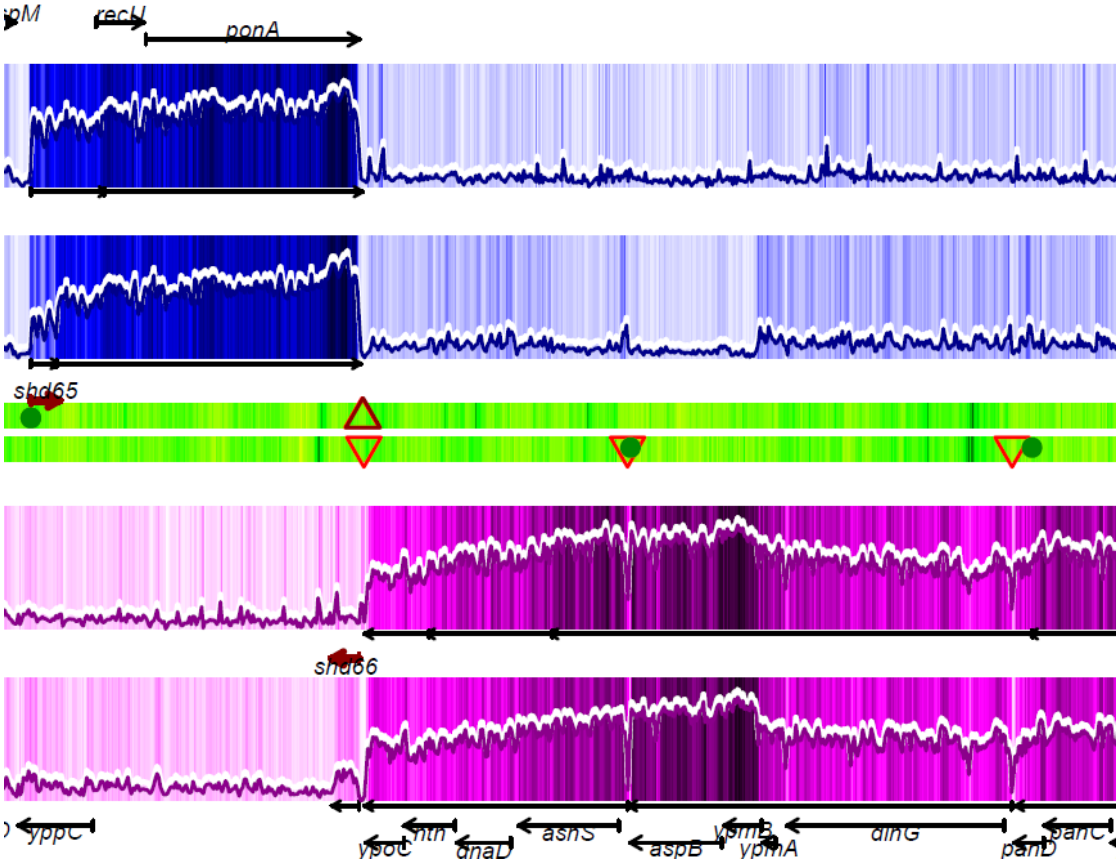

Figure 4.8. Expression of the *dinG ypmA ypmB aspB* operon.
Excerpt from *B. subtilis* tiling array with strand specific probes, top strand shown in blue, bottom strand in pink. The upper panels of each strand correspond to gene expression in rich (LB), the lower panels in minimal medium (M9).The higher the graph/darker the color the higher the expression. Red triangles illustrate predicted terminators; green circles indicate predicted σ factor binding sites (56).

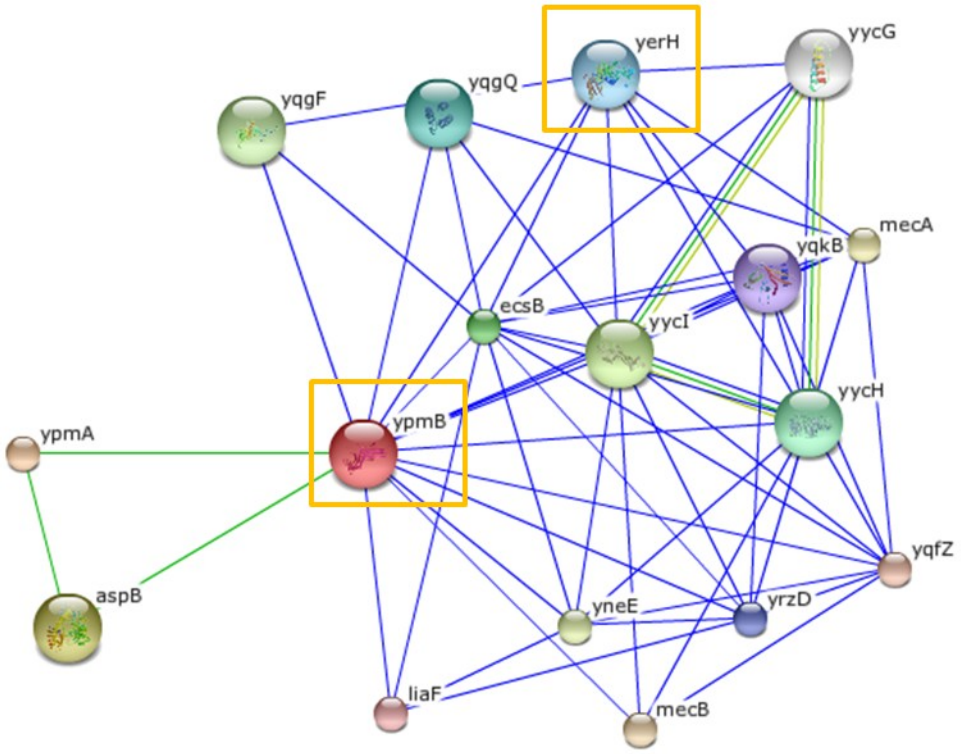

Figure 4.9. Putative interaction network of *ypmB*.
STRING analysis of protein associations based on: co-ocurrence across genomes (blue), genetic neighborhood (green), text mining (yellow). Displayed connections have a confidence score of 0.5 or higher. Adapted from http://string.embl.de/ (30)

Insertions in *dinG* – a polar effect on *ypmB*? Two independent Tn7SX insertions occurred in *dinG* in the wild-type CU1065. Disruption of the ATP-dependent helicase is suspicious, because of the close proximity to the downstream genes *ypmA* and *ypmB* (24). A total of 12 insertions in three different backgrounds (W168, CU1065, and *pbpDFG*) were found in *ypmB*, leading to moenomycin resistance. It could be possible, that the Tn7SX insertions in *dinG* have a polar effect on the downstream genes *ypmA ypmB aspB* (Fig. 4.8).

Xylose dependent moenomycin resistance through a Tn7SX insertion in *ytrP*. One Tn7SX insertion was detected in *ytrP*, in the *sigM* deletion background. YtrP is a putative diguanylate cyclase-related enzyme (9). Using blast, close hits also report similarity to a histidine kinase, but a corresponding reponse regulator is missing. Since resistance to moenomycin was observed after addition of xylose, we assume that a downstream gene is affected. Downstream (in the same orientation as the P_{xylA} promoter) is the monocistronic gene *yttP*. Little is known about *yttP*, which has similarity to a transcriptional regulator (TetR/AcrR family). Allenby *et al.*, list *yttP* as a member of the PhoP regulon where it was induced in response to phosphate starvation (2, 54). Fujita *et al.,* however, found *yttP* to be a high-threshold member of the Spo0A regulon, (21, 45, 55). Rahn-Lee *et al.* tested effects of a *yttP* deletion on inhibition of replication, but were unable to observe a phenotype (55). Overexpression of *yttP* , in wild-type and a *sigM* deletion background might give clues about a relation to moenomycin resistance.

YebC, a member of the σ^M regulon. Three independent insertions are located in *yebC*, in the W168 and *pbpDFG* backgrounds. YebC has similarity to integral inner membrane proteins, or permeases (not to be confused with *E. coli yebC* which encodes a different protein) (23, 27, 36, 63). Disruption of *yebC* by the transposon leads to high resistance to moenomycin, both in liquid susceptibility studies and when tested in disc diffusions assays with moenomycin soaked filter discs. Interestingly, *yebC* is a member of the σ^M regulon, and is mildly induced in microarrays upon moenomycin treatment (unpublished results, see chapter 5) (18). Since σ^M was found to confer resistance to moenomycin, this seems counterintuitive. To test effects of σ^M on this

mutant, we transformed a *sigM::kan* LFH deletion into a *yebC*::Tn7SX insertion strain. This deletion was now much more sensitive to moenomycin, indicating a possible connection between the resistance and σ^M regulon members.

Psd and YbfM – alterations in the phospholipid content of the membrane are likely to affect moenomycin anchoring. In total, five Tn7SX insertions were found in the *pssA-ybfM-psd* operon. This operon, as already described for selection of duramycin resistant Tn7SX isolates, is involved in the synthesis of phosphatidylserine and phosphatidylethanolamine, two important members of membrane phospholipids (Fig. 4.2, Fig. 4.10) (71). Insertions in both *ybfM* and *psd* result in inhibition of the zwitter-ionic phophatidylethanolamine production, thereby increasing amounts of the negatively charged precursor phosphatidylserine. This could alter the overall phospholipid composition in the membrane. Nishi *et al.* showed previously that transposon insertions in *mprF*, which synthesizes the positively charged membrane lipid lysyl-phosphatidylglycerol, led to moenomycin resistant mutants in *S. aureus* (47). This also indicates that an increase in negatively charged membrane lipids affects susceptibility to moenomycin.

Two aspects could be responsible for the decreased susceptibility to moenomycin. First, for full activity, moenomycin needs to anchor in the membrane with its moenocinol side chain, a C_{25} branched acyl chain. It was shown that a shortened side chain (C_{10}) was able to interact with the target transglycosylase, but was unable to exert biological activity, inhibiting its function (1, 4). By changing properties of the membrane, the anchoring ability of moenomycin could be impaired.

Second, moenomycin also needs to interact with the trans-membrane domain of the transglycosylase to be active (Fig 4.11) (13). By changing the phospholipid content of the membrane, this interaction could be hindered or changed, for example through conformational changes of the transglycosylase. To fully answer the question which of these two options plays a role, binding and activity studies could be done with moenomycin, and perhaps compared to moenomycin with altered side chain lengths. Furthermore, titration experiments with ectopically inducible copies of *psd* could indicate whether a certain threshold is needed for this effect. This could be coupled with ESI-MS based quantification of membrane phospholipids.

Lastly, why these Tn7SX insertions were only found in the *pbpDFG* background, but not in wild-type *B. subtilis*, remains to be answered. Perhaps, if PonA is the only remaining transglycosylase, membrane charge and conformation characteristics have a greater impact on moenomycin binding and activity. We conducted growth inhibition studies with *psd* deletions in the wild-type background, and found this strain to be less susceptible to moenomycin as well, although to a lesser extent, than in the *pbpDFG* background.

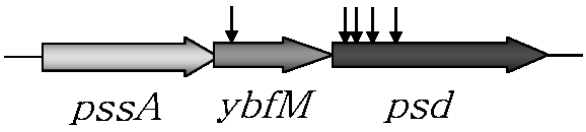

Figure 4.10. Tn7SX transposon insertions in *ybfM* and *psd*.
Five independent insertions were found in the *pssA-ybfM-psd* operon.

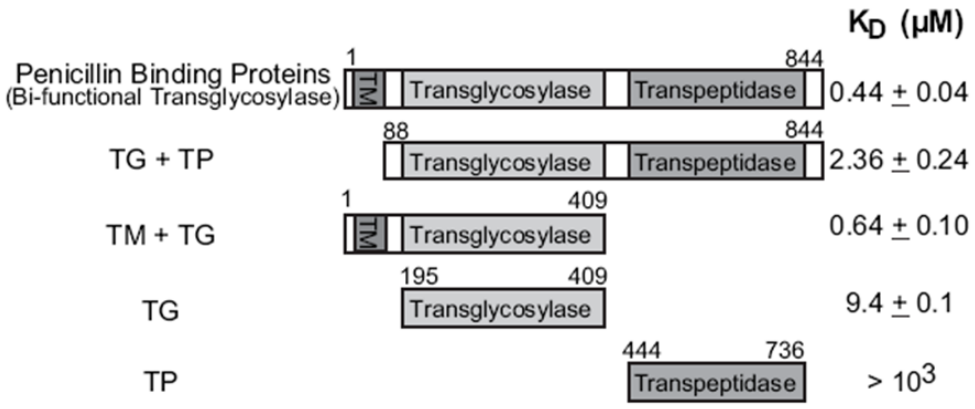

Figure 4.11. Affinity of moenomycin to truncated HMW PBPs.
Binding constants of moenomycin with different domains of PBPs are listed. Presence of a transmembrane domain increased moenomycin binding (13).

***dinB* insertions increase moenomycin resistance in a *sigM* deletion strain.**

A transposon insertion in the nuclease inhibitor *dinB* (33, 72) does have no apparent advantage regarding moenomycin resistance. Here, we only obtained Tn7SX insertions in the *sigM* deletion background, which is otherwise very susceptible to moenomycin. The P_{xylA} promoter is oriented facing the downstream gene *ydgF*, which has been renamed *aapA*, an amino-acid permease, transporting d-serine/d-alanine/glycine. In fact, the moenomycin resistance of this Tn7SX insertion was slightly dependent on xylose addition. It could be argued that induction of the membrane protein AapA leads to increased transport of these amino acids, compensating for defects in the *sigM* mutant or affecting the membrane potential, and subsequently moenomycin activity. To confirm a dependency on the *sigM* deletion, or on AapA, this transposon could be transformed into *B. subtilis* wild-type background, and could be coupled with a deletion of *aapA*.

Four insertions in close proximity, YokA and YokD. Two Tn7SX insertions each are located inside *yokA* and *yokD*, respectively. YokD has similarity to an aminoglycoside N3-acetyltransferase and YokA to a DNA site-specific recombinase. These insertions could be independent, the close chromosomal proximity, however, might suggest a connection. In all cases, the insertions are in the CU1065 wild-type background strain. The xylose inducible promoters in *yokD* face in direction of the 2kb downstream *yokA*, whereas the insertions in *yokA* face the opposite orientation towards *yokB*, which has similarity to a lipoprotein. Addition of xylose to the insertions in *yokD* could perhaps affect expression of *yokA*; whereas xylose added to Tn7SX in *yokA* could affect expression of *yokB*. From the resistance studies, we can see a slight increase in resistance, when xylose is added to the insertion in *yokA*, the insertions in *yokD* had not yet been tested with xylose.

Transposon insertions in the aminoglycoside N3-acetyltransferase are interesting in terms of antibiotic resistance. This enzymatic group (EC:2.3.1.81) catalyses the acetyl transfer to 2-deoxystreptamine antibiotics, leading to N3'-acetyl-2-deoxystreptamine antibiotics, thereby inactivating for example gentamicin, kanamycin, neomycin and others (according to the NCBI Conserved Domain Database (CDD)(41)). A functional relationship to moenomycin is not apparent, as it is a phospho-glycolipid. Besides having the ability to inactivate aminoglycosides, an additional function of a YokD homolog was observed in *Providencia stuartii*: O-acetylation of peptidoglycan (48). If YokD has similar functions in *B. subtilis* is still unknown.

Increased expression of proteases by disruption of the transcriptional regulator ScoC (Hpr)? Hpr, renamed to ScoC, is a transcriptional regulator of the MarR family. It negatively regulates sporulation and extracellular protease genes (aprE, nprE, sin), as well as peptide transport genes (appABCDF and oppABCDF) (31). These extracellular proteases are produced in large quantities at the end of logarithmic growth to degrade extracellular high-molecular-weight materials to serve as nutrients. Their regulation is important because their production is very energy consuming. Next to AbrB, SinR, and Pai, ScoC is a negative regulator of AprE, binding directly upstream of *aprE* (Fig 4.12) (32).

Even though the regulation of the degradative proteases is complex, it was shown that for example SenS, is able to supress transcription of ScoC, and in turn increase levels of AprE (32). A disruption of ScoC by Tn7SX probably leads to elevated expression of secreted proteases. Whether this affects moenomycin directly, or rather indirectly, remains to be answered.

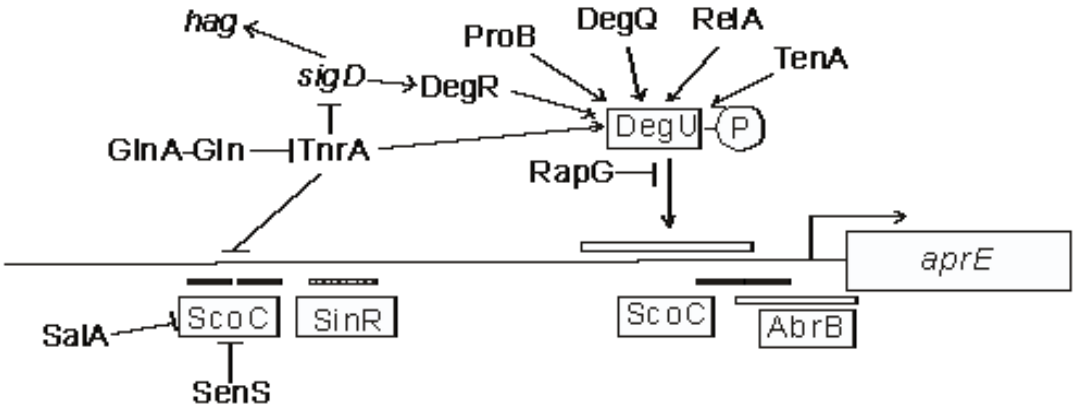

Figure 4.12. *aprE* regulatory network.
The negative regulator of *aprE*, ScoC, can be repressed by SenS and SalA.
Adapted from T. Tanaka, Saitama University, Japan (http://www.molbiol.saitama-u.ac.jp/091028.gif)

Insertions in the cytochrome quinol oxidase gene *qoxB*. Two insertions are in *qoxB*, coding for subunit I of the cytochrome aa3 quinol oxidase. *B. subitilis* is known to have three different terminal oxidases that transfer electrons from reducing equivalents to oxygen. While cytochrome c is the minor oxidase, the major ones are the quinol oxidases cytochrome bd (*cydABCD*) and aa_3 (*qoxABCD*), which translocate one to two protons per electron transferred to oxygen (69). Oxygen levels determine which oxidase is predominantly used. During aerobic growth conditions the cytochrome aa_3 oxidases are predominant, at low oxygen levels the cytochrome bd oxidases. The quinol oxidases are synthetically lethal. Either one is sufficient, but both cannot be replaced by cytochrome c (69).

Zamboni *et al*. have examined effects of a *qox* mutant in *B. subtilis*. They observed acetate overflow during carbon metabolism, which they suggest is due to kinetic limitation of the terminal oxidases. At the maximum growth rate the remaining oxidases were insufficient to oxidize all catabolically generated NADH (70). How this translates to the transposon insertion in *qoxB* and moenomycin resistance is not clear. The kinetic limitation could perhaps result in slower metabolism, and consequently reduced growth rate and cell wall synthesis, thereby presenting fewer targets to moenomycin.

Of note is that the gene upstream of *qoxB*, *ywzA*, encodes a transglycosylase associated protein. *ywzA*, a member of the σ^B regulon, was shown to be induced by phenol and salicylic acid and downregulated by ComK (5, 51).

Insertion in the usually inactive plipastatin synthase operon. *ppsD* is part of the 38.4-kb plipastatin synthesis operon *ppsABCDE*. Plipastatin is a non-ribosomal peptide (NRP) that is usually not synthesized by *B. subtilis* W168 because of a frame-shift mutation in *sfp* and a mutation in the promoter region of *degQ* (Fig 4.13). Sfp, a phosphopantetheinyl transferase is necessary to convert the peptidyl carrier domains of the plipastatin synthetase from the inactive apo-forms to active holo-forms. DegQ is a putative regulator for expression of the *ppsABCDE* operon (66).

It is surprising that the Tn7SX insertion in *ppsD* showed a moenomycin resistance phenotype, because the background strain is supposedly a non-producer of plipastatin. The P_{xylA} promoter should have no effect here, because it is facing in the opposite orientation of *ppsD*. Attempts to delete *ppsD* via LFH deletion have failed probably because of the large size of the gene (10.8 kb).

To further investigate the effects of *ppsD* on moenomycin resistance, we received two strains from Dr. Kenji Tsuge (Keio University): BEST8628, which produces plipastatin (due to reversal of the mutations in sfp^0 and $degQ^0$); and BEST8666, which does not produce plipastatin due to deletion of the *pps* operon, *sfp*, and *degQ* (66). When tested for moenomycin sensitivity, neither of the strains showed differences compared to wild-type W168. This does not confirm our transposon phenotype. Perhaps this strain has another mutation close to the Tn7SX insertion site that co-transformed during our linkage tests.

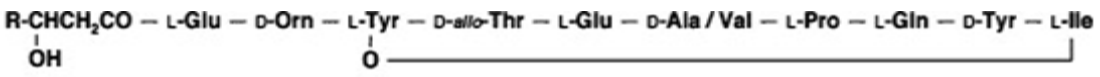

Figure 4.13. Structure of the NRPS produced lipopeptide plipastatin.
R = alkyl chain, usually C_{14} to C_{16} (66).

Tn7SX insertion downstream of *yheA* and *yhaZ*. The Tn7SX insertion downstream of the genes *yheA* and *yhaZ* does not have an obvious genetic effect. The xylose inducible promoter is oriented opposite to *yheA*, in direction of *yheC*, which is similar to a spore coat associated protein, a UDP-MurNAc-tripeptide-D-ala-D-ala ligase. *yheC* and *yheD* were found to be upregulated by SpoIIID (19). YheD forms a ring during spore coat formation, but is not essential for sporulation. The fact that this transposon insertion is not directly dependent on xylose, and the distance of about 2kb from the insertion site to the start of *yheC*, do not support a likely induction of *yheC*, unless the promoter is slightly leaky. The relation to moenomycin resistance is unclear at this point.

Effects of transposon insertion upstream of *bsaA*. One insertion was located upstream of *bsaA*. BsaA is similar to glutathione peroxidases, but since *B. subtilis* lacks glutathione, this function is unlikely. Instead, it could be a peroxidase using other low molecular weight thiols in the cell (e.g., bacillithiol (22, 46)). The Tn7SX insertion is upstream of *bsaA* with the P_{xylA} promoter in the same orientation as the gene. An effect could therefore either be caused by induction of *bsaA* or by the downstream gene *ypgQ*, which is a putative metal-dependent phosphohydrolase. These options still remain to be tested.

Isolation of fosfomycin sensitive mutants. We used Tn7SX to select for sensitivity to fosfomycin, an antibiotic produced by *Streptomyces* species and used in the treatment of lower urinary tract infections (57). Fosfomycin enters the cell via the GlpT ABC transporter transporter, where it inactivates MurA, a cytoplasmic enzyme involved in the first step of peptidoglycan biosynthesis (37). Mutations in *glpT* of *E. coli* result in increased fosfomycin resistance, and in *B. subtilis*, the *glpT* locus was originally mapped by selection for Fos^r mutants (39). *B. subtilis* was found to become resistant to fosfomycin by its inactivation through addition of L-cysteine (57). This step is catalyzed by bacillithiol and the bacillithiol-S-transferase enzyme FosB (11, 22).

Bacillithiol (BSH) is a recently characterized low-molecular-weight thiol, similar to glutathione or mycothiol, which helps the cell maintain a reduced cytosolic state by detoxifying electrophiles (22, 46). BSH is synthesized by the BshA glycosyltransferase, BshB1 or BshB2 deacetylase and a methylglyoxal synthase (Fig. 4.14). BshC, the cysteine adding enzyme was not known, which encouraged us to utilize the highly random insertion power of the Tn7SX library to screen for candidates that would disrupt BSH production, and thereby render the cells susceptible to the antibiotic fosfomycin. Since BshB1 and BshB2 are partially redundant, likely candidates of Tn7SX insertions would be *bshA*, *bshC*, or *fosB*. However, if BshC is an essential enzyme, the transposon mutagenesis will not be successful.

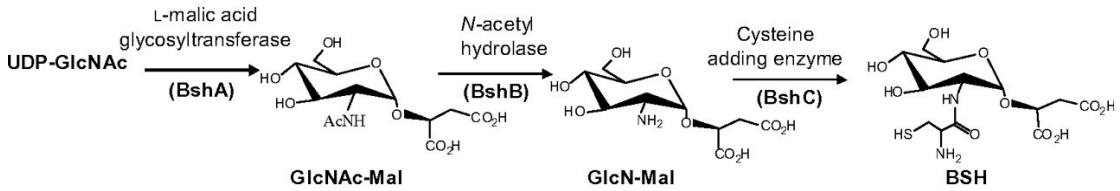

Figure 4.14. Synthesis of the low-molecular-weight thiol bacillithiol in *B. subtilis*. Bacillithiol (BSH) synthesis is catalysed by BshA (glycosyltransferase), BshB (*N*-acetylhydrolase), and BshC (cysteine-adding enzyme) (22).

In order to screen for fosfomycin sensitivity, cells were plated on LB plates containing spectinomycin (with or without xylose) after transformation of W168 with the Tn7SX amplified library. Colonies were then transferred to microtiter plates, from which they were replica plated onto plates containing spectinomycin, and 30 µg/ml of fosfomycin, a concentration that wild-type W168 can tolerate. Half of the plates contained 2% xylose. In total, 10 microtiter plates were employed, resulting in 960 colonies tested (with and without xylose). We found more than 18 colonies that were not able to grow at the selected concentration of fosfomycin.

Results of the insertion mapping are listed in Table 4.7. The fact that we obtained a Tn7SX insertion in *bshA*, the first gene involved in BSH synthesis, indicates that the screen was successful for our purpose. Another insertion indirectly relevant to fosfomycin detoxification is in *ecsB*. EcsB is part of an operon with EcsA, an ATP binding cassette (ABC) of an ABC transporter (38). Heinrich *et al.* report that mutants of *ecsA* inhibit proteolysis of ECF anti-σ^W factor RsiW by the intramembrane cleaving protease RasP (26). In wild-type, σ^W is sequesterd by its anti-σ^W factor RsiW, and after stress-induced degradation by regulated intramembrane proteolysis, σ^W is released and can activate the transcription of σ^W-controlled genes. It is plausible, that the *ecsB* mutant from this Tn7SX sceen also fails to proteolytically degrade RsiW,

causing σ^W to be inactive. Since σ^W is normally necessary for *fosB* activation, the resulting low levels of FosB are likely insufficient to detoxify fosfomycin.

When tested in liquid growth curves for sensitivity to fosfomycin, strains with Tn7SX insertions in *bshA, yvzA, ecsB*, upstream of *bglA* and *cypC*, as well as a *fosB* deletion as positive control had an MIC of 100 μg/ml or less, whereas wild-type W168 has an MIC of 200 μg/ml. The different Tn7SX insertion mutants can be tested for their effect on BSH and fosfomycin degradation. However, while these studies were conducted, John D. Helmann and Ahmed Gaballa discovered a candidate for BshC using phylogenomic methods, namely YllA. This gene was not found in the first rounds of sequencing mutants from the Tn7SX library screen. Nonetheless, the remaining mutants might give clues to other aspects of fosfomycin detoxification.

Table 4.7. Fosfomycin sensitive Tn7SX insertions in W168.

ID #	Insertion in…	Gene function	At position	Tn7SX orientation vs. gene
6H2	us of *ybxI* and *cypC*	*ybxI*: similar to β-lactamase *cypC*: fatty acid β -hydroxylating CYP450	(-106) *ybxI*, (-67) *cypC*	same as *cypC*
8C1	*bshA*	*bshA*, BSH synthesis	601 of 1131	opposite
6F8	*citB*	aconitate hydratase	502 of 2727	opposite
4D8	*murAA*	UDP-GlucNAc-1-carboxyvinyltransferase	46 of 1308	opposite
4C1	us of *bglA*	6-phospho-beta-glucosidase	(-25)	same
4G10	*yvzA*	unknown, part of the LiaRS regulon ?	291 of 357	opposite
4H8	*yfmI*	similar to macrolide-efflux transporter	284 of 1218	opposite
8H1	*ecsB*	ABC transporter (membrane protein)	1004 of 1224	opposite
5G11	possibly in *cwlH*	N-acetylmuramoyl-L-alanine amidase (sporulation)	373 of 750	opposite
5C4	*yetI*	similar to positive regulator of σ^B	950 of 1083	opposite
5D3	us of *cysK*	cysteine synthetase A	(-33)	opposite
3/21	*citB*	aconitate hydratase	504 of 2727	opposite
12/24	*yfmI*	similar to macrolide-efflux transporter	284 of 1218	opposite
4G7	*murAA*	UDP-GlucNAc-1-carboxyvinyltransferase	1261 of 1308	opposite
10E5	*yhaJ*	unknown	47 of 237	opposite
10E8	*ylmD*	unknown	571 of 834	opposite

4.4 Conclusions.

Stress response to cell envelope active antibiotics by ECF σ factors and TCS can result in upregulation of alternative cell wall synthesis pathways and thereby confer resistance. Use of moenomycin serves as a valuable tool to study proteins involved in cell wall synthesis and its regulation. σ^M regulates genes that confer resistance to moenomycin via a still unknown mechanism. Here, we investigated aspects of cell wall synthesis and resistance to moenomycin with the help of Tn7SX transposon mutagenesis.

Interestingly, amongst the 25 different Tn7SX insertions, only one mutant is part of the *sigM* regulon, *yebC*, which has similarity to a membrane permease. In addition, most mutants are different from the genes induced by moenomycin (see transcriptional analysis of moenomycin treatment, Chapter 5, Table 5.3). An insertion in the histidine kinase of the YdfHI TCS was found to confer resistance to moenomycin, perhaps by regulating Ldt expression which is part of an alternative peptidoglycan synthesis pathway. Additional members of this pathway including the transglycosylase and the D,D-carboxypeptidase that provides the tetrapeptide substrate for Ldt still need to be investigated.Insertions in the phosphatidylethanol synthesis operon *pssA-ybfM-psd* alter the phospholipid composition of the membrane, increasing the net negative charge. This might affect the ability of moenomycin to insert into the membrane, or to interact with the trans-membrane domain of the transglycosylase.

Here, a shortcoming of using the amplified Tn7SX library is the occurrence of siblings amongst the insertion hits, especially as some insertions have a growth advantage over others and are present in higher copy numbers, resulting in lower

randomness as the direct transformation after transposition. However, using this library multiple times, we still obtained moenomycin resistant insertions in different genes, indicating, that the selection is close to, but not yet saturated.

The technique used in this work also has its limitations. The transposon mutagenesis can be unsuccessful if a good screening method is not found, if the spectinomycin resistance cassette poses a problem, or if more than one mutation is needed for resistance. The latter was the case in an attempt to use Tn7SX to select for resistance to the cell membrane perturbing antibiotic daptomycin. We only obtained insertions with minimal decreases in susceptibility, which is likely due to the fact that multiple mutations are needed for resistance, or a point mutation in essential genes.

Altogether, the high number of different insertions that conferred resistance to moenomycin is remarkable. The mutations opened up many new aspects related to the mechanism of action and resistance of moenomycin, and linked to cell wall synthesis that remain subjects worthy of further investigation. The findings of mutants potentially involved in fosfomycin detoxification by screening for drug sensitivity highlight the versatility of the Tn7SX transposon system.

REFERENCES

1. **Adachi, M., Y. Zhang, C. Leimkuhler, B. Sun, J. V. LaTour, and D. E. Kahne.** 2006. Degradation and reconstruction of moenomycin A and derivatives: dissecting the function of the isoprenoid chain. J Am Chem Soc **128:**14012-3.

2. **Allenby, N. E., N. O'Connor, Z. Pragai, A. C. Ward, A. Wipat, and C. R. Harwood.** 2005. Genome-wide transcriptional analysis of the phosphate starvation stimulon of Bacillus subtilis. J Bacteriol **187:**8063-80.

3. **An, F. Y., M. C. Sulavik, and D. B. Clewell.** 1999. Identification and characterization of a determinant (eep) on the Enterococcus faecalis chromosome that is involved in production of the peptide sex pheromone cAD1. J Bacteriol **181:**5915-21.

4. **Anikin, A., A. Buchynskyy, U. Kempin, K. Stembera, P. Welzel, and G. Lantzsch.** 1999. Membrane Anchoring and Intervesicle Transfer of a Derivative of the Antibiotic Moenomycin A. Angew Chem Int Ed Engl **38:**3703-3707.

5. **Berka, R. M., J. Hahn, M. Albano, I. Draskovic, M. Persuh, X. Cui, A. Sloma, W. Widner, and D. Dubnau.** 2002. Microarray analysis of the Bacillus subtilis K-state: genome-wide expression changes dependent on ComK. Mol Microbiol **43:**1331-45.

6. **Bordi, C., B. G. Butcher, Q. Shi, A. B. Hachmann, J. E. Peters, and J. D. Helmann.** 2008. In vitro mutagenesis of Bacillus subtilis by using a modified Tn7 transposon with an outward-facing inducible promoter. Appl Environ Microbiol **74:**3419-25.

7. **Bramkamp, M.** 2009. The putative Bacillus subtilis L,D: -transpeptidase YciB is a lipoprotein that localizes to the cell poles in a divisome-dependent manner. Arch Microbiol.

8. **Brockmeier, U.** 2006. New strategies to optimize the secretion capacity for heterologous proteins in Bacillus subtilis. Dissertation.

9. **Budde, I., L. Steil, C. Scharf, U. Volker, and E. Bremer.** 2006. Adaptation of Bacillus subtilis to growth at low temperature: a combined transcriptomic and proteomic appraisal. Microbiology **152:**831-53.

10. **Butaye, P., L. A. Devriese, and F. Haesebrouck.** 2001. Differences in antibiotic resistance patterns of Enterococcus faecalis and Enterococcus faecium strains isolated from farm and pet animals. Antimicrob Agents

Chemother **45:**1374-8.

11. **Cao, M., B. A. Bernat, Z. Wang, R. N. Armstrong, and J. D. Helmann.** 2001. FosB, a cysteine-dependent fosfomycin resistance protein under the control of sigma(W), an extracytoplasmic-function sigma factor in Bacillus subtilis. J Bacteriol **183:**2380-3.

12. **Cao, M., T. Wang, R. Ye, and J. D. Helmann.** 2002. Antibiotics that inhibit cell wall biosynthesis induce expression of the Bacillus subtilis sigma(W) and sigma(M) regulons. Mol Microbiol **45:**1267-76.

13. **Cheng, T. J., M. T. Sung, H. Y. Liao, Y. F. Chang, C. W. Chen, C. Y. Huang, L. Y. Chou, Y. D. Wu, Y. H. Chen, Y. S. Cheng, C. H. Wong, C. Ma, and W. C. Cheng.** 2008. Domain requirement of moenomycin binding to bifunctional transglycosylases and development of high-throughput discovery of antibiotics. Proc Natl Acad Sci U S A **105:**431-6.

14. **Cremniter, J., J. L. Mainardi, N. Josseaume, J. C. Quincampoix, L. Dubost, J. E. Hugonnet, A. Marie, L. Gutmann, L. B. Rice, and M. Arthur.** 2006. Novel mechanism of resistance to glycopeptide antibiotics in Enterococcus faecium. J Biol Chem **281:**32254-62.

15. **Denham, E. L., P. N. Ward, and J. A. Leigh.** 2008. Lipoprotein signal peptides are processed by Lsp and Eep of Streptococcus uberis. J Bacteriol **190:**4641-7.

16. **Dunkley, E. A., Jr., S. Clejan, A. A. Guffanti, and T. A. Krulwich.** 1988. Large decreases in membrane phosphatidylethanolamine and diphosphatidylglycerol upon mutation to duramycin resistance do not change the protonophore resistance of Bacillus subtilis. Biochim Biophys Acta **943:**13-8.

17. **Duy, N. V., U. Mader, N. P. Tran, J. F. Cavin, T. Tam le, D. Albrecht, M. Hecker, and H. Antelmann.** 2007. The proteome and transcriptome analysis of Bacillus subtilis in response to salicylic acid. Proteomics **7:**698-710.

18. **Eiamphungporn, W., and J. D. Helmann.** 2008. The Bacillus subtilis sigma(M) regulon and its contribution to cell envelope stress responses. Mol Microbiol **67:**830-48.

19. **Eichenberger, P., M. Fujita, S. T. Jensen, E. M. Conlon, D. Z. Rudner, S. T. Wang, C. Ferguson, K. Haga, T. Sato, J. S. Liu, and R. Losick.** 2004. The program of gene transcription for a single differentiating cell type during sporulation in Bacillus subtilis. PLoS Biol **2:**e328.

20. **Flannagan, S. E., and D. B. Clewell.** 2002. Identification and characterization of genes encoding sex pheromone cAM373 activity in Enterococcus faecalis and Staphylococcus aureus. Mol Microbiol **44:**803-17.

21. **Fujita, M., J. E. Gonzalez-Pastor, and R. Losick.** 2005. High- and low-threshold genes in the Spo0A regulon of Bacillus subtilis. J Bacteriol **187:**1357-68.

22. **Gaballa, A., G. L. Newton, H. Antelmann, D. Parsonage, H. Upton, M. Rawat, A. Claiborne, R. C. Fahey, and J. D. Helmann.** Biosynthesis and functions of bacillithiol, a major low-molecular-weight thiol in Bacilli. Proc Natl Acad Sci U S A **107:**6482-6.

23. **Galperin, M. Y., and E. V. Koonin.** 2004. 'Conserved hypothetical' proteins: prioritization of targets for experimental study. Nucleic Acids Res **32:**5452-63.

24. **Gioia, J., S. Yerrapragada, X. Qin, H. Jiang, O. C. Igboeli, D. Muzny, S. Dugan-Rocha, Y. Ding, A. Hawes, W. Liu, L. Perez, C. Kovar, H. Dinh, S. Lee, L. Nazareth, P. Blyth, M. Holder, C. Buhay, M. R. Tirumalai, Y. Liu, I. Dasgupta, L. Bokhetache, M. Fujita, F. Karouia, P. Eswara Moorthy, J. Siefert, A. Uzman, P. Buzumbo, A. Verma, H. Zwiya, B. D. McWilliams, A. Olowu, K. D. Clinkenbeard, D. Newcombe, L. Golebiewski, J. F. Petrosino, W. L. Nicholson, G. E. Fox, K. Venkateswaran, S. K. Highlander, and G. M. Weinstock.** 2007. Paradoxical DNA Repair and Peroxide Resistance Gene Conservation in Bacillus pumilus SAFR-032. PLoS ONE **2:**e928.

25. **Halliday, J., D. McKeveney, C. Muldoon, P. Rajaratnam, and W. Meutermans.** 2006. Targeting the forgotten transglycosylases. Biochem Pharmacol **71:**957-67.

26. **Heinrich, J., T. Lunden, V. P. Kontinen, and T. Wiegert.** 2008. The Bacillus subtilis ABC transporter EcsAB influences intramembrane proteolysis through RasP. Microbiology **154:**1989-97.

27. **Henry, T., F. Garcia-Del Portillo, and J. P. Gorvel.** 2005. Identification of Salmonella functions critical for bacterial cell division within eukaryotic cells. Mol Microbiol **56:**252-67.

28. **Hornbaek, T., M. Jakobsen, J. Dynesen, and A. K. Nielsen.** 2004. Global transcription profiles and intracellular pH regulation measured in Bacillus licheniformis upon external pH upshifts. Arch Microbiol **182:**467-74.

29. **Iwamoto, K., T. Hayakawa, M. Murate, A. Makino, K. Ito, T. Fujisawa, and T. Kobayashi.** 2007. Curvature-dependent recognition of ethanolamine phospholipids by duramycin and cinnamycin. Biophys J **93:**1608-19.

30. **Jensen, L. J., M. Kuhn, M. Stark, S. Chaffron, C. Creevey, J. Muller, T. Doerks, P. Julien, A. Roth, M. Simonovic, P. Bork, and C. von Mering.** 2009. STRING 8--a global view on proteins and their functional interactions in 630 organisms. Nucleic Acids Res **37:**D412-6.

31. **Kallio, P. T., J. E. Fagelson, J. A. Hoch, and M. A. Strauch.** 1991. The transition state regulator Hpr of Bacillus subtilis is a DNA-binding protein. J Biol Chem **266:**13411-7.

32. **Kawachi, E., S. Abe, and T. Tanaka.** 2005. Inhibition of Bacillus subtilis scoC expression by multicopy senS. J Bacteriol **187:**8526-30.

33. **Kikukawa, T., S. Miyauchi, T. Araiso, N. Kamo, and T. Nara.** 2007. Anti-parallel membrane topology of two components of EbrAB, a multidrug transporter. Biochem Biophys Res Commun **358:**1071-5.

34. **Kobayashi, K., M. Ogura, H. Yamaguchi, K. Yoshida, N. Ogasawara, T. Tanaka, and Y. Fujita.** 2001. Comprehensive DNA microarray analysis of Bacillus subtilis two-component regulatory systems. J Bacteriol **183:**7365-70.

35. **Kodama, T., H. Takamatsu, K. Asai, N. Ogasawara, Y. Sadaie, and K. Watabe.** 2000. Synthesis and characterization of the spore proteins of Bacillus subtilis YdhD, YkuD, and YkvP, which carry a motif conserved among cell wall binding proteins. J Biochem **128:**655-63.

36. **Kolker, E., K. S. Makarova, S. Shabalina, A. F. Picone, S. Purvine, T. Holzman, T. Cherny, D. Armbruster, R. S. Munson, Jr., G. Kolesov, D. Frishman, and M. Y. Galperin.** 2004. Identification and functional analysis of 'hypothetical' genes expressed in Haemophilus influenzae. Nucleic Acids Res **32:**2353-61.

37. **Lemieux, M. J., Y. Huang, and D. N. Wang.** 2004. Glycerol-3-phosphate transporter of Escherichia coli: structure, function and regulation. Res Microbiol **155:**623-9.

38. **Leskela, S., V. P. Kontinen, and M. Sarvas.** 1996. Molecular analysis of an operon in Bacillus subtilis encoding a novel ABC transporter with a role in exoprotein production, sporulation and competence. Microbiology **142 (Pt 1):**71-7.

39. **Lindgren, V.** 1978. Mapping of a genetic locus that affects glycerol 3-phosphate transport in Bacillus subtilis. J Bacteriol **133:**667-70.

40. **Magnet, S., A. Arbeloa, J. L. Mainardi, J. E. Hugonnet, M. Fourgeaud, L. Dubost, A. Marie, V. Delfosse, C. Mayer, L. B. Rice, and M. Arthur.** 2007. Specificity of L,D-transpeptidases from gram-positive bacteria producing different peptidoglycan chemotypes. J Biol Chem **282:**13151-9.

41. **Marchler-Bauer, A., J. B. Anderson, F. Chitsaz, M. K. Derbyshire, C. DeWeese-Scott, J. H. Fong, L. Y. Geer, R. C. Geer, N. R. Gonzales, M. Gwadz, S. He, D. I. Hurwitz, J. D. Jackson, Z. Ke, C. J. Lanczycki, C. A. Liebert, C. Liu, F. Lu, S. Lu, G. H. Marchler, M. Mullokandov, J. S. Song, A. Tasneem, N. Thanki, R. A. Yamashita, D. Zhang, N. Zhang, and S. H.**

Bryant. 2009. CDD: specific functional annotation with the Conserved Domain Database. Nucleic Acids Res **37:**D205-10.

42. **Mascher, T., N. G. Margulis, T. Wang, R. W. Ye, and J. D. Helmann.** 2003. Cell wall stress responses in Bacillus subtilis: the regulatory network of the bacitracin stimulon. Mol Microbiol **50:**1591-604.

43. **McPherson, D. C., A. Driks, and D. L. Popham.** 2001. Two class A high-molecular-weight penicillin-binding proteins of Bacillus subtilis play redundant roles in sporulation. J Bacteriol **183:**6046-53.

44. **McPherson, D. C., and D. L. Popham.** 2003. Peptidoglycan synthesis in the absence of class A penicillin-binding proteins in Bacillus subtilis. J Bacteriol **185:**1423-31.

45. **Molle, V., M. Fujita, S. T. Jensen, P. Eichenberger, J. E. Gonzalez-Pastor, J. S. Liu, and R. Losick.** 2003. The Spo0A regulon of Bacillus subtilis. Mol Microbiol **50:**1683-701.

46. **Newton, G. L., M. Rawat, J. J. La Clair, V. K. Jothivasan, T. Budiarto, C. J. Hamilton, A. Claiborne, J. D. Helmann, and R. C. Fahey.** 2009. Bacillithiol is an antioxidant thiol produced in Bacilli. Nat Chem Biol **5:**625-7.

47. **Nishi, H., H. Komatsuzawa, T. Fujiwara, N. McCallum, and M. Sugai.** 2004. Reduced content of lysyl-phosphatidylglycerol in the cytoplasmic membrane affects susceptibility to moenomycin, as well as vancomycin, gentamicin, and antimicrobial peptides, in Staphylococcus aureus. Antimicrob Agents Chemother **48:**4800-7.

48. **Payie, K. G., P. N. Rather, and A. J. Clarke.** 1995. Contribution of gentamicin 2'-N-acetyltransferase to the O acetylation of peptidoglycan in Providencia stuartii. J Bacteriol **177:**4303-10.

49. **Pedersen, L. B., E. R. Angert, and P. Setlow.** 1999. Septal localization of penicillin-binding protein 1 in Bacillus subtilis. J Bacteriol **181:**3201-11.

50. **Peters, J. E., and N. L. Craig.** 2001. Tn7: smarter than we thought. Nat Rev Mol Cell Biol **2:**806-14.

51. **Petersohn, A., M. Brigulla, S. Haas, J. D. Hoheisel, U. Volker, and M. Hecker.** 2001. Global analysis of the general stress response of Bacillus subtilis. J Bacteriol **183:**5617-31.

52. **Petit, M. A., and S. D. Ehrlich.** 2000. The NAD-dependent ligase encoded by yerG is an essential gene of Bacillus subtilis. Nucleic Acids Res **28:**4642-8.

53. **Popham, D. L., and P. Setlow.** 1995. Cloning, nucleotide sequence, and mutagenesis of the Bacillus subtilis ponA operon, which codes for penicillin-

binding protein (PBP) 1 and a PBP-related factor. J Bacteriol **177:**326-35.

54. **Pragai, Z., and C. R. Harwood.** 2002. Regulatory interactions between the Pho and sigma(B)-dependent general stress regulons of Bacillus subtilis. Microbiology **148:**1593-602.

55. **Rahn-Lee, L., B. Gorbatyuk, O. Skovgaard, and R. Losick.** 2009. The conserved sporulation protein YneE inhibits DNA replication in Bacillus subtilis. J Bacteriol **191:**3736-9.

56. **Rasmussen, S., H. B. Nielsen, and H. Jarmer.** 2009. The transcriptionally active regions in the genome of Bacillus subtilis. Mol Microbiol **73:**1043-57.

57. **Rigsby, R. E., K. L. Fillgrove, L. A. Beihoffer, and R. N. Armstrong.** 2005. Fosfomycin resistance proteins: a nexus of glutathione transferases and epoxide hydrolases in a metalloenzyme superfamily. Methods Enzymol **401:**367-79.

58. **Ruiz-Maso, J. A., S. P. Anand, M. Espinosa, S. A. Khan, and G. del Solar.** 2006. Genetic and biochemical characterization of the Streptococcus pneumoniae PcrA helicase and its role in plasmid rolling circle replication. J Bacteriol **188:**7416-25.

59. **Salipante, S. J., M. Barlow, and B. G. Hall.** 2003. GeneHunter, a transposon tool for identification and isolation of cryptic antibiotic resistance genes. Antimicrob Agents Chemother **47:**3840-5.

60. **Salzberg, L. I., and J. D. Helmann.** 2008. Phenotypic and transcriptomic characterization of Bacillus subtilis mutants with grossly altered membrane composition. J Bacteriol **190:**7797-807.

61. **Scheffers, D. J.** 2005. Dynamic localization of penicillin-binding proteins during spore development in Bacillus subtilis. Microbiology **151:**999-1012.

62. **Scheffers, D. J., L. J. Jones, and J. Errington.** 2004. Several distinct localization patterns for penicillin-binding proteins in Bacillus subtilis. Mol Microbiol **51:**749-64.

63. **Shin, D. H., H. Yokota, R. Kim, and S. H. Kim.** 2002. Crystal structure of conserved hypothetical protein Aq1575 from Aquifex aeolicus. Proc Natl Acad Sci U S A **99:**7980-5.

64. **Stothard, P., G. Van Domselaar, S. Shrivastava, A. Guo, B. O'Neill, J. Cruz, M. Ellison, and D. S. Wishart.** 2005. BacMap: an interactive picture atlas of annotated bacterial genomes. Nucleic Acids Res **33:**D317-20.

65. **Tjalsma, H.** 2007. Feature-based reappraisal of the Bacillus subtilis exoproteome. Proteomics **7:**73-81.

66. **Tsuge, K., K. Matsui, and M. Itaya.** 2007. Production of the non-ribosomal peptide plipastatin in Bacillus subtilis regulated by three relevant gene blocks assembled in a single movable DNA segment. J Biotechnol **129:**592-603.

67. **Vander Horn, P. B., and S. A. Zahler.** 1992. Cloning and nucleotide sequence of the leucyl-tRNA synthetase gene of Bacillus subtilis. J Bacteriol **174:**3928-35.

68. **Wach, A.** 1996. PCR-synthesis of marker cassettes with long flanking homology regions for gene disruptions in S. cerevisiae. Yeast **12:**259-65.

69. **Winstedt, L., and C. von Wachenfeldt.** 2000. Terminal oxidases of Bacillus subtilis strain 168: one quinol oxidase, cytochrome aa(3) or cytochrome bd, is required for aerobic growth. J Bacteriol **182:**6557-64.

70. **Zamboni, N., and U. Sauer.** 2003. Knockout of the high-coupling cytochrome aa3 oxidase reduces TCA cycle fluxes in Bacillus subtilis. FEMS Microbiol Lett **226:**121-6.

71. **Zhang, Y. M., and C. O. Rock.** 2008. Membrane lipid homeostasis in bacteria. Nat Rev Microbiol **6:**222-33.

72. **Zhang, Z., C. Ma, O. Pornillos, X. Xiu, G. Chang, and M. H. Saier, Jr.** 2007. Functional characterization of the heterooligomeric EbrAB multidrug efflux transporter of Bacillus subtilis. Biochemistry **46:**5218-25.

CHAPTER 5

THE TRANSGLYCOSYLATION INHIBITORS RAMOPLANIN AND MOENOMYCIN INDUCE DISTINCT TRANSCRIPTIONAL RESPONSES

The transglycosylation step of cell wall synthesis is an important antibiotic target because it is essential and specific to bacteria. Moenomycin and ramoplanin are two antibiotics targeting this step, albeit by different mechanisms. The glycolipid moenomycin binds to the transglycosylase domain of penicillin binding proteins, while the lipoglycopeptide ramoplanin binds to lipid II, the enzyme and substrate during the transglycosylation reaction, respectively. In order to study how bacteria respond to inhibition of cell wall synthesis at the transglycosylation step, we have determined transcriptional profiles after treatment with moenomycin and ramoplanin in the Gram-positive model organism *Bacillus subtilis*. Contrary to our expectations, the antibiotics did not stimulate overlapping responses. Ramoplanin strongly induced the LiaRS two component system, which was previously shown to be induced by cell envelope active antibiotics, like vancomycin and daptomycin. LiaRS controls expression of the phage-shock-protein LiaH, which is assumed to protect against membrane perturbation. Moenomycin, however, almost exclusively induced genes that are part of the extracytoplasmic function σ factor σ^M regulon. σ^M regulates genes that are involved in cell wall synthesis, division, or cell shape determination. While a *liaH* deletion was not more susceptible to ramoplanin, a *sigM* deletion was much more sensitive to moenomycin. Overexpression of σ^V, which led to induction of a large fraction of the σ^M regulon, was not able to compensate for moenomycin susceptibility. The roles of σ^M and σ^V are discussed in the context of moenomycin resistance.

The majority of the studies in this chapter were performed by A. B. Hachmann. Thorsten Mascher (Ludwig-Maximilians-University Munich, Germany) contributed to the ramoplanin microarrays. Bronwyn Butcher (Cornell University) constructed the σ^V overexpression strain and did the σ^V microarrays. The data analysis was completed by A. B. Hachmann.

5.1 Introduction

Ramoplanin is a lipoglycodepsipeptide that inhibits cell wall synthesis of Gram-positive bacteria (Fig. 5.1). As a non-ribosomal peptide synthesis product of *Actinoplanes* ATCC 33076, it was found in at least three forms, A1, A2, and A3, which differ in their acyl chain substituents. With an overall positive charge, it comprises 17 amino acids that form a 49-member lactone ring with a di-mannose group and a polyprenyl tail (4, 19). It is in phase III clinical trials for the treatment of *Clostridium difficile*-associated diarrhea (CDAD) (2). In addition, it is also active against methicillin resistant *Staphylococcus aureus* and vancomycin resistant enterococci; though a systemic administration is not yet developed, because of ramoplanin's hydrolytic instability and potential to aggregate into insoluble fibrils (15, 16, 18).

Initial reports in 1990 on the mechanism of action of ramoplanin suggested that it targets lipid I and MurG (27). Then, it was not known that MurG and lipid I are intracellular targets. Walker *et al.*, however, found that ramoplanin inhibits transglycosylation by binding to extracellular lipid II, in a 2:1 ratio (Fig. 5.2) (18). It was shown to bind to the reducing end of the nascent glycan chain, at the initiation sites of PG synthesis and lipid II (16, 32). Figure 5.3 shows an x-ray crystal structure

(at 1.4 Å resolution) of a ramoplanin dimer appearing as two stacked antiparallel half-disks (19). By sequestering lipid II, the substrate for transglycosylation and transpeptidation, formation of the mature, fully cross-linked peptidoglycan is inhibited, which leads to a mechanically weakened cell wall and bacterial death from osmotic lysis (19).

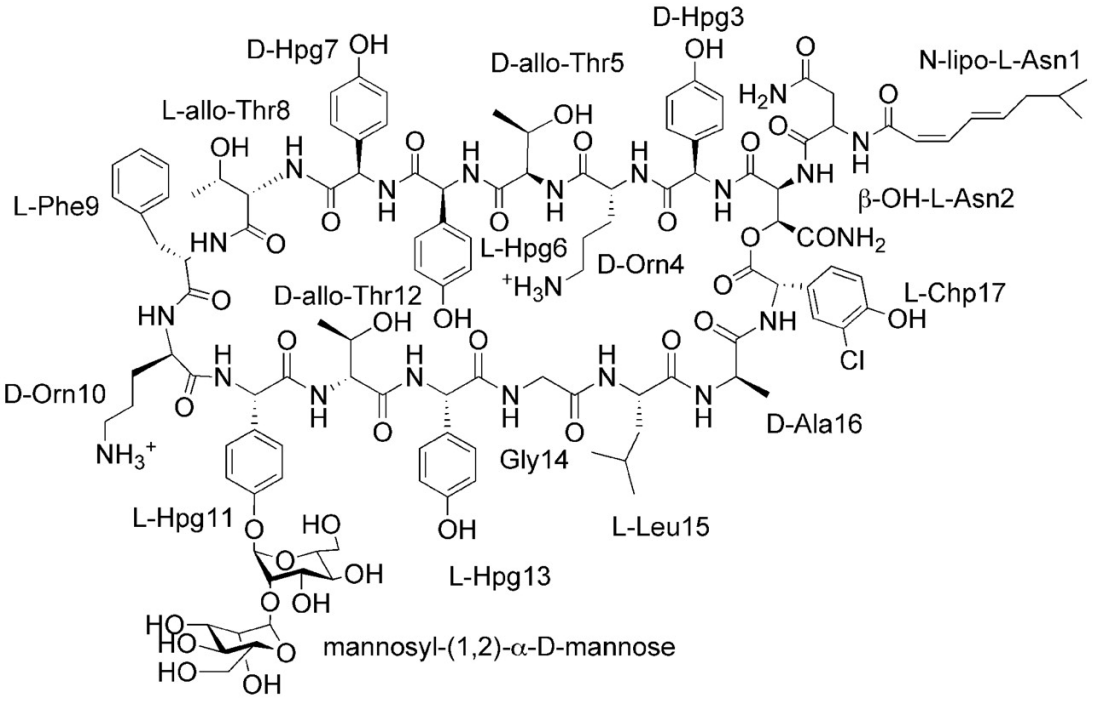

Figure 5.1. Structure of the lipoglycodepsipeptide ramoplanin (19).

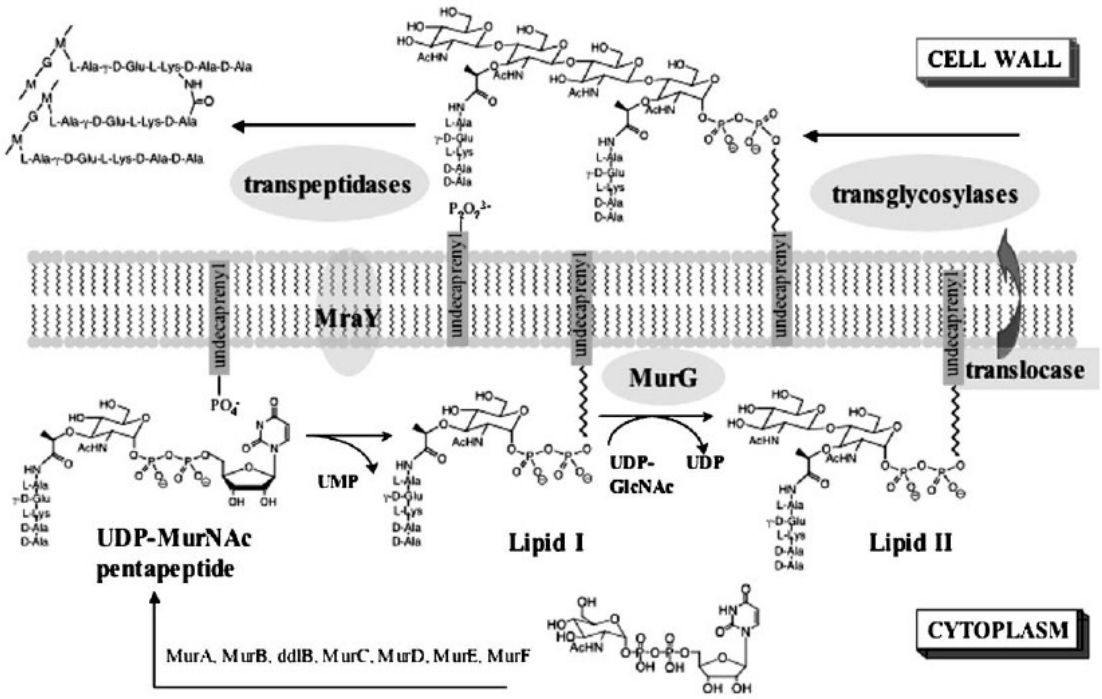

Figure 5.2. Ramoplanin inhibits transglycosylation by binding extracellular lipid II (16).

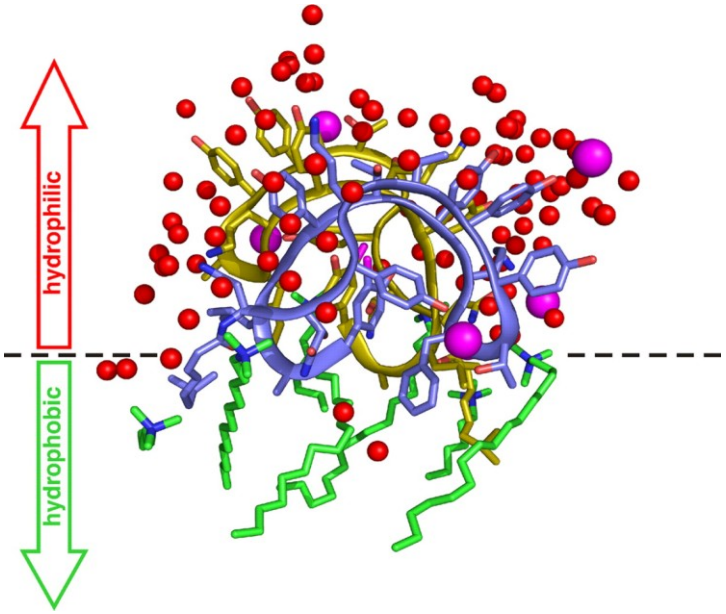

Figure 5.3. Structure of a ramoplanin dimer at the membrane interface (dotted line). Monomers are colored blue and yellow. Water: red spheres, chloride ions: magenta spheres, detergent molecules: green. The positions of the solvents illustrate the hydrophobicity distribution, PDB ID 1DSR (19).

Another well-characterized antibiotic targeting the transglycosylation step of Gram-positive bacteria is moenomycin (see also Chapter 1 and 4). Moenomycin is a glycolipid that was shown to bind to transglycosylase by mimicking lipid IV (dimer of two lipid II molecules) during peptidoglycan synthesis (Fig 5.4) (23, 29).

Here, we examined the transcriptional response to two antibiotics that both inhibit the transglycosylation step during cell wall synthesis in *B. subtilis*. The results prompted us to further investigate the regulons of the LiaRS two-component system and the extracytoplasmic function (ECF) σ factors σ^M and σ^V.

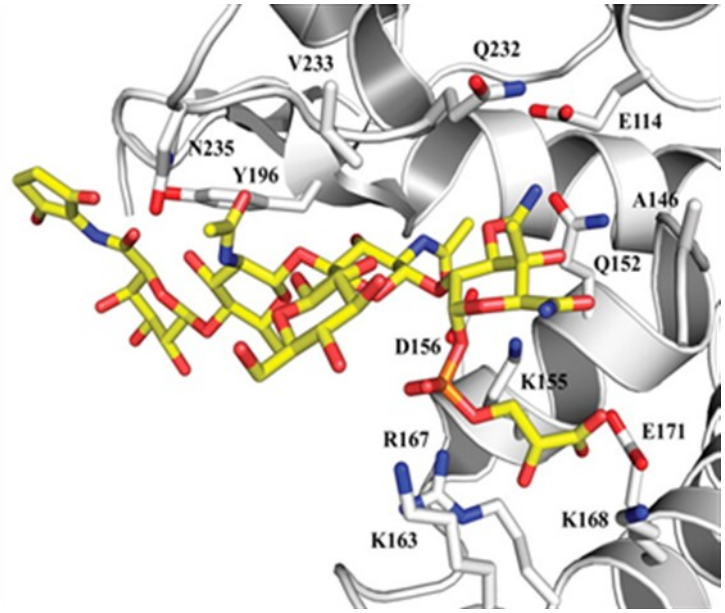

Figure 5.4. Crystal structure of moenomycin.
Sites of interaction with amino acids of the glycosyltransferase subunit of PBP2 of *S. aureus* are indicated, PDB ID 2OLV(23).

5.2 Materials and Methods

Bacterial strains and growth conditions. Bacteria were cultured at 37°C with vigorous shaking using Luria Bertani (LB) as growth medium. The following antibiotics were used for selection when necessary: spectinomycin 100 μg/ml, kanamycin 10 μg/ml, chloramphenicol 10 μg/ml, tetracycline 20 μg/ml, and erythromycin 1 μg/ml with lincomycin 25 μg/ml (mls: macrolide-lincomycin-streptogramin B resistance). The strains used in this study were derived from *Bacillus subtilis* wild-types W168 (*trpC2*) and CU1065 (W168 *trpC2 att*SPβ) and are listed in Table 5.1. Gene deletions were generated by replacing open reading frames with antibiotic resistance cassettes using long-flanking-homology PCR (25, 31). Moenomycin was kindly provided by Biovet JSC (Bulgaria). Minimal inhibitory concentrations (MIC) were determined by diluting overnight cultures 1:100, growing to OD_{600} of 0.4, and re-diluteding to 5 x 10^5 CFU/ml in microtiter plates with a total inoculum of 200 μl. Growth was measured spectrophotometrically (OD_{600}) using a Bioscreen incubator (Growth Curves USA, Piscataway, NJ) at 37°C with vigorous shaking. The absorbance was recorded every 20 minutes for 24 hours. Inhibition was defined as a final $OD_{600} < 0.05$ (at the 24 hour time point). In most cases, *B. subtilis* wild-type or mutants treated with moenomycin did not result in a clear determinable MIC, but rather in a delayed lag phase. After 24h W168 was able to grow even with addition of 500μ/ml or 2000μ/ml moenomycin. Here, to compare different mutants, we used the ability to outgrow a certain moenomycin concentration after a particular time as a measure of susceptibility. Zone of inhibition assays were performed as described previously (10).

RNA preparation and microarray analyses. Cultures were grown to mid-log phase (OD_{600} of 0.4) and split into two flasks. For ramoplanin, one sample was treated with 5 μg/ml for 10 mintues, for moenomycin, one sample was treated with 1 μg/ml for 15 minutes, for σ^V overexpression, 1mM IPTG was added for 20 minutes; the other sample was used as non-treated control. Total RNA was isolated from three different biological replicas with the RNeasy Mini Kit (Qiagen Sciences, Maryland). After DNase treatment with TURBO DNA-free™ (Ambion), RNA concentrations were quantified using a NanoDrop spectrophotometer (NanoDrop Tech. Inc., Wilmington, DE). The corresponding cDNA was synthesized from 20 μg total RNA and differentially labeled according to manufacturer's instructions using the SuperScript™ Plus Indirect cDNA labeling System (Invitrogen). Before and after indirect labeling with Alexa Fluor 555 or Alexa Fluor 647 (at least 3 h at room temperature) cDNA was purified using the Qiagen PCR purification kit (Qiagen, Maryland) and quantified with NanoDrop. Both labeled cDNA populations were combined (approximately 100 pmoles coupled cDNA each), denatured, and hybridized to a microarray slide overnight at 42°C for 16-18 h. After washing, hybridized microarray slides were scanned with a GenePix™ 4000B array scanner (Axon Instruments, Inc.). Our *B. subtilis* W168 microarrays, consisting of 4109 gene-specific antisense oligonucleotides (65-mers; Sigma-Genosys), were printed at the W.M. Keck Foundation Biotechnology Resource Laboratory, Yale University. Each slide contains 8,447 features corresponding to duplicates of each ORF-specific oligonucleotide, additional oligonucleotides of control genes, and 50% DMSO blank controls. Images were processed using the GenePix Pro 4.0 software package which produces (R,G) fluorescence intensity pairs for each gene. Each expression value is represented by at

least six separate measurements (duplicate spots on each of three arrays). Mean values and standard deviations were calculated with MS Excel. The normalized microarray datasets were filtered to remove those genes that were not expressed at levels significantly above background in either condition (sum of mean fluorescence intensity <20). In addition, the mean and standard deviation of the fluorescence intensities were computed for each gene and those where the standard deviation was greater than the mean value were ignored. The fold induction values were calculated by using the signal intensities of treated samples divided by untreated samples.

Cluster analysis. Results of whole genome microarray analyses of *B. subtilis* with a set of antimicrobial compounds from our data and from a study by Hutter *et al.* (20) was compared by complete linkage clustering (arrangement based on treatment and genetic response similarity) using the Gene Cluster 3.0 software. The resulting cluster was visualized with Treeview 1.60 written by Michael Eisen (14).

Table 5.1. Strains and oligonucleotides used in this study.

Strains	**Genotype, remarks**	**Reference**
W168	*trpC2*	BGSC no. 1A1
CU1065	W168 *trpC2 att*SPß	lab stock (30)
HB5121	W168 *liaIHGFSR::spc*	(17)
HB0933	CU1065 *liaR::kan*	(25)
HB0031	CU1065 *sigM::kan*	(11)
BSU2007	Δ7 ECF σ factor unmarked deletion	(1)

5.3 Results and Discussion

Unexpected stress responses to the transglycosylation inhibitors ramoplanin and moenomycin. Ramoplanin and moenomycin target the same step during peptidoglycan formation, with the former binding to the substrate (lipid II), and the latter the enzyme (HMW PBP) (Fig. 5.4) (18). In order to compare the transcriptional response to these two molecules that both inhibit transglycosylation, we performed microarrays of *B. subtilis* treated with the antibiotics.

Surprisingly, the transcriptional response showed no obvious overlap between the two antibiotics. Moenomycin treatment strongly induced the σ^M regulon, which is known to be upregulated by cell wall active antibiotics (Table 5.3). This is in contrast to earlier studies with vancomycin or bacitracin, where the induction of σ^M genes was almost always accompanied by induction of other ECF σ factors and TCS (e.g., σ^W, or LiaRS TCS) (8, 13). Here, we mainly saw members of the σ^M regulon, which confirmed Eiamphungporn's recent findings about the regulon (13).

Ramoplanin treatment, in turn, did not strongly induce the σ^M regulon. Instead, treatment resulted in upregulation of the LiaRS TCS and potential regulon members. Overall, the transcriptional response resembled more that of daptomycin treatment in *B. subtilis* (detailed in Chapter 2). This indicates that both antibiotics instigate different stresses in the cell envelope, and correspondingly lead to different responses.

The transcriptional response to ramoplanin. In order to learn more about the transcriptional response of *B. subtilis* to the lipid II-binding antibiotic ramoplanin, we conducted microarray experiments. Upon treatment with the drug we observed a strong induction of LiaRS TCS regulon members (Table 5.2, Fig. 5.5). LiaRS was originally named for Lipid II Interacting Antibiotics, because it was strongly

upregulated after treatment with the lipid II targeting antibiotics vancomycin or bacitracin (26). More recently, though, we found that *liaRS* is also induced by the membrane active antibiotic daptomycin (see Chapter 2, (17)). In fact, the response to daptomycin is very similar to that of ramoplanin (Fig 5.8). However, the two antibiotics differ with regard to mutant susceptibility; a *liaIH* deletion is more susceptible than wild-type to daptomycin, but not to ramoplanin. W168 and *liaIH* have an MIC of 0.4 μg/ml ramoplanin.

The low expression of other regulon members in the ramoplanin microarray was unexpected, as e.g., σ^M regulated genes were known to be strongly induced by other cell wall active antibiotics, like vancomycin, which also binds lipid II. To test whether other genes would be induced more strongly in the absence of the LiaRS TCS, we repeated the microarray with ramoplanin in the absence of the LiaR response regulator (Fig 5.6, Fig. 5.7). The *liaR* deletion strain shows some compensation by σ^M and spx regulated genes as well as other regulon members. Nonetheless, the role of the LiaRS TCS is clearly important in the stress response to these antibiotics. A question that still remains is why the two antibiotics, that each target different parts of the cell envelope, induce such a similar transcriptional response.

Table 5.2. Ramoplanin stimulon.
Genes induced or repressed more than two-fold are shown with their respective regulator.

Gene	Fold Change	Regulon	Gene	Fold Change	Regulon	Gene	Fold Change	Regulon
liaH	551.36	LiaRS	*yjbC*	6.95	ECF	*gabD*	6.02	Spx
liaI	176.84	LiaRS	*yceD*	2.89	ECF	*yhfJ*	4.33	Spx
liaF	54.30	LiaRS	*yceE*	2.67	ECF	*yfjR*	3.92	Spx
liaG	53.72	LiaRS	*yceF*	3.39	ECF	*ydiP*	3.92	Spx
liaR	31.51	LiaRS	*yceG*	2.63	ECF	*nfrA*	3.84	Spx
liaS	26.06	LiaRS	*yceH*	2.77	ECF	*yugJ*	3.44	Spx
yhcZ	3.52	LiaRS	*yrhI*	2.95	ECF	*yuaE*	3.20	Spx
yvrI	63.36	yvrIHa	*yrhH*	2.90	ECF	*yhfK*	3.06	Spx
yvrL	15.74	yvrIHa	*divIC*	2.51	ECF	*yjbH*	2.98	Spx
yvrH	4.70	yvrIHa	*abh*	2.43	ECF	*trxB*	2.83	Spx
oxdC	2.04	yvrIHa	*ywnJ*	2.03	ECF	*ywnF*	2.70	Spx
sigM	2.64	σ^M	*ylaC*	2.07	ECF	*yfiC*	2.63	Spx
yhdK	2.47	σ^M	*qoxD*	0.53	ECF	*sodA*	2.63	Spx
yhdL	3.00	σ^M	*yxlD*	3.21	σ^Y	*ymfH*	2.54	Spx
yqjL	10.44	σ^M σ^W	*yxlE*	2.07	σ^Y	*yqjM*	2.51	Spx
mreB	4.99	σ^M	*yxlF*	3.17	σ^Y	*ytzB*	2.51	Spx
mreD	2.65	σ^M	*yxlG*	2.07	σ^Y	*yvgP*	2.48	Spx
ytpA	4.01	σ^M	*xpaC*	2.37	σ^W	*ytcI*	2.44	Spx
divIB	3.98	σ^M	*yfhL*	2.35	σ^W	*yqiG*	2.42	Spx
yebC	3.83	σ^M	*ydjP*	2.11	σ^W	*yckI*	2.38	Spx
yfnI	3.55	σ^M	*yteJ*	0.52	σ^W	*yraA*	2.37	Spx
ydaH	3.27	σ^M	*ywbO*	2.77	σ^X	*yrzF*	2.34	Spx
hprT	3.16	σ^M	*ywjC*	3.33	σ^B	*trxA*	2.32	Spx
ycgQ	3.15	σ^M	*yvyD*	2.33	σ^B	*yugP*	2.25	Spx
ytpB	3.07	σ^M	*ykzA*	2.27	σ^B	*yvrD*	2.15	Spx
ypbG	2.59	σ^M	*ytkL*	2.18	σ^B	*yrzG*	2.14	Spx
yacC	2.05	σ^M	*ydaE*	2.13	σ^B	*ywrO*	2.13	Spx
yacK	2.49	σ^M	*ydaG*	2.10	σ^B	*yjbQ*	2.11	Spx
yacL	2.26	σ^M	*ytrA*	2.80	YtrA	*ywoB*	2.21	
sbp	2.48	σ^M	*ytrB*	2.68	YtrA	*ywoC*	5.05	
murB	2.32	σ^M	*ytrC*	3.26	YtrA	*ywoD*	3.73	
ypuA	2.23	σ^M	*ytrD*	3.83	YtrA	*ypbH*	2.02	
ypuD	2.07	σ^M	*ytrE*	2.28	YtrA			
			ytrF	2.28	YtrA			

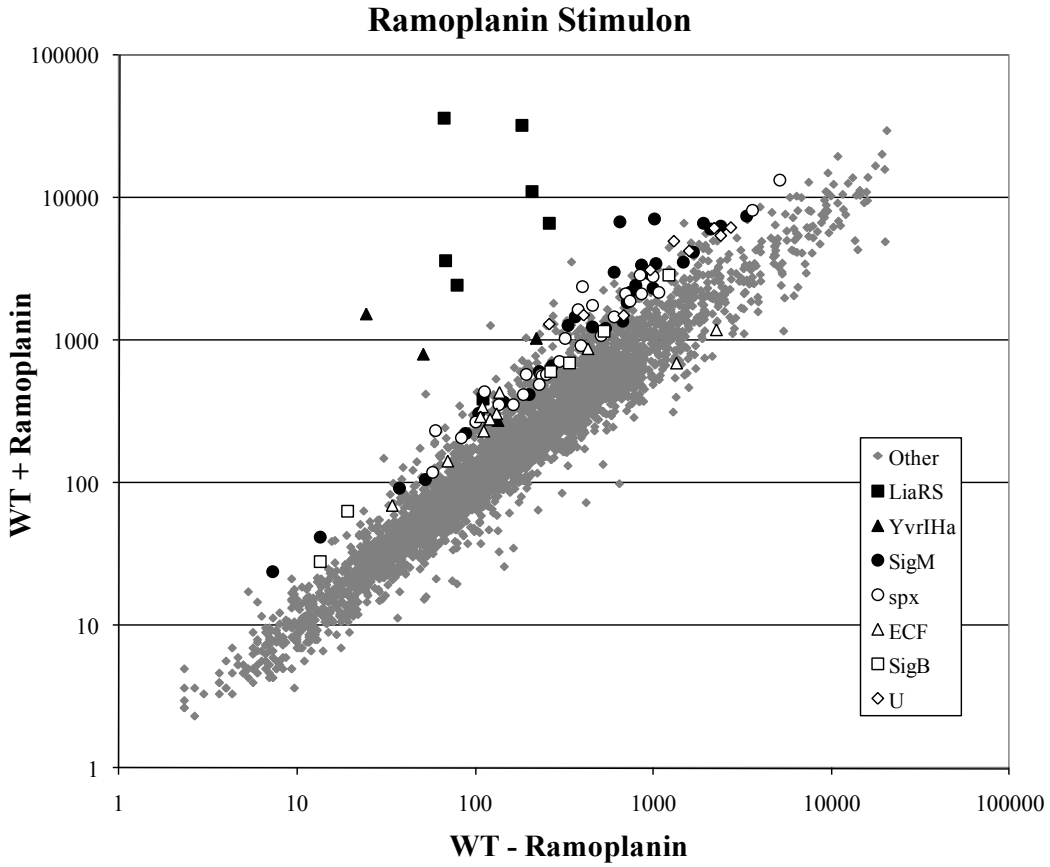

Figure 5.5. Ramoplanin stimulon in *B. subtilis*.
The scatterplot represents the average expression levels of treated versus untreated cultures of *B. subtilis* CU1065 (ramoplanin at 5 μg/mL, treated for 10 minutes) of triplicate microarray analyses. The legend lists highly expressed genes as grouped by their corresponding transcriptional regulators.

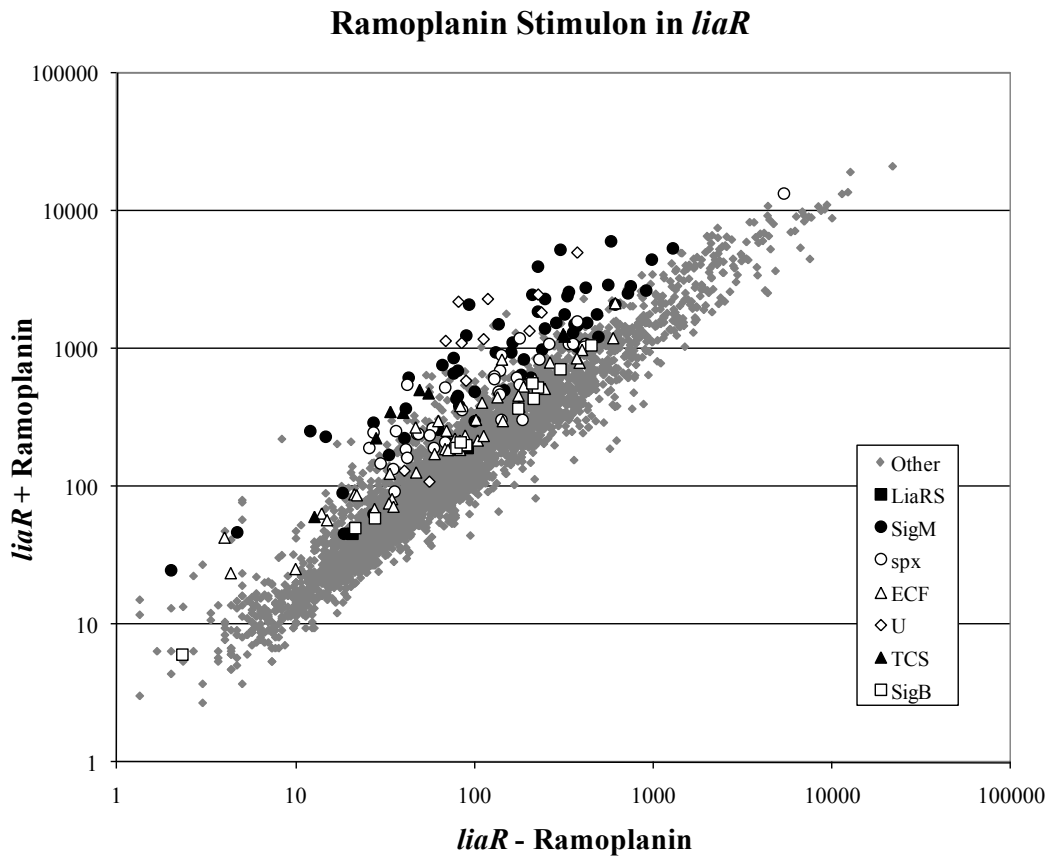

Figure 5.6. Ramoplanin stimulon in *B. subtilis liaR* deletion.
The scatterplot represents the average expression levels of treated versus untreated cultures of *B. subtilis liaR* (ramoplanin at 5 μg/mL, 10 minutes) of triplicate microarray analyses.

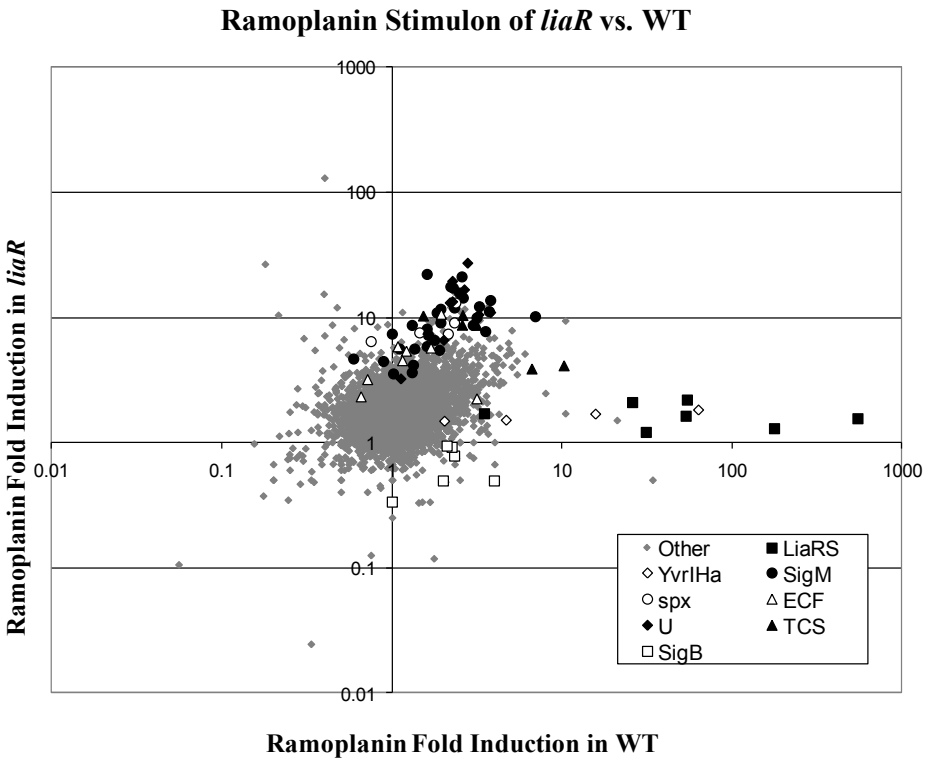

Figure 5.7. Ramoplanin stimulon of a *liaR* deletion versus wild-type CU1065.
The scatterplot represents the fold change of average expression levels of treated versus untreated cultures of *B. subtilis liaR* versus CU1065 (ramoplanin at 5 µg/mL, 10 minutes) of triplicate microarray analyses.

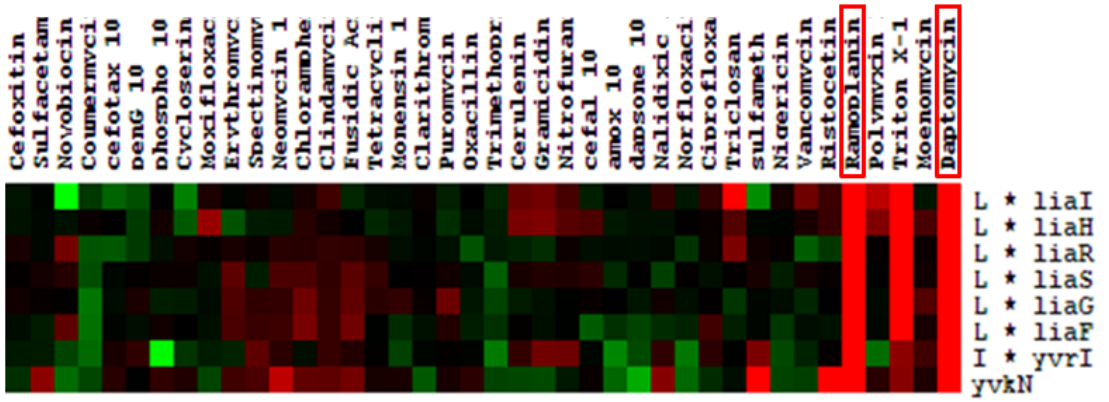

Figure 5.8. Cluster analysis of *B. subtilis* with 40 antibiotics.
LiaRS TCS regulon members cluster together and are strongly induced by ramoplanin and daptomycin. Gene expression profiles from Hutter *et al.* (20) and our data after treatment with 40 different antibiotics, complete linkage clustered, i.e. by treatment and fold change of gene expression. Red indicates induction and green repression after treatment, whereas black corresponds to unchanged gene expression.

Role of the LiaRS TCS in response to ramoplanin. Initial experiments with daptomycin suggested a mechanism of action involving inhibition of lipoteichoic acid synthesis, because of accumulation of lipoteichoic acid precursors (6), but later studies could not confirm these findings (28). However, a link to teichoic acids could also be deduced from ramoplanin's mechanism of action, binding to lipid II. Figure 5.9 shows the connection between peptidoglycan and teichoic acid synthesis (3). Upon treatment with ramoplanin, one could expect that the cell tries to compensate for the loss of lipid II (that is sequestered by ramoplanin), by producing more lipid II. However, the number of lipid II molecules is limited, as it usually is recycled during cell wall synthesis, and can only be compensated by drawing lipid II from the teichoic synthesis pathway. This could create an imbalance towards accumulation of toxic precursors, which was shown to be the likely reason for toxicity, when late teichoic acid synthesis enzymes were deleted (3, 12). Moreover, a decrease of teichoic acids also decreases the negative net charge of the cell envelope, probably causing further envelope stress. Whether the comparable response seen with ramoplanin and daptomycin is related to effects on teichoic acids, or has to do with secondary effects caused by accumulation of teichoic acid precursors, or effects of envelope charge alterations, can be the topic of future studies. Another aspect that both molecules have in common is that they are positively charged antimicrobial peptides (daptomycin indirectly by its complexation with Ca^{2+}), and that both anchor into the cell membrane with an acyl side chain.

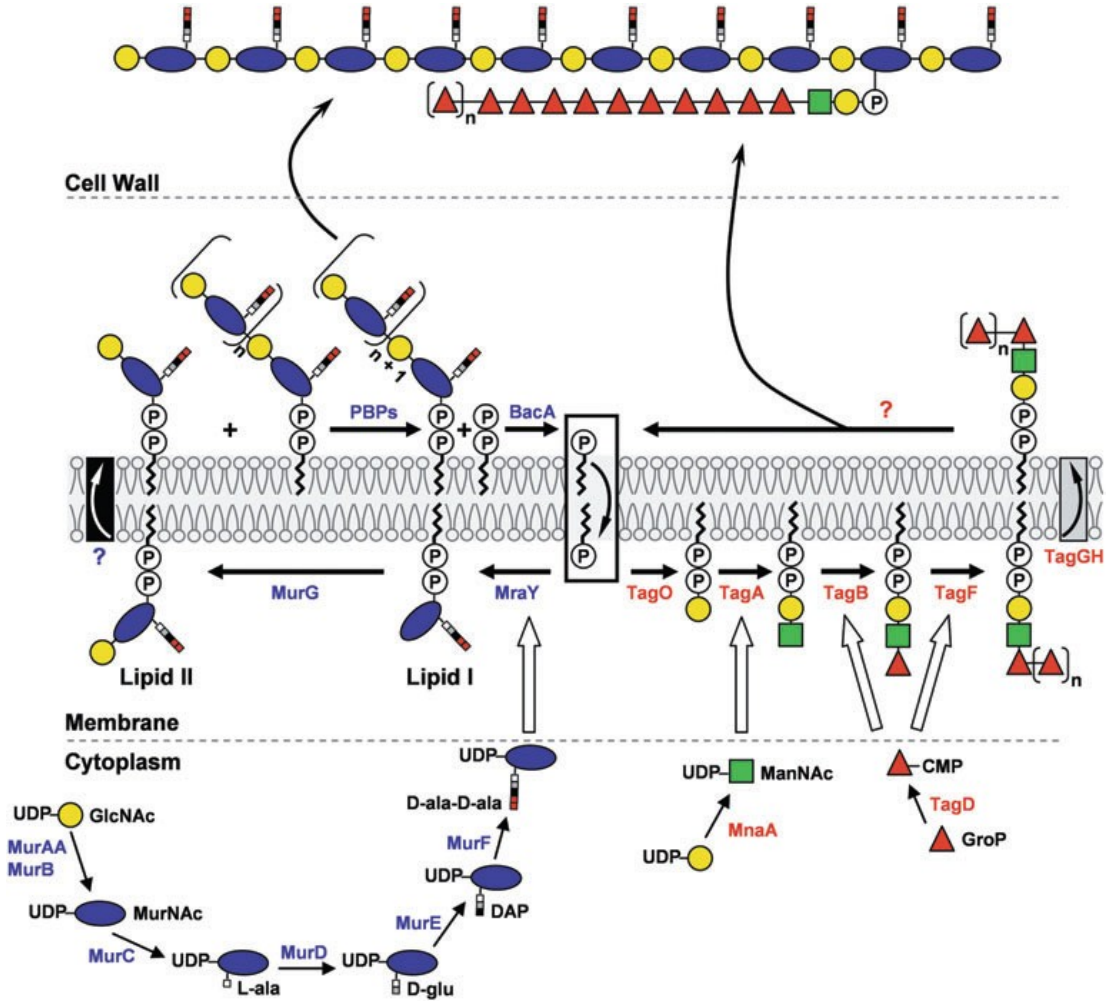

Figure 5.9. Teichoic acid and peptidoglycan synthesis.
Peptidoglycan on left and teichoic acid synthesis on right, with common substrate undecaprenyl-phosphate (in black rectangle). Teichoic acids are polymerized intracellularly, and peptidoglycan extracellularly. Solid arrows: enzyme catalysed step, block arrows: activated substrate, question mark: unknown enzymatic reactions (3).

The transcriptional response to moenomycin. We wondered whether moenomycin and ramoplanin induce a similar stress response in *B. subtilis*, since both antibiotics inhibit the transglycosylation step during cell wall synthesis. Treatment with moenomycin, however, resulted in a different response; it induced a large fraction of the σ^M regulon genes (Fig. 5.10). The σ^M regulon comprises about 60 genes, most of them involved in cell envelope synthesis, cell division and shape control, as well as DNA repair. The activation of its anti σ factor, YhdKL, is not yet known. σ^M is induced by cell wall active antibiotics, like vancomycin or bacitracin, and by heat stress or ethanol (11, 13, 21, 22). Table 5.3 summarizes the response of *B. subtilis* to moenomycin treatment. After 15 minutes treatment, 40 genes of the σ^M regulon were induced (20 minutes treatment caused even more σ^M genes to be induced, data not shown). Amongst them is *yebC*, a putative integral inner membrane protein, which was 3.3 fold induced, and which conferred resistance to moenomycin when disrupted by the Tn7SX transposon (see Chapter 4).

The induction of the σ^M regulon is in line with a similar induction by vancomycin, which also binds lipid II. Yet, as this response almost exclusively consists of σ^M regulon members, we wondered how a *sigM* deletion mutant would react to moenomycin. The response was overall less strong, but the fact that we still saw a subset of σ^M genes induced including *sigV* was intriguing. To get a clearer picture of the σ^V regulon we therefore performed transcriptional profiling on a strain that overexpressed σ^V in the absence of all other ECF σ factors.

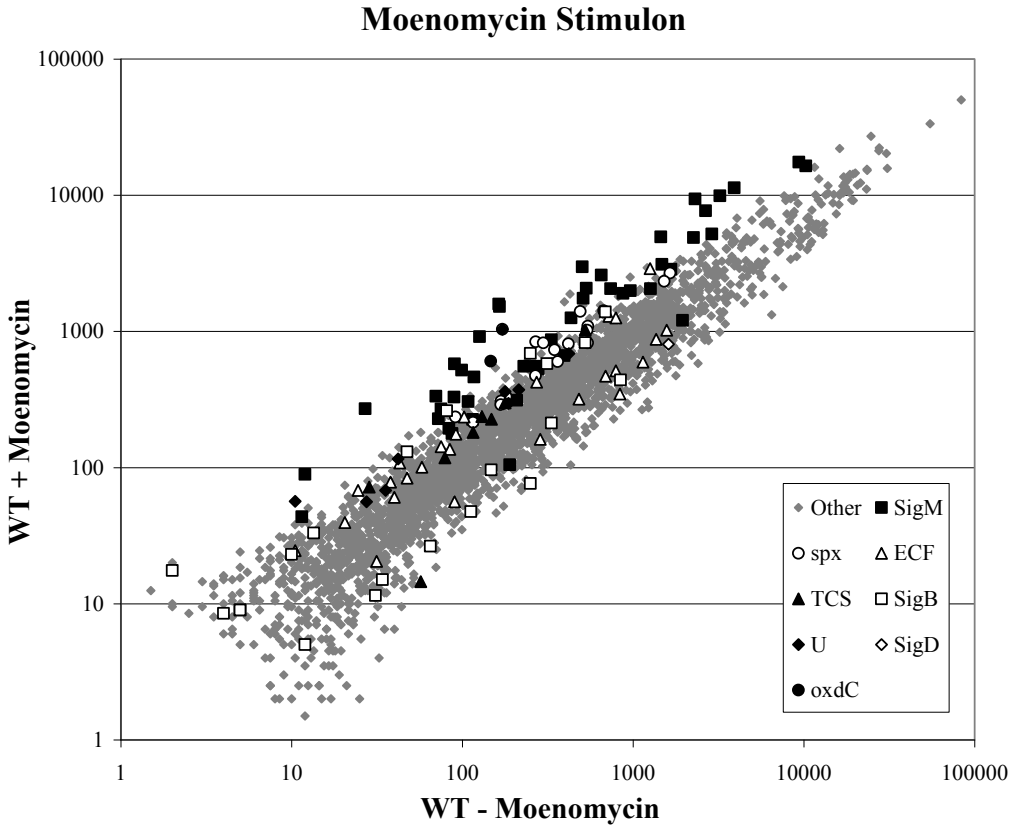

Figure 5.10. Moenomycin stimulon in *B. subtilis*.
The scatterplot represents average expression levels of treated versus untreated cultures of *B. subtilis* CU1065 (moenomycin at 1 µg/mL, 15 minutes). The legend lists highly expressed genes as grouped by their corresponding transcriptional regulators (U stands for unknown regulated group, e.g., ytr operon). Spots are labeled up to 1.5-fold induction or repression.

Table 5.3. Moenomycin stimulon and σ^V regulon.
Genes induced or repressed >1.5-fold are shown with their respective regulator.

Gene	Fold Change		Regulon	Gene	Fold Change		Regulon
	MOE	σ^V			MOE	σ^V	
yqjL	12.01	619.06	σ^M	*trxA*	2.84	-	Spx
murG	6.97	4.43	σ^M	*yvrD*	2.70	-	Spx
ypbG	6.21	2.25	σ^M	*yfiC*	2.62	-	Spx
murB	4.05	3.14	σ^M	*ywnF*	2.59	-	Spx
ywaC	3.58	56.90	σ^M	*nfrA*	2.54	-	Spx
yfnI	3.48	3.07	σ^M	*trxB*	2.49	-	Spx
ylxW	3.44	2.20	σ^M	*yuaE*	2.47	-	Spx
ydaH	3.26	899.95	σ^M	*gabD*	2.41	-	Spx
yhdK	3.25	2.08	σ^M	*yqiG*	2.33	-	Spx
yebC	3.25	13.94	σ^M	*yrzF*	2.17	-	Spx
yrhJ	2.98	5.08	σ^M	*yrzG*	2.14	-	Spx
divIB	2.93	2.39	σ^M	*yvgP*	2.10	-	Spx
ylxX	2.88	1.60	σ^M	*yckK*	2.09	-	Spx
maf	2.83	10.34	σ^M	*yugP*	2.02	-	Spx
ywnJ	2.62	360.14	σ^M	*yqjM*	1.81	-	Spx
yhdL	2.59	1.54	σ^M	*yckI*	1.80	-	Spx
dltE	2.50	12.13	σ^M	*ywrO*	1.69	-	Spx
ycgR	2.50	20.92	σ^M	*yraA*	1.67	-	Spx
ycgQ	2.49	52.37	σ^M	*yhfK*	1.63	-	Spx
yrhI	2.29	6.83	σ^M	*ymfH*	1.59	-	Spx
yacK	2.26	3.01	σ^M	*ydiP*	1.57	-	Spx
sbp	2.25	1.45	σ^M	*yjbI*	0.55	-	Spx
ywtF	2.21	7.66	σ^M	*yjbH*	0.39	-	Spx
ypuD	1.95	352.45	σ^M	*sodA*	0.31	-	Spx
sigM	1.93	-	σ^M	*sigZ*	2.72	-	σ^Z
mreC	1.92	3.45	σ^M	*yrpG*	1.98	-	σ^Z
mreB	1.90	4.01	σ^M	*ywhE*	2.67	-	ECF
yceC	1.88	4.41	σ^M	*ylaA*	2.41	7.33	ECF
yceD	1.84	3.69	σ^M	*qoxB*	0.69	-	ECF
mreD	1.67	3.73	σ^M	*ylaB*	0.48	12.76	ECF
minC	1.64	2.33	σ^M	*sigV*	2.56	47.21	σ^V
ytpA	1.59	0.94	σ^M	*yrhK*	2.13	16.29	σ^V
recU	1.58	1.37	σ^M	*yrhL*	3.19	13.15	σ^V
pbpX	1.56	5.41	σ^M	*ydcA*	2.31	-	σ^W
ywoA	1.55	24.11	σ^M	*yknW*	0.68	473.04	σ^W
abh	1.53	6.57	σ^M	*yuaI*	0.68	-	σ^W
divIC	1.53	4.26	σ^M	*ysdB*	0.57	-	σ^W
rodA	1.50	5.51	σ^M	*ythQ*	0.53	1.66	σ^W
yacA	1.56	1.49	σ^M	*yoaG*	0.53	4.46	σ^W
ponA	2.12	1.29	σ^M	*yozO*	0.35	21.47	σ^W
ywoB	1.80	-	YtrA	*sigX*	0.57	-	σ^X
ytrF	1.58	-	YtrA	*oxdC*	2.05	-	YvrHI
ywoC	1.51	-	YtrA	*yvrI*	1.82	-	YvrHI
ytrA	0.70	-	YtrA	*yvrL*	1.51	-	YvrHI
yycG	1.70	-	YycFG	*csbC*	1.94	-	σ^B
yxlF	1.61	92.77	σ^Y	*ytkL*	1.75	-	σ^B
yxlG	1.60	5.16	σ^Y	*csbB*	0.40	-	σ^B
yhcY	1.50	-	LiaRS	*nap*	0.32	-	σ^B

The σ^V regulon. σ^V belongs to the group of four ECF σ factors σ^V, σ^Y, σ^Z, and YlaC, that have not been studied extensively (24). Here, we wanted to elucidate the role of σ^V. We carried out microarray analyses with overexpression of σ^V in wild-type and in the absence of all seven ECF σ factors. The latter is a strain, which we obtained from Kei Asai, Japan (1). It has unmarked deletions of all seven ECF σ actors, which makes it a great tool to study each single σ factor individually. Here, this strain is called Δ7. We constructed an ectopic IPTG inducible (Pspac) copy of *sigV* into these strains. Cultures were grown to mid-exponential phase and split in two. One culture was induced for 20 minutes, and RNA was harvested from both for transcriptional profiling.

Surprisingly, overexpression of *sigV* in wild-type showed increased expression of 39 genes that are part of the σ^M regulon and four genes that are part of the σ^W regulon (Table 5.3) (Fig. 5.11). This opened up the question, whether σ^V induced expression of *sigM* and *sigW*, and thereby indirectly their regulon members, or whether σ^V induced those genes directly.

In order to address this, we repeated the σ^V overexpression microarray, but this time in the Δ7 background (Fig. 5.12). Again, a similar set of σ^M and σ^W regulon members was induced, but now much stronger. As this strain is missing all other ECF σ factors, we concluded that this is due to direct regulation by σ^V. Why a subset of the σ^M and σ^W regulated genes was present and not the whole operon is likely a result of closer similarity to the σ^V promoter consensus sequence (Fig. 5.14).

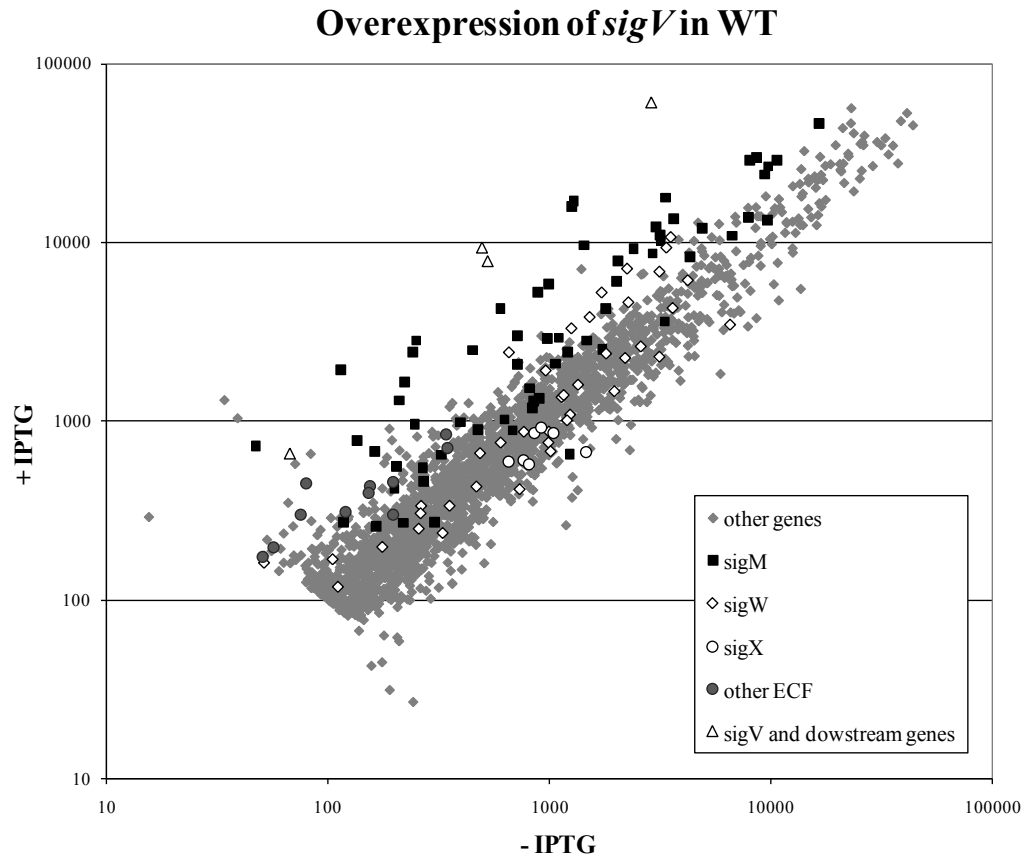

Figure 5.11. Overexpression of *sigV* in *B. subtilis* W168.
The scatterplot represents average expression levels of IPTG induced versus uninduced cultures of W168. The legend lists highly expressed genes as grouped by their corresponding transcriptional regulators.

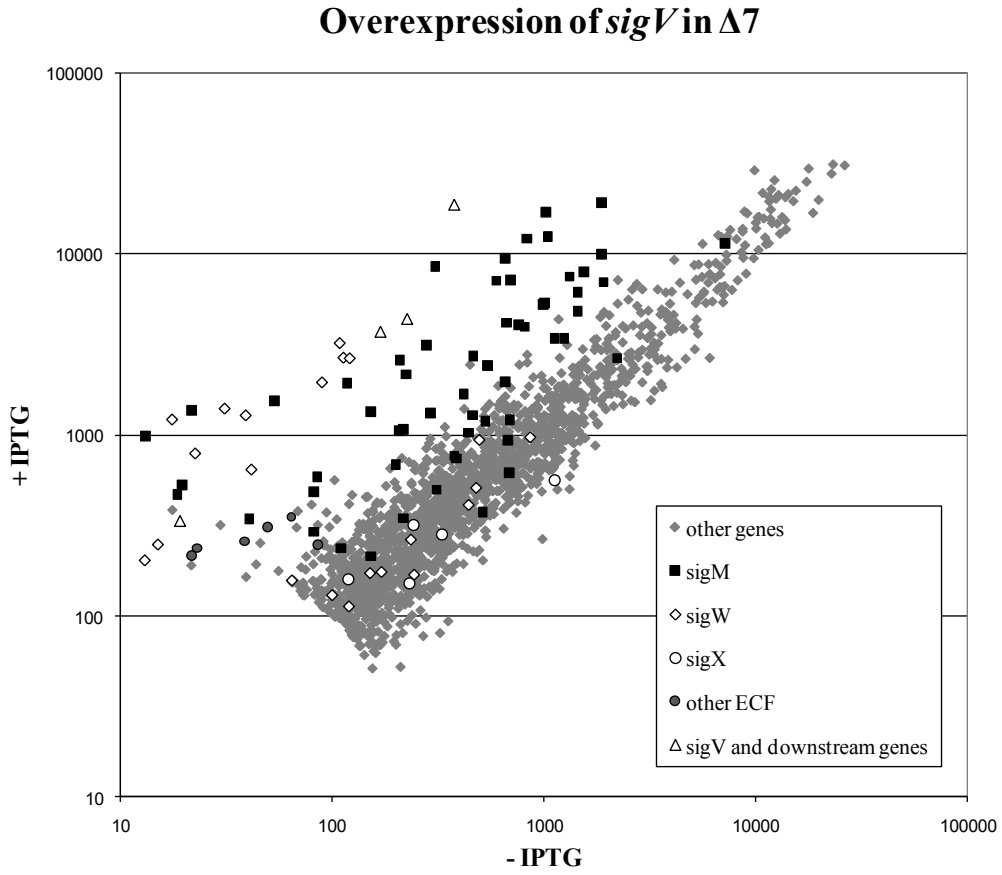

Figure 5.12. Overexpression of *sigV* in *B. subtilis* Δ7 ECF deletion strain.
The scatterplot represents average expression levels of IPTG induced versus uninduced cultures of Δ7. The legend lists highly expressed genes as grouped by their corresponding transcriptional regulators.

Overlapping promoter recognition of ECF σ factors. We have found earlier indications of promoter overlap among ECF σ factors when we compared antibiotic susceptibility of single, double, and triple mutants of *sigM, sigW,* and *sigX* in zone of inhibition assays (Fig 5.13) (24). When treated with the MurAA inhibitor fosfomycin, we saw that mainly σ^W was responsible for conferring resistance to the drug; as was σ^M for the transglycosylase inhibitor moenomycin. However, if the cells were treated with D-cycloserine, each single or double mutant had no significant effect, only in the

triple mutant, *sigMWX*, were the cells much more susceptible to the drug. This could be explained by a very similar promoter consensus sequence (Fig 5.14) (24).

The regulon overlap during overexpression of *sigV* could be due to promoter occlusion, where the three prominent ECF σ factors are hindering σ^V from binding to RNA polymerase, as they are expressed at much higher levels than σ^V. The overexpression allows σ^V to now bind to RNA polymerase in the presence of the other σ factors, and even stronger in their absence.

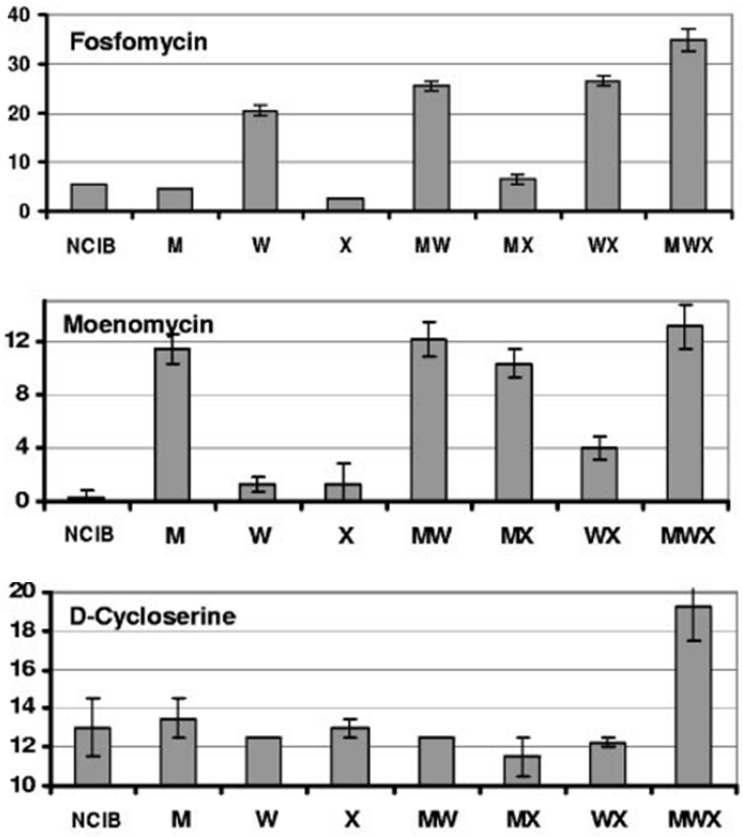

Figure 5.13. Antibiotic sensitivity profile of ECF σ mutants.
Each bar represents the average zone of inhibition of at least two assays performed with two independent clones of each deletion mutant (deleted sigma factors are shown on the *x* axis). The *y* axis shows the zone of inhibition (in millimeters), expressed as total diameter minus diameter of the filter paper disk (5.5 mm). NCIB: wild-type NCIB3610.

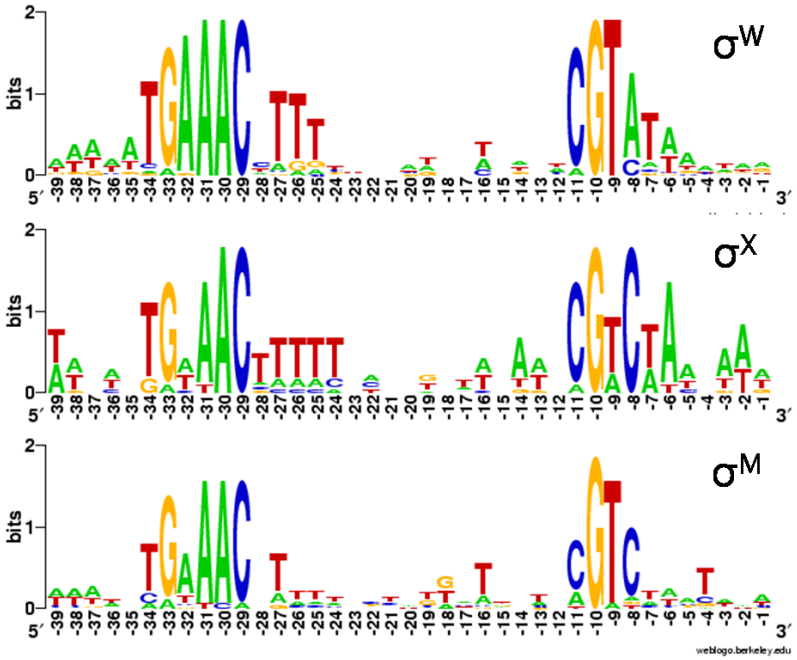

Figure 5.14. Promoter consensus sequence of σ^W, σ^X, and σ^M.
Weblogo representation of the position weight matrices for recognition by σ^M, σ^W, and σ^X. The promoters used for determining the consensus sequences are derived from published data (5, 7, 9, 13, 21) (generated at http://weblogo.berkeley.edu/logo.cgi).

Role of σ^V and σ^M in moenomycin resistance. Since σ^V regulates the expression of a large subset of genes from the σ^M regulon, we wondered whether σ^V overexpression could also confer resistance to moenomycin, like σ^M does (Fig 5.13, see also Chapter 4) (24). We tested this with liquid growth inhibition assays by measuring the minimal inhibitory concentration (MIC) after 10 hours of treatment with moenomycin. It turned out that a *sigM* deletion was very sensitive compared to the W168 wild-type, with an MIC of 0.4 µg/ml vs. 10 µg/ml, respectively. Overexpression of σ^V in the Δ7 background did not restore wild-type levels of susceptibility. In fact, this strain was as sensitive as the *sigM* deletion. This indicates that the resistance to moenomycin is conferred by regulon members that are exclusively regulated by σ^M and not by σ^V. The putative σ^V regulon is currently being

confirmed by other methods.

Exclusive members of the σ^M regulon and their promoter consensus sequence are listed in the left column of Table 5.4 and top panel of Figure 5.15, respectively. This table summarizes the results from comparing the known σ^M regulon with the putative σ^V regulon. The genes/operons in the right column were induced by *sigV* overexpression. Note the possibility that the Δ7 strain may have defects in the cell envelope or synthesis, which could lead to activation of other stress responses.

It is not yet known, which of the σ^M regulated genes is responsible for resistance to moenomycin. A likely candidate is PBP1 (*ponA*), because it is a target of moenomycin. Yet, when we tested a *ponA* deletion strain for moenomycin susceptibility, we did not see any difference compared to wild-type. This still leaves several genes as potential candidates. It is worth noting, that none of the moenomycin resistant mutations that were obtained through transposon mutagenesis (see Chapter 4) are among the genes that are exclusively regulated by σ^M.

Table 5.4. σ^V and σ^M specific regulon members.
About 15 operons are exclusively regulated by σ^M (putative) and 23 operons are putatively regulated by both, $\sigma^V$and σ^M.

operons exclusively regulated by σ^M	operons putatively regulated by σ^M and σ^V	
sigM yhdLK	*yqjL*	*ywtF*
ypbG	*ydaH*	*rodA*
ypuA	*yfnI*	*ypuD*
bcrC	*maf*	*ywaC*
yngC	*mreBCDminCD*	*yrhHIJ*
recUponA	*yacLM*	*abh*
(ydbO-ydbP(as))	*divIC*	*dltABCDE*
ytpAB	*(murG)murB*	*ywnJ*
yjbC spx	*divIBylxXW sbp*	*yceCDEFG*
rapD	*ycgRQ*	*pbpX*
secDF	*ddlmurF*	*ywbNO*
metA	*yebC*	
yacAhprTftsH		
yacBC		
ytnA		

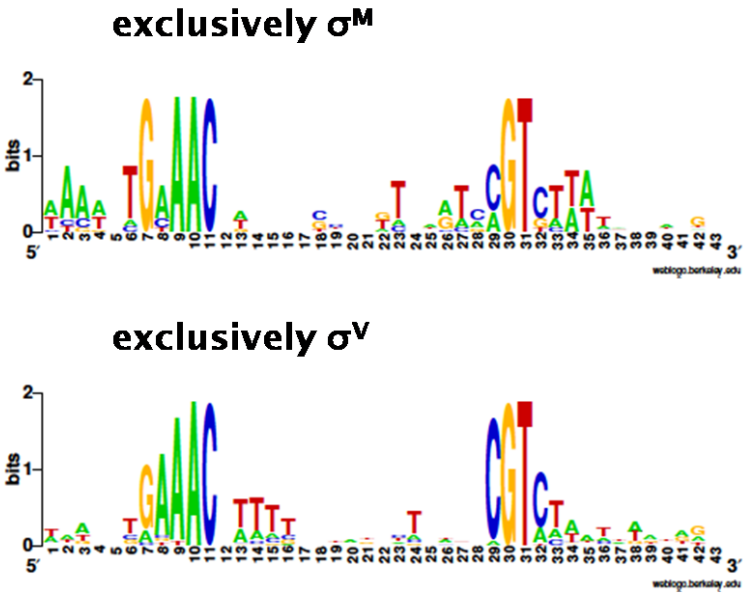

Figure 5.15. Promoter consensus sequence of σ^M and σ^V.
Weblogo representation of the position weight matrices for the potential recognition by σ^M or σ^V exclusively. The promoters used for determining the consensus sequences are derived from results of our expression profiling (weblogo generated at http://weblogo.berkeley.edu/logo.cgi).

5.4 Conclusions.

Even though the mechanism of action of an antibiotic has been studied, secondary effects, and stress responses are not quite apparent. Understanding these responses is of great importance to learn more about regulatory and structural aspects of the cell, as well as potential resistance mechanisms.

Here, we investigated stress responses to the cell wall active antibiotics moenomycin and ramoplanin. In contrast to our expectations, *B. subtilis* responded differently to antibiotics that target the same step during cell wall synthesis. Moenomycin induced the ECF σ factor σ^M, and ramoplanin the LiaRS TCS. Members of the σ^M regulon also conferred resistance to moenomycin. In addition, we showed that σ^V has an overlapping but smaller regulon compared to σ^M. The σ^V regulon is currently being studied and confirmed by other methods by Veronica Guariglia. Further experiments with ramoplanin were not carried to completion due to compound limitations.

The presented results focus on cell envelope stress response in *B. subtilis*, in particular on antibiotics that target the cell envelope, because of the rise in antibiotic resistance coupled with the slow rate of antibiotics discovery. New findings about stress responses and resistance can contribute to advance our understanding of the molecular nature of genetic systems involved in antibiotic resistance.

REFERENCES

1. **Asai, K., K. Ishiwata, K. Matsuzaki, and Y. Sadaie.** 2008. A viable Bacillus subtilis strain without functional extracytoplasmic function sigma genes. J Bacteriol **190:**2633-6.

2. **Balagopal, A., and C. L. Sears.** 2007. Clostridium difficile: new therapeutic options. Curr Opin Pharmacol **7:**455-8.

3. **Bhavsar, A. P., L. K. Erdman, J. W. Schertzer, and E. D. Brown.** 2004. Teichoic acid is an essential polymer in Bacillus subtilis that is functionally distinct from teichuronic acid. J Bacteriol **186:**7865-73.

4. **Breukink, E., and B. de Kruijff.** 2006. Lipid II as a target for antibiotics. Nat Rev Drug Discov **5:**321-32.

5. **Butcher, B. G., and J. D. Helmann.** 2006. Identification of Bacillus subtilis sigma-dependent genes that provide intrinsic resistance to antimicrobial compounds produced by Bacilli. Mol Microbiol **60:**765-82.

6. **Canepari, P., and M. Boaretti.** 1996. Lipoteichoic acid as a target for antimicrobial action. Microb Drug Resist **2:**85-9.

7. **Cao, M., and J. D. Helmann.** 2004. The Bacillus subtilis extracytoplasmic-function sigmaX factor regulates modification of the cell envelope and resistance to cationic antimicrobial peptides. J Bacteriol **186:**1136-46.

8. **Cao, M., and J. D. Helmann.** 2002. Regulation of the Bacillus subtilis bcrC bacitracin resistance gene by two extracytoplasmic function sigma factors. J Bacteriol **184:**6123-9.

9. **Cao, M., P. A. Kobel, M. M. Morshedi, M. F. Wu, C. Paddon, and J. D. Helmann.** 2002. Defining the Bacillus subtilis sigma(W) regulon: a comparative analysis of promoter consensus search, run-off transcription/macroarray analysis (ROMA), and transcriptional profiling approaches. J Mol Biol **316:**443-57.

10. **Cao, M., C. M. Moore, and J. D. Helmann.** 2005. Bacillus subtilis paraquat resistance is directed by sigmaM, an extracytoplasmic function sigma factor, and is conferred by YqjL and BcrC. J Bacteriol **187:**2948-56.

11. **Cao, M., T. Wang, R. Ye, and J. D. Helmann.** 2002. Antibiotics that inhibit cell wall biosynthesis induce expression of the Bacillus subtilis sigma(W) and sigma(M) regulons. Mol Microbiol **45:**1267-76.

12. **D'Elia, M. A., K. E. Millar, T. J. Beveridge, and E. D. Brown.** 2006. Wall teichoic acid polymers are dispensable for cell viability in Bacillus subtilis. J Bacteriol **188:**8313-6.

13. **Eiamphungporn, W., and J. D. Helmann.** 2008. The Bacillus subtilis sigma(M) regulon and its contribution to cell envelope stress responses. Mol Microbiol **67:**830-48.

14. **Eisen, M. B., P. T. Spellman, P. O. Brown, and D. Botstein.** 1998. Cluster analysis and display of genome-wide expression patterns. Proc Natl Acad Sci U S A **95:**14863-8.

15. **Fang, X., J. Nam, D. Shin, Y. Rew, D. L. Boger, and S. Walker.** 2009. Functional and biochemical analysis of a key series of ramoplanin analogues. Bioorg Med Chem Lett **19:**6189-91.

16. **Fang, X., K. Tiyanont, Y. Zhang, J. Wanner, D. Boger, and S. Walker.** 2006. The mechanism of action of ramoplanin and enduracidin. Mol Biosyst **2:**69-76.

17. **Hachmann, A. B., E. R. Angert, and J. D. Helmann.** 2009. Genetic analysis of factors affecting susceptibility of Bacillus subtilis to daptomycin. Antimicrob Agents Chemother **53:**1598-609.

18. **Halliday, J., D. McKeveney, C. Muldoon, P. Rajaratnam, and W. Meutermans.** 2006. Targeting the forgotten transglycosylases. Biochem Pharmacol **71:**957-67.

19. **Hamburger, J. B., A. J. Hoertz, A. Lee, R. J. Senturia, D. G. McCafferty, and P. J. Loll.** 2009. A crystal structure of a dimer of the antibiotic ramoplanin illustrates membrane positioning and a potential Lipid II docking interface. Proc Natl Acad Sci U S A **106:**13759-64.

20. **Hutter, B., C. Schaab, S. Albrecht, M. Borgmann, N. A. Brunner, C. Freiberg, K. Ziegelbauer, C. O. Rock, I. Ivanov, and H. Loferer.** 2004. Prediction of mechanisms of action of antibacterial compounds by gene expression profiling. Antimicrob Agents Chemother **48:**2838-44.

21. **Jervis, A. J., P. D. Thackray, C. W. Houston, M. J. Horsburgh, and A. Moir.** 2007. SigM-responsive genes of Bacillus subtilis and their promoters. J Bacteriol **189:**4534-8.

22. **Jordan, S., M. I. Hutchings, and T. Mascher.** 2008. Cell envelope stress response in Gram-positive bacteria. FEMS Microbiol Rev **32:**107-46.

23. **Lovering, A. L., L. H. de Castro, D. Lim, and N. C. Strynadka.** 2007. Structural insight into the transglycosylation step of bacterial cell-wall biosynthesis. Science **315:**1402-5.

24. **Mascher, T., A. B. Hachmann, and J. D. Helmann.** 2007. Regulatory overlap and functional redundancy among Bacillus subtilis extracytoplasmic function sigma factors. J Bacteriol **189:**6919-27.

25. **Mascher, T., N. G. Margulis, T. Wang, R. W. Ye, and J. D. Helmann.** 2003. Cell wall stress responses in Bacillus subtilis: the regulatory network of the bacitracin stimulon. Mol Microbiol **50:**1591-604.

26. **Mascher, T., S. L. Zimmer, T. A. Smith, and J. D. Helmann.** 2004. Antibiotic-inducible promoter regulated by the cell envelope stress-sensing two-component system LiaRS of Bacillus subtilis. Antimicrob Agents Chemother **48:**2888-96.

27. **Reynolds, P. E., and E. A. Somner.** 1990. Comparison of the target sites and mechanisms of action of glycopeptide and lipoglycodepsipeptide antibiotics. Drugs Exp Clin Res **16:**385-9.

28. **Silverman, J. A., N. G. Perlmutter, and H. M. Shapiro.** 2003. Correlation of daptomycin bactericidal activity and membrane depolarization in Staphylococcus aureus. Antimicrob Agents Chemother **47:**2538-44.

29. **Sung, M. T., Y. T. Lai, C. Y. Huang, L. Y. Chou, H. W. Shih, W. C. Cheng, C. H. Wong, and C. Ma.** 2009. Crystal structure of the membrane-bound bifunctional transglycosylase PBP1b from Escherichia coli. Proc Natl Acad Sci U S A **106:**8824-9.

30. **Vander Horn, P. B., and S. A. Zahler.** 1992. Cloning and nucleotide sequence of the leucyl-tRNA synthetase gene of Bacillus subtilis. J Bacteriol **174:**3928-35.

31. **Wach, A.** 1996. PCR-synthesis of marker cassettes with long flanking homology regions for gene disruptions in S. cerevisiae. Yeast **12:**259-65.

32. **Walker, S., L. Chen, Y. Hu, Y. Rew, D. Shin, and D. L. Boger.** 2005. Chemistry and biology of ramoplanin: a lipoglycodepsipeptide with potent antibiotic activity. Chem Rev **105:**449-76.

APPENDIX

Table S3.1. Differential quantification of gene expression of Dap^R1 and W168 without daptomycin treatment. Genes induced or repressed >2.5-fold are shown.

Gene	Signal Intensity Dap^{R}1	W168	Fold Change	Function of Gene Product
yrkP	1670	104	16.1	TCS response regulator (regulates *yrkR, yrkO, yrkN, ykcC, ykcB*)
yrkQ	1151	135	8.6	TCS histidine kinase
yrkR	6561	63.8	102.9	*psiE*, phosphate starvation inducible protein
yrkO	84	24.3	3.5	similarity to transporter
yrkN	58	10.3	5.7	GCN5-related N-acetyltransferase
ykcB	1128	3.3	347	similar to glycosyltransferase
ykcC	2239	66.8	33.5	similar to glycosyltransferase
bioA	1373	91	15.1	biotin biosynthesis
bioB	1781	94.5	18.8	biotin biosynthesis
bioD	2151	140	15.4	biotin biosynthesis
bioI	1407	54.3	25.9	biotin biosynthesis
yuiG	408	97.8	4.2	biotin biosynthesis
yycA	438	118	3.7	similar to *ykcB* (glycosyltransferase)
yorJ	314	1	314	putative DNA primase
yorH	329	168	2.0	unknown
liaI	2091	192	10.9	putative membrane protein
liaH	1642	127	13.0	PspA homolog, cell membrane protection
liaG	275	87.5	3.1	putative membrane anchored protein
liaF	331	164	2.0	negative regulator of LiaR
liaS	304	145	2.1	TCS histidine kinase
liaR	113	69	1.6	TCS response regulator
yvrI	76	14.8	5.2	σ factor YvrI
yvrH	158	63	2.5	TCS response regulator
yvrG	378	176	2.2	TCS histidine kinase
oxdC	312.8	122	2.6	oxalate decarboxylase
bcrC	277	48	5.7	bacteriocin transport/UPP phosphatase
yqjL	504	55	9.2	hydrolase; paraquat resistance
ypbG	385	39.8	9.7	phosphoesterase
ypbH	412	159	2.6	similar to negative regulation of competence; MecA
ywlC	112	52.8	2.1	sua5/yciO/yrdC/ywlC family protein
ywlD	99.8	6.5	15.4	putative integral inner membrane protein
ysbA	178	13.3	13.4	murein hydrolase regulator LrgA
ysbB	167	28.5	5.9	antiholin-like protein LrgB
yobE	68.5	31.3	2.2	similar to general secretion pathway protein
yobJ	90.3	41.3	2.2	helix-turn-helix domain protein
yobQ	173	65	2.7	AraC/XylS family
yobR	230	34	6.8	GCN5-related N-acetyltransferase
yobS	293	38.3	7.7	TetR family transcriptional regulator
yobT	520	41	12.6	metallo-beta-lactamase family protein
yvfR	371	41	9.0	similar to ABC transporter (ATP-binding)
yvfS	310	30.1	10.1	similar to ABC transporter transmembrane subunit
yvfT	237	48.8	4.9	similar to TCS histidine kinase
yvfU	128	22	5.8	similar to TCS response regulator
yfhD	227	88.8	2.6	hypothetical protein
yfhE	347	141	2.5	hypothetical protein
yfhK	2153	841	2.6	similar to cell-division inhibitor
yfhL	651	230	2.83	hypothetical protein
yfhM	792	315	2.5	similar to epoxide hydrolase; induced by phosphate starvation (sigma-B-dependent, PhoPR-independent)
yfhO	504	214	2.4	similar to multidrug resistance protein
yhfR	1088	337	3.2	similar to 2,3-diphosphoglycerate-dependent phosphoglycerate mutase
yhfT	558	195	2.9	similar to long-chain fatty-acid-CoA ligase
yhfU	152	18.8	8.1	similar to biotin biosynthesis
yclF	93.3	46.8	2.0	similar to di-tripeptide ABC transporter (membrane protein)

Table S3.1. (Continued)

Gene	Signal Intensity Dap^{R}1	Signal Intensity W168	Fold Change	Function of Gene Product
yclH	299	42	7.1	similar to ABC transporter (permease)
cotC	74.5	10.8	6.9	spore coat protein, late sporulation; σ^K controlled
ytbJ	807	377	2.1	thiamin biosynthesis
ytbQ	651	98	6.7	similar to epimerase/dehydratase
yqhA	101	15.5	6.5	similar to positive regulator of σ^B-activity, negative regulator of σ^B-activity in unstressed cells; acts with RsbR, YkoB, and YojH; similar to RsbR
xlyA	173	86.5	2.0	N-acetylmuramoyl-L-alanine amidase, major role in defective prophage PBSX-mediated lysis, endolysin; similar to CwlA of the skin element
xlyB	126	19.8	6.4	N-acetylmuramoyl-L-alanine amidase, major role in defective prophage PBSX-mediated lysis
coxA	317	51.5	6.2	spore cortex protein, located within the spore integument
ycgA	158	27	5.9	putative short-chain fatty acids transport protein
ycgQ	160	56.8	2.8	similar to ABC transporter, substrate-binding protein
ycgR	103	52.5	2.0	similar to ABC transporter, permease protein
yebC	184	31.5	5.9	putative permease
yebG	259	129	2.0	hypothetical protein
ywaC	339	65	5.2	similar to GTP-pyrophosphokinase, RelA/SpoT domain
ypnP	135	26.3	5.1	putative drug/sodium antiporter
des	1560	322.8	4.8	desaturase
desR	175	40.8	4.3	TCS response regulator, regulating desaturase
yaaH	81.3	33.5	2.4	spore protein required for L-alanine-stimulated germination; cell wall binding motif probably involved in assembly of the forespore; σ^E -dependent; similar to cortical fragment-lytic enzyme
yaaK	1059	522	2.0	unknown
yaaL	360	74.8	4.8	unknown
yaaN	264	119	2.2	putative toxic anion resistance protein
sigW	2573	602	4.3	ECF σ factor
rsiW	518	125	4.1	ECF anti-σ factor
sigM	109	45	2.4	ECF σ factor
yhdL	194	72.5	2.7	ECF anti-σ factor
sigY	206	105	2.0	ECF σ factor
sigX	621	386	1.6	ECF σ factor
rsiX	261	128	2.1	ECF anti-σ factor
mlpA	958	227	4.2	regulation of aprE, mitochondrial processing peptidase-like, zinc protease
yozE	84.3	21	4.0	similar to serine-type D-Ala-D-Ala carboxypeptidase
yqiB	657	260	2.5	exodeoxyribonuclease
yqiC	303	77.5	3.9	exodeoxyribonuclease
truA	112	29	3.8	pseudouridylate synthase A
truB	536	278	1.9	tRNA pseudouridine 55 synthase B
yoqA	154	46	3.3	unknown
yoqB	76.5	20	3.8	unknown
yoqC	196	67.3	2.9	unknown
yocD	290	113	2.6	similar to phage-related DNA-binding protein anti-repressor
yoqE	101	38.8	2.6	unknown
yoqF	127	1	127	unknown
yoqG	198	1	198	unknown
yoqH	79.3	30.8	2.6	unknown
yoqJ	81.8	42.5	1.9	unknown
yoqK	158	67.5	2.3	unknown
yoqU	87.3	45.5	1.9	unknown
divIB	1212	318	3.8	cell division
ylxX	771	229	3.4	cell division
ylxW	310	96.8	3.2	cell division
sbp	841	327	2.6	cell division

Table S3.1. (Continued)

Gene	Signal Intensity Dap^{R}1	Signal Intensity W168	Fold Change	Function of Gene Product
yxjA	742	279	2.7	nucleoside transporter
yxjI	416	110	2.7	similar to UDP-N-acetylenolpyruvoylglucosamine reductase
tdk	171	45	3.8	thymidine kinase
leuD	110	30	3.7	3-isopropylmalate dehydratase (small subunit)
abrB	1152	319	3.6	transcriptional pleiotropic regulator of transition state genes
abh	3303	1293	2.6	transcriptional regulator of transition state genes (AbrB-like)
radC	960	267	3.6	DNA repair protein
yopX	265	119	2.2	Unknown
yopY	184	51.5	3.6	Unknown
bofA	433	122	3.6	inhibition of pro-sigma-K processing
yhaX	126	35.8	3.5	similar to HAD superfamily hydrolase
yosI	271	129	2.1	SPBc2 prophage-derived uncharacterized protein yosI
yosJ	197	82.8	2.4	hypothetical protein
yosK	452	179	2.5	hypothetical protein
yosL	187	52.5	3.6	hypothetical protein
yosM	127	36.8	3.5	ribonucleotide reductase stimulatory protein
proI	93.8	27.3	3.4	pyrroline-5-carboxylate reductase
proS	4098	1563	2.6	prolyl-tRNA synthetase
ykkC	220	76.8	2.9	ykkCD coexpression in *E. coli* gives rise to a broad specificity, multidrug-resistant phenotype; similar to molecular chaperone; ykkC and ykkD are tandemly duplicated genes
ykkD	231	84	2.8	small multidrug resistance protein
ykkE	327	97.3	3.4	similar to formyltetrahydrofolate deformylase
ymaA	829	335	2.5	similar to NrdI protein
ymaB	540	163	3.3	mutt/nudix family
spoVT	555	170	3.3	transcriptional positive and negative regulator of sigma-G-dependent genes
spoVC	862	370	2.3	peptidyl-tRNA hydrolase
ykuR	1292	636	2.0	N-acetyl-diaminopimelate deacetylase
ykuS	508	241	2.1	hypothetical protein
ykuT	143	43.8	3.3	similar to MscS, small conductance mechanosenstive ion channel protein
ywrE	209	64.3	3.3	Unknown
ydpI	474	148	3.2	similar to permease
ywqE	139	43.5	3.2	similar to capsular polysaccharide biosynthesis
ywqF	225	112	2.0	similar to UDP-glucose 6-dehydrogenase
ymfE	104	52	2.0	similar to multidrug resistance protein
ymfI	357	113	3.2	short-chain dehydrogenase
ymfJ	360	142	2.5	Unknown
araR	415	131	3.2	negative regulation of the L-arabinose metabolic operon (araABDLMNPQ-abfA) and of the araE/araR genes
ydaB	47.8	15.3	3.1	similar to long-chain-fatty-acid--CoA ligase
ydaD	218	85	2.6	similar to short-chain dehydrogenase/reductase
ydaE	171	70.8	2.4	similar to ABC-type sugar transport system
ydaG	2549	1178	2.2	similar to general stress protein (sigB dependent)
ydaJ	47	16.8	2.8	putative glycosyl hydrolase lipoprotein
ydaK	61.3	22.8	2.7	putative membrane protein, diguanylate cyclase domain
ydaN	59	21.3	2.8	similar to cellulose synthase domain protein
ykrI	119	55.8	2.1	Anti-sigma-I factor rsgI
ykrL	398	160	2.5	heat shock protein HtpX (zinc dependent protease)
ykrS	94.8	41	2.3	methylthioribose-1-phosphate isomerase (methionine salvage pathway)
ykrX	337	109	3.1	2-OH-3-keto-5-methylthiopentenyl-1-P- phosphatase
ykrY	354	123	2.9	methylthioribulose-1-phosphate dehydratase
gspA	4970	1611	3.1	general stress protein (sigB dependent)

Table S3.1. (Continued)

Gene	Signal Intensity Dap^{R}1	Signal Intensity W168	Fold Change	Function of Gene Product
xhlA	311	112	2.8	involved in cell lysis upon induction of defective prophage PBSX
xhlB	671	218	3.1	involved in cell lysis upon induction of defective prophage PBSX
ykgA	905	295	3.1	similar to N-Dimethylarginine dimethylaminohydrolase
murB	1345	454	3.0	peptidoglycan synthesis
murG	812	265	3.1	peptidoglycan synthesis
pbpA	2233	989	2.3	cell wall elongation in spore outgrowth
pbpX	421	169	2.5	penicillin-binding protein, beta lactamase
ponA	1270	594	2.1	penicillin-binding proteins 1A/1B; required for vegetative growth or spore outgrowth under divalent cation limitation conditions; localized to and has an important function in the division septum in vegetative cells; mutant cells display a significant septation defect and FtsZ rings with aberrant structure or improper localization
mreB	1123	564	2.0	cell-shape determining protein
pbpB	1421	736	1.9	formation of the cell-division septum (late stage), required for both the initiation of division and continued septal ingrowth; recruited to the division site, continually during septal ingrowth; present transiently in the asymmetrical septum of sporulating cells; closely related to pbpB of E. coli
yvrD	841	276	3.1	similar to ketoacyl-carrier protein reductase
yvgW	176	57.8	3.0	similar to heavy metal-transporting ATPase
yvgY	175	87.3	2.0	copZ, copper insertion chaperone and transporter component
yvaD	70.3	23.3	3.0	putative integral inner membrane protein
yvaE	87.8	37.3	2.4	similar to multidrug-efflux transporter
ywkE	399	133	3.0	Protein hemK
ywkF	152	62.8	2.4	hypothetical protein
yfjS	55	18.5	3.0	exported N-acetylmuramic acid deacetylase
yptA	344	117	2.9	hypothetical protein
maf	677	235	2.9	septum formation
yuzF	232	81.3	2.9	hypothetical protein
yeaA	731	260	2.8	hypothetical protein
glpD	483	172	2.8	glycerol-3-phosphate dehydrogenase
ymzA	708	253	2.8	unknown
ymzC	71.3	30.3	2.4	hypothetical protein
ytzG	133	47.8	2.8	similar to 16S pseudouridylate synthase
xkdF	538	255	2.8	PBSX prophage, similar to YqbD of the skin element
xkdG	300	110	2.8	PBSX prophage, similar to YqbE of the skin element
xkdH	298	134	2.2	PBSX prophage, similar to YqbH of the skin element
xkdI	497	245	2.0	PBSX prophage, similar to YqbI of the skin element
xkdJ	312	139	2.3	PBSX prophage, similar to YqbJ of the skin element
xkdK	149	96.8	2.6	PBSX prophage, similar to sheath tail protein
xkdM	166	59.5	2.8	PBSX prophage, similar to YqbM of the skin element
xkdO	178	74.5	2.4	PBSX prophage, putative lytic transglycosylase
xkdQ	186	102	1.8	PBSX prophage, putative phage cell wall hydrolase
xkdU	130	47.3	2.8	PBSX prophage, similar to YqcA of the skin element
xkdV	128	56.3	2.3	PBSX prophage, similar to YqcC of the skin element
xkdW	140	60.8	2.3	PBSX prophage, similar to YqcD of the skin element
xkdX	135	46.8	2.9	PBSX prophage, similar to YqcE of the skin element
ybaE	1296	470	2.8	similar to ABC/cobalt transporter
ybaF	411	167	2.5	similar to ABC/cobalt transporter
yybS	630	231	2.7	hypothetical protein
yybT	869	412	2.1	similar to diguanylate cyclase and phosphoesterase
dltA	4819	1825	2.6	LTA/WTA synthesis
dltB	5417	1995	2.7	LTA/WTA synthesis
dltC	2199	827	2.7	LTA/WTA synthesis
dltD	4698	1785	2.6	LTA/WTA synthesis
dltE	1487	489	3.0	LTA/WTA synthesis

Table S3.1. (Continued)

Gene	Signal Intensity Dap^{R}1	Signal Intensity W168	Fold Change	Function of Gene Product
tlp	324	120	2.7	small acid-soluble spore protein (thioredoxin-like protein)
yitL	56.8	21	2.7	hypothetical protein
ykoX	309	115	2.7	hypothetical protein
ydjN	229	99.5	2.3	unknown
ydjP	482	179	2.7	unknown
yvkC	605	226	2.7	phosphoenolpyruvate synthase
ytxD	323	122	2.7	similar to flagellar motor protein
ytxE	133	52.5	2.5	similar to motility protein
ytxJ	3491	1527	2.3	general stress regulon controlled by σ^B; induced by salt addition during logarithmical growth
mtlA	441	191	2.3	phosphotransferase system (PTS) mannitol-specific enzyme IICBA component
mtlD	1659	627	2.7	mannitol-1-phosphate dehydrogenase
ypuD	265	100	2.6	hypothetical membrane lipoprotein
thyB	478	181	2.6	thymidylate synthase
yodS	77.8	29.5	2.6	similar to putative aminoacyloate CoA-transferase
clpE	44.8	17	2.6	ATP-dependent Clp protease-like (class III stress gene)
uvrB	292	111	2.6	excinuclease ABC (subunit B)
uvrC	177	73.8	2.4	excinuclease ABC (subunit C)
yabD	457	220	2.1	metal-dependent DNase
yabK	1067	407	2.6	hypothetical protein
xepA	126	48	2.6	lytic exoenzyme associated with defective prophage PBSX, unlikely to be involved in host cell lysis; similar to YqxG of the skin element
yceG	4872	1903	2.6	tellurium resistance protein
yceH	2037	931	2.2	similar to toxic anion resistance protein
safA	3710	1458	2.5	morphogenetic protein associated with SpoVID during the early stage of coat assembly; localized in the cortex, near the interface with the coat in mature spores; mutant spores have defective coats which are missing several proteins (CotG); cell wall binding motif probably involved in assembly on the forespore; sigma-E-dependent
yxiT	305	120	2.5	hypothetical protein
dxr	1547	611	2.5	1-deoxy-D-xylulose-5-phosphate reductoisomerase
yndN	277	110	2.5	Metallothiol transferase fosB
yoaF	564	251	2.2	similar to sortase family protein
yoaG	86	34	2.5	similar to bacitracin resistance protein?
ybxA	401	161	2.5	similar to cobalt transporter ATP-binding subunit
sspA	510	206	2.5	small acid-soluble spore protein (alpha-type SASP), major; localized on the nucleoid in developing forespores; localized to the ring-shaped nucleoid of the germinating spore
ahrC	787	321	2.5	negative regulation of arginine biosynthesis
gid	1112	468	2.4	glucose-inhibited division protein
uppS	2078	910	2.3	undecaprenyl pyrophosphate synthetase
ywiE	845	374	2.3	similar to cardiolipin synthetase
yfnI	2659	1267	2.1	exported glycerol phosphate lipoteichoic acid synthetase and anion-binding protein
idh	547	1983	0.28	myo-inositol 2-dehydrogenase
malL	5265	19093	0.28	maltose-inducible alpha-glucosidase
yuxI	41.3	151	0.27	hypothetical protein
lacR	23.3	85.5	0.27	negative regulation of beta-galactosidase (lacA)
ybbC	33.3	124	0.27	similar to beta-lactamase
mmsA	277	1044	0.26	methylmalonate-semialdehyde dehydrogenase

Table S3.1. (Continued)

Gene	Signal Intensity Dap^{R}1	Signal Intensity W168	Fold Change	Function of Gene Product
yqaR	21.8	83.8	0.26	hypothetical protein
yoaP	88.8	346	0.26	uncharacterized N-acetyltransferase
opuCA	80.3	203	0.40	glycine betaine/carnitine/choline ABC transporter (ATP-binding protein)
opuCB	89.3	313	0.28	glycine betaine/carnitine/choline ABC transporter (membrane protein)
opuCC	108	443	0.24	glycine betaine/carnitine/choline ABC transporter (osmoprotectant-binding)
opuCD	144	459	0.31	glycine betaine/carnitine/choline ABC transporter (membrane protein)
yczF	58.3	239	0.24	hypothetical protein
iolB	783	2874	0.27	myo-inositol catabolism
iolC	373	1247	0.30	myo-inositol catabolism
iolD	244	1004	0.24	myo-inositol catabolism
iolE	163	640	0.26	myo-inositol catabolism
iolF	528	1597	0.33	myo-inositol catabolism
iolH	225	630	0.36	myo-inositol catabolism
iolI	99.5	285	0.35	myo-inositol catabolism
yvbI	64.8	194	0.33	putative permease
yvbJ	197	820	0.24	hypothetical protein
htrA	450	1889	0.24	serine protease Do (heat-shock protein), probably involved in processing, maturation, or secretion of extracellular enzymes
yurI	18.5	82.8	0.22	extracellular ribonuclease
yxeL	44.0	200	0.22	similar to GCN5-related N-acetyltransferase
yxeM	45.0	163	0.28	putative ABC transporter, extracellular solute binding protein, polar amino acid transporter
yxeN	39.8	119	0.33	putative ABC transporter, permease
yxeO	83.5	194.5	0.43	putative ABC transporter, ATP-binding protein
yxeP	29.3	70.5	0.41	putative carboxypeptidase, aminohydrolase
yxeQ	45.5	102	0.45	MmgE/PrpD family protein, propionate catabolism
ytiB	2889	13333	0.22	carbonic anhydrase
ytmA	36.3	182	0.20	putative hydrolase
ytmI	41.0	109	0.38	putative N-acetyltransferase
araB	26.8	82.3	0.33	L-ribulokinase
araD	69.0	231	0.30	L-ribulose-5-phosphate 4-epimerase
araL	48.8	132	0.37	L-arabinose operon, putative phosphatase
araM	3187	16405	0.19	Glycerol-1-phosphate dehydrogenase
araP	56.3	148	0.38	L-arabinose transport
yvdA	64.3	138	0.47	similar to carbonic anhydrase
yvdF	2090	5557	0.38	glucan 1,4-alpha-maltohydrolase
yvdG	8787	29262	0.30	maltose/maltodextrin-binding lipoprotein
yvdH	3556	24806	0.24	maltodextrin ABC transport system (permease)
yvdI	5467	24465	0.22	maltodextrin ABC transporter (permease)
yvdJ	4340	22404	0.19	putative component of transporter
yvdK	5594	22591	0.25	maltose phosphorylase
yvdO	50.5	195	0.26	spore coat protein assembly factor CotR
yqbR	45.5	250	0.18	conserved hypothetical protein; skin element
ctaC	534	2805	0.19	cytochrome caa3 oxidase
ctaD	699	3878	0.18	cytochrome caa3 oxidase
ctaE	895	5266	0.17	cytochrome caa3 oxidase
ctaF	401	2228	0.18	cytochrome caa3 oxidase
ctaG	2166	4506	0.48	cytochrome aa(3) assembly factor
ctaO	19	99.8	0.19	protoheme IX farnesyltransferase (heme O synthase)
qcrA	908	6094	0.15	menaquinol:cytochrome c oxidoreductase
qcrB	1385	9258	0.15	menaquinol:cytochrome c oxidoreductase
qcrC	656	3739	0.18	menaquinol:cytochrome c oxidoreductase
yveA	20	135	0.15	L-aspartate/L-glutamate permease
yveF	139	295	0.47	hypothetical protein

Table S3.1. (Continued)

Gene	Signal Intensity Dap^{R}1	Signal Intensity W168	Fold Change	Function of Gene Product
yveK	35.5	92	0.39	modulator of protein tyrosine kinase EpsB, epsA
yveM	10.8	57	0.19	Probable polysaccharide biosynthesis protein epsC
yveO	26.8	70.8	0.38	similar to glycosyltransferase, epsE
yveP	47	95.5	0.49	similar to glycosyltransferase, epsF
yveQ	46.8	120	0.39	biofilm extracellular matrix formation enzyme, epsG
yydC	94	276	0.34	hypothetical protein
yydI	55.0	195	0.28	ABC transporter
yydJ	10.8	73.5	0.15	putative permease for export of a regulatory peptide
arfM	117	802	0.15	regulation of anaerobic genes
lctP	1937	13382	0.14	L-lactate permease
yisN	49.5	358	0.14	hypothetical protein
rbsA	658	4537	0.15	ribose ABC
rbsB	1323	8676	0.15	ribose ABC
rbsC	690	5069	0.14	ribose ABC
rbsD	653	3203	0.20	ribose ABC
rbsK	717	2030	0.35	ribokinase
rbsR	538	1635	0.33	negative regulation of the ribose operon (rbsRKDACB)
appA	179	1349	0.13	oligopeptide ABC transporter
appB	95.0	692.8	0.14	oligopeptide ABC transporter
appC	72.3	387	0.19	oligopeptide ABC transporter
appF	189	1060	0.18	oligopeptide ABC transporter
narG	299	1744	0.17	nitrite extrusion protein, nitrate reductase
narH	2201	17613	0.12	nitrite extrusion protein, nitrate reductase
narI	542	3755	0.14	nitrite extrusion protein, nitrate reductase
narJ	902	6895	0.13	nitrite extrusion protein, nitrate reductase
narK	177	1361	0.13	nitrite extrusion protein, nitrate reductase
wprA	80.8	654	0.12	cell wall-associated protein precursor
tnrA	283	2385	0.12	global nitrogen regulation (positive regulation of nrgAB, nasBCDEF, gabP, ureABC, guaD; negative regulation of glnRA, gltAB)
abnA	19.0	165	0.11	arabinan-endo 1,5-alpha-L-arabinase
glpT	192	1962	0.10	glycerol-3-phosphate permease
citB	49.5	192	0.26	aconitate hydratase
acoA	114	385	0.30	acetoin dehydrogenase
acoB	29.0	347	0.08	acetoin dehydrogenase
acoC	71.3	452	0.16	acetoin dehydrogenase
acoL	59.0	371	0.16	acetoin dehydrogenase
ptsG	142	1720	0.08	glucose transport and phosphorylation
ptsH	4952	8698	0.57	histidine-containing phosphocarrier protein of the phosphotransferase system (PTS) (HPr protein)
msmE	50.5	614	0.08	multiple sugar-binding protein
msmR	53.5	137	0.39	transcriptional regulator (LacI family)
msmX	289	1434	0.20	ATP-binding protein
melA	79.8	981	0.08	α -D-galactoside galactohydrolase
yesL	105	216	0.48	putative permease, similar to membrane enzyme for rhamnogalaturonan degradation
yesY	41	535	0.08	similar to rhamnogalacturonan acetylesterase
comP	269	807	0.33	two-component sensor histidine kinase, involved in early competence, phosphorylation of ComA
comQ	342	822	0.42	transcriptional regulator, required for the processing, modification, and release of active competence pheromone ComX, regulation of late competence operon (comG) and surfactin expression (srfA)

Table S3.1. (Continued)

Gene	Signal Intensity Dap^{R}1	Signal Intensity W168	Fold Change	Function of Gene Product
comX	65.8	235	0.28	competence pheromone precursor, required for the development of genetic competence possibly by activating ComA through extracellular signaling of Spo0K
comGG	19.8	78.8	0.25	required for exogenous DNA-binding
comS	354	5287	0.07	competence regulation
ylqB	130	2498	0.05	unknown
amyC	44.8	1003	0.04	maltose transport
yvaW	14.3	151	0.09	Sporulation-delaying protein sdpA, export of killing factor
yvaX	5.8	135	0.04	Sporulation-delaying protein sdpB, exporter of killing factor
yvaY	39	332	0.12	killing factor SdpC
yvfA	39	176	0.37	possible polysaccharide biosynthesis protein, epsK
yvfB	149	309	0.48	possible polysaccharide biosynthesis protein, epsK, similar to O-antigen and teichoic acid export protein
yvfC	44.0	101	0.44	putative undecaprenyl-phosphate galactose phosphotransferase, epsL
yvfD	77.8	141	0.55	putative acetyltransferase epsM
yvfH	241	907	0.27	L-lactate permease
yvfK	270	4204	0.06	maltose/maltodextrin-binding protein
yvfL	357	7324	0.05	maltodextrin transport system permease
yvfM	175	4479	0.04	maltodextrin transport system permease
yvfO	83.5	1581	0.05	arabinogalactan endo-1,4- β -galactosidase
yvfV	2260	4334	0.52	putative iron-sulfur heterodisulfide reductase, similar to Glycolate oxidase
yvfW	9646	15342	0.63	iron-sulfur oxidoreductase
srfAA	115	2481	0.05	surfactin synthetase/competence
srfAD	2.5	87.3	0.03	surfactin production and competence
srfAB	2.0	76.0	0.03	surfactin production and competence

Table S3. 2. Differential quantification of gene expression of Dap^{R}1 and W168 with daptomycin treatment. Genes with fold changes >2 are shown.

Gene	Signal Intensity		Fold Change	Signal Intensity		Fold Change	Function of Gene Product[3]
	W168 +	W168[1] -	W168[2] +/-	Dap^{R}1 +	Dap^{R}1 -	Dap^{R}1 +/-	
liaI	58519	44.5	1315	3397	1279	2.7	putative membrane protein
liaH	58516	43.5	1345	5096	1438	3.5	PspA homolog
liaG	28172	95.8	294	686	230	3.0	putative membrane anchored protein
liaF	39778	248	160	944	518	1.8	negative regulator of LiaR
liaS	11803	89.7	132	643	304	2.1	TCS histidine kinase
liaR	2549	35.5	71.8	163	116	1.4	TCS response regulator
yvrI	1826	3.5	522	68.8	25.3	2.7	σ factor YvrI
yvrL	933	1.8	509	34.3	21.9	1.6	negative regulator of yvrI
yvzA	277	32.2	8.6	36.9	27.8	1.3	hypothetical protein
yvzC	170	5.5	31.0	33.8	16.8	2.0	hypothetical protein
yvcB	836	33.8	24.7	83.3	72.0	1.2	hypothetical protein
yhcY	115	34.5	3.3	122	104	1.2	TCS histidine kinase
yhcZ	466	209	2.2	380	388	1.0	TCS response regulator
yvkN	202	8.7	23.3	33.6	28.0	1.2	hypothetical protein
yvpB	167	14.0	12.0	33.8	35.0	1.0	hypothetical protein
yknU	2912	296	9.8	121	140	0.9	ABC transporter (ATP-binding protein)
sdpI	1566	181	8.7	195	185	1.1	immunity protein for SdpC
ywdD	125	24.0	5.2	52.4	53.5	1.0	hypothetical protein
ywdE	340	39.2	8.7	40.3	32.9	1.2	hypothetical protein
ywdI	1075	548	2.0	763	785	1.0	similar to uracil-DNA glycosylase
yqjL	237	28.5	8.3	1547	1441	1.1	hydrolase; paraquat resistance
bcrC	293	85.7	3.4	2409	2593	0.9	bacteriocin transport permease
ypbG	172	43.7	3.9	1029	1002	1.0	marker for inhibition of cell wall biosynthesis
ydaH	268	38.0	7.0	682	752	0.9	uncharacterized membrane protein
ywfB	194	28.7	6.8	44.3	37.9	1.2	similar to Bacilysin biosynthesis protein
yuaF	535	107	5.0	1267	135	0.9	hypothetical protein
yuaG	238	123	1.9	278	237	1.2	flotillin-like protein
yfiC	11470	2555	4.5	2180	2180	1.0	ABC transporter (ATP-binding protein)
yitI	563	151	3.7	207	236	0.9	probable acetyltransferase
yebC	119	32.5	3.7	627	589	1.1	putative permease
ywaC	96.3	26.5	3.6	665	626	1.1	ppGpp synthase
fabHA	972	381	2.5	667	533	1.3	fatty acid biosynthesis
fabHB	58.8	19.2	3.1	34.1	22.9	1.5	fatty acid biosynthesis
fabF	1526	759	2.0	1375	1212	1.1	beta-ketoacyl-acyl carrier protein synthase II
sigM	160	69.7	2.3	588	606	1.0	ECF σ factor
yhdK	77.3	37.8	2.0	280	305	0.9	ECF anti-σ factor
yhdL	169	61.7	2.7	405	432	0.9	ECF anti-σ factor
rodA	118	42.5	2.8	386	370	1.0	cell-division membrane protein
radC	450	168	2.7	1213	1259	1.0	DNA repair protein
maf	469	177	2.6	2744	2556	1.1	cell division and shape determination
ypeB	237	96.8	2.4	15.8	11.6	1.0	sporulation protein
murB	548	262	2.1	4252	5161	0.8	UDP-N-acetylenolpyruvoylglucosamine reductase
murG	284	118	2.4	2662	2712	1.0	peptidoglycan biosynthesis
yoeB	2165	938	2.3	406	507	0.8	protection against autolysins
yumB	121	51.2	2.4	103	74.5	1.4	NADH dehydrogenase
yheJ	151	63.8	2.4	30.0	27.0	1.1	unknown
ytfI	518	223	2.3	273	329	0.8	hypothetical protein
ywrE	121	54.2	2.2	175	189	0.9	unknown
yxjI	106	49.8	2.1	378	342	1.1	unknown
ylbQ	145	68.2	2.1	277	303	0.9	2-dehydropantoate 2-reductase

Table S3.2. (Continued)

Gene	Signal Intensity		Fold Change	Signal Intensity		Fold Change	Function of Gene Product[3]
	W168	W168[1]	W168[2]	Dap^R1	Dap^R1	Dap^R1	
	+	-	+/-	+	-	+/-	
yhdA	144	69.8	2.1	94.4	114	0.8	NAD(P)H-FMN and ferric iron reductase
glpD	156	76.7	2.0	415	411	1.0	glycerol-3-phosphate dehydrogenase
liaI	58519	44.5	1315	3397	1279	2.7	putative membrane protein
glpF	214	112	1.9	1707	1698	1.0	glycerol uptake facilitator
yojI	141	69.5	2.0	55.4	59.9	0.9	multidrug efflux protein
trpF	195	97.5	2.0	206	175	1.2	phosphoribosyl anthranilate isomerase
cdsA	109	55.8	2.0	599	625	1.0	phosphatidate cytidylyltransferase
ygxB	253	131	1.9	94.9	50.6	1.9	putative membrane protein
ywtF	264	142	1.9	1051	1113	0.9	similar to transcriptional regulator LytR
yvaV	515	278	1.9	333	310	1.1	putative HTH-type transcriptional regulator
licA	113	78.5	1.4	724	1165	0.6	PTS, lichenan degradation
nadA	2467	2285	1.1	1809	3050	0.6	quinolinate synthetase
ywiC	341	445	0.8	64.4	114	0.6	putative membrane protein
ytrP	61.8	41.8	1.5	343	613	0.6	TCS histidine kinase
yolB	1662	2578	0.6	1646	1477	1.1	SPBc2 prophage-derived uncharacterized protein
yckI	156	243	0.6	806	730	1.1	L-cystine import ATP-binding protein
yscB	165	257	0.6	282	210	1.3	hypothetical protein
yqzC	253	397	0.6	664	724	0.9	hypothetical protein
rplI	354	563	0.6	1372	1301	1.1	ribosomal protein L9
mcpB	435	692	0.6	1928	1648	1.2	methyl-accepting chemotaxis protein
yheA	536	857	0.6	1508	1480	1.0	hypothetical protein
hbs	3435	5532	0.6	6845	7406	0.9	non-specific DNA-binding protein
yrvJ	309	511	0.6	451	438	1.0	similar to N-acetylmuramoyl-L-alanine amidase
yhdN	164	273	0.6	7667	537	1.4	aldo/keto reductase specific for NADPH
lmrB	255	426	0.6	106	127	0.8	lincomycin-resistance
rpmB	671	1155	0.6	2384	2096	1.1	ribosomal protein L28
degR	83.0	153	0.5	101	97.1	1.0	activation of degradative enzymes (AprE, NprE, SacB)
ydaL	208	384	0.5	22.0	19.9	1.1	hypothetical protein
rpsT	408	802	0.5	996	1070	0.9	ribosomal protein S20
ywhB	213	364	0.6	687	695	1.0	4-oxalocrotonate tautomerase
ywhE	371	737	0.5	78.6	93.3	0.8	*pbpG*, penicillin-binding protein (sporulation)
yocH	531	1074	0.5	5743	6754	0.9	similar to cell wall-binding protein (autolysin)
ywjC	79.7	168	0.5	137	122	1.1	unknown
yxeL	31.8	69.2	0.5	33.6	52.3	0.6	similar to GCN5-related N-acetyltransferase
yxeM	55.8	120	0.5	67.6	78.4	0.9	putative ABC transporter
yxeN	34.3	60.7	0.6	33.1	27.6	1.2	putative ABC transporter, permease
yxeO	64.2	118	0.5	84.0	89.8	0.9	putative ABC transporter, ATP-binding protein
yxeP	27.3	53.3	0.5	46.9	37.3	1.3	putative carboxypeptidase, aminohydrolase
yxeQ	51.2	92.7	0.6	62.9	65.3	1.0	MmgE/PrpD family protein, propionate catabolism
arfM	515	726	0.7	93.3	241	0.4	regulation of anaerobic genes

[1] "+" or "-" correspond to average triplicates of signal intensities of daptomycin-treated or untreated samples, respectively.
[2] "+/-" corresponds to the fold change between daptomycin-treated and untreated samples.
[3] Functions were assigned based on the SubtiList database or BSORF entries.